



Thesis submitted for the degree of Doctor of Philosophy (PhD)

**Removal of Humic Substances from Water Using Solar  
Irradiation and Granular Activated Carbon Adsorption**

Xiaohui Liu

March 2010

University College London

Civil, Environmental and Geomatic Engineering

Chadwick Building – Gower Street- London - WC1E 6BT – UK

I, Xiaohui Liu, confirm that the work presented in this thesis is my own. Where information has been derived from other sources, I confirm that this has been indicated in the thesis.

## ACKNOWLEDGEMENTS

This work would not have been completed without the financial support of the Overseas Research Students (ORS) Award and the Great Britain-China Educational Trust (GBCET).

I would like to thank Prof. Caroline Fitzpatrick for her support over the past three years.

I'm very grateful to Prof. Nick Tyler, Prof. Nigel Graham, Prof. John Gregory and Dr. Luiza Campos for their valuable advice and support to this work. I would also like to thank Dr. Emma Goslan (Cranfield University), Andrew Wetherill (Yorkshire Water), Dr. Karl Smith (Imperial College) and Mark Beswick (Met Office) for their contribution in different aspects of this work and this is grateful acknowledged.

Many thanks to all my friends, particularly Shang, Rui, Sunday, Jianhong, Bo, Max, Steven and Tony, for encouraging me with their friendship. I would especially like to thank Ian and Judith for all their support and encouragement over these years.

Finally and most of all, I would like to thank my beloved parents, to whom this thesis is dedicated. Their constant love and inspiration supported me through the difficult times and encouraged me to complete this thesis.

## ABSTRACT

For the existing water treatment processes, difficulties in removing humic substances (HS) to improve drinking water quality, and safety, have created the demand for exploring novel options to enhance HS removal. Here a combination of solar irradiation and granular activated carbon (GAC) adsorption is proposed. It aims to make use of the most freely available and abundant energy source, sunlight, to improve the performance of GAC adsorption process. An investigation into how characteristics of HS vary under natural sunlight and how this influences the subsequent removal of HS by GAC adsorption was carried out. Bulk water parameters, and more specifically, UV absorbance at 254 nm ( $UV_{254}$ ), as well as dissolved organic carbon (DOC) were used in conjunction with molecular weight (MW) to evaluate the performance of the solar-GAC method. The observation was made that solar irradiation led to a decrease in DOC,  $UV_{254}$  and MW of HS. The high MW components were photodegraded into smaller molecules, even with very low solar intensity in winter. Significant photodegradation of small molecules was also achievable by exposure to natural sunlight alone. Pre-treatment using solar irradiation was shown to successfully improve the GAC adsorption performance on HS removal, increasing the DOC removal from 69 % to 95 %. An up to three-fold increase in the adsorption capacity of GAC for the irradiated HS was observed. Solar collectors were found to effectively enhance the photodegradation of HS, and consequently enhance the removal of HS by GAC adsorption. The application of solar collectors could be a viable option for humic water treatment. The proposed solar irradiation-GAC adsorption method provides a new approach for the treatment of humic rich waters. The utilization of solar irradiation in water treatment processes is considered a sustainable and promising field.

# TABLE OF CONTENTS

	<b>Page</b>
Acknowledgement .....	3
Abstract .....	4
Table of contents .....	5
List of tables .....	9
List of figures .....	11
Abbreviations and notation .....	17
<b>CHAPTER 1 INTRODUCTION .....</b>	<b>20</b>
1.1 Background and motivation for work .....	20
1.2 Scope of work .....	21
1.3 Thesis overview .....	22
<b>CHAPTER 2 LITERATURE REVIEW .....</b>	<b>25</b>
2.1 Introduction .....	25
2.2 Humic substances .....	25
2.2.1 <i>A brief review of HS</i> .....	25
2.2.2 <i>Bulk characterization of HS</i> .....	29
2.2.2.1 Ultraviolet and visible light absorbance .....	30
2.2.2.2 Organic carbon content .....	32
2.2.2.3 Molecular size .....	33
2.2.3 <i>HS as precursors for chlorination by-products</i> .....	35
2.3 Sunlight in water treatment .....	38
2.3.1 <i>Solar irradiation as source of energy</i> .....	38
2.3.1.1 Solar spectrum .....	39
2.3.1.2 World distribution of solar irradiation .....	42
2.3.1.3 Natural sunlight vs. solar simulator .....	43
2.3.2 <i>Photodegradation of HS</i> .....	45
2.3.2.1 Photodegradation process .....	45
2.3.2.2 Effects of irradiation on properties of HS .....	46

2.3.3	<i>Water treatment with solar energy</i> .....	54
2.3.3.1	Using solar energy in drinking water treatment.....	54
2.3.3.2	Solar collectors.....	56
2.4	GAC adsorption .....	62
2.4.1	<i>GAC properties</i> .....	63
2.4.2	<i>Effects of physicochemical characteristics on HS adsorption</i> .....	64
2.4.2.1	Physical aspect .....	64
2.4.2.2	Chemical aspect .....	66
2.4.3	<i>Approaches to evaluate the adsorption of HS</i> .....	67
2.4.3.1	Isotherm models.....	67
2.4.3.2	Continuous flow adsorption process .....	70
2.5	Water treatment processes for removing HS – a brief review .....	73
2.5.1	<i>Membrane filtration</i> .....	75
2.5.2	<i>Coagulation</i> .....	77
2.5.3	<i>Advanced Oxidation Processes (AOPs)</i> .....	78
2.6	Conclusions.....	80
<b>CHAPTER 3 AIMS AND OBJECTIVES.....</b>		<b>82</b>
<b>CHAPTER 4 MATERIALS AND METHODS.....</b>		<b>84</b>
4.1	Introduction.....	84
4.2	Hypothesis and approach .....	84
4.3	HS samples.....	85
4.3.1	<i>Description of HS</i> .....	85
4.3.2	<i>Preparation of HS solutions</i> .....	87
4.3.2.1	Stock Solution .....	87
4.3.2.2	Experimental solutions.....	87
4.4	Analytical methods .....	88
4.4.1	<i>Sampling</i> .....	88
4.4.2	<i>UV<sub>254</sub> measurement</i> .....	89
4.4.3	<i>DOC</i> .....	89
4.4.4	<i>SUVA</i> .....	90
4.4.5	<i>HPSEC</i> .....	90

4.4.5.1 Instrumentation .....	90
4.4.5.2 Column calibration.....	91
4.4.5.3 Calculating MW .....	93
4.4.6 <i>pH</i> .....	95
4.5 Solar irradiation experiment.....	96
4.5.1 <i>Basic experimental set-up</i> .....	96
4.5.2 <i>PET bottles</i> .....	98
4.5.3 <i>Solar collectors</i> .....	100
4.5.4 <i>Solar irradiation measurement</i> .....	105
4.6 Granular activated carbon adsorption experiment .....	106
4.6.1 <i>Characterizing GAC</i> .....	106
4.6.2 <i>Adsorption isotherm study (batch experiments)</i> .....	107
4.6.3 <i>Small column experiments</i> .....	108
4.6.3.1 GAC preparation .....	109
4.6.3.2 Column set-up .....	109
<b>CHAPTER 5 RESULTS AND DISCUSSIONS.....</b>	<b>112</b>
5.1 Introduction.....	112
5.2 Effects of solar irradiation on the properties of HS .....	114
5.2.1 <i>Evaluation of solar irradiation</i> .....	114
5.2.2 <i>Light transmission characteristics of experimental bottles</i> .....	119
5.2.3 <i>Seasonal evaluation of solar irradiation on HS characteristics</i> .....	123
5.2.3.1 Winter experiment.....	123
5.2.3.2 Spring experiment .....	131
5.2.3.3 Summer experiment .....	135
5.2.4 <i>Factors affecting the photodegradation of HS</i> .....	144
5.2.4.1 Microbial effects .....	145
5.2.4.2 pH effects .....	147
5.2.4.3 Effects of solar irradiation on aquatic FA .....	151
5.2.5 <i>Evaluation of natural water source</i> .....	153
5.2.6 <i>Summary of solar irradiation results</i> .....	160
5.3 Effects of solar irradiation on the adsorption of HS by GAC .....	164
5.3.1 <i>Characteristics of GAC</i> .....	164

5.3.2 Seasonal evaluation of solar irradiation effect on GAC adsorption of HS .....	165
5.3.2.1 Winter experiment.....	166
5.3.2.2 Spring experiment .....	175
5.3.2.3 Summer experiment .....	189
5.3.3 Effect of pH .....	195
5.3.4 Adsorption of FA .....	198
5.3.5 Evaluation of natural water source.....	199
5.3.6 GAC column adsorption.....	204
5.3.7 Summary of GAC adsorption results .....	212
<b>CHAPTER 6 OVERALL COMPARISONS AND DISCUSSIONS .....</b>	<b>215</b>
6.1 Introduction.....	215
6.2 Overall comparisons of different processes on HS removal.....	216
<b>CHAPTER 7 CONCLUSIONS AND RECOMMENDATIONS .....</b>	<b>227</b>
7.1 Conclusions.....	227
7.2 Recommendations.....	230
<b>CHAPTER 8 REFERENCES .....</b>	<b>232</b>
<b>PAPERS AND COMMUNICATIONS .....</b>	<b>247</b>

## LIST OF TABLES

	<b>Page</b>
<b>Table 2.1</b> DOC concentration and distribution of HS in natural waters (Thurman, 1985). .....	26
<b>Table 2.2</b> Physicochemical characteristics of HS (Reckhow <i>et al.</i> , 1990; Karanfil <i>et al.</i> , 1996a). .....	28
<b>Table 2.3</b> A summary of the applications of UV-visible spectroscopy to characterize HS. ....	31
<b>Table 2.4</b> Irradiation effects on the UV <sub>254</sub> removal of HS (Allard <i>et al.</i> , 1994; Corin <i>et al.</i> , 1998; Hongve, 1998; Goslan <i>et al.</i> , 2006; Chow <i>et al.</i> , 2008). .....	48
<b>Table 2.5</b> Irradiation effects on the DOC removal of HS (Allard <i>et al.</i> , 1994; Corin <i>et al.</i> , 1998; Hongve, 1998; Pullin <i>et al.</i> , 2004; Winter <i>et al.</i> , 2007; Rodríguez-Zúñiga <i>et al.</i> , 2008). .....	50
<b>Table 2.6</b> Classifications of solar collectors (Rodríguez <i>et al.</i> , 2004). .....	57
<b>Table 2.7</b> Advantages and disadvantages of the non-concentrating and concentrating solar collectors (Malato <i>et al.</i> , 2002; Rodríguez <i>et al.</i> , 2004). .....	59
<b>Table 2.8</b> Examples of water treatment methods and their natural HS removal performances (Owen <i>et al.</i> , 1993; Fu <i>et al.</i> , 1994; Goel <i>et al.</i> , 1995; Jacangelo <i>et al.</i> , 1995; Lambert and Graham, 1995; Volk <i>et al.</i> , 2000; Parkinson <i>et al.</i> , 2003; Chin and Bérubé, 2005). .....	74
<b>Table 2.9</b> Examples of water treatment methods and their AHA removal performances (Allard <i>et al.</i> , 1994; Rebhun <i>et al.</i> , 1998; Chen and Wu, 2004; Murray and Parsons, 2004; Wiszniewski <i>et al.</i> , 2004; Listiarini <i>et al.</i> , 2009). .....	75
<b>Table 2.10</b> Published data for colour and DOC removals by slow sand filtration with pre-ozonation (Graham, 1999). .....	80
<b>Table 4.1</b> Details of solar irradiation experiments, including experimental duration, solar collectors used and sampling frequency. ....	97
<b>Table 4.2</b> Sizes of solar collectors (PC, CPC and BPC) used in this research. ....	102
<b>Table 4.3</b> A summary of the rapid small scale column test (RSSCT) parameters used in this study. ....	110
<b>Table 5.1</b> Accumulative solar dose during irradiation experiments at Chadwick Building of UCL, London, UK. ....	114
<b>Table 5.2</b> Characteristics of HS solutions prior to solar irradiation in winter experiments (solar dose $1.44 \times 10^5$ kJ/m <sup>2</sup> ). .....	123
<b>Table 5.3</b> First-order decay rate constants of HS irradiated in different solar collectors in winter experiment (DOC removal 11-15 %, UV <sub>254</sub> removal 14-20 %, solar dose $1.44 \times 10^5$ kJ/m <sup>2</sup> ). .....	127
<b>Table 5.4</b> Characteristics of HS solutions prior to solar irradiation in spring experiment (solar dose $2.61 \times 10^5$ kJ/m <sup>2</sup> ). .....	131
<b>Table 5.5</b> First-order decay rate constants of HS irradiated in different solar collectors in spring experiment (DOC removal 18-31 %, UV <sub>254</sub> removal 28-45 %, solar dose $2.61 \times 10^5$ kJ/m <sup>2</sup> ). .....	133
<b>Table 5.6</b> Characteristics of HS solutions prior to solar irradiation in summer experiment (solar dose $5.97 \times 10^5$ kJ/m <sup>2</sup> ). .....	136

<b>Table 5.7</b>	First-order decay rate constants of HS irradiation in different solar collectors in summer (DOC removal 50-62 % and UV <sub>254</sub> removal 60-84 %, solar dose $5.97 \times 10^5$ kJ/m <sup>2</sup> ).	138
<b>Table 5.8</b>	Characteristics of AHA and SRFA solutions prior to solar irradiation (solar dose $1.96 \times 10^5$ kJ/m <sup>2</sup> ).	151
<b>Table 5.9</b>	Characteristics of the natural CH water and AHA water prior to solar irradiation in autumn (solar dose $1.42 \times 10^5$ kJ/m <sup>2</sup> ).	154
<b>Table 5.10</b>	First-order decay rate constants of CH water and AHA water irradiated in BPC and flat tray in autumn (DOC removal 21-29 % for CH water and 14-24 % for AHA water, solar dose $1.42 \times 10^5$ kJ/m <sup>2</sup> ).	159
<b>Table 5.11</b>	Basic characteristics of the Aquasorb 101 GAC (Universal Mineral Supplies, UK).	165
<b>Table 5.12</b>	Modified Freundlich isotherm parameters for the irradiated and non-irradiated HS solutions in winter experiment (initial DOC 8.50 mg/L, DOC removal 11-15 %, solar dose $1.44 \times 10^5$ kJ/m <sup>2</sup> ).	173
<b>Table 5.13</b>	Modified Freundlich isotherm parameters for irradiated and non-irradiated HS solutions in spring experiment. (initial DOC 8.29 mg/L, DOC removal 18-31 %, solar dose $2.61 \times 10^5$ kJ/m <sup>2</sup> ).	177
<b>Table 5.14</b>	Modified Freundlich isotherm parameters for the irradiated and non-irradiated HS solutions in summer experiment (initial DOC 8.51 mg/L, DOC removal 50-62 %, solar dose $5.97 \times 10^5$ kJ/m <sup>2</sup> ).	192
<b>Table 5.15</b>	Modified Freundlich isotherm parameters for CH water and AHA water on GAC (DOC removal 21-29 % for CH water and 14-24 % for AHA water, solar dose $1.42 \times 10^5$ kJ/m <sup>2</sup> ).	202
<b>Table 5.16</b>	Characteristics of HS solutions used in small column studies.	205
<b>Table 6.1</b>	Experimental conditions corresponding to the treatment process listed in Figure 6.1 regarding the removal of UV <sub>254</sub> of AHA (Allard <i>et al.</i> , 1994; Murray and Parsons, 2004; Wiszniowski <i>et al.</i> , 2004; Listiarini <i>et al.</i> , 2009).	218
<b>Table 6.2</b>	Experimental conditions corresponding to the treatment process listed in Figure 6.2 regarding the removal of DOC of AHA (Rebhun <i>et al.</i> , 1998; Wang <i>et al.</i> , 2000; Wiszniowski <i>et al.</i> , 2002 and 2004; Chen and Wu, 2004; Murray and Parsons, 2004).	223

## LIST OF FIGURES

	<b>Page</b>
<b>Figure 2.1</b> Proposed structure of humic acid (Stevenson, 1982).....	27
<b>Figure 2.2</b> Proposed structure of fulvic acid (Leenheer <i>et al.</i> , 1998).....	28
<b>Figure 2.3</b> UV/visible spectra of several lake waters with different DOC of HS (Zuo and Jones, 1997).....	30
<b>Figure 2.4</b> Relationship between DOC and UV <sub>254</sub> for a variety of water samples (Collins <i>et al.</i> , 1986; Chow <i>et al.</i> , 1999; Nokes <i>et al.</i> , 1999; Bergamaschi <i>et al.</i> , 2000; Volk <i>et al.</i> , 2000; Singer and Bilyk, 2002; Chow <i>et al.</i> , 2008).....	33
<b>Figure 2.5</b> Effect of MW on HS properties and reactivity (Cabaniss <i>et al.</i> , 2000). .....	34
<b>Figure 2.6</b> Relationship between (a) DBP formation and UV <sub>254</sub> (White <i>et al.</i> , 2003); and (b) DBP formation and UV <sub>254</sub> (Singer, 1999).....	37
<b>Figure 2.7</b> Diffuse and direct solar irradiation (Rodríguez, 2003).....	39
<b>Figure 2.8</b> Distribution of the components of sunlight.....	40
<b>Figure 2.9</b> Solar spectrum of the direct irradiation on the ground level on a clear day (ASTM, 1992). (W/m <sup>2</sup> nm is the unit of irradiation intensity of each wavelength).....	41
<b>Figure 2.10</b> Examples of the spectral distribution and irradiation of (a) a solar simulator (Doll and Frimmel, 2003) and (b) a mercury lamp (Patel-Sorrentino <i>et al.</i> , 2004) used in HS photodegradation studies. .....	44
<b>Figure 2.11</b> Relationship between irradiation and absorbance removal (Parkinson <i>et al.</i> , 2003). A is the absorbance.....	46
<b>Figure 2.12</b> HPSEC chromatograms of HS before and after irradiation under different atmospheres (Lou and Xie, 2006).....	51
<b>Figure 2.13</b> MW fractions of different water samples before and after UV irradiation (Lehtola <i>et al.</i> , 2003). Samples A, B and C were raw waters from three Finnish waterworks. Samples A and B were ground waters and sample C was surface water. Numbering with decreasing order of MW. ....	53
<b>Figure 2.14</b> Non-concentrating solar collectors - flat plates at PSA, Spain (source: <a href="http://www.psa.es/webeng/instalaciones/desalacion.php">http://www.psa.es/webeng/instalaciones/desalacion.php</a> ). PSA: Plataforma Solar de Almería. ....	57
<b>Figure 2.15</b> Medium-concentrating solar collectors - parabolic trough collectors at PSA, Spain (source: <a href="http://www.psa.es/webeng/instalaciones/parabolicos.php">http://www.psa.es/webeng/instalaciones/parabolicos.php</a> ).....	58
<b>Figure 2.16</b> High-concentrating solar collectors - parabolic dish at PSA, Spain (source: <a href="http://www.psa.es/webeng/instalaciones/discos.php">http://www.psa.es/webeng/instalaciones/discos.php</a> ). ....	58
<b>Figure 2.17</b> (a) Simulations of the incident sunlight reflected by a compound parabolic collector onto the bottle located in the centre (Blanco <i>et al.</i> , 1999), and (b) an example of the CPC application (Rodríguez, 2003). .....	60
<b>Figure 2.18</b> Representative shape of the breakthrough curve with breakthrough at 5 % of the influent concentration (André, 2006). ....	71

<b>Figure 2.19</b>	Schematic of the combination of pre-treatment and membrane filtration for drinking water treatment (Jacangelo <i>et al.</i> , 1997). (RO represents the reverse osmosis).....	77
<b>Figure 4.1</b>	Schematic diagram of the HS sample treatment methodology.....	85
<b>Figure 4.2</b>	An example of HPSEC chromatograms of PSS standards having MWs of 891, 6430, 15800 and 33500 Da as well as acetone for the purpose of calibrating HS. ....	92
<b>Figure 4.3</b>	An example of the calibration function obtained by linear regression of the log MW and retention time of calibration standards.....	93
<b>Figure 4.4</b>	Solar irradiation experimental set-up on the roof of Chadwick Building, UCL, London. From left to right: bigger parabolic collector (BPC), compound parabolic collector (CPC) and parabolic collector (PC). ....	98
<b>Figure 4.5</b>	The PET bottle used for solar irradiation experiment (source: Medfor Ltd., UK). ....	99
<b>Figure 4.6</b>	Schematic of parabolic curve, showing the reflection of sunlight perpendicular to the parabolic collector aperture plane. ....	102
<b>Figure 4.7</b>	Pictures of three solar collectors used in this research: (a) PC, (b) BPC, and (c) CPC. ....	103
<b>Figure 4.8</b>	Schematic of the compound parabolic curve (height 10 cm and width 25 cm) with 8 cm as the bottle diameter. ....	104
<b>Figure 4.9</b>	Schematic of the rapid small scale column test (RSSCT) experiment. ....	110
<b>Figure 5.1</b>	Distribution of daily solar dose for four seasons: data recorded at UCL and by Met Office. ....	115
<b>Figure 5.2</b>	Distribution of daily UV intensity for four seasons.....	116
<b>Figure 5.3</b>	Light transmission characteristics of quartz, borosilicate glass and PET materials as a function of wavelength, measured on a UV-visible spectrophotometer. ....	120
<b>Figure 5.4</b>	Changes in (1) UV <sub>254</sub> absorbance and (2) UV/visible absorption spectrum of HS solutions in PET and glass bottles due to solar irradiation in spring (solar dose $3.39 \times 10^4$ kJ/m <sup>2</sup> ) and summer (solar dose $8.59 \times 10^4$ kJ/m <sup>2</sup> ) with initial UV <sub>254</sub> =0.37 cm <sup>-1</sup> .....	122
<b>Figure 5.5</b>	Effect of solar irradiation on the DOC concentration of HS in different solar collectors in winter (initial DOC 8.50 mg/L, solar dose $1.44 \times 10^5$ kJ/m <sup>2</sup> ). ....	124
<b>Figure 5.6</b>	Effect of solar irradiation on the UV <sub>254</sub> absorbance of HS in different solar collectors in winter (initial UV <sub>254</sub> 0.67 cm <sup>-1</sup> , solar dose $1.44 \times 10^5$ kJ/m <sup>2</sup> ). ....	125
<b>Figure 5.7</b>	Chromatograms of HS before and after solar irradiation in winter and destruction/formation (D/F) curves (initial DOC 8.50 mg/L and UV <sub>254</sub> 0.67 cm <sup>-1</sup> , DOC removal 11-15 % and UV <sub>254</sub> removal 14-20 %, solar dose $1.44 \times 10^5$ kJ/m <sup>2</sup> ). ....	129
<b>Figure 5.8</b>	Effect of solar irradiation on the DOC concentration of HS in different solar collectors in spring (initial DOC 8.29 mg/L, solar dose $2.61 \times 10^5$ kJ/m <sup>2</sup> ). ....	132
<b>Figure 5.9</b>	Effect of solar irradiation on the UV <sub>254</sub> absorbance of HS in different solar collectors in spring (initial UV <sub>254</sub> 0.67 cm <sup>-1</sup> , solar dose $2.61 \times 10^5$ kJ/m <sup>2</sup> ). ....	132

<b>Figure 5.10</b> Chromatograms of HS before and after solar irradiation in spring and destruction/formation (D/F) curves (initial DOC 8.29 mg/L and $UV_{254}$ 0.67 $cm^{-1}$ , DOC removal 18-31 % and $UV_{254}$ removal 28-45 %, solar dose $2.61 \times 10^5$ $kJ/m^2$ ). .....	134
<b>Figure 5.11</b> Effect of solar irradiation on the DOC concentration of HS in different solar collectors in summer (initial DOC 8.51 mg/L, solar dose $5.97 \times 10^5$ $kJ/m^2$ ). .....	137
<b>Figure 5.12</b> Effect of solar irradiation on the $UV_{254}$ absorbance of HS in different solar collectors in summer (initial $UV_{254}$ 0.68 $cm^{-1}$ , solar dose $5.97 \times 10^5$ $kJ/m^2$ ). .....	137
<b>Figure 5.13</b> Chromatograms of HS before and after solar irradiation in summer and destruction/formation (D/F) curves (initial DOC 8.51 mg/L and $UV_{254}$ 0.68 $cm^{-1}$ , DOC removal 50-62 % and $UV_{254}$ removal 60-84 %, solar dose $5.97 \times 10^5$ $kJ/m^2$ ). .....	139
<b>Figure 5.14</b> (a) HPSEC chromatograms of HS irradiated in BPC during summer; (b) removal of different MW fractions of HS irradiated in BPC due to solar irradiation during summer. ....	140
<b>Figure 5.15</b> (a) HPSEC chromatograms of HS irradiated in the tray during summer, (b) removal of different MW fractions of HS irradiated in the tray due to solar irradiation during summer. ....	143
<b>Figure 5.16</b> Evolution of the properties of irradiated HS solutions in BPC after the completion solar irradiation experiments in winter (solar dose $1.44 \times 10^5$ $kJ/m^2$ ), spring (solar dose $2.61 \times 10^5$ $kJ/m^2$ ) and summer (solar dose $5.97 \times 10^5$ $kJ/m^2$ ). .....	146
<b>Figure 5.17</b> Removal of HS in terms of $UV_{254}$ and DOC due to solar irradiation and further degradation after irradiation. ....	147
<b>Figure 5.18</b> Removal of HS with initial pH values of 4.2, 7.5 and 9.7 by solar irradiation (initial DOC 8.30 mg/L and $UV_{254}$ 0.67 $cm^{-1}$ , solar dose $1.59 \times 10^5$ $kJ/m^2$ ). ....	148
<b>Figure 5.19</b> HPSEC chromatograms and destruction/formation (D/F) curves of HS solutions at three different initial pH values (4.2, 7.5 and 9.7) before and after solar irradiation: (a) HS irradiated in CPC, and (b) HS irradiated in tray (initial DOC 8.30 mg/L and $UV_{254}$ 0.67 $cm^{-1}$ , solar dose $1.59 \times 10^5$ $kJ/m^2$ ). .....	150
<b>Figure 5.20</b> Total removals of SRFA and AHA with respect to DOC and $UV_{254}$ due to solar irradiation (initial DOC 5.06mg/L (SRFA) and 3.80 mg/L (AHA), initial 0.20 $cm^{-1}$ (SRFA) and 0.25 $cm^{-1}$ (AHA), solar dose $1.96 \times 10^5$ $kJ/m^2$ ). .....	152
<b>Figure 5.21</b> HPSEC chromatograms of CH water and AHA water before and after solar irradiation in autumn (initial DOC 12.90 mg/L for CH water and 8.83 mg/L for AHA water, initial $UV_{254}$ 0.72 $cm^{-1}$ for CH water and 0.71 $cm^{-1}$ for AHA water, solar dose $1.42 \times 10^5$ $kJ/m^2$ ). .	156
<b>Figure 5.22</b> Effect of solar irradiation on the DOC concentration of CH water and AHA water in BPC and flat tray in autumn (initial DOC 12.90 mg/L for CH water and 8.83 mg/L for AHA water, solar dose $1.42 \times 10^5$ $kJ/m^2$ ). ....	156
<b>Figure 5.23</b> Effect of solar irradiation on the $UV_{254}$ absorbance of the CH water and AHA water in BPC and flat tray in autumn (initial $UV_{254}$ 0.72	

	cm <sup>-1</sup> for CH water and 0.71 cm <sup>-1</sup> for AHA water, solar dose 1.42×10 <sup>5</sup> kJ/m <sup>2</sup> ). .....	156
<b>Figure 5.24</b>	Removal of different MW fractions of CH water and AHA water in BPC and tray due to solar irradiation in autumn (initial DOC 12.90 mg/L for CH water and 8.83 mg/L for AHA water, DOC removal 21-29 % for CH water and 14-24 % for AHA water, solar dose 1.42×10 <sup>5</sup> kJ/m <sup>2</sup> ). .....	159
<b>Figure 5.25</b>	Summary of the first-order decay rate constants for HS solutions irradiated in different seasons: (a) <i>k<sub>1</sub></i> for DOC, and (b) <i>k<sub>2</sub></i> for UV <sub>254</sub> . .....	162
<b>Figure 5.26</b>	Correlations between first-order decay rate constants of HS solutions irradiated in the flat tray and solar doses in four seasonal experiments. .....	163
<b>Figure 5.27</b>	Adsorption isotherms of the irradiated and non-irradiated HS solutions by GAC in winter experiment (initial DOC 8.50 mg/L, DOC removal 11-15 %, solar dose 1.44×10 <sup>5</sup> kJ/m <sup>2</sup> ). .....	168
<b>Figure 5.28</b>	Comparisons of experimental value and computed value of <i>q<sub>e</sub></i> based on the Langmuir, Freundlich and modified Freundlich models: (a) non-irradiated HS (DOC 8.50 mg/L) and (b) HS irradiated in BPC (DOC 7.23 mg/L). The dashed lines represent 10 % uncertainty... ..	170
<b>Figure 5.29</b>	Adsorption of the irradiated and non-irradiated HS solutions by GAC in winter experiments. Solid and dashed lines represent the fitting of the modified Freundlich model to experimental data (initial DOC 8.50 mg/L, DOC removal 11-15 %, solar dose 1.44×10 <sup>5</sup> kJ/m <sup>2</sup> ). .....	172
<b>Figure 5.30</b>	Chromatograms of the non-irradiated and irradiated HS solutions after adsorption by GAC (1000 mg/L) in winter experiment (initial DOC 8.50mg/L, DOC removal 11-15 %, solar dose 1.44×10 <sup>5</sup> kJ/m <sup>2</sup> ). .....	174
<b>Figure 5.31</b>	Adsorption isotherms of irradiated and non-irradiated HS solutions by GAC in spring experiment (initial DOC 8.29 mg/L, DOC removal 18-31 %, solar dose 2.61×10 <sup>5</sup> kJ/m <sup>2</sup> ). .....	176
<b>Figure 5.32</b>	Adsorption of irradiated and non-irradiated HS solutions by GAC in spring experiment. Solid and dashed lines represent the fitting of the modified Freundlich model to experimental data. (initial DOC 8.29 mg/L, DOC removal 18-31 %, solar dose 2.61×10 <sup>5</sup> kJ/m <sup>2</sup> ).... ..	176
<b>Figure 5.33</b>	HPSEC chromatograms of HS remaining in solution after GAC adsorption in spring experiment: (a) HS irradiated in BPC, (b) HS irradiated in tray, and (c) non-irradiated HS (DOC removal 18-31 %, solar dose 2.61×10 <sup>5</sup> kJ/m <sup>2</sup> ). .....	179
<b>Figure 5.34</b>	Correlations between MW of the non-irradiated and irradiated HS and adsorption parameters: (a) <i>K<sub>F</sub></i> and (b) <i>n<sup>-1</sup></i> . (The solid and dashed lines suggest the trend).....	181
<b>Figure 5.35</b>	Correlations between the aromaticity of the non-irradiated and irradiated HS and adsorption parameters of HS: (a) <i>K<sub>F</sub></i> , and (b) <i>n<sup>-1</sup></i> . (The solid and dashed lines suggest the trend.) .....	182
<b>Figure 5.36</b>	SUVA values of the irradiated and non-irradiated HS remaining in solutions after adsorption by various doses of GAC in spring experiment (DOC removal 18-31 %, solar dose 2.61×10 <sup>5</sup> kJ/m <sup>2</sup> ).. ..	183

<b>Figure 5.37</b> Changes in the MW of HS solutions remaining in the solutions after adsorption by various GAC doses in spring experiment: (a) weight-average MW, and (b) number-average MW.....	185
<b>Figure 5.38</b> Changes in the polydispersity of the non-irradiated and irradiated HS solutions remaining in solution after adsorption by various GAC doses in spring experiment.....	186
<b>Figure 5.39</b> Adsorption isotherms of the non-irradiated and irradiated HS with similar initial concentrations.....	188
<b>Figure 5.40</b> Comparisons of the adsorption parameters of irradiated and diluted HS solutions with similar initial concentrations.....	189
<b>Figure 5.41</b> Adsorption isotherms of the irradiated and non-irradiated HS solutions by GAC in summer experiment (initial DOC 8.51 mg/L, DOC removal 50-62 %, solar dose $5.97 \times 10^5$ kJ/m <sup>2</sup> ).....	191
<b>Figure 5.42</b> Adsorption of the irradiated and non-irradiated HS by GAC in summer experiment. Solid and dashed lines show the fitting of the modified Freundlich model to the experimental data (initial DOC 8.51 mg/L, DOC removal 50-62 %, solar dose $5.97 \times 10^5$ kJ/m <sup>2</sup> )....	191
<b>Figure 5.43</b> Chromatograms of HS remaining in the solutions after adsorption by GAC in summer experiment: (a) HS irradiated in BPC, and (b) HS irradiated in the flat tray (DOC removal 50-62 %, solar dose $5.97 \times 10^5$ kJ/m <sup>2</sup> ).....	193
<b>Figure 5.44</b> SUVA values of HS remaining in the solutions after adsorption by various dose of GAC in summer experiment (DOC removal 50-62 %, solar dose $5.97 \times 10^5$ kJ/m <sup>2</sup> ).....	193
<b>Figure 5.45</b> Effect of MW on the adsorption behaviour of HS by GAC in summer experiment: (a) $K_F$ and (b) $n^{-1}$ . The solid and dashed lines suggest the trend.....	194
<b>Figure 5.46</b> Freundlich adsorption parameter $K_F$ of the non-irradiated and irradiated HS solutions with different initial pH values (4.2, 7.5 and 9.7).....	196
<b>Figure 5.47</b> Adsorption isotherms of AHA and SRFA solutions before and after solar irradiation (solar dose $1.96 \times 10^5$ kJ/m <sup>2</sup> ): (a) conventional isotherms and (b) modified Freundlich isotherms.....	197
<b>Figure 5.48</b> Changes in adsorption parameters of the non-irradiated and irradiated SRFA and AHA solutions.....	198
<b>Figure 5.49</b> Isotherms of the non-irradiated and irradiated CH water and AHA water by GAC: (a) conventional isotherms and (b) modified Freundlich isotherms (DOC removal 21-29 % for CH water and 14-24 % for AHA water, solar dose $1.42 \times 10^5$ kJ/m <sup>2</sup> ).....	200
<b>Figure 5.50</b> Chromatograms of the non-irradiated and irradiated CH water and AHA water before and after adsorption by 2000 mg GAC/L (DOC removal 21-29 % for CH water and 14-24 % for AHA water, solar dose $1.42 \times 10^5$ kJ/m <sup>2</sup> ).....	202
<b>Figure 5.51</b> Changes in the MW of CH water and AHA water remaining in solutions after adsorption by various doses of GAC.....	203
<b>Figure 5.52</b> Changes in the polydispersity of CH water and AHA water remaining in solutions after adsorption by various doses of GAC.....	204
<b>Figure 5.53</b> MWD of the non-irradiation and irradiated HS solutions measured by HPSEC before column feeding (initial DOC 7.2, 6.8 and 3.1 mg/L	

for the non-irradiated, irradiated A and irradiated B samples, respectively).....	206
<b>Figure 5.54</b> Breakthrough curves of the non-irradiated and irradiated HS solutions by small GAC columns using the RSSCT method (initial DOC 7.2, 6.8 and 3.1mg/L for the non-irradiated, irradiated A and irradiated B samples, respectively).....	207
<b>Figure 5.55</b> Chromatograms of HS remaining in the effluent after passing through the small GAC column: (a) non-irradiated HS, (b) irradiated A HS, and (c) irradiated B HS (initial DOC 7.2, 6.8 and 3.1 mg/L for non-irradiated, irradiated A and irradiated B, respectively).....	212
<b>Figure 5.56</b> Maximum removals of HS following solar irradiation and GAC adsorption.....	213
<b>Figure 5.57</b> Enhancement in the adsorbability of HS by GAC due to solar irradiation.....	214
<b>Figure 5.58</b> Maximum adsorption load of HS on GAC following solar irradiation and GAC adsorption.....	214
<b>Figure 6.1</b> Comparison of different treatment processes for the removal of UV <sub>254</sub> absorbance of AHA. (1) Allard <i>et al.</i> (1994); (2) Murray and Parsons (2004); (3) Wiszniowski <i>et al.</i> (2004); (4) and (5) Listiarini <i>et al.</i> (2009); (6) results in this research.....	217
<b>Figure 6.2</b> Comparison of different treatment processes for the removal of DOC content of AHA. (1) Rebhun <i>et al.</i> (1998); (2) and (3) Wang <i>et al.</i> (2000); (4) Wiszniowski <i>et al.</i> (2002); (5) Wiszniowski <i>et al.</i> (2004); (6) Chen and Wu (2004); (7) Murray and Parsons (2004); (8) results in this research.....	222

## ABBREVIATIONS AND NOTATION

AA	Acetic acids	
AHA	Aldrich humic acid	
AOP	Advanced oxidation process	
ASTM	American Society for Testing and Material	
BET	Brunauer Emmett and Teller	
BPC	Big parabolic collector	
CH	Chellow Heights	
CPC	Compound parabolic collector	
Da	Dalton	
DBP	Disinfection by-product	
DOC	Dissolved organic carbon	(mg/L)
EAWAG	Swiss Federal Institute of Aquatic Science & Technology	
EBCT	Empty bed contact time	(s)
<i>E.coli</i>	<i>Escherichia coli</i>	
EPR	Electron paramagnetic resonance	
F200	Filtrisorb 200	
F400	Filtrisorb 400	
FA	Fulvic acid	
FAF	Fulvic acid fraction	
FTIR	Fourier transform infrared spectroscopy	
GAC	Granular activated carbon	
HA	Humic acid	
HAA	Haloacetic acid	
HAF	Humic acid fration	
HS	Humic substances	
HPLC	High performance liquid chromatography	
HPIA	Hydrophilic fraction	
HPINA	Hydrophilic non acid	
HPSEC	High performance size exclusion chromatography	
IC	Inorganic carbon	(mg/L)
IHSS	International Humic Substances Society	

$K_F$	Modified Freundlich isotherm parameter	$(\text{mg/g GAC})^{1-1/n}$
MF	Microfiltration	
$M_n$	Number-average molecular weight	(Daltons)
MTZ	Mass transfer zone	
$M_w$	Weight-average molecular weight	(Daltons)
MW	Molecular weight	(Daltons)
MWCO	Molecular weight cut-off	
MWD	Molecular weight distribution	
NF	Nanofiltration	
NMR	Nuclear magnetic resonance	
NOM	Natural organic matter	
NTU	Nephelometric turbidity unit	
$\rho$	Polydispersity	
PAC	Power activated carbon	
PAH	Polycyclic aromatic hydrocarbons	
PC	Parabolic collector	
PET	Polyethylene terephthalate	
$\text{pH}_{\text{pzc}}$	Zero point of charge	
PSA	Plataforma Solar de Almería	
PSS	Polystyrene sodium sulphonate	
PTC	Parabolic trough collector	
PVA	Polyvinyl chloride	
RO	Reverse osmosis	
RSD	Relative standard deviation	
RSSCT	Rapid small-scale column test	
SODIS	Solar Water Disinfection	
SRFA	Suwanee River fulvic acid	
SRHA	Suwanee River humic acid	
SUVA	Specific UV absorbance	(L/mg m)
TC	Total carbon	(mg/L)
THM	Trihalomethane	
TOC	Total organic carbon	(mg/L)
UF	Ultrafiltration	
USEPA	United States Environmental Protection Agency	
UV	Ultraviolet	

UV <sub>254</sub>	UV absorbance at 254 nm	(cm <sup>-1</sup> )
WHO	World Health Organisation	
WTW	Water treatment works	

## CHAPTER 1

### INTRODUCTION

#### 1.1 Background and motivation for work

Humic substances (HS) are the main constituent of the dissolved natural organic matter (NOM) and account for up to 90 % of the dissolved organic carbon (DOC) in all natural waters (Thurman, 1985). Although HS themselves are regarded as non-toxic, several problems may arise during drinking water treatment. These problems include:

- HS have aesthetic effects which are the colour, odour and taste of water;
- HS enhance the transportation and distribution of synthetic compounds and heavy metals (Ding and Wu, 1997);
- HS can lower the efficiency of other water treatment processes, reducing the removal of target pollutants (Newcombe *et al.*, 2002b);
- During the water disinfection step, HS can react with chlorination and cause the formation of disinfection by-products (DBPs), such as trihalomethanes (THMs) and haloacetic acids (HAAs) (Singer, 1999; Barrett *et al.*, 2000). It is suspected that DBPs can cause cancer to humans.

An increase of HS content has been observed in water sources in many countries over the past 20 years (Worrall *et al.*, 2004; Skjelkvåle *et al.*, 2005; Vuorenmaa *et*

*al.*, 2006). Freeman *et al.* (2001) have reported increases of DOC of up to 65 % for 11 streams and 11 lake catchments over a timescale of 12 years in the UK. The increased DOC greatly challenges the water treatment works (WTWs) to guarantee water quality and provide safe potable water to the public.

Current water treatment processes are not specifically designed for removing HS. The conventional processes (comprising of coagulation, sedimentation and sand filtration) can generally remove 10-90 %, with an average of 30 % of dissolved organic matter (Li *et al.*, 2003). Improving DOC removal by increasing coagulant dose will result in an increased amount of sludge production and extra cost. Interest in the use of advanced oxidation processes (AOPs) has risen over the years; nevertheless, it is typically associated with high cost, by-products with unknown toxicity and undesired chemical residuals. The need therefore rises for exploring new approaches to improve HS removal, with emphasis on low energy consumption, low chemical addition, and low cost.

## **1.2 Scope of work**

The general aim of this research is to propose and investigate a new approach for removing HS from water, for the purpose of improving the already existing treatment process. More specifically, the research work is focused on using solar irradiation as a pre-treatment method to enhance the adsorption of HS by granular activated carbon (GAC). This will be achieved by a series of investigations conducted at different times of the year and on different water samples containing HS, looking at:

- changes in the characteristics of HS following natural sunlight irradiation;
- improvement in the GAC adsorption performance of the irradiated HS.

This thesis is the first to evaluate the use of solar energy as a pre-treatment method for improving HS removal by GAC, and makes an important contribution to the knowledge of this subject.

### **1.3 Thesis overview**

Chapter 2 initially presents a review of available literature on the characteristics of HS, which is helpful in selecting the most relevant analytical methods to represent HS and in linking those characteristics with the proposed treatment method, within the scope of this research. Here by targeting the treatment method, the review will be focused on two aspects – solar irradiation and GAC adsorption. In the section on solar irradiation, characteristics of sunlight, applications of solar irradiation in drinking water treatment and solar collector technologies are discussed. A detailed review is carried out on the physicochemical changes of HS resulting from irradiation, keeping in mind that most of the referred work carried out by other researchers is performed using artificial light sources. In the section on GAC adsorption, factors that control the adsorption of HS by GAC are thoroughly reviewed. Properties of GAC, adsorption models and continuous flow mode are also presented. Finally, some of the water treatment processes with respect to HS removal are briefly reviewed.

In Chapter 3, specific objectives are defined here to achieve the aim of this investigation.

Chapter 4 describes various aspects of the experimental design for the work conducted, including materials, analytical methods, solar irradiation experimental set-up, batch and column adsorption studies.

In Chapter 5, experimental results are presented and discussed. In the section on solar irradiation effects, the solar measurement data and light transmission property of the experimental container are first examined, which is useful for interpreting and comparing the results for all the experiments carried out. The effects of solar irradiation on HS are reported according to the time order of the seasonal experiments conducted – winter, spring and summer. The kinetics of HS removal in terms of DOC and UV absorbance at 254 nm ( $UV_{254}$ ) are determined to quantitatively compare the solar effects, in particular the improvement by using solar collectors. Since the hypothesis of this work is based on the size exclusion effects between HS and GAC, it is important to know the changes in molecular size of HS upon solar irradiation. More attention is therefore paid on the molecular weight (MW) changes during solar irradiation. Some factors, such as pH and microbial activity that may affect the photodegradation of HS are also discussed. Further investigations on aqueous fulvic acid (FA) and a natural water sample allow a better understanding and evaluation of the solar-GAC method, and these results are then presented.

A section on adsorption is also presented in Chapter 5. It starts with a brief description of the Aquasorb 101 GAC used in this research, based on the information from the supplier and lab analytical data. The equilibrium isotherms are examined to describe the adsorption behaviour, followed by a comparison of adsorption parameters in order to quantitatively evaluate the improvement in the adsorption of the irradiated HS. The role of the molecular size of HS in the adsorption process is also carefully examined, which is useful in understanding and explaining the experimental observations. The GAC adsorption is normally used as a continuous flow process in water treatment, it is important to examine the effects of solar irradiation on HS adsorption under continuous flow conditions

in order to provide information for the large-scale applications; these results are then presented.

To date, the work presented in this thesis is the first to examine a combination of solar irradiation and GAC adsorption to improve the removal of HS. It is useful to compare findings in this study with relevant external researches so as to enable a theoretical assessment of the proposed method. A comparison of results from different researchers is presented in Chapter 6.

Finally, in Chapter 7, conclusions are drawn based on the findings throughout the experimental work. Several suggestions that would require more attention for future work are also made.

## CHAPTER 2

### LITERATURE REVIEW

#### 2.1 Introduction

Health and safety concerns with respect to the presence of humic substances (HS) in water supply are arising. In this chapter, a literature review is carried out as background work to explore the potential for using solar irradiation to enhance the removal of HS. Topics reviewed on HS are composition and structure, bulk characterization, as well as the role of HS in disinfection by-product (DBP) formation. Recent findings on the changes of HS due to irradiation are discussed, together with a description of solar spectrum, applications of sunlight in water treatment and solar technologies with respect to the development of solar collectors. Additional interest is also given on the granular activated carbon (GAC) adsorption process, as it has been recommended as one of the best available methods to remove HS and can potentially be combined with solar irradiation. Finally, other available water treatment processes in terms of HS removal are briefly reviewed.

#### 2.2 Humic substances

##### *2.2.1 A brief review of HS*

HS are the dominant group of natural organic matter (NOM) and are ubiquitous in aquatic and terrestrial environments (Thurman, 1985). They are developed

randomly from the decomposition and transformation of plant tissues or animal residues (MacCarthy, 2001). Terrestrial streams continuously carry HS through soils and eventually into water bodies. The soils of watersheds, especially pH values, mineral composition and cations directly affect the amount and composition of aquatic HS (Hayes and Clapp, 2001). Environmental conditions, such as climate, biosphere and geography, also greatly influence the properties of HS (Piccolo, 2001). The concentration and distribution of HS vary for different water sources. For example, ground water and sea water have the lowest dissolved organic carbon (DOC) concentration of HS, while tea-coloured rivers or dystrophic lakes may contain HS of 30 mg DOC/L or greater. An extensive review has been carried out by Thurman (1985) and a summary of the representative data is presented in Table 2.1.

**Table 2.1** DOC concentration and distribution of HS in natural waters (Thurman, 1985).

Water source	DOC of HS (mg/L)	HS of total DOC (%)
Lake water	0.5-5	40
River water	0.05-10	50
Ground Water	0.03-0.1	25
Sea Water	0.06-0.6	25
Wetland	10-50	75

HS are considered to be a complex mixture of organic compounds of highly heterogeneous nature. The elemental contents of HS are Carbon (C), Hydrogen (H) and Oxygen (O) as well as a small percentage of Nitrogen (N), Sulphur (S) and other constituents (Rice and MacCarthy, 1991). The major functional

groups in HS are carboxylic and phenolic groups. The presence of functional groups is very important with respect to the behaviour of HS in the environment and during water treatment. Negative charges of HS, solubility, binding metal ions and organic contaminants, as well as adsorption onto mineral surfaces are all related to functional groups (Chen *et al.*, 2002). Despite extensive studies on elemental contents, functional groups and physicochemical reactions, little is known about the actual structure of HS to date. It is traditionally accepted that HS are polymers constituted of aromatic or aliphatic units with a diverse array of functional groups. The distribution of functional groups and arrangement of molecules vary from macromolecule to macromolecule, but the overall chemical characteristics are not sufficiently different to allow HS to be separated to individual components on a chemical basis (Summers and Roberts, 1988a). The macromolecular self-association of relatively small molecules through weak binding forces such as van der Waals forces, charge transfer, hydrophobic interactions and hydrogen bonding also complicates the HS analysis (Summers and Roberts, 1998a; Piccolo, 2001). Some models have been suggested to assist the understanding of HS structures and two of them are presented in Figures 2.1 and 2.2.

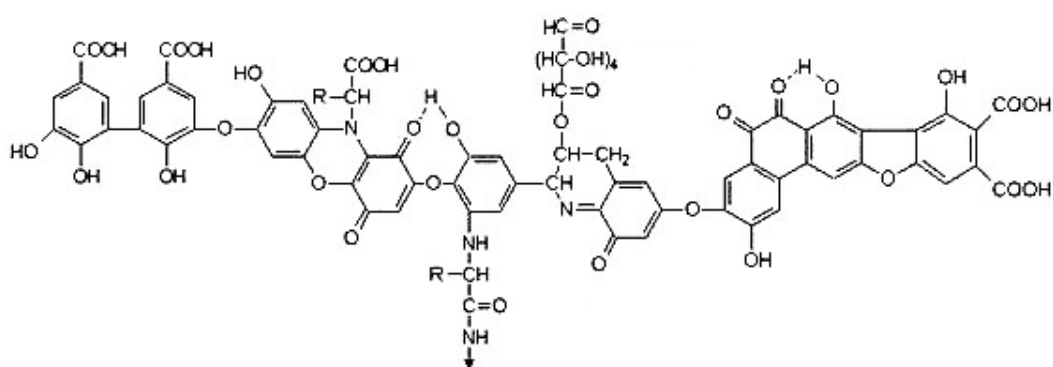


**Figure 2.1** Proposed structure of humic acid (Stevenson, 1982).

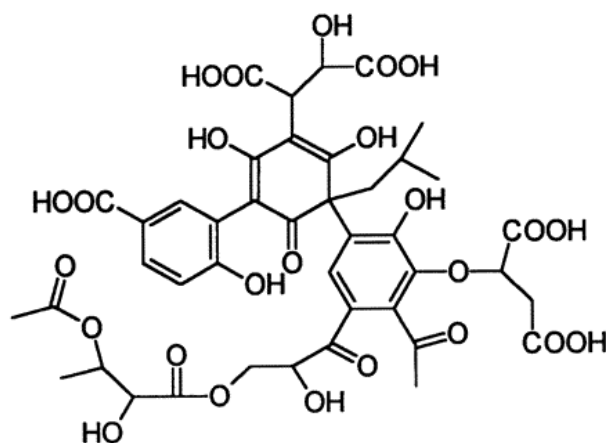


**Figure 2.2** Proposed structure of fulvic acid (Leenheer *et al.*, 1998).

**Table 2.2** Physicochemical characteristics of HS (Reckhow *et al.*, 1990; Karanfil *et al.*, 1996a).

HS	Aromaticity (%)	Carboxylic acidity (meq/g)	Phenolic acidity (meq/g)	M <sub>w</sub> <sup>a</sup> (Da)
Ohio River HA	34	3.8	1.5	9.0 Å <sup>b</sup>
Ohio River FA	14	5.0	1.0	5.5 Å
Laurentian HA	33.4	8.9	5.7	3982
Laurentian FA	28.2	11.7	9.3	2402
SRFA <sup>c</sup>	24.8	8.1	3.3	1920
AHA <sup>d</sup>	57.7	7.9	3.6	4006

M<sub>w</sub>: Weigh-average molecular weight

Å: Molecular size 10<sup>-10</sup> m

SRFA: Suwannee River fulvic acid

AHA: Aldrich humic acid

A classic definition is to divide soluble HS into humic acid (HA) and fulvic acid (FA) based on their solubility in water as a function of the pH value of the extraction medium (MacCarthy, 2001). HA is the fraction that is not soluble at

pH lower than 2, but soluble at higher pH. The fraction that can dissolve at all pH values is FA. In general, FA accounts for a larger fraction than HA in natural waters, whereas in soils the HA content is higher than the FA content (Nikolaou and Lekkas, 2001). Table 2.2 presents a summary of the physiochemical data of FA and HA from different sources (Reckhow *et al.*, 1990; Karanfil *et al.*, 1996a).

From the above data and graphs, it can be seen that HA is generally of higher molecular weight (MW) and a lower proportion of oxygen containing functional groups compared to FA. It has been revealed that FA has large relatively immobile aliphatic structures with many carboxylic groups and HA has a high aromaticity with many carbonates and phenolic groups (Cook and Langford, 1998). Chen *et al.* (2002) reported that soil derived HS have a relative abundance of aromatic functional groups compared to aquatic HS while the latter possesses more carboxylic functional groups compared to the former. From the data in Table 2.2, it is clearly seen that HA and FA isolated from various sources exhibit different characteristics, confirming the heterogeneous nature of HS. As a result, the reactivity and treatability of HS may differ from source to source when looking at water treatment processes. AHA and SRFA are commonly used as reference materials in HS research, enabling inter-laboratory comparisons under different experimental conditions.

### 2.2.2 Bulk characterization of HS

The amorphous mixture nature makes it impossible to characterize a unique fraction of HS. Therefore, characteristic data of HS obtained by current techniques refer to average properties (MacCarthy, 2001). Likewise, due to the complexity of HS, a single analytical method can only yield data of limited usefulness (Peuravuori and Pihlaja, 1997; Chen *et al.*, 2002).

### 2.2.2.1 Ultraviolet and visible light absorbance

Absorption of ultraviolet (UV) or visible irradiation by organic molecules corresponds to the excitation of electrons and is related to certain functional groups. HS contain a variety of chromophores absorbing light of a wide wavelength range found in the solar spectrum. The most prominent chromophores are aromatic structures and conjugated bonds.

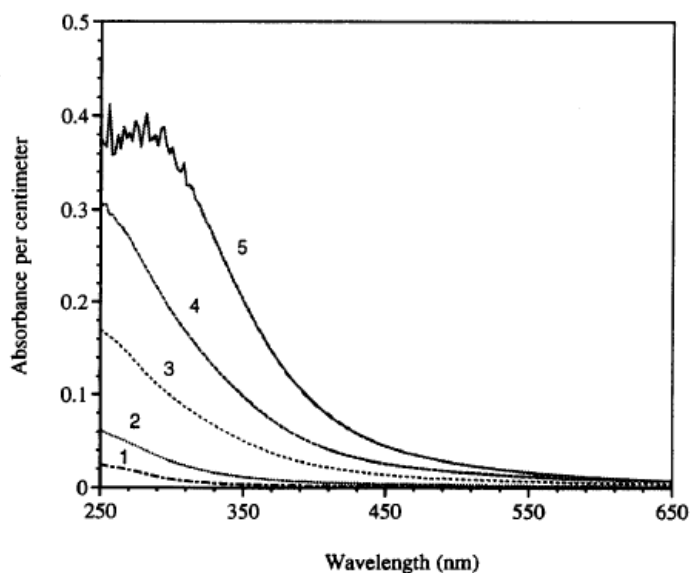


**Figure 2.3** UV/visible spectra of several lake waters with different DOC of HS (Zuo and Jones, 1997).

In the visible range (400-800 nm), HS absorb mostly the short wavelength part of light. The typical yellow-brown colour of natural water is a consequence and a raw correlation between colour and humic content or MW exists (Wang *et al.*, 1990; Hautala *et al.*, 2000). Absorbance at wavelengths between 400 nm and 465 nm has been recommended for measuring the colour of HS (Bennett and Drikas, 1993; Hautala *et al.*, 2000).

In the UV range (200-400 nm), unlike many other organic compounds, HS do not exhibit distinguishable peaks when scanned with a UV spectrophotometer. Instead, a smooth increase of absorbance with decreasing wavelength is observed. An example of this is given in Figure 2.3, which shows a gradually decreasing absorbance as the wavelength increases. This observation is explained by the existence of numerous high energetic bonds and aromatic rings which do not have distinguishable absorption spectra.

**Table 2.3** A summary of the applications of UV-visible spectroscopy to characterize HS.

Wavelength	Correlative properties	References
254 nm	DOC, HS content, aromaticity, formation of DBPs	Dobbs <i>et al.</i> , 1972; Reckhow <i>et al.</i> , 1990; Deflandre and Gagne, 2001; White <i>et al.</i> , 2003 ; Ates <i>et al.</i> , 2007
400, 410, 456, 465 nm	Colour	Bennett and Drikas, 1993; Hautala <i>et al.</i> , 2000
272 nm	Aromatic rings, formation of DBPs	Li <i>et al.</i> , 1998; Korshin <i>et al.</i> , 2002
280 nm	MW	Chin <i>et al.</i> , 1994; Peuravuori and Pihlaja, 1997
250/365 nm ( $E_2^*/E_3$ )	Aromaticity, MW	Peuravuori and Pihlaja, 1997; Chen <i>et al.</i> , 2002
465/665 nm ( $E_4/E_6$ )	Humification, MW, aromaticity	Thurman, 1985; Chin <i>et al.</i> , 1994; Schmitt-Kopplin <i>et al.</i> , 1998

\* E is the absorbance.

The light absorbing properties are of great importance in characterizing HS. A summary of some applications of UV-visible spectroscopy from different researchers is given in Table 2.3. Among them, UV absorbance at 254 nm ( $UV_{254}$ ) is singled out as the most commonly used parameter for characterizing HS; this is due to the fact that it is a highly specific indicator of aromatic and conjugated character of organics, and also convenient to measure.

#### 2.2.2.2 Organic carbon content

Another surrogate parameter, widely used for characterizing HS, is DOC concentration, which is measured instead of total organic carbon (TOC) by passing the solution through a 0.45  $\mu\text{m}$  membrane filter (Standard Methods for the Examination of Water and Wastewater, 1998). A good correlation has been obtained between  $UV_{254}$  and DOC (with an  $R^2$  value of 0.93) from data collected from a number of water sources and references, as illustrated in Figure 2.4. In general, the higher the DOC, the higher the  $UV_{254}$  value is. It should be noted that this observation is based on data collected from a variety of untreated water samples. After physicochemical treatment, changes in  $UV_{254}$  and DOC of HS will differ. For example, some non-humic fractions which are available for biodegradation may account for DOC concentration but absorb little UV. As a result, one might observe no decrease in  $UV_{254}$  after treatment, although these fractions may have been utilised by bacteria.

The ratio of  $UV_{254}$  and DOC can be used to evaluate the relative change. This ratio is called specific UV absorbance (SUVA) and is often used as an indicator of the aromatic carbon content of HS (Weishaar *et al.*, 2003; Singer, 1999). The higher the SUVA value, the more aromatic the HS are. Edzwald and Tobiason

(1999) have related the SUVA value with hydrophobicity and hydrophilicity of HS. Generally, the SUVA value is higher for HS with high hydrophobicity.

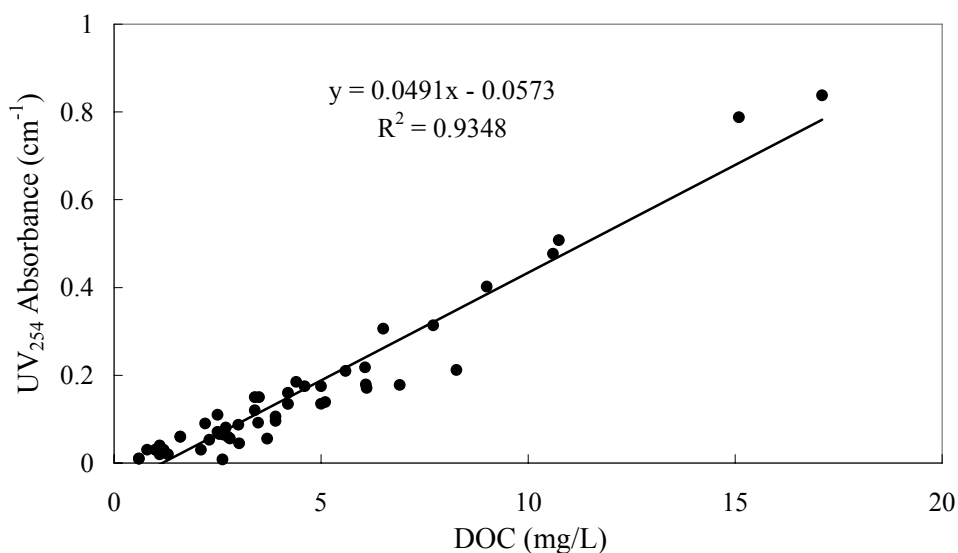


**Figure 2.4** Relationship between DOC and UV<sub>254</sub> for a variety of water samples (Collins *et al.*, 1986; Chow *et al.*, 1999; Nokes *et al.*, 1999; Bergamaschi *et al.*, 2000; Volk *et al.*, 2000; Singer and Bilyk, 2002; Chow *et al.*, 2008).

### 2.2.2.3 Molecular size

The size of humic molecules is an important characteristic of HS. It has been found that the molecular size is related to nearly all physicochemical aspects of HS, such as DBP formation (Reckhow *et al.*, 1990), coagulation efficiencies (Ratnaweera *et al.*, 1999), complexation of metals (Leenheer *et al.*, 1998), adsorption of HS onto mineral and carbon (Kilduff *et al.*, 1996; André, 2006), and partitioning of organic pollutants. The size of organic molecules has been shown to be directly proportional to the MW (Cornel *et al.*, 1986) and therefore commonly represented as MW. An illustration of the effects of MW on HS

properties and reactivity is adapted from Cabaniss *et al.* (2000) and shown in Figure 2.5.

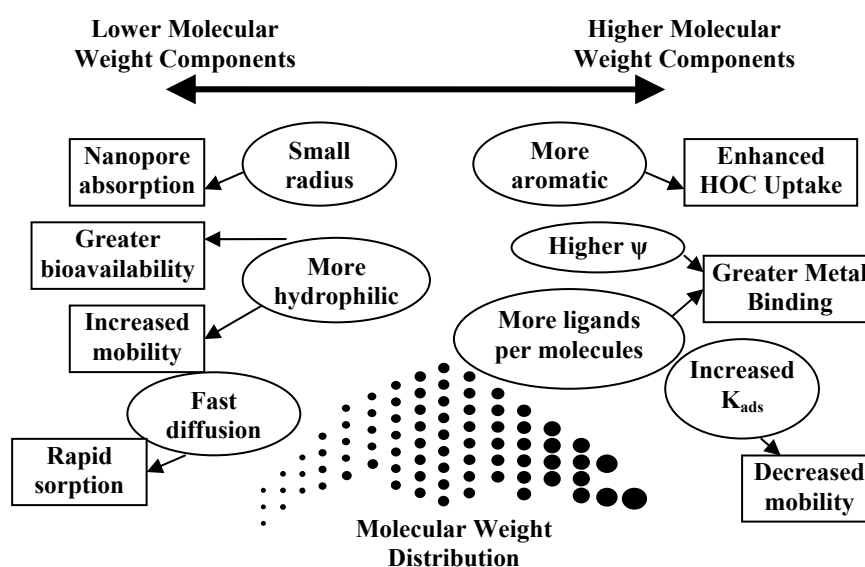


**Figure 2.5** Effect of MW on HS properties and reactivity (Cabaniss *et al.*, 2000).

Literature values indicate that the MW of HS can vary from a few hundreds to more than  $1 \times 10^6$  Dalton (Da). Recent research shows that HA has an average MW in the range of 2,000-5,000 Da and FA has an average MW varying from 500 to 2,000 Da (Thurman, 1985). Recently, the measurement of molecular size has been widely conducted by means of high performance size-exclusion chromatography (HPSEC). This technique is based on different accessibility of molecules of various sizes into the column pores. As a HS sample passes through the column, smaller components are relatively easily accessible to the column pores thus have a longer retention time. Consequently, large components will elute earlier from the column than small ones (Chin *et al.*, 1994). HPSEC analysis is carried out without pre-isolation of aquatic HS and requires only a small amount of sample (less than 5ml) as well as a short running time (normally 10 to 20 minutes).

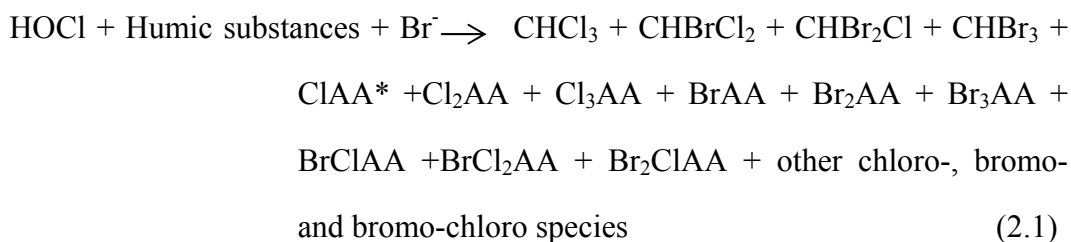
Commonly employed HPSEC columns for HS analysis are TSK, Protein-Pak and Biosep columns, all packed with silica gels (Chin *et al.*, 1994; Peuravuori and Pihlaja, 1997). Conte and Piccolo (1999) compared the performance of Biosep and TSK columns on the MW determination of HS. They found that both TSK and Biosep columns can adequately be used to monitor relative changes in MW but values are not absolute.

HPSEC can simultaneously provide number average molecular weight ( $M_n$ ), weight average molecular weight ( $M_w$ ) and polydispersity ( $\rho$ ) by using polystyrene sodium sulphonates (PSS) standards to calibrate the column (Chin *et al.*, 1994; Pelekani *et al.*, 1999). Salicylic acid and acetone are sometimes used as low MW standards (Karanfil *et al.*, 1996a; Zhou *et al.*, 2000). Baseline corrections, MW cutoffs (MWCOS) of the chromatogram, and UV detection wavelength can also influence the MW determination (Zhou *et al.*, 2000).

Other characterization techniques include Fluorescence Emission Spectrometry, Fourier Transform Infrared Spectroscopy (FTIR), Nuclear Magnetic Resonance (NMR) and Electron Paramagnetic Resonance (EPR) (Nikolaou and Lekkas, 2001; Chen *et al.*, 2002).

### 2.2.3 HS as precursors for chlorination by-products

Since the early work of Rook (1974), HS have been strongly implicated as principle precursors for carcinogenic DBPs during chlorination of drinking water and this has led to much attention paid on the adverse aspects of HS on drinking water safety. HS react with chlorine to produce trihalomethanes (THMs), haloacetic acids (HAAs) and some other by-products. An equation to model the reaction of HS with chlorine is (Singer, 1999):



\* AA: acetic acids

A number of factors can control the extent of DBP formation, such as temperature, pH, bromide (Br) content, amount and characteristics of HS (Ye *et al.*, 2009). For example, the formation of THMs and HAAs increases with increasing temperature, so DBP levels would be higher during the warmer months of the year (Singer, 1999), which could be a plausible reason in this study to make use of sunlight for HS removal so as to control the DBP formation.

Among these factors, characteristics and concentrations of HS have been found to have the major influence on the DBP formation and many studies have reported a simple and reliable correlation between surrogate parameters of HS and DBP formation (Korshin *et al.*, 1997; Kitis *et al.*, 2001; Weishaar *et al.*, 2003). White *et al.* (2003) found that  $\text{UV}_{254}$  is a good indicator for DBP formation, whereas DOC is less correlated to DBP formation. Reckhow *et al.* (1990) and Singer (1999) reported that DBP production correlates well with SUVA and aromatic carbon content. Representative results are shown in Figure 2.6. The good correlation between SUVA or  $\text{UV}_{254}$  and DBP formation potential can possibly be explained by the fact that the electron-rich sites of HS, including activated aromatic structures and conjugated bonds, are primarily attacked by chlorine (Ates *et al.*, 2007). Collins *et al.* (1986) observed that the reactivity of HS in forming THMs varies as a function of MW. That is, THM formation increases with increasing MW.

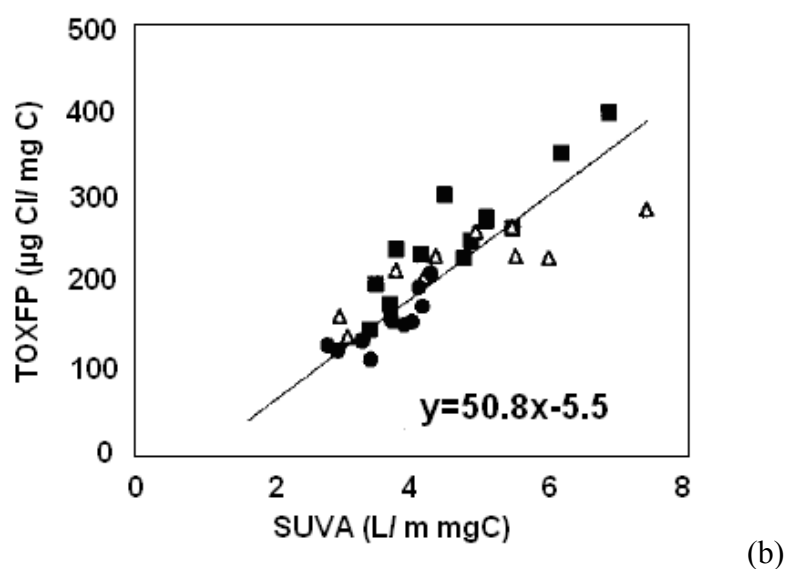
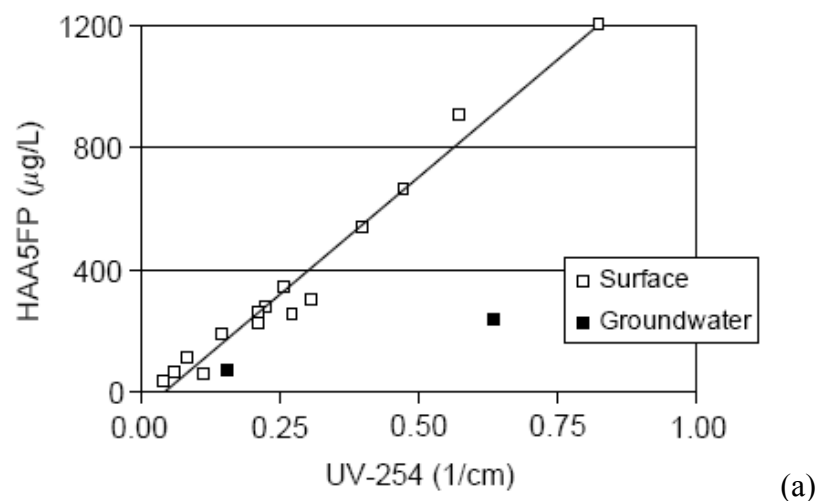


**Figure 2.6** Relationship between (a) DBP formation and  $UV_{254}$  (White *et al.*, 2003); and (b) DBP formation and  $UV_{254}$  (Singer, 1999).

It should be noted that the good correlations reported above are for a single water with a high humic content in each study. HS characteristics may vary significantly depending on water sources, leading to different DBP formation potentials. Goslan (2003) found that when a range of water sources that did not have a high humic content were investigated, the correlations between water characteristics and THM formation were very weak. Jung and Son (2008)

reported that the THM formation potential for raw waters with high aromaticity showed high correlations with SUVA while raw waters with low aromaticity had low correlations with SUVA.

It can therefore be concluded that, for a specific set of water system, in particular, a water source with a high humic content, the key correlations are:

- The higher the  $UV_{254}$ , the more DBP will be formed;
- The higher the SUVA, the higher the aromaticity, and the more DBP will be formed;
- The higher the MW, the more DBP will be formed.

Thus, to control the DBP formation of a water that contains a large amount of HS, potentially one should give priority to reducing the aromaticity,  $UV_{254}$ , SUVA and MW of humic waters and hence reduce the concentration of precursors.

## **2.3 Sunlight in water treatment**

### *2.3.1 Solar irradiation as source of energy*

The sun is the most freely available and renewable energy source on the earth. The earth receives  $1.7 \times 10^{14}$  kW energy ( $1.5 \times 10^{18}$  kWh per year) coming from the sun, which is approximately 28,000 times the consumption of the entire world during that period (Rodríguez, 2003). Solar irradiation outside the atmosphere has wavelengths from 0.2  $\mu\text{m}$  to 50  $\mu\text{m}$ . Due to the absorption, scattering and reflection by different components in the atmosphere, such as ozone, oxygen,

clouds and aerosols, the irradiation is attenuated to wavelengths between 0.3  $\mu\text{m}$  and 3  $\mu\text{m}$  when reaching the earth surface.

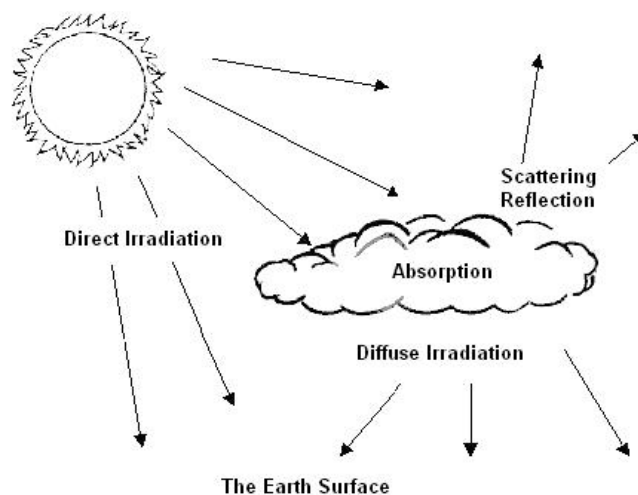


**Figure 2.7** Diffuse and direct solar irradiation (Rodríguez, 2003).

Global irradiation is composed of direct and diffuse irradiation (Figure 2.7). Direct irradiation is the irradiation which reaches the earth without being absorbed or reflected in the atmosphere. Diffuse irradiation is the irradiation that has been dispersed in the atmosphere and reaches the ground level at random directions. The total direct irradiation in clear days is at its maximum and the diffuse irradiation is at its minimum. The opposite situation is in cloudy days.

### 2.3.1.1 Solar spectrum

The solar spectrum is commonly divided into various regions (or bands) and sub-regions on the basis of wavelength (Figure 2.8). The chemical and biological reactivity, as well as the photon energy of sunlight components, increase with the wavelength decreasing from longer to shorter. UV-C is commonly referred to as the germicidal irradiation of the highest energy that can

alter DNA molecules and cause cell death. A prolonged exposure to UV-B irradiation can lead to sunburn and skin cancer. UV-A is considered less harmful but can indirectly distort DNA molecules of living organisms by producing highly reactive chemical radicals such as hydroxyl radical. The visible spectrum of sunlight can be detected by human eyes by colours (Figure 2.8). Visible irradiation is considered less or non-harmful to living organisms. Visible light in the violet and blue bands from 400 to 500 nm has higher frequency and energy than the light in other bands, which is also called high-energy visible light.

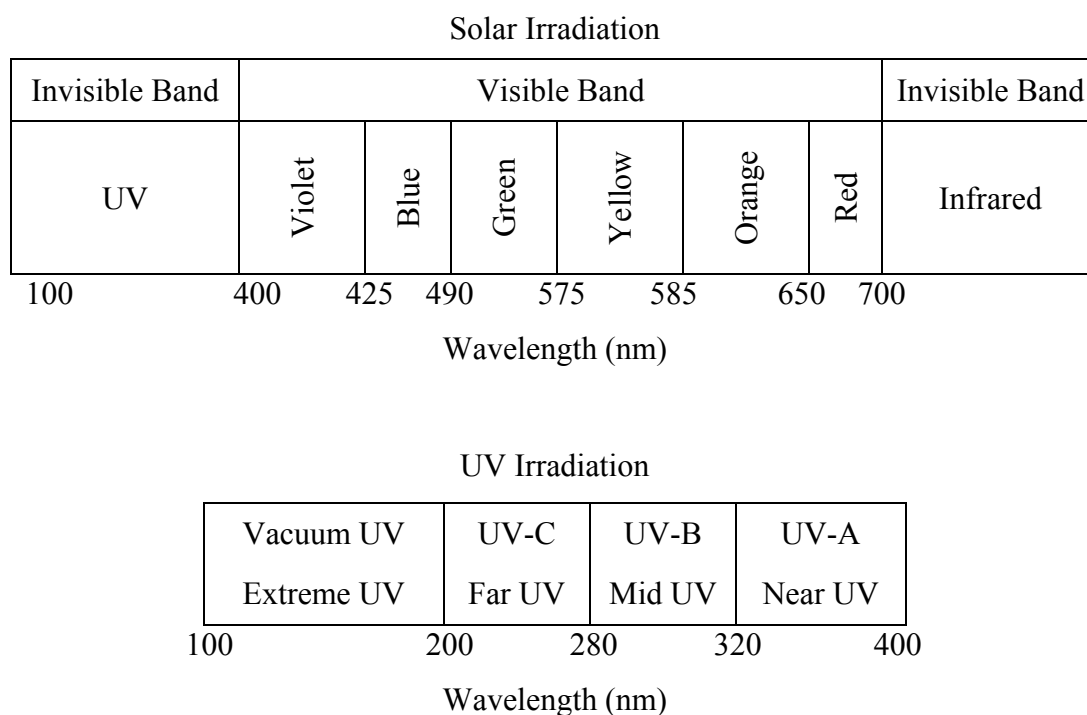


**Figure 2.8** Distribution of the components of sunlight.

A standard sunlight spectrum (ASTM, 1992) is presented in Figure 2.9. The standard spectrum represents the solar irradiation on the earth surface in a clear day. It is clearly seen that UV irradiation only accounts for a very small

proportion of the solar spectrum, with only up to 4 % of the total solar energy (Corin *et al.*, 1998). This is because, when passing through the atmosphere, all UV-C irradiation and 90 % of UV-B irradiation are absorbed by ozone, or other atmospheric components, while UV-A irradiation is less affected by the atmosphere. Consequently, the UV irradiation reaching the earth's surface is largely UV-A and only a small amount is UV-B (World Health Organisation, WHO). The solar intensity and the UV level vary with time of day and time of year. They are also affected by latitude, altitude, thickness of ozone layer and weather conditions (WHO). This variability makes it of great importance to measure solar data on-site and at real time, with respect to the experiments that will be discussed in chapter 5.

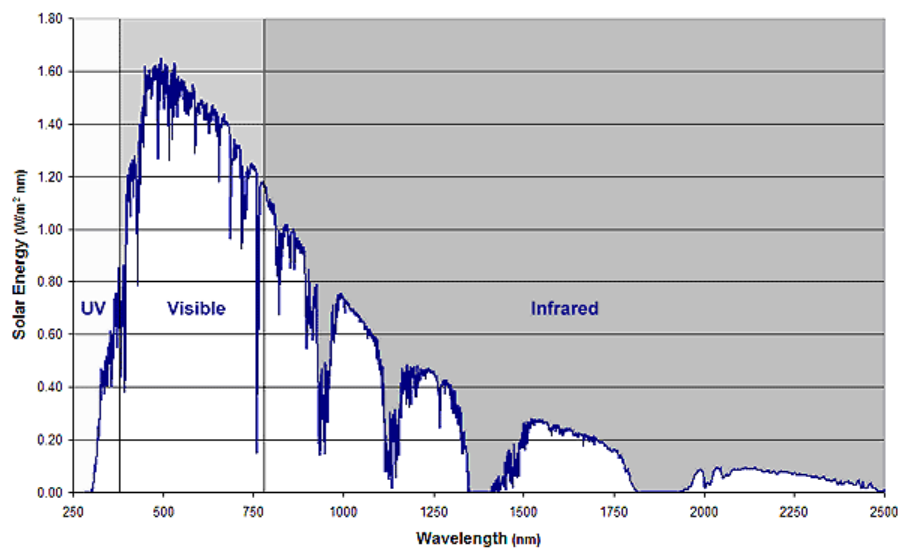


**Figure 2.9** Solar spectrum of the direct irradiation on the ground level on a clear day (ASTM, 1992). ( $\text{W/m}^2 \text{ nm}$  is the unit of irradiation intensity of each wavelength)

### 2.3.1.2 World distribution of solar irradiation

The distribution of solar irradiation all over the world varies from one location to another depending on geographic conditions, season, and time of day. According to Acra *et al.* (1984), the global geographic distribution of solar irradiation is generally divided into four belts. A brief description with respect to the northern hemisphere is given by Acra *et al.* (1984):

- The most favourable belt (15-35 °N). This region has the greatest amount of sunlight and is most favourable for solar energy applications because of limited rainfall and cloud coverage. The sunshine duration is on average 3000 h/year. Many of developing countries in northern Africa and southern Asia are within this region.

- The moderately favourable belt (0-15 °N). This region has high humidity and frequent cloud coverage. There is usually 2500 h of sunlight per year. The solar intensity all over the year is relatively uniform due to the slight seasonal variations.

- The less favourable belt (35-45 °N). The average solar irradiation intensity is similar to that of the above two regions. Nevertheless, there are significant seasonal variations in solar intensity and daylight hours in this region. Moreover, cloudiness and atmospheric pollution significantly reduce the solar intensity.

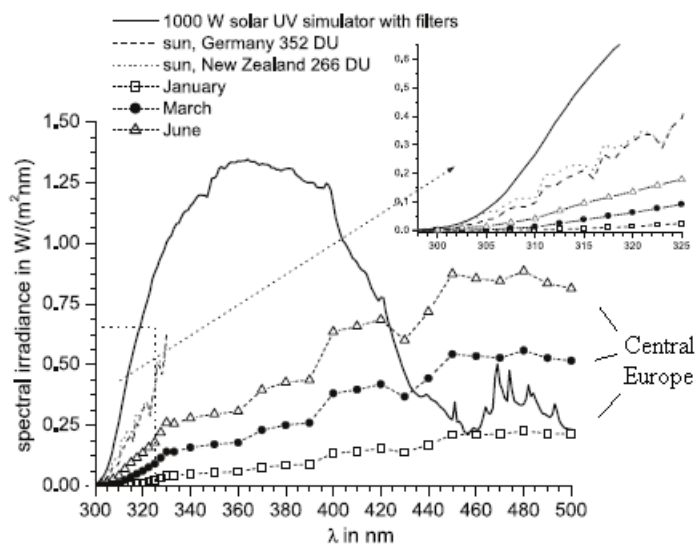
- The least favourable belt (45 °N and above). Most parts of North America and northern Europe are located within this belt. Due to the higher latitude and lower solar altitude, half of the total irradiation is diffuse irradiation, with a relatively higher proportion in winter.

London (with latitude around  $51^\circ$ ) is located within the least favourable belt. The weather in London features a mixture of sunshine, cloudiness and wetness. During winter months, daylight hours are short and solar intensity is low. In the summertime, there are more sunny days, with frequently rain and cloud. Despite this, the absence of published information (regarding the use of solar irradiation, and in particular under natural conditions, as a pre-treatment method prior to GAC adsorption to remove HS from water) encouraged a series of investigations to be carried out in London. This research could provide important information to those areas with more favourable conditions for solar applications.

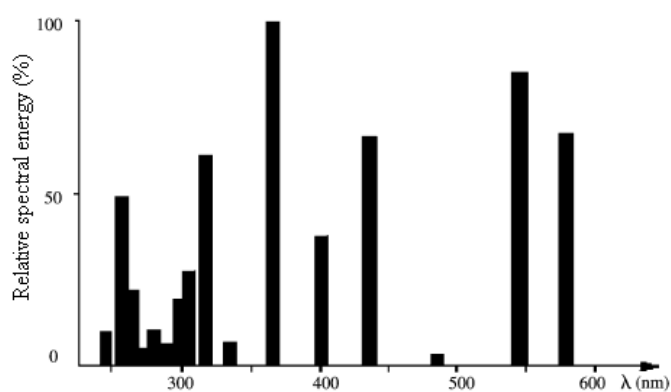
### 2.3.1.3 Natural sunlight vs. solar simulator

The solar spectrum contains all wavelengths that can be found in the emission from different lamps used in laboratory studies. Figure 2.10 shows two examples of the spectral distribution and irradiation of a mercury lamp and a solar simulator that were used for HS photodegradation studies in the lab (Doll and Frimmel, 2003; Patel-Sorrentino *et al.*, 2004). A comparison between Figure 2.9 and Figure 2.10 clearly demonstrates the difference in spectral distribution between simulated light and natural sunlight. The intensity of artificial light in the UV range which is more effective in photooxidation is much higher than that in natural sunlight. Patel-Sorrentino *et al.* (2004) reported that the photon energy from a mercury lamp (Figure 2.10b) was approximately 30 times greater than the solar photon energy. In the work by Chow *et al.* (2008), it was estimated that an exposure of 24 h in the solar simulator is equivalent to 4 days of full, clear and sunny day exposure. This implies that the photodegradation process under natural sunlight would be much slower than that observed under artificial light. Figure 2.10a also shows the sunlight spectral irradiation in different regions, including central Europe for different months of a year (January, March and

June), New Zealand and Germany. As it can be seen, solar intensity varies depending on season and location, as well as time of day. Therefore, lab studies using the simulated sunlight only provide useful information to understand the photodegradation of HS within a short period. However, under natural sunlight conditions, solar intensities are not as constant as those under artificial light. If solar irradiation is to be used as the energy source for application purposes, more investigations should be conducted under natural sunlight and this is one of the main drives for the research work presented in this thesis.



(a)



(b)

**Figure 2.10** Examples of the spectral distribution and irradiation of (a) a solar simulator (Doll and Frimmel, 2003) and (b) a mercury lamp (Patel-Sorrentino *et al.*, 2004) used in HS photodegradation studies.

### 2.3.2 Photodegradation of HS

HS contain many chromophoric groups that absorb irradiation at both UV and visible wavelengths. In natural environments, HS are the main light absorbing constituent of natural water. The yellow-brown to black colour of natural waters is the consequence of light absorbing. The absorption of light by these chromophores leads to structural modification and gradual decomposition, which is known as photodegradation (Rodríguez-Zúñiga *et al.*, 2008).

#### 2.3.2.1 Photodegradation process

Photodegradation of HS by solar irradiation involves the formation of excited states and highly reactive species, such as singlet oxygen ( $^1\text{O}_2$ ), hydrogen peroxide ( $\text{H}_2\text{O}_2$ ), hydroxyl radical ( $\cdot\text{OH}$ ), superoxide ( $\text{O}_2^-$ ), and hydrated electrons ( $e^-_{\text{aq}}$ ) (Frimmel, 1994; Thomas-Smith and Blough, 2001; Goldstone *et al.*, 2002; Paul *et al.*, 2006). The excited states decay rapidly. The reactive species are powerful oxidants that can react fast with numerous organic components present in water. It has been found that pH, metals and compositions of HS affect the production of oxidant radicals.

Photodegradation by solar irradiation has been suggested to proceed via both direct and indirect photochemical pathways (Goldstone *et al.*, 2002). Absorption of photons by chromophores can directly result in a rapid rearrangement or breakdown of chromophoric structures and formation of non-chromophoric photoproducts. Consequently, the loss of absorbance is higher at the spectral output of the irradiation source (Del Vecchio and Blough, 2002; Parkinson *et al.*, 2003). An example is presented in Figure 2.11, which clearly shows that the biggest loss in absorbance occurred with chromophores at the irradiation

wavelength. The loss of absorbance over the entire spectrum can be attributed to the indirect photodegradation. The excited chromophores might act as precursors (sensitizers) for the production of reactive species which can oxidize both UV and non-UV absorbing chromophores. Therefore, if direct photoreactions dominate, the rate of photodegradation will be proportional to the amount of light absorbed by HS. If indirect photoreactions also play an important role, photodegradation of humic compositions which are not chromophoric may occur (Goldstone *et al.*, 2002).

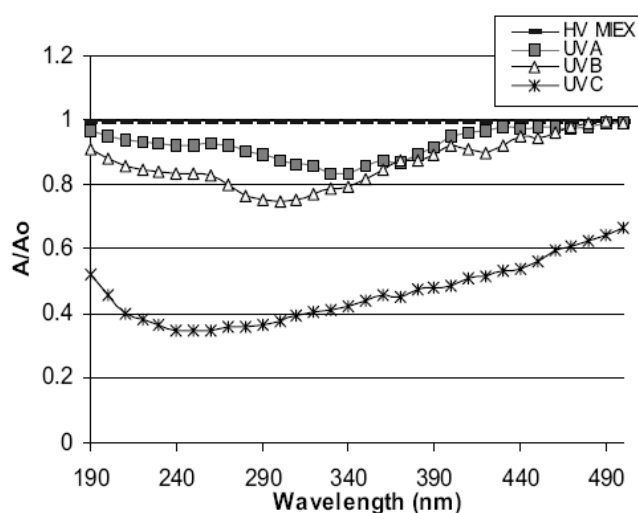


**Figure 2.11** Relationship between irradiation and absorbance removal (Parkinson *et al.*, 2003).  $A$  is the absorbance.

### 2.3.2.2 Effects of irradiation on properties of HS

Following the absorption of irradiation, a series of photoreactions occur in HS, leading to photobleaching (Allard *et al.*, 1994; Reche *et al.*, 1999; Chow *et al.*, 2008), DOC loss (Corin *et al.*, 1996; Patel-Sorrentino *et al.*, 2004), MW decrease (Frimmel 1998; Lou and Xie, 2006), production of CO, CO<sub>2</sub> and low MW organic compounds (Zuo and Jones, 1997; Brinkmann *et al.*, 2003; Lehtola

*et al.*, 2003; Xie *et al.*, 2004), which in turn influence the physical, chemical and biological aspects of HS.

*Photobleaching* – Photobleaching is a result of the destruction of chromophores (i.e. breakdown of aromatic structures or conjugated bonds), reflected by a loss of absorbance. However, irradiation does not affect all chromophores in HS to the same extent, as a result, a nonuniform loss of absorbance across the entire wavelength range is observed using a spectrophotometer. Figure 2.11 is a good example to illustrate this from Parkinson *et al.* (2003). Del Vecchio and Blough (2002) who studied irradiation of humic samples using irradiation at different wavelengths found that the largest losses in absorbance always occurred at the irradiation wavelength. A non-uniform loss in absorbance (200-550 nm) was also observed by Rodríguez-Zúñiga *et al.* (2008). Corin *et al.* (1997) found that the UV<sub>254</sub> absorbance decreased more rapidly than the absorbance at 460 nm for a lake water sample under UV irradiation, suggesting that the chromophores absorbing in the UV range are less stable against the radical attack than the chromophores responsible for the yellow colour of natural humic waters. Results from these studies imply two effects: (1) the primary photoreaction of chromophores that match the irradiation wavelength, and (2) the secondary photodegradation of chromophores with reactive species generated from the primary photoreaction. This corresponds to the direct and indirect photodegradation pathways as previously described.

Due to the heterogeneous nature of HS, a comparison of the removal of HS by different researchers is difficult unless exactly the same light source and HS samples are used. The light irradiance is commonly expressed as the light ‘intensity’ in W/m<sup>2</sup>, or the light ‘dose’ in kJ/m<sup>2</sup>, which is determined from the intensity and the irradiation time. Published work however shows that

irradiation could result in  $UV_{254}$  reduction of HS, as presented in Table 2.4.  $UV_{254}$  absorbance is a commonly used surrogate to evaluate the irradiation effect on HS properties. The available data demonstrate that:

- (1) the removal of  $UV_{254}$  is dependent on HS characteristics as well as irradiation wavelengths and intensities;
- (2) for the same water, the reduction of  $UV_{254}$  increases with increasing irradiation.

**Table 2.4** Irradiation effects on the  $UV_{254}$  removal of HS (Allard *et al.*, 1994; Corin *et al.*, 1998; Hongve, 1998; Goslan *et al.*, 2006; Chow *et al.*, 2008).

	Irradiation		$UV_{254}$ absorbance		References	
	Source	Intensity	Duration (h)	Initial ( $cm^{-1}$ )		Removal (%)
Aquatic FA	UV lamp at 254 nm	16 $W/m^2$	12	N/A	95	Allard <i>et al.</i> , 1994
Soil HA			58	N/A	95	
Lake water	UV lamp at 254 nm	0.42 $W/m^2$	8	0.816	31	Corin <i>et al.</i> , 1998
			168		85	
Reservoir water	UV lamp at 254 nm	34 $W/m^2$	90	0.536	85	Goslan <i>et al.</i> , 2006
Wetland water				0.306	25	
Drainage water	Solar Simulator	650 $W/m^2$	24	0.218	24	Chow <i>et al.</i> , 2008
Aqueduct water				0.087	38	
River water				0.053	35	

*DOC loss* – A summary of the published DOC removal data with respect to irradiation is presented in Table 2.5; it is shown that irradiation leads to a decrease in DOC concentration of HS. Contradictive findings to the listed research have been reported by Goslan *et al.* (2006) and Chow *et al.* (2008) who found that irradiation did not lead to any DOC change, possibly due to the high resistance of organics to complete mineralization. These results indicate that the removal of DOC is also greatly affected by the characteristics of both HS and irradiation source.

The decrease of DOC is attributed to the mineralization of dissolved organic molecules to CO, CO<sub>2</sub> and other inorganic dissolved organic matter. The CO and CO<sub>2</sub> are transferred into the atmosphere, leading to a direct loss of DOC (Zuo and Jones, 1997; Xie *et al.*, 2004).

When HS are exposed to irradiation under different types of atmosphere (oxygen, nitrogen and air), the DOC loss differs. Schmitt-Kopplin *et al.* (1998) found that the decrease of colour and TOC was much higher in the presence of oxygen compared to nitrogen. Patel-Sorrentino *et al.* (2004) and Xie *et al.*, (2004) reported a notable loss of DOC under oxygen (up to 46 %) and an extremely small DOC loss under nitrogen (2 %), while there was an insignificant difference in DOC loss between samples under oxygen and air atmospheres. These results, on one hand, suggest the consumption of oxygen in the photodegradation process of HS. Oxygen may act as an electron acceptor and a participant in secondary reactions to form photoproducts (Zuo and Jones, 1997; Patel-Sorrentino *et al.*, 2004). On the other hand, it seems likely that the quantity of oxygen in the air is sufficient to support the photodegradation process.

**Table 2.5** Irradiation effects on the DOC removal of HS (Allard *et al.*, 1994; Corin *et al.*, 1998; Hongve, 1998; Pullin *et al.*, 2004; Winter *et al.*, 2007; Rodríguez-Zúñiga *et al.*, 2008).

	Irradiation			DOC		References
	Source	Intensity	Duration (h)	Initial (mg/L)	Removal (%)	
Aquatic FA	UV lamp at 254 nm	16 W/m <sup>2</sup>	30	10	50	Allard <i>et al.</i> , 1994
			71		75	
Lake water	UV lamp at 254 nm	0.42 W/m <sup>2</sup>	8	17.7	19	Corin <i>et al.</i> , 1998
			168		42	
Pond water	Natural sunlight	157 W/m <sup>2</sup>	288	12	32	Hongve, 1998
Creek water	Solar simulator	750 W/m <sup>2</sup>	48	27.4	16	Pullin <i>et al.</i> , 2004
Lake water				7.0	10	
Pond water	Natural sunlight	N/A	312 (13d)	11.9	24	Winter <i>et al.</i> , 2007
Aldrich HA				10.9	26	
River water (winter)	Hg-Xe lamp at 290-475 nm	58 W/m <sup>2</sup>	48	11.2	68	Rodríguez-Zúñiga <i>et al.</i> , 2008
River water (summer)			48	10.9	79	

*MW decrease* – The reduction in UV<sub>254</sub> and DOC indicates the breakdown of certain structures and formation of photoproducts due to irradiation. This may in turn influence the MW, which is a key parameter on the physical, chemical and biological properties of HS. Some researchers have looked at the changes in

MW due to the photodegradation of HS, finding that following the absorption of light, there is a decrease in the average MW of HS (Lepane *et al.*, 2003; Buchanan *et al.*, 2005; Lou and Xie, 2006; Carvalho *et al.*, 2008). Representative HPSEC chromatograms of HS before and after irradiation are shown in Figure 2.12 (Lou and Xie, 2006). It can be seen that the total peak area of chromatograms decreased after irradiation, suggesting a decrease in the MW of the irradiated HS. One should keep in mind that the decrease in MW measured by HPSEC only represents the changes of chromophores, i.e. destruction of carbon double bonds or degradation of large components to smaller compounds which do not absorb light to the same extent as their parent molecules.

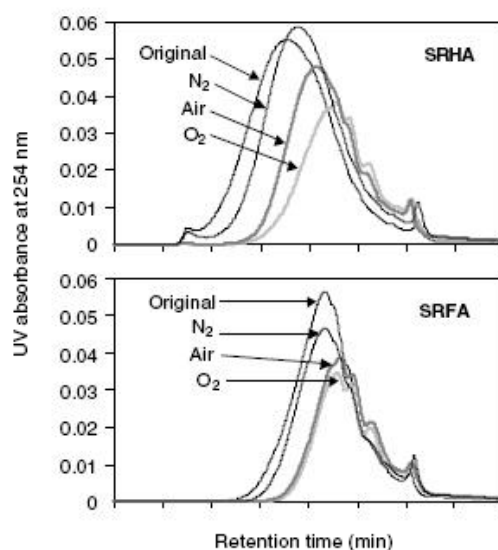


**Figure 2.12** HPSEC chromatograms of HS before and after irradiation under different atmospheres (Lou and Xie, 2006).

HS are a mixture of organic compounds with a wide range of MW. Changes in different MW fractions may vary, and therefore affect the overall MW. Studies on the reduction of MW fractions in HS have been performed on the fractionated HS or by means of HPSEC measurement. Carvalho *et al.* (2008) fractionated

FA samples into four MW fractions (>10, 10-5, 5-1 and <1 kDa) using ultrafiltration (UF). Following solar irradiation, the authors found a dramatic increase in the lowest MW fraction (<1 kDa) and a significant decrease in the fraction with MW >10 kDa. Buchanan *et al.* (2005) observed that the high MW hydrophobic molecules were susceptible to photoirradiation. As a result of photodegradation, non-UV absorbing and low MW hydrophilic molecules were formed. Lehtola *et al.* (2003) studied the changes in the MW by dividing HPSEC chromatograms into several fractions and making a comparison of each MW fraction before and after UV irradiation (Figure 2.13). As shown, the highest removal was observed in the fractions with large molecular size, especially in sample B where fractions 1, 2 and 3 were undetected in the chromatograms after irradiation. Changes in medium and small fractions varied. In contrast to an increase in fraction 5 of sample A, reductions in medium MW fractions were observed in the other two samples. The increase in the smaller fractions was more significant for samples A and B. It is apparent that the overall MW reduction is a result of the photodegradation of MW fractions. The photodegradability of different fractions varies within the same humic mixture and can also be affected by the raw water characteristics.

Moran and Zepp (1997) have suggested that four classes of degradation products of HS are formed during solar irradiation:

- (1) low MW organic compounds;
- (2) carbon gases (CO, CO<sub>2</sub> and other forms of inorganic carbon);
- (3) unidentified bleached organic matter; and
- (4) nitrogen- and phosphorus-rich compounds.

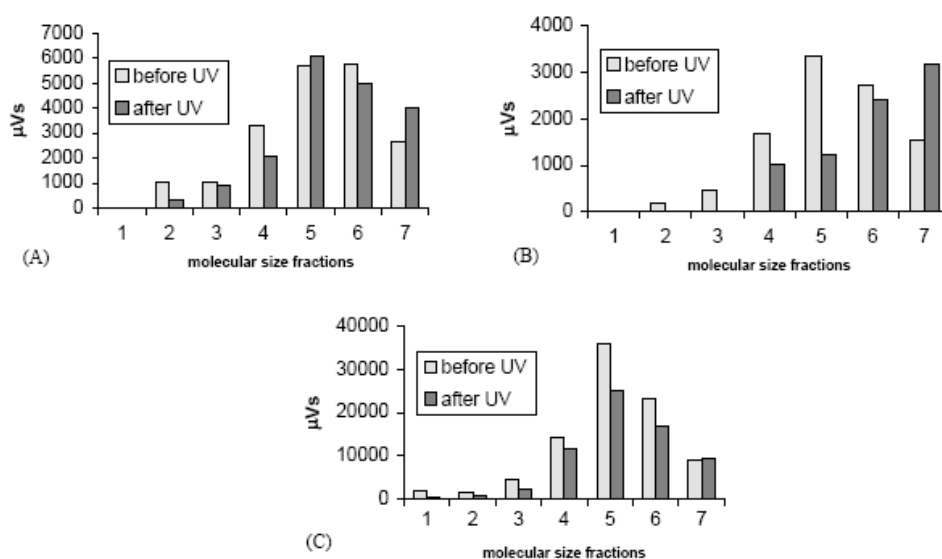


**Figure 2.13** MW fractions of different water samples before and after UV irradiation (Lehtola *et al.*, 2003). Samples A, B and C were raw waters from three Finnish waterworks. Samples A and B were ground waters and sample C was surface water. Numbering with decreasing order of MW.

All of the identified small organic photoproducts are carbonyl compounds, most of which have the MW less than 100 Da (Moran and Zepp, 1997). Decreases in pH values during irradiation have been observed (Corin *et al.*, 1996; Lepane *et al.*, 2003; Lou and Xie, 2006), which is a result of the photoproduction of small organic acids. The formation of photoproducts is consistent with the decrease in  $\text{UV}_{254}$ , DOC and MW. The physical and chemical characteristics of the irradiated HS are therefore different from the non-irradiated HS.

There is no doubt that UV irradiation in sunlight greatly affects the photodegradation of HS. However, it does not necessarily mean that UV irradiation is the only active irradiation for HS photodegradation. Several studies have suggested a less effective action of the violet and blue light (wavelengths between 400 and 490 nm) in the visible region with respect to the

removal of HS (Archibald and Roy-Arcand, 1995; Moran and Zepp, 1997; Frimmel, 1998; Lou and Xie, 2006). Lou and Xie (2006) compared the contributions of UV-B, UV-A and visible irradiation to the MW decrease of several HS waters and found that visible light was responsible for up to 40 % of the MW decrease, indicating the important influence of visible irradiation on HS properties. This further justifies the possibility of making use of natural sunlight for the purpose of removing HS from water in the research presented in this thesis. However, considering the low intensity of UV irradiation and the less effective action of visible light, the photodegradation of HS by natural sunlight may proceed with relatively slow kinetics and hence is less effective. A further treatment stage is therefore required.

### 2.3.3 *Water treatment with solar energy*

#### 2.3.3.1 Using solar energy in drinking water treatment

Treating drinking water with natural sunlight is a promising and sustainable approach. Solar irradiation can remove a number of organic chemicals and microorganisms from water and avoid generation of harmful by-products from chemical addition (Caslake *et al.*, 2004).

Sunlight is known to remove a variety of pathogenic bacteria by direct exposure, which is called solar disinfection (Blanco *et al.*, 1999; Kehoe *et al.*, 2000; McLoughlin *et al.*, 2004). Solar disinfection involves both heating and photochemical effects. Photons of sunlight are absorbed by light-sensitizers which can be excited and react with surrounding oxygen to generate highly reactive radicals. These radicals can distort the DNA molecules or break the chain structures. As a consequence, the replication process of microorganisms is

blocked and bacteria are inactivated. Kehoe *et al.* (2000) reported that by exposing *Escherichia coli* (*E.coli*) containing water to natural sunlight for 8 h with solar intensity of  $97.6 \text{ mW/m}^2$ , total inactivation was achieved for a highly turbid water of 300 NTU (nephelometric turbidity unit). Ubomba-Jaswa *et al.* (2009) found that for complete inactivation, the minimum UV-A dose should be above  $108 \text{ kJ/m}^2$ . As suggested by the Solar Water Disinfection (SODIS) method, contaminated water placed in a transparent PET-bottle or glass bottle and simply exposed to the sun for 6 hours can provide safe drinking water for people in developing countries.

By exposure to solar irradiation alone, a number of organic contaminants, such as pesticides, polycyclic aromatic hydrocarbons (PAHs) and pharmaceuticals, can be photodegraded (Bertilsson and Widenfalk, 2002; Doll and Frimmel, 2003; Matamoros *et al.*, 2009). For example, Bertilsson and Wildenfalk (2002) found that the photodegradation of three types of PAHs followed first-order kinetics. Under  $1.6 \text{ W/m}^2$  UV-B and  $13.3 \text{ W/m}^2$  UV-A irradiations, anthracene and phenanthrene were rapidly photodegraded (half-lives of 1 and 20.4 h, respectively), while the half-life of naphthalene was more than 100 h. Matamoros *et al.* (2009) studied the photodegradation of four pharmaceuticals (carbamazepine, ibuprofen, 17 alpha-ethinylestradiol and ketoprofen) under natural sunlight (daily average  $270 \text{ W/m}^2$ ) and a solar simulator ( $507.5 \text{ W/m}^2$ ). The authors found that the half-lives of four pharmaceuticals varied from 0.54 min to 39 h when exposure to simulated light, while their half-lives are 5 to 111 longer with natural sunlight. The mechanism for the photodegradation of organic contaminants follows the basic photochemical processes (as described in section 2.3.2.1), involving electronic excitation and generation of reactive species.

Examples above illustrate that solar-induced photodegradation can remove various contaminants. However, the photodegradation efficiency depends on a number of factors, such as irradiation intensity, exposure time, characteristics of chemicals and turbidity of water. As shown, exposure to natural sunlight is a relatively slower process than using artificial light source. To accelerate the photodegradation process, in solar applications, photocatalysts (such as titanium dioxide (TiO<sub>2</sub>) and Fenton reagent (addition of H<sub>2</sub>O<sub>2</sub> to Fe<sup>2+</sup> salt)) have been introduced (Malato *et al.*, 1997; Blanco *et al.*, 1999; Fernández-Ibáñez *et al.*, 2003; McLoughlin *et al.*, 2004; Mavronikola *et al.*, 2009). The reactive radicals generated through catalysts can destroy most of microorganisms and organic molecules. In addition, artificial UV irradiation is often employed instead of natural sunlight to accelerate the process (Cho *et al.*, 2005; Paleologou *et al.*, 2007). However, it is inevitably associated with extra cost.

#### 2.3.3.2 Solar collectors

The practical use of solar-driven photochemical processes has been largely enabled by the design and construction of different types of solar collectors. The solar collector is a device that is designed to efficiently collect solar photons and introduce them to target waters to promote specific chemical reactions. Solar collectors are traditionally classified into three categories according to their thermal performance (Rodríguez *et al.*, 2004), which are summarized in Table 2.6.

A non-concentrating solar collector is a static system without any solar tracking mechanisms (Figure 2.14). The flat plate is usually aiming to the sun at a specific tilt depending on the geographic location, and in particular the latitude of the site. Their main advantages are low manufacturing cost and simplicity.

Non-concentrating collectors are typically encountered in applications that require only a small scale use.

**Table 2.6** Classifications of solar collectors (Rodríguez *et al.*, 2004).

Type of Solar Collector	Featured Collectors	Concentration Ratio
Non-concentrating	Flat Plate	< 1.5
Medium-concentrating	Parabolic Trough Collector	5 - 50
High-concentrating	Parabolic Dish	100 - 10,000



**Figure 2.14** Non-concentrating solar collectors - flat plates at PSA, Spain (source: <http://www.psa.es/webeng/instalaciones/desalacion.php>). PSA: Plataforma Solar de Almería.

The parabolic trough collector (PTC) is a good representative of medium-concentrating solar collectors (Figure 2.15). This device has a structure with a parabolic reflective surface and is normally equipped with either single- or two-axis sun tracking devices, which enable the incoming sunlight to be always perpendicular to the collector aperture. All the direct irradiation reaching the

aperture is therefore reflected and concentrated onto the tubular receiver installed along the linear focus of the parabola. PTCs can concentrate the sunlight intensity between 5 and 50 times, depending on the sun tracking system and the parabola size.



**Figure 2.15** Medium-concentrating solar collectors - parabolic trough collectors at PSA, Spain (source: <http://www.psa.es/webeng/instalaciones/parabolicos.php>).

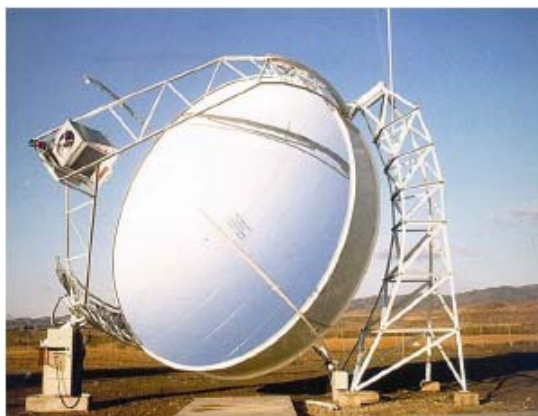


**Figure 2.16** High-concentrating solar collectors - parabolic dish at PSA, Spain (source: <http://www.psa.es/webeng/instalaciones/discos.php>).

The parabolic dish is a high-concentrating collector that has a focal point instead of a linear focus (Figure 2.16). It features a paraboloid with solar tracking

mechanisms. For effective sun tracking, high-precision optical systems are required. The solar intensity concentration achieved by a high-concentrating collector can be up to 10,000 times of what can be achieved with a non-concentrating solar collector.

The advantages and disadvantages of non-concentrating and concentrating solar collectors are summarized in Table 2.7 based on the reviews by Malato *et al.* (2002) and Rodríguez *et al.* (2004) who studied solar photocatalysis for water treatment. In general, concentrating collectors have significantly better performance but they require sun tracking systems, which lead to increased installation and maintenance cost.

**Table 2.7** Advantages and disadvantages of the non-concentrating and concentrating solar collectors (Malato *et al.*, 2002; Rodríguez *et al.*, 2004).

Type	Advantages	Disadvantages
Non-concentrating collector (flat plate type)	<ul style="list-style-type: none"> <li>a. More economic due to lower maintenance requirements;</li> <li>b. More suitable for small scale use;</li> <li>c. Simple installation;</li> <li>d. Use both direct and diffuse irradiation.</li> </ul>	Less efficient in concentrating sunlight on an energy basis
Concentrating collector (parabolic trough or dish type)	<ul style="list-style-type: none"> <li>a. Receiving a large amount of energy per area of the containers;</li> <li>b. Suitable for supporting catalysts.</li> </ul>	<ul style="list-style-type: none"> <li>a. Relatively expensive;</li> <li>b. Design to only use direct irradiation;</li> <li>c. Water overheating may occur.</li> </ul>

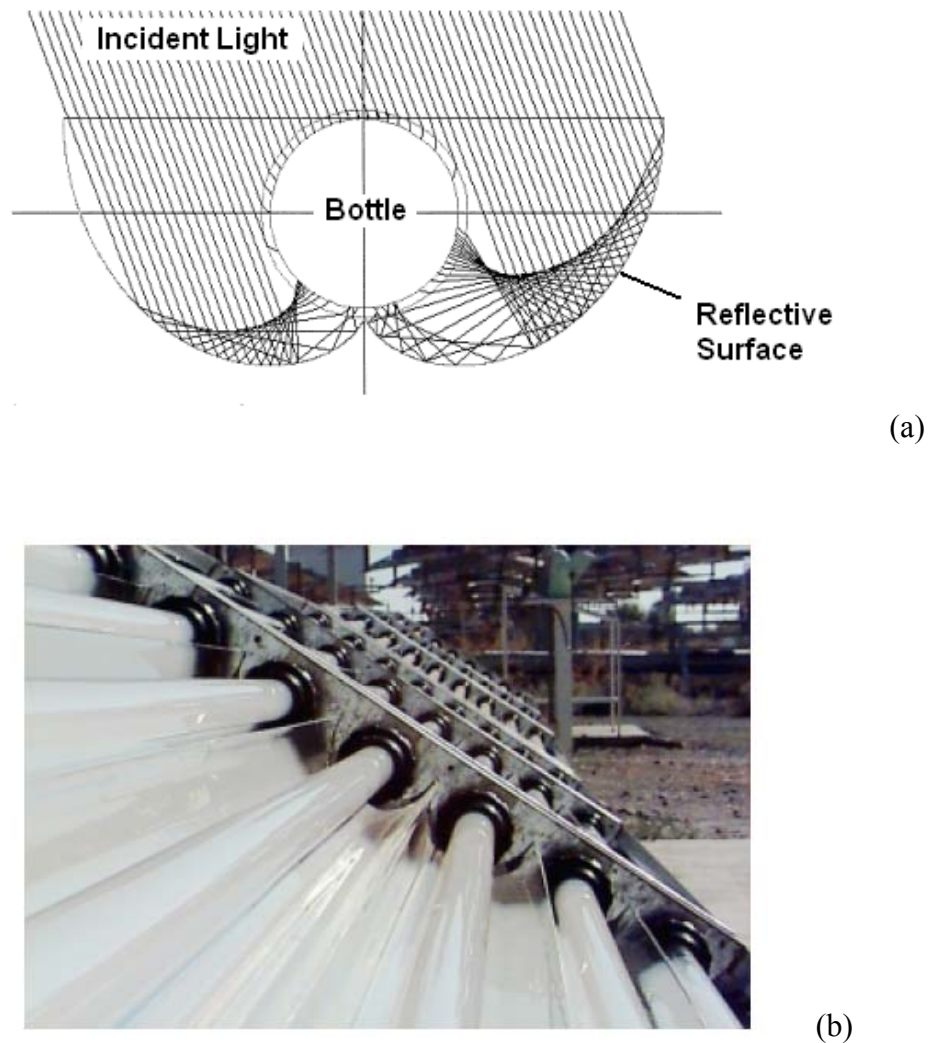


**Figure 2.17** (a) Simulations of the incident sunlight reflected by a compound parabolic collector onto the bottle located in the centre (Blanco *et al.*, 1999), and (b) an example of the CPC application (Rodríguez, 2003).

In addition to the above applications, compound parabolic collectors (CPCs) are of growing interest in solar applications. The CPC is a static collector with a reflective surface describing an involute around a cylindrical tube (Figure 2.17a). As there are no tracking mechanisms of CPCs, they are more economic than solar tracking collectors. The CPC is proposed as a combination of parabolic collectors and flat plate systems, therefore, it is able to concentrate direct solar

irradiation, and also have the properties of flat static plates using diffuse irradiation (Malato *et al.*, 1997; Ajona and Vidal, 2000; Rodríguez *et al.*, 2004). Figure 2.17a is an illustration given by Blanco *et al.* (1999), showing that the incident light (including direct and diffuse) can be effectively collected and reflected by a CPC onto the bottle located in the centre. An example of a CPC type collector is presented in Figure 2.17b (Rodríguez, 2003).

Instead of the pilot scale solar applications, a variety of small scale water treatment studies have been carried out using simple and static solar collectors, including plastic pouches or plastic bottles with light reflective and absorptive surfaces (Kehoe *et al.*, 2001; Walker *et al.*, 2004; Mani *et al.*, 2006), dark grey polyvinyl chloride (PVA) base covered by acrylic plate (Caslake *et al.*, 2004), and V-groove, parabolic and compound parabolic reactors (McLoughlin *et al.*, 2004).

A number of laboratory and field tests have proven the effective use of solar collectors in water treatment (Malato *et al.*, 1997; Blanco *et al.*, 1999; Rodríguez *et al.*, 2003 and 2004; Navntoft *et al.*, 2008; Remoundaki *et al.*, 2009). For example, Navntoft *et al.* (2008) studied the inactivation of *E.coli* in a well water using CPC under sunlight and found that complete inactivation was achieved in the CPC system when  $150 \text{ kJ/m}^2$  irradiation received from the sun, while the water without CPC needed  $210 \text{ kJ/m}^2$ , which means that complete inactivation using CPC was achieved sooner than that without CPC.

Other studies on the removal of HS from water by photocatalytic methods using solar collectors have been reported recently (Moncayo-Lasso *et al.*, 2008; Remoundaki *et al.*, 2009), however, there is limited information regarding using solar irradiation alone to treat humic rich waters. It is therefore of interest to conduct research work using different types of solar collectors to evaluate the

effect of sunlight alone and performance of solar collectors on the properties of HS.

## 2.4 GAC adsorption

The GAC adsorption process is of great importance in water industry. It can be used to remove a variety of contaminants, such as taste and odour compounds, algal toxins, industrial chemicals and natural organic materials (Newcombe, 1999). Adsorption by GAC is considered to be one of the best available and recommended technologies for the removal of HS (Jacangelo *et al.*, 1995; Karanfil *et al.*, 2000). However, it has been found in practice that the presence of HS significantly reduces the effectiveness of GAC adsorbers with respect to equilibrium capacity, adsorption rates and removal of the target contaminants (Carter and Weber, 1994; Newcombe *et al.*, 2002a). As a result, the operational life of fixed-bed GAC adsorbers is significantly reduced. The rapid saturation of GAC requires frequent replacement or regeneration, resulting in an increase in treatment costs and a loss of GAC capability to produce high quality water. Typical high removal efficiencies of HS by GAC adsorption process have been reported to be 60-80% (Owen *et al.*, 1993; Lambert and Graham, 1995). A study on a Finnish water treatment plant which involved GAC adsorption process showed that only a 47 % removal of TOC was achieved (Matilainen *et al.*, 2002).

A fundamental understanding of the factors that influence the GAC adsorption process is essential in order to optimise the existing method, or tailor new strategies to improve the HS removal.

### 2.4.1 GAC properties

The main raw materials for GAC production include wood, coal, peat, coconuts or bones (Crittenden *et al.*, 2005; Newcombe, 2006). The activation processes include treatment with carbon dioxide and high temperature steam (900-1100°C) or air. Carbons with high internal surface and porous structures are therefore generated. The surface area of GAC is normally referred to as the internal area, due to the fact that the external surface area of GAC is less than 1/100 of the internal area (Newcombe, 2006). Therefore, the internal area provides the majority of the sites for adsorption. The surface area of GAC is usually about 1000 m<sup>2</sup>/g with a maximum value of roughly 1400 m<sup>2</sup>/g (Fettig, 1999). The pores on GAC can be classified into three categories, according to their size (Crittenden *et al.*, 2005):

- Macropores (> 50 nm)
- Mesopores (2 nm - 50 nm)
- Micropores (< 2 nm)

The surface area, total pore volumes, and pore size distribution can vary significantly among different carbons, depending on the type of raw materials and production processes. For example, the micropores could account for between 30 % and 80 % of the total surface area (Fettig, 1999).

Carbon (C) is the most abundant element in GAC (80-98 %), followed by oxygen (2-20 %) which mainly exists in oxygen-containing functional groups, such as carboxylic and phenolic groups (Newcombe, 2006). These functional groups are believed to greatly influence GAC surface chemistry, such as hydrophobicity,

heterogeneity and point of zero charge ( $\text{pH}_{\text{pzc}}$ ) (Fettig, 1999). In addition to oxygen, GAC also contains a variety of elements such as S, Cl, Na, K, Si and Fe, depending on the composition of raw materials and the methods of generation.

Cheng *et al.* (2005) applied two aspects of modification to commercial carbons: (1) high temperature ammonia treatment to enlarge the surface, and (2) impregnation with iron. Both treatments led to a dramatic increase in the adsorption of HS, implying that pore size and surface chemistry of GAC are two aspects that could be improved to enhance the HS removal.

#### *2.4.2 Effects of physicochemical characteristics on HS adsorption*

Adsorption is a surface phenomenon. The surface characteristics of adsorbates and adsorbents play a major role in controlling the adsorption behaviour of the system. The interactions between GAC and HS can be explained from the physical and chemical perspectives.

##### 2.4.2.1 Physical aspect

For the physical aspect, the ability of humic molecules to access GAC pores is of great importance in controlling adsorption. Available data about size distribution of HS and pore size distribution of GAC have revealed that most pores of commercially available GAC are smaller than the average molecular size of HS (Dastgheib *et al.*, 2004). For example, Filtrasorb 400 (F400), a commonly used GAC in water treatment, has approximately  $1000 \text{ m}^2/\text{g}$  specific surface area and about 86 % of the surface area falls into pores smaller than 1 nm in width (Kilduff *et al.*, 1996). The average molecular sizes of HS have been reported to be between 0.4 and 4 nm, using various analytical techniques to measure them

(Cornel *et al.*, 1986; Aiken and Malcolm, 1987; Karanfil *et al.*, 1999). Apparently, some larger humic fractions would be excluded from the small GAC pores due to size exclusion effects.

Evidence for size exclusion effects can be found in some investigations which were carried out on bulk water or different fractions of HS (Summers and Roberts, 1988; Kilduff *et al.*, 1996; Yasua *et al.*, 1997; Karanfil *et al.*, 1999; Newcombe *et al.*, 2002a; Schreiber *et al.*, 2005). Kilduff *et al.* (1996), Yasua *et al.* (1997) and Schreiber *et al.* (2005) reported that humic waters with lower initial average MW can be treated to a greater extent, which could be attributed to the good accessibility of small molecules to the micropores of GAC. By looking into different MW fractions which were fractionated using UF from the whole humic solutions, Kilduff *et al.* (1996) found that the GAC adsorption capacity of smaller molecules (MW 1400 Da) increased by more than a factor of 5, compared to the fractions with MW about 6800 Da, based on the Freundlich modelling results. Karanfil *et al.* (1999) compared the HS adsorption using several commercial coal-based carbons and found that the adsorption capacity increased with an increasing surface area in the meso- and macropore size range.

Studies listed above provide experimental evidence that adsorption effectiveness is highly related to size exclusion effects. It is therefore important to have a good compatibility between pore size distribution of the GAC used and molecular size distribution of HS. On one hand, for a given size distribution of humic molecules in waters, benefits arise from having adsorbents with sufficiently accessible surface areas, or large pores, to adsorb HS. On the other hand, for a given probable pore size distribution of the GAC used, benefits to the adsorption of HS also arise from using the pre-treatment to reduce the amount, or size, of large molecules. Previous studies have proven that coagulation and ozonation

can significantly increase the GAC adsorption capacity of HS due to the elimination of high MW components through pre-treatment processes (Hooper *et al.*, 1996; Matilainen *et al.*, 2006). In some cases, the GAC adsorbers can also host microorganisms and partly act as biological filters after an oxidation treatment (Graham, 1999). Biological GAC filters have been found to be effective in removing low MW humic fractions.

#### 2.4.2.2 Chemical aspect

For the chemical aspect, surface chemistry of GAC, molecular structures of HS and solution chemistry are important factors that affect the interactions between HS and GAC (Dastgheib *et al.*, 2005). Similar functional groups, such as carboxylic and phenolic groups, have been identified both on GAC surface and within HS structures. The repulsive forces between these functional groups may be responsible for the low adsorption capacity of GAC for HS. Carboxylic groups deprotonate at pH values of 4 to 5 and phenolic groups deprotonate at pH values of 9 to 10. Therefore, for the pH range typically encountered in water treatment (6.5-8), HS are expected to be negatively charged. To enhance the adsorption of HS, the GAC surface should exhibit positive charge (basic surface area) to create the attractive forces between GAC and HS. Karanfil *et al.* (1999) carried out comprehensive investigations with four representative humic samples and seventeen activated carbons to study the role of GAC surface chemistry on the adsorption of organic compounds. The authors found that the repulsive forces between strongly acidic functionalities within the humic structure and on the GAC surface may significantly reduce adsorption capacity, and HS removal decreased with increasing GAC surface acidity.

The pH value of the solution appears to have a significant influence on the adsorption of HS by GAC; decreasing pH will increase the HS adsorption. Possible reasons are as follows (Newcombe, 1999):

- decrease in negative charge of HS, or increase in the positive charge on GAC, which can increase attractive forces between HS and GAC surface;
- decrease in the solubility of HS due to protonation of carboxylic groups, which can increase driving forces for adsorption onto the hydrophobic GAC surface.

Apart from pH, ionic strength, presence of calcium (Ca) cations, and dissolved oxygen have all been reported to influence HS adsorption by GAC (Summers and Roberts, 1988; Karanfil *et al.*, 1996b; Fettig, 1999). For example, the sensitivity of adsorption to dissolved oxygen has been found to depend on MW, polydispersity, aromaticity and acidity for natural NOM, while the soil derived HA is relatively not sensitive to the presence or absence of oxygen.

### 2.4.3 Approaches to evaluate the adsorption of HS

#### 2.4.3.1 Isotherm models

Adsorption isotherms can be obtained by performing a series of batch experiments to examine the adsorbent capacity for the target adsorbate. Previous adsorption investigations have led to the development of a large amount of theoretical equilibrium isotherm models, which provide a good quantitative description and representation of experimentally obtained data, as well as a useful tool for predicting the full-scale continuous flow process. The main equilibrium

isotherm models that have been previously applied in the HS-GAC adsorption system and are of interest within the scope of this research include:

*- The Langmuir model*

The well-known Langmuir equation describes monolayer adsorption onto homogeneous adsorbent. There is a stoichiometry between the number of sites and the number of adsorbate molecules. It is assumed that all the sites have the equal energy of adsorption. The relevant equation is:

$$q_e = \frac{v_m b C_e}{1 + b C_e} \quad (2.2)$$

where  $q_e$ : adsorbed amount of adsorbate on the adsorbent at equilibrium concentration  $C_e$  [mg/g]

$v_m$ : maximum adsorption amount of adsorbate adsorbed per unit weight of adsorbent [mg/g]

$b$ : constant related to the energy of adsorption

$C_e$ : adsorbate concentration in solution at equilibrium [mg/L]

Equation 2.3 can be linearised to become:

$$\frac{1}{q_e} = \frac{1}{v_m} + \frac{1}{v_m b C_e} \quad (2.3)$$

Constants  $q_e$  and  $C_e$  can then be calculated from the plot of  $1/q_e$  vs.  $1/C_e$ .

- *The Freundlich model*

The Freundlich model is empirical and accounts for the heterogeneity of the adsorbent surface. Each adsorption site is considered to have a specific energy. Multilayers can be formed on the adsorbent surface. The equation is:

$$q_e = K_F C_e^{1/n} \quad (2.4)$$

The Freundlich parameters  $K_F$  and  $1/n$  can be obtained by plotting  $q_e$  versus  $C_e$  in a logarithmic scale, i.e.:

$$\text{Log } q_e = \text{Log } K_F + \frac{1}{n} \text{Log } C_e \quad (2.5)$$

$K_F$  indicates the adsorption capability of the adsorbate. The larger the  $K_F$ , the larger the  $q_e$  value will be. The exponential constant  $1/n$  is related to the distribution of energy sites.

- *The modified Freundlich model*

A modified Freundlich model has been recommended by several researchers to describe the adsorption of commercial and natural HS by GAC (Summers and Roberts, 1988a and 1998b; Karanfil *et al.*, 1996a and 1996b; Kilduff *et al.*, 1996). It expresses the equilibrium condition in terms of the amount of unadsorbed components per unit of adsorbent, rather than the traditional equilibrium DOC concentration in solution. This modified form of Freundlich isotherm is described as:

$$q_e = K_F (C_e/D)^{1/n} \quad (2.6)$$

where the  $q_e$  and  $C_e$  are as before;  $D$  is the GAC dose (g/L);  $K_F$  is the Freundlich parameter, representing the adsorption capacity at a value of  $C_e/D$  equal to unity; and  $1/n$  is the exponential constant. The modified Freundlich parameters  $K_F$  and  $1/n$  can be obtained by plotting  $\log q_e$  versus  $\log C_e/D$ , as follows:

$$\text{Log } q_e = \text{Log } K_F + \frac{1}{n} \text{Log } C_e/D \quad (2.7)$$

#### 2.4.3.2 Continuous flow adsorption process

In drinking water treatment practice, GAC is often applied in a fixed-bed column. The column can be regarded as numerous batch adsorption operations in series. Adsorption occurs in a particular region in the bed, known as the mass transfer zone (MTZ) which moves with time (Crittenden *et al.*, 2005). As the solution passes through the bed, the adsorbent is gradually consumed till the MTZ reaching the end of the contact bed. It is usually considered that the breakthrough occurs when the effluent concentration is 5 % of the influent concentration, hence a breakthrough at time  $t_B$ . At the final stage, the target compounds are no longer eliminated from the effluent as the bed has reached its capacity. Figure 2.18 qualitatively illustrates the breakthrough curve ‘S’ shape for an ideal adsorption system where the adsorbate has small size and a simple structure.

Compared to batch adsorption studies, continuous flow studies are considered more effective in assessing and predicting the performance of GAC adsorbers (Li *et al.*, 2003). The operation of full-scale adsorbers is time-consuming, expensive and impractical to be conducted in a laboratory environment. The rapid small-scale column test (RSSCT), which is a scale down version of the full-scale

GAC column has been developed (Crittenden *et al.*, 1986, 1987 and 1991). A number of studies have proven that the RSSCT method can successfully simulate the full-scale plant operation and produce identical breakthrough profiles for a full-scale GAC column (Crittenden *et al.*, 1984, 1986 and 1991). The use of RSSCT method offers the following advantages: less time, reduced water volume requirement, reduced operating cost, and no requirement for isotherms and kinetics studies.

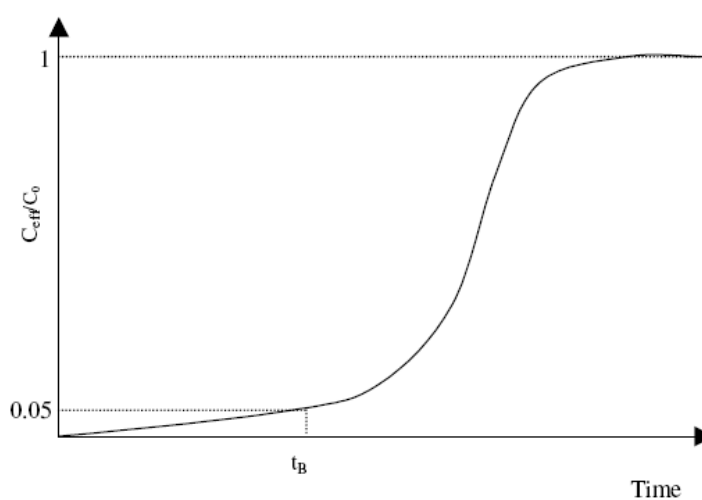


**Figure 2.18** Representative shape of the breakthrough curve with breakthrough at 5 % of the influent concentration (André, 2006).

In the RSSCT method, mathematical models are used to define the scaling relationship between the small- and full-scale columns so as to maintain perfect similarity between the performances of adsorbers (Crittenden *et al.*, 2005). In the RSSCT column, GAC of smaller size is used, prepared from the GAC used in the full-scale column. The scaling relationships are a function of the carbon particle sizes used in RSSCT and full-scale columns. A review of previous studies by Summers *et al.* (1995) has shown that the RSSCT method can be used successfully to assess the full-scale column performance with respect to the

control of NOM and DBP formation. The equations used to determine the RSSCT parameters are summarized as follows (Crittenden *et al.*, 2005):

The critical RSSCT design and operating parameters are the empty bed contact time (EBCT) and the loading rate, as can be calculated using the following equations:

$$\frac{EBCT_{SC}}{EBCT_{LC}} = \left[ \frac{D_{SC}}{D_{LC}} \right]^{2-X} \quad (2.8)$$

in which: D – the particle size of GAC [nm]

SC – small column

LC – large column

X – diffusivity factor

It is recommended that a value of 1 be used for the X parameter when HS are the target compounds (Summers *et al.*, 1995).

The hydraulic loadings of the small- and full-scale columns are related to the particle size according to the following equation:

$$\frac{V_{SC}}{V_{LC}} = \frac{D_{LC}}{D_{SC}} \quad (2.9)$$

in which: V – loading rate [m/h]

The flow rate and length of the column can easily be determined from Equations 2.10 and 2.11:

$$Q_{SC} = V_{SC} A_{SC} \quad (2.10)$$

in which: Q – flow rate [ml/min]

A – area of the cross section of the column [cm<sup>2</sup>]

$$L_{SC} = V_{SC} EBCT_{SC} \quad (2.11)$$

in which: L – length of the contact bed [cm]

The mass of GAC in the RSSCT column can be calculated as:

$$M_{SC} = Q_{SC} EBCT_{SC} \rho_{LC} \quad (2.12)$$

in which: M – mass of adsorbent [g]

$\rho$  – bulk density of the full-scale column [g/ml]

## 2.5 Water treatment processes for removing HS – a brief review

A number of physical, chemical and biological technologies have been proven being capable of removing HS from natural water sources (Owen *et al.*, 1993; Fu *et al.*, 1994; Goel *et al.*, 1995; Jacangelo *et al.*, 1995; Lambert and Graham, 1995; Volk *et al.*, 2000; Parkinson *et al.*, 2003; Chin and Bérubé, 2005). Some examples are shown in Table 2.8. As can be seen, HS removal efficiencies greatly vary from water source to water source and from process to process. This is due to the heterogeneous nature of HS waters and variations in water treatment conditions. It is therefore more appropriate to evaluate the removal efficiencies of HS by different water treatment processes on the same water source.

**Table 2.8** Examples of water treatment methods and their natural HS removal performances (Owen *et al.*, 1993; Fu *et al.*, 1994; Goel *et al.*, 1995; Jacangelo *et al.*, 1995; Lambert and Graham, 1995; Volk *et al.*, 2000; Parkinson *et al.*, 2003; Chin and Bérubé, 2005).

Method		Initial DOC (mg/L)	DOC Removal (%)	References
Photo-oxidation	UV alone	8.2	36	Parkinson <i>et al.</i> , 2003
	O <sub>3</sub> /UV	1.9	50	Chin and Bérubé, 2005
Adsorption	GAC	7.8	69	Lambert and Graham, 1995
	γ-Al <sub>2</sub> O <sub>3</sub>	7.8	46	Lambert and Graham, 1995
Membrane	UF, NF	8.2	80-100	Fu <i>et al.</i> , 1994; Jacangelo <i>et al.</i> , 1995
Coagulation	Aluminium	2.5-15.1	10-40	Owen <i>et al.</i> , 1993; Volk <i>et al.</i> , 2000
Oxidation	O <sub>3</sub> only	10	27	Goel <i>et al.</i> , 1995
	O <sub>3</sub> + biodegradation	10	75	Goel <i>et al.</i> , 1995

As Aldrich humic acid (AHA) will be the target compound used in this research, examples on treating this model humic material using different water treatment processes are illustrated in Table 2.9 (Allard *et al.*, 1994; Rebhun *et al.*, 1998; Chen and Wu, 2004; Murray and Parsons, 2004; Wiszniowski *et al.*, 2004; Buchanan *et al.*, 2008; Listiarini *et al.*, 2009; Bond *et al.*, 2010). Likewise, different processes exhibit different capabilities in HS removal. All the technologies have their advantages and disadvantages. Representative processes will be discussed in the following sections.

**Table 2.9** Examples of water treatment methods and their AHA removal performances (Allard *et al.*, 1994; Rebhun *et al.*, 1998; Chen and Wu, 2004; Murray and Parsons, 2004; Wiszniowski *et al.*, 2004; Listiarini *et al.*, 2009).

Method	Initial DOC (mg/L)	DOC Removal (%)	References
Photocatalytic degradation (solar irradiation + TiO <sub>2</sub> )	100	86-93	Wiszniowski <i>et al.</i> , 2004
GAC	10	50-80	Chen and Wu, 2004
NF	10	82-98	Listiarini <i>et al.</i> , 2009
Coagulation (alum or ferric chloride)	16.5-50	93-98	Rebhun <i>et al.</i> , 1998
UV-C irradiation	10	95	Allard <i>et al.</i> , 1994
AOP (Fenton process)	10.5	90	Murray and Parsons, 2004

NF: Nanofiltration

AOP: advanced oxidation process

### 2.5.1 Membrane filtration

Membrane filtration, including microfiltration (MF), ultrafiltration (UF) and nanofiltration (NF), has grown rapidly as a drinking water treatment method over the past decade. It features many advantages over conventional treatment methods, such as smaller size, easier operation and maintenance as well as good water quality. However, the application of membrane filtration in practical applications has been restricted by fouling issues (Zularisam *et al.*, 2006). Even

a small portion of HS can lead to serious and irreversible fouling. Recent research has highlighted the influence of high MW components, high aromatic hydrophobic acids, and organic colloidal materials of HS in the fouling of membranes (Amy and Cho, 1999; Fan *et al.*, 2001). Problems of hydraulic resistances, frequent regeneration or replacement, as well as high operating and maintenance cost therefore arise.

MF and UF are considered inadequate in removing HS due to the pore sizes of the membranes being significantly larger than most of humic molecules. For that reason, NF is more effective in removing HS. Pre-treatment, such as MF or UF, pH adjustment, and conventional treatment followed by ozonation, is required for NF applications due to fouling problems. Coagulation treatment prior to membrane filtration has been used to enhance the removal of HS and reduce fouling by aggregating fine particles to form a highly porous and less dense cake on the surface, that can be easily removed by backwashing (Fabris *et al.*, 2007). Powered activated carbon (PAC) adsorption is another pre-treatment method used for reducing HS levels through the rapid adsorption of dissolved foulants to alleviate membrane fouling. Flux decrease and accumulation of carbon on the membrane surface are problems typically associated with PAC addition. It is essential to tailor pre-treatment strategies for difference water sources. Representative schematics of the combination of pre-treatment and membrane filtration for drinking water treatment are illustrated in Figure 2.19 (Jacangelo *et al.*, 1997).

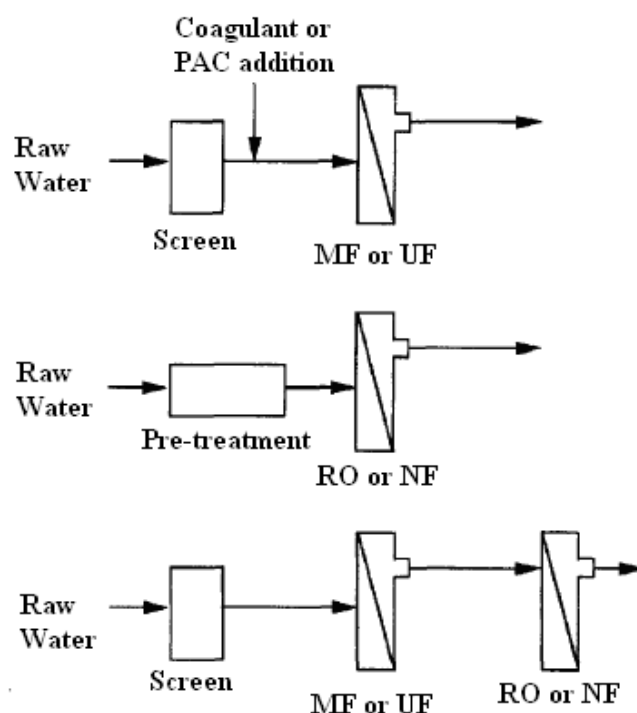


**Figure 2.19** Schematic of the combination of pre-treatment and membrane filtration for drinking water treatment (Jacangelo *et al.*, 1997). (RO represents the reverse osmosis)

### 2.5.2 Coagulation

Chemical coagulation is the major HS removal process for drinking water treatment in many countries (Ratnaweera *et al.*, 1999). When coagulants (normally aluminium or ferric salts) are added to the water, several mechanisms begin to work with respect to HS removal (Chow *et al.*, 2009): (1) charge neutralisation – the cationic metal interacts with negatively charged HS; (2) adsorption of molecules on the metal hydroxides; and (3) formation of insoluble metal hydroxides where HS are removed by sweep coagulation. Many factors can influence the removal of HS by coagulation, such as concentrations and properties of HS, charge and dosage of coagulant as well as pH and temperature

(Kam and Gregory, 1999; Ratnaweera *et al.*, 1999; Chow *et al.*, 2009). Sharp *et al.* (2006) used XAD resin adsorption techniques to fractionate moorland waters into hydrophilic fraction (HPIA), humic acid fraction (HAF), fulvic acid fraction (FAF) and hydrophilic non acid (HPINA). The authors found that the hydrophobic fractions, including HAF and FAF, were more readily removed by the coagulation process, while the HPINA was least amenable to be removed by coagulation due to a negligible charge density. Results revealed that the organic make up of raw water may greatly influence treatability and coagulation performance.

Enhanced coagulation by adding excess coagulants, or adjusting pH, has been proposed by the United States Environment Protection Agency (USEPA) for improving the removal of DBP precursors from conventional water treatment processes (Jiang and Graham, 1996). However, increasing coagulant doses could result in more sludge production, unwanted metal ion residue and associated high operating cost.

### 2.5.3 Advanced Oxidation Processes (AOPs)

The use of AOPs for improving the performance of water treatment is of growing interest in recent years. A number of AOPs, such as UV/H<sub>2</sub>O<sub>2</sub>, UV/O<sub>3</sub>, Fenton process, and UV/TiO<sub>2</sub>, have been investigated for treating refractory organics, bacteria and HS in water (Legrini *et al.*, 1993; Graham, 1999; Wang *et al.*, 2000; Murray and Parsons, 2004; Goslan *et al.*, 2006). AOPs typically involve the rapid generation of strong oxidants, such as hydroxyl radicals, to destroy the refractory organic structures. For example, in UV/H<sub>2</sub>O<sub>2</sub> or UV/O<sub>3</sub> processes, the generation of oxidants can be described as the following mechanisms:



where  $h\nu$  is the photon energy from UV irradiation. The attack of the oxidant to HS is non-selective and capable of rapidly oxidising HS in water. Chin and Bérubé (2005) reported that  $\text{O}_3/\text{UV}$  led to 50 % reduction in DOC concentration and 70 % reduction in HAA formation potential.

UV irradiation is typically considered to be used as a pre-treatment method, as it alone is generally considered to be an ineffective procedure for HS removal (Legrini *et al.*, 1993). Thomson *et al.* (2002) investigated the potential of UV-C irradiation in facilitating biological treatment and improving the water quality. It was found that the low MW photoproducts generated by UV-C irradiation were significantly removed by the bio-treatment and the water quality was greatly improved as measured by the decreased chlorine demand, DOC and  $\text{UV}_{254}$ . Similar observation has also been made by Buchanan *et al.* (2008) who found that using vacuum UV (185 nm + 254 nm) irradiation followed by a biological carbon adsorption treatment improved the reduction of DOC concentration of HS from 29% to 54 %. The advantages of using UV irradiation to treat HS compared to other processes are: no requirement for recycling of the substrate, no chemical addition, and no sludge by-products formed (Parkinson *et al.*, 2003). However, it is associated with extra operating cost due to the usage of UV light.

Ozonation has also been tested as a pre-treatment unit prior to conventional treatment processes, such as slow sand filtration and coagulation. According to Graham (1999), for water sources with DOC being principally composed of HS, the typical colour removal for slow sand filtration is approximately 42 %, whereas the DOC removal is only of 9 to 15 %. By introducing pre-ozonation, higher

colour and DOC removals were observed (Table 2.9). As a result, the THM formation potential was reduced. The removal of HS is dependent on the ozone doses and also affected by the nature of water sources (Goel *et al.*, 1995).

**Table 2.10** Published data for colour and DOC removals by slow sand filtration with pre-ozonation (Graham, 1999).

Water Source	Ozone Dose (mg O <sub>3</sub> /L)	DOC Removal (%)	Colour Removal (%)
Seagahan, UK	5	25	70-80
Lake Vyrnwy, UK	1.1-2.5	26.5	52
River Dee, UK	0.5*	28	58
Model Water	6-7	34-40	67-82

\* mg O<sub>3</sub>/mg TOC

## 2.6 Conclusions

From the available literature reviewed above, the following conclusions may be drawn:

- UV<sub>254</sub> absorbance, DOC and HPSEC allow rapid measurements of HS properties and give information that can be linked to the DBP formation potential for a water source with a high humic content;
- irradiation can alter the physicochemical properties of HS (reflected as a decrease in DOC, UV<sub>254</sub> and molecular size). The nature of HS waters may greatly influence the photodegradation of HS;
- not only the UV irradiation, but also the visible irradiation can photodegrade HS. Both of them can be found in the natural sunlight spectrum;

- no research work known to the author has related the solar-induced photodegradation of HS with the subsequent GAC adsorption process to enhance the removal of HS from water;
  - sunlight is the most freely available and abundant energy source. It is a promising field in water treatment;
  - solar collectors can be applied to promote the sunlight-induced photoreaction. The solar tracking concentrating collectors have high optical efficiency but require high capital investment. The simple non-tracking solar collectors are of low cost and more suitable for a small scale use;
  - the adsorption of HS by GAC can be affected by physical as well as chemical factors. Improvement of adsorption can be achieved by modification on either aspect;
  - for a chemically compatible adsorption system, low MW components are preferentially removed from the humic mixture by GAC due to the better accessibility to GAC pores;
  - adding pre-treatment units prior to conventional treatment processes, or a combination of processes, may significantly benefit the removal of HS;
- and,
- the solar irradiation – GAC adsorption method is considered to be a possible combination to enhance the removal of HS from water, with the potential advantages of low energy consumption, low chemical addition, and associated low cost on waste handling .

## CHAPTER 3

### AIMS AND OBJECTIVES

The aim of this work was to investigate a new and alternative water treatment method for removing humic substances (HS) from water, using a combination of granular activated carbon (GAC) adsorption and sunlight, a renewable energy source.

The following objectives were set:

- Evaluate the impact of natural sunlight on the properties of HS with respect to UV absorbance at 254 nm ( $UV_{254}$ ), dissolved organic carbon (DOC) concentration and molecular weight (MW) and establish the relationship between solar irradiation and HS changes;
- Investigate the use of static solar collectors, including two parabolic collectors and a compound parabolic collector, for promoting the photodegradation process of HS, and therefore their removal by GAC adsorption;
- Compare the adsorption behaviour of the irradiated and non-irradiated HS by Aquasorb 101 GAC in order to determine the effect of pre-treatment with sunlight on the overall HS removal;
- Evaluate the possibility of treating HS using natural sunlight at different times of the year, followed by GAC adsorption;

- Evaluate the treatability of HS waters with different properties (Aldrich humic acid water, Suwanee River fulvic acid water, and natural water) using the proposed solar irradiation-GAC adsorption method.

## **CHAPTER 4**

### **MATERIALS AND METHODS**

#### **4.1 Introduction**

To address the goal of this research, a series of laboratory investigations have been carried out. This chapter describes various aspects of the experimental framework, including the experimental set-up and analytical techniques. First, a general description of the hypothesis and approach of this study is given. Selection, collection and preparation of humic substances (HS) samples, as well as analytical methods (including UV absorbance at 254 nm (UV<sub>254</sub>), dissolved organic carbon (DOC) concentration and molecular weight (MW)) which have been implemented throughout this study are described in detail. The focus is then given on the solar irradiation experimental set-up. In this part, selection of containers for HS samples, design of solar collectors, and measurement of solar irradiation are discussed. Finally, a description is given on the studies performed on the adsorption of HS by granular activated carbon (GAC), including batch isotherm experiments and small column tests.

#### **4.2 Hypothesis and approach**

Considering that GAC preferentially adsorbs smaller molecules from the humic mixture, and that photodegradation decreases the MW of HS by breaking down high MW components into smaller molecules, a hypothesis is made that solar

irradiation increases the adsorption capability of GAC for the irradiated HS. This hypothesis was examined in the present work by comparing the adsorption behaviour of irradiated and non-irradiated HS by GAC. For the purpose of exploring a new approach with low energy consumption and low cost. Natural sunlight was used as the energy source. A commercially available GAC was used without modifications. A schematic diagram of the sample treatment methodology is given below (Figure 4.1). A more detailed description will be given in the following sections.

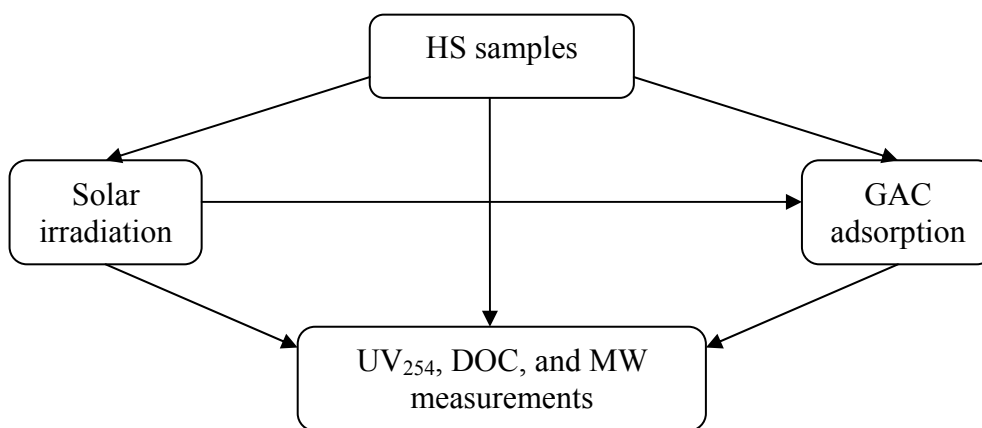


**Figure 4.1** Schematic diagram of the HS sample treatment methodology.

### 4.3 HS samples

#### 4.3.1 Description of HS

HS samples used in this research included aqueous solutions prepared from the commercially available Aldrich humic acid (AHA) sodium salt, Suwanee River fulvic acid (SRFA), and a natural water sample collected from a water treatment works (WTW) of Yorkshire Water.

AHA (lot number H1-675-2) was purchased from Sigma-Aldrich, UK. It was selected to be used in most of the experiments. This is because:

- it is a very well-defined reference material and has been widely used in HS research (Allard *et al.*, 1994; Karanfil *et al.*, 1996a; Schmitt-Kopplin *et al.*, 1998; Selcuk *et al.*, 2003);
- complex physicochemical background and seasonal variations of natural waters make it difficult to evaluate the solar irradiation effects alone on the removal of HS in this study;
- techniques for extracting HS from natural waters are sophisticated and expensive, it was beyond the budget of this project;
- a large amount of HS containing water was needed.

SRFA was purchased from the International Humic Substances Society (IHSS). It is also a common reference material. The removal of SRFA was studied to evaluate the treatability of fulvic acid (FA) compared to humic acid (HA) using the solar-GAC method.

A natural water sample was collected from the inlet channel prior to any chemical treatment at the Chellow Heights Water Treatment Works (Bradford, UK) in autumn. The sample was collected using two 5 L polyethylene containers and transported to the environmental engineering lab at University College London (UCL) the next day after collection. This water was a mixture of waters from Upper Baden, Scar House and Angram Reservoirs in North Yorkshire. It was a typical upland water of dark colour which was a consequence of water passing through peat, the major soil type in the upland areas of Yorkshire.

### 4.3.2 Preparation of HS solutions

Deionised water was obtained by passing municipal water through an ion-exchange system (Purite Limited, Thame, UK) and used to prepare AHA and SRFA solutions.

#### 4.3.2.1 Stock Solution

To prepare the stock solution, 5 g of AHA powder were dissolved in one litre of deionised water. The mixture was stirred for a few minutes and left to settle. The supernatant solution was filtered progressively using Whatman number 1 filter paper (11  $\mu\text{m}$ ), Whatman number 3 filter paper (6  $\mu\text{m}$ ) and finally on a Whatman 0.45  $\mu\text{m}$  cellulose nitrate membrane filter. Prior to use, each cellulose nitrate filter was rinsed with 500 ml of deionised water to prevent organic compounds leaching from filters to interfere the HS measurement (Karanfil *et al.*, 2003; Khan and Subramania-Pillai, 2007). The filtered stock solution was stored at 4 °C if not in use.

#### 4.3.2.2 Experimental solutions

*AHA* – experimental solutions were prepared by diluting the stock solution. An appropriate amount of stock solution was taken with a pipette, dissolved in 1 L of deionised water and stirred to mix completely. The prepared 1 L experimental solution was then transferred to a 1 L pre-washed transparent polyethylene terephthalate (PET) bottle and ready for use.

*SRFA* – in the SRFA experiment, similar amounts of SRFA and AHA powders were separately weighed, dissolved in 1 L of deionised water and well mixed.

Before transferring to 1 L bottles, solutions were filtered through 0.45  $\mu\text{m}$  filters.

*Natural water sample* – the natural water sample was filtered through 0.45  $\mu\text{m}$  filters to remove suspended particles as soon as it was delivered to the laboratory at UCL. 1 L aliquots of the filtered water were transferred into 1 L PET bottles. The solar irradiation experiment using natural water started within one week after sample collection.

All the experimental solutions were stored in the fridge at 4 °C if not in use.

#### **4.4 Analytical methods**

##### *4.4.1 Sampling*

All samples were analysed for UV<sub>254</sub> absorbance, DOC concentration, molecular weight distribution (MWD) and pH. The sampling procedure was as follows:

- Prior to sampling, 0.45  $\mu\text{m}$  syringe filters (polypropylene and cellulose, 25 mm, Sartorius Minisart RC) were pre-washed to prevent cellulose acetate from causing a reading at 254 nm. Approximately 100 ml of deionised water was used to wash each filter until the UV<sub>254</sub> of filtrate was zero.
- Filter 15 ml of sample through a 0.45  $\mu\text{m}$  syringe filter. The first 5 ml of filtrate was discarded.
- Approximately 3 ml were used for UV<sub>254</sub> measurement immediately, and then returned to its corresponding experimental solution after the measurement.
- About 6 ml of filtrate was kept in a Pyrex glass tube sealed with parafilm for further DOC analysis. All tubes were soaked in a 10 % nitric acid bath

overnight, thoroughly rinsed with deionised water and dried at 105 °C in advance. Checks on tubes filled with deionised water were undertaken every time when DOC analysis was conducted so as to make sure no interference of DOC coming from the glass tube into the HS solution.

- About 1 ml of filtrate was injected into a small sampling vial with a sealed cap (Perkin Elmer, UK) for high performance size exclusion chromatography (HPSEC) measurement.

The filtrates for DOC and HPSEC measurements were kept in the fridge at 4 °C. Duplicate experiments were performed.

#### *4.4.2 UV<sub>254</sub> measurement*

UV<sub>254</sub> measurement was made on a double-beam Camspec UV-visible spectrophotometer (UK) with an optical path length of 1 cm in a quartz glass cuvette in the Chadwick laboratory of Environmental Engineering, UCL. Deionised water was used as a blank to adjust zero. Measurement of deionised water was made every 10-15 samples to check the stability of the instrument. The cuvette was regularly soaked in hydrochloric acid (HCl) overnight, washed with acetone and deionised water to avoid any interference from the contaminants attached on the cuvette wall. The relative standard deviation (RSD), determined from replicate experiments, was less than 3 %.

#### *4.4.3 DOC*

DOC was measured on a Shimadzu TOC-5000A analyser (Shimadzu, Milton Keynes, UK) in the chemistry laboratory of Centre for Water Science at Cranfield University, UK. The system consists of a TOC-5000A analyser coupled with an

autosampler module. The analyser was operated using the combustion/non-dispersive infrared gas analysis method. The total organic carbon (TOC) was calculated by measuring the total carbon (TC) and the inorganic carbon (IC) and then subtracting the IC from the TC. The machine was calibrated regularly. Working standards were diluted from 1000 mg/L TC and IC standards to the appropriated concentrations with deionised water. Working standards were also inserted and measured in every 10-15 samples in order to check the stability of the TOC analyser. The analyser was recalibrated as soon as the value of the standard was beyond 10% of the expected value. As samples were filtered through 0.45µm filters, DOC was measured instead of TOC (Standard Methods for the Examination of Water and Wastewater, 1998). The RSD, determined from selected samples, was less than 5 %.

#### 4.4.4 SUVA

The specific UV absorbance (SUVA) was determined as a ratio of  $UV_{254}$  ( $m^{-1}$ ) with DOC (mg/L), using the unit of litre per milligram carbon per meter.

#### 4.4.5 HPSEC

##### 4.4.5.1 Instrumentation

The MWD of HS was measured using the HPSEC method which is based on the theory that small compounds more easily diffuse into the pores of column packing materials therefore elute out of the column later than larger molecules (Chin *et al.*, 1994; Peuravuori and Pihlaja, 1997; Cabaniss *et al.*, 2000). HPSEC was performed on a high performance liquid chromatography (HPLC) system (Perkin Elmer, UK), equipped with a series 200 pump, an autosampler and a UV detector

set to 254 nm. The mobile phase was 0.01 M sodium acetate (HPLC grade, Fisher Scientific, UK) at a flow rate of 1 ml/min at room temperature. The column was a BIOSEP-SEC-S3000 (Phenomenex, UK) 7.8 mm (ID) × 30 cm and the guard column was the ‘Security Guard’ fitted with a GFC-3000 disc 4 mm (ID) × 3 mm (Phenomenex, UK). The guard column was checked regularly and the cartridge was replaced as soon as the packing material was “dirty” (showing visual contaminants). Chromatograms were recorded and processed with the TotalChrom Navigator software for HPLC (Perkin Elmer, UK). A chromatogram of detector response vs. time was generated for each sample. In addition, an inter-laboratory comparison was made between UCL and Cranfield University where the same column and method were used. The comparison showed a similar distribution of chromatograms of the same HS sample.

#### 4.4.5.2 Column calibration

The column was calibrated using a set of sodium polystyrene sulfonates (PSS, purchased through Kromatek, UK, from Polymer Standards Service GmbH, Germany) with peak MWs of 891, 6430, 15800 and 33500 daltons (Da). The concentration of each standard was made to 1 g/L. An example of HPSEC chromatograms of these standards is presented in Figure 4.2. Each PSS standard exhibited a single peak in their chromatograms, except for the PSS 891 Da standard, of which multiple peaks were observed in the chromatogram. This is in agreement with the previous finding by Zhou *et al.* (2000). The PSS standard of the smallest MW was therefore excluded from employment to calibrate HS. Instead, acetone (MW = 58 Da, HPLC grade, Aldrich) was used to calibrate the low end of the MWD and an individual peak was obtained by HPSEC measurement, as illustrated in Figure 4.2. A combination of PSS and acetone as standards to characterize HS has been used in several studies (Karanfil *et al.*,

1996a; Zhou *et al.*, 2001; Pullin *et al.*, 2004). However, the use of PSS standard of low MW ( $\leq 1000$  Da) for HS calibration has been reported in some work, in which multiple peaks in the chromatogram of the low MW PSS standard were not mentioned (Świetlik *et al.*, 2002; Carvalho *et al.*, 2008).

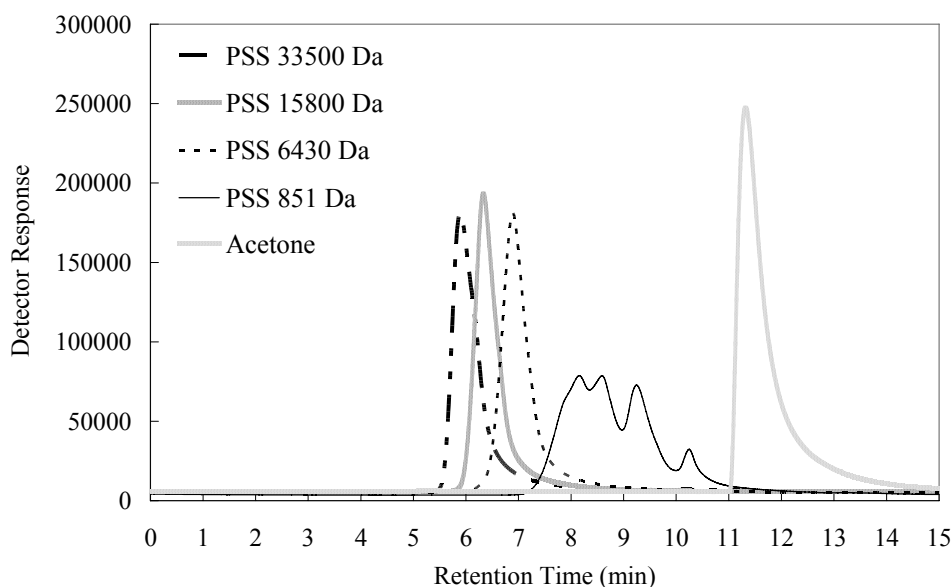


**Figure 4.2** An example of HPSEC chromatograms of PSS standards having MWs of 891, 6430, 15800 and 33500 Da as well as acetone for the purpose of calibrating HS.

It should be noted that the PSS standards used in the calibration of HS covered a wide range of MW. This was due to the fact that at the present time, no good standards for the intermediate MW range (i.e. 200-4000 Da) have been identified (Zhou *et al.*, 2000). There is no doubt that the identification of standards in this range could improve the calibration of the MW of HS.

A linear regression between the log peak MW and the retention time ( $t$ ) was used for the calibration of the MW of HS (Pelekani *et al.*, 1999; Zhou *et al.*, 2000), in the form of:

$$\log (MW) = a - b(t) \quad (4.1)$$

An example of the calibration curve is shown in Figure 4.3. A correlation factor of  $R^2 > 0.99$  was consistently obtained for the calibration throughout this research. Using equation 4.1, the MW of each humic fraction can therefore be obtained according to the time they elute out of the HPSEC column.

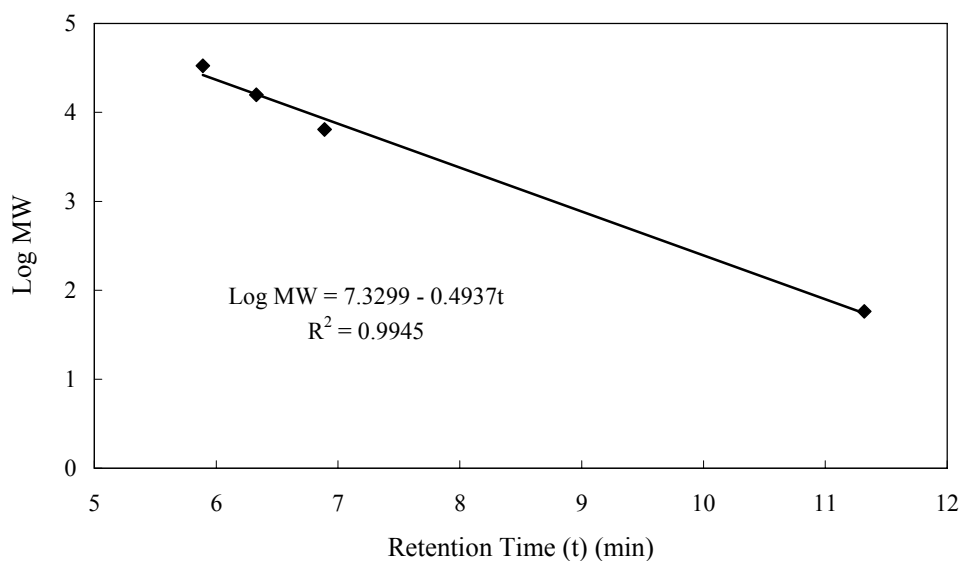


**Figure 4.3** An example of the calibration function obtained by linear regression of the log MW and retention time of calibration standards.

#### 4.4.5.3 Calculating MW

Number-average MW ( $M_n$ ), weight-average MW ( $M_w$ ), and polydispersity ( $\rho$ ) of HS were determined using following equations (Chin *et al.*, 1994; Peuravuori and Pihlaja, 1997; Zhou *et al.*, 2000):

$$M_n = \frac{\sum_{i=1}^n h_i}{\sum_{i=1}^n \frac{h_i}{M_i}} \quad (4.2)$$

$$M_w = \frac{\sum_{i=1}^n h_i M_i}{\sum_{i=1}^n h_i} \quad (4.3)$$

$$\rho = \frac{M_w}{M_n} \quad (4.4)$$

where  $h_i$  is the height of the chromatogram curve of HS at retention time  $t$ ;  $M_i$  is the MW of molecules at retention time  $t$ , which was determined according to the calibration results (equation 4.1).

Data processing of HPSEC chromatograms, including baseline corrections and molecular weight cut-offs (MWCOs), is critical in determining the MW of HS (Zhou *et al.*, 2000). Various combinations of MWCOs at high and low MWs (for example, low MWCO of 2 % and high MWCO of 1 %, or low MWCO of 1 % and high MWCO of 1 %) were evaluated on determining the MW 6430 Da PSS standard. The calculated MW values obtained from different combinations of MWCOs were then compared with the information from the supplier (Polymer Standards Service GmbH, Germany). As a result, the high MWCO and low MWCO at 1% of the maximum response were determined in MW calculation because the calculated MW value of PSS standard was closest to the value provided by the supplier.

The MWCO was based on the linear fitting baseline correction because linear fitting is simple and reproducible with common spreadsheet programs. After

baseline correction and determination of MWCOs,  $M_n$ ,  $M_w$  and  $\rho$  were then calculated using spreadsheet programs. Calibration was carried out every time when analysing HS samples. A day-to-day difference of approximately 5 % RSD for MW of AHA was observed.

Once the calibration condition and data analysis method have been decided, it was then tested on the calculation of the MW of AHA and SRFA which are model humic materials commonly used in HS research. The obtained MW values were found to be close to the published data (see chapter 5). An accurate calibration and calculation of MW would enable an inter-laboratory comparison. However, it should be kept in mind that due to the absence of PSS standards with intermediate MW and the heterogeneous nature of HS, an uncertainty of MW value obtained in this work might arise. It is therefore more appropriate to interpret the molecular size alteration of HS by their relative changes in MWD rather than their absolute values. In the following chapter, both the absolute MW values and the relative MW changes will be given and discussed.

In addition, destruction/formation curves were obtained by subtracting chromatograms of the irradiated HS from the non-irradiated HS, as suggested by Frimmel *et al.* (1998) and Lepane *et al.* (2003). Destruction/formation curves can directly provide information regarding the removal and accumulation of MW fractions. Results will be discussed in detail in chapter 5.

#### 4.4.6 pH

pH values were recorded using a Conductivity & pH meter (Jenway Ltd., UK). The pH meter was calibrated with pH buffer solutions 4.01, 7.01, and 10.01 every time prior to analysis.

## 4.5 Solar irradiation experiment

### 4.5.1 Basic experimental set-up

Before exposure to sunlight,  $UV_{254}$ , DOC, MWD and pH of HS solution in each bottle were measured. PET bottles containing HS solutions were placed in three collectors: compound parabolic collector (CPC), parabolic collector (PC) and bigger parabolic collector (BPC), which were located on the roof of Chadwick building, UCL. Each collector can place up to 4 bottles and the number of samples was determined according to each experimental design. Details of irradiation experiments are shown in Table 4.1, including duration, number of samples and sampling frequency. Each solar collector was positioned as a non-tracking static system inclined  $51^\circ$  (the latitude of London), and the bottles were aligned in an east-west orientation to maximise sunlight capture (Rodríguez *et al.*, 2004). The solar irradiation values were recorded during irradiation experiments by a CS300 pyranometer (Campbell Scientific, UK) which was mounted adjacent to solar collectors. Figure 4.4 presents a photograph of the solar irradiation experimental set-up taken on site.

HS solutions were placed in a flat tray which was covered by an aluminium foil sheet at the same experimental site (the tray can not be seen in Figure 4.4). These samples are also referred to as the HS solutions irradiated without concentrating sunlight. Some HS solutions were stored in the dark at room temperature, serving as a control which is referred to as the non-irradiated HS in this thesis.

**Table 4.1** Details of solar irradiation experiments, including experimental duration, solar collectors used and sampling frequency.

Experiment	Season	Duration	Initial DOC of HS sample (mg/L)	Solar collectors used	Sampling frequency*
Winter experiment	Winter	23/11/07-31/01/08	AHA 8.5	All	Every week
Spring experiment	Spring	08/03/08-17/04/08	AHA 8.3	All	Every week
Effects of pH value	Spring	08/05/08-22/05/08	AHA 8.3	CPC and Tray	Every 3 days
Summer experiment	Summer	01/07/08-04/09/08	AHA 8.5	All	Every 3-4 days
SRFA vs. AHA	Autumn	08/09/08-10/10/08	AHA 3.8 SRFA 5.1	BPC and Tray	Every 3-4 days
AHA vs. natural HS	Autumn	11/10/08-27/11/08	AHA 8.8 Natural 12.9	All	Every week
Column study	Winter-Spring	22/12/08-25/05/09	AHA 7.2	Tray	N/A

\*All experiments were duplicated



**Figure 4.4** Solar irradiation experimental set-up on the roof of Chadwick Building, UCL, London. From left to right: bigger parabolic collector (BPC), compound parabolic collector (CPC) and parabolic collector (PC).

After the completion of solar irradiation experiments, all the irradiated HS solutions were kept in the fridge at 4 °C for analysis and future adsorption experiments which were carried out within two weeks. All experiments were duplicated.

#### 4.5.2 PET bottles

To choose suitable containers for HS in solar irradiation experiments, several factors should be taken into account: (1) light transmission characteristics, (2) durability, (3) chemical stability, (4) availability, (5) cost, and (6) weight. Containers commonly used for HS photodegradation studies are made of quartz and Pyrex borosilicate glass materials (Schmitt-Kopplin *et al.*, 1998; Del Vecchio and Blough, 2002; McLoughlin *et al.*, 2004; Chow *et al.*, 2008). An alternative and cost-effective approach for small-scale solar applications is to use transparent PET bottles, which has been recommended by the Swiss Federal Institute of Aquatic Science and Technology (EAWAG) for the Solar Water Disinfection

(SODIS) project. The feasibility of using PET containers in drinking water disinfection treatment has been reported in several studies (Walker *et al.*, 2004; Mani *et al.*, 2006).

Quartz glass can transmit significantly more UV radiation than most of other materials, but is of very high cost. Glass bottles are relatively easily broken and of heavy weight. PET is an uncoloured transparent plastic material and widely used as the material for soft drink bottles. The advantages of using PET bottles are low weight, relatively unbreakable and of low cost. However, glass and PET materials selectively absorb some wavelengths of irradiation.



**Figure 4.5** The PET bottle used for solar irradiation experiment (source: Medfor Ltd., UK).

Difference in the light transmission properties of different materials was evaluated by means of UV/visible spectrophotometry and photodegradation tests on HS solutions. Transmittance of borosilicate glass (represented by a glass cuvette), quartz glass (represented by a quartz cuvette) and a plastic sheet (cut from a PET bottle into  $1 \times 3.5$  cm then inserted in a quartz cuvette) was compared at wavelengths from 300 to 700 nm using a spectrophotometer. Deionised water was served as a blank. Photodegradation experiments were carried out during a

good sunny week in April and a good sunny week in July. Considering the high cost of quartz bottles, only glass and PET containers were used. The comparison results will be discussed in chapter 5.

A picture of a PET bottle (Medfor Ltd., UK) used in solar irradiation experiments is presented in Figure 4.5. The bottle was round in cross-section with a diameter of 8 cm. It came with a white PP tamper-evident screw cap. In the preliminary experiments, PET bottles containing deionised water were exposed to sunlight for a few weeks and the  $UV_{254}$  absorbance of the irradiated deionised water was regularly checked. The observed results proved that no interference was generated from bottles by solar irradiation, indicating the chemical stability of PET material.

#### *4.5.3 Solar collectors*

Solar collectors used in this research were all static systems without sunlight tracking mechanisms. One collector had a compound parabolic profile and the other two had a parabolic profile. This was due, on one hand, to the easier installation and lower manufacturing cost of the static system than the sophisticated solar tracking systems at the laboratory trial level. In the second place, this study was the first to assess a possible combination of solar irradiation with GAC adsorption to enhance HS removal, applying simplified collectors would be sufficient to verify the hypothesis of this research and provide general information for solar collector applications with respect to the proposed solar-GAC method. As a consequence of the simplification, solar collectors used in this study would exhibit reduced sunlight concentrating efficiencies compared to those with sunlight tracking devices.

The size of each collector was designed according to the given PET bottle size (diameter of 8 cm). For the parabolic profile, the geometric focus of the parabola was 4 cm above the base to allow the PET bottle centre to meet the parabola focus (Figure 4.6). In theory, direct solar irradiation perpendicular to the parabolic collector aperture plane is reflected by the parabola to its focus. Parabolic collectors were made into two different sizes, the term BPC was used to distinguish the one of bigger size from the smaller one which was called PC thereafter. Both BPC and PC were designed on the basis of the following equation, written as (Gray *et al.*, 1997):

$$y = x^2/4f \quad (4.5)$$

where  $f$  is the distance of the focal point to the parabola bottom, which is 4 cm in this work. According to equation 4.5, the parabola was then plotted using the AutoCAD software. Table 4.2 presents the actual sizes of PC and BPC employed in this research. The profile of PC and BPC was the same as they were designed from the same equation, while the height of PC was only 1/3 of that of BPC. The size of PC was determined according to that of CPC (see Table 4.2 and Figure 4.8) in order to evaluate and compare the solar concentrating efficiencies of collectors with different profiles but similar aperture areas. The graphic design was then printed out at its actual designed size. The wooden frame of collector was fabricated first according to the graphic design. The reflective mirror surface was then placed firmly into the frame and cut to fit the frame. Pictures of PC and BPC are given in Figures 4.7a and 4.7b, respectively.

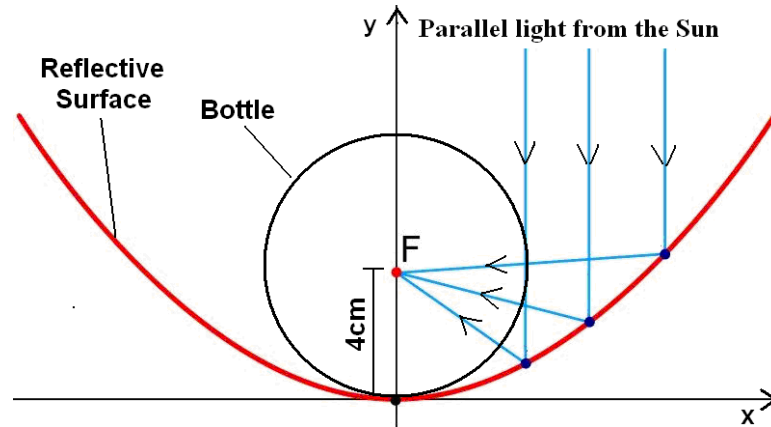


**Figure 4.6** Schematic of parabolic curve, showing the reflection of sunlight perpendicular to the parabolic collector aperture plane.

**Table 4.2** Sizes of solar collectors (PC, CPC and BPC) used in this research.

Solar collectors	Width (cm)	Height (cm)	Bottle centre above base (cm)
PC	25	10	4
BPC	40	32	4
CPC	25	10	6

The CPC has a surface area following an involute around a tubular container. The design of CPC in this study was based on the work by Blanco *et al.* (1999) and Rodríguez *et al.* (2004). Data in the CPC graph in these publications were extracted using the Engauge Digitizer software, transferred into Excel software and then plotted using the AutoCAD software. The graphic design was printed out at its actual size (given in Table 4.2) and the fabrication procedure was the same as that for the parabolic ones. Figures 4.8 and 4.7c present a schematic of CPC and a picture of CPC used in this research, respectively.

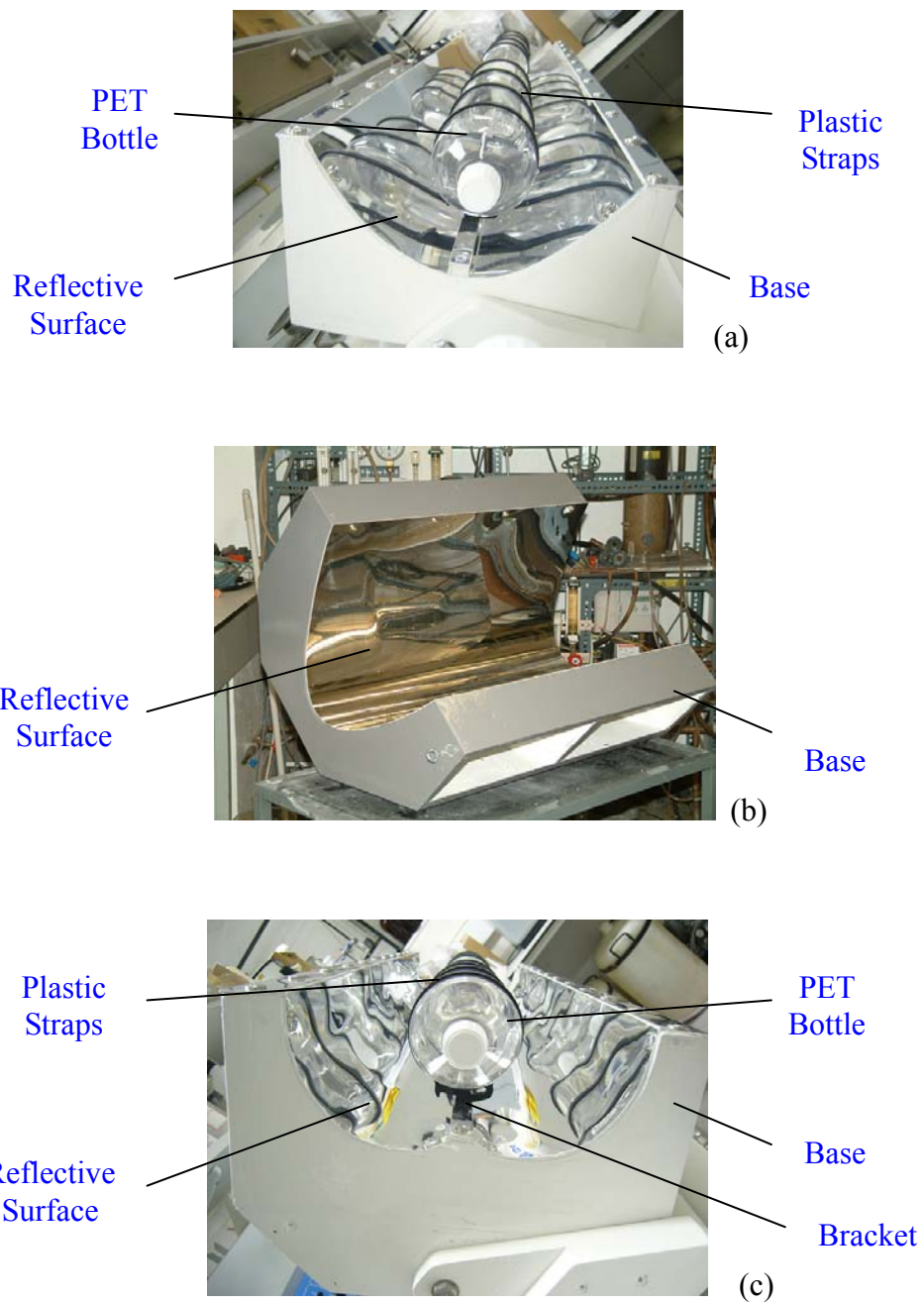


**Figure 4.7** Pictures of three solar collectors used in this research: (a) PC, (b) BPC, and (c) CPC.

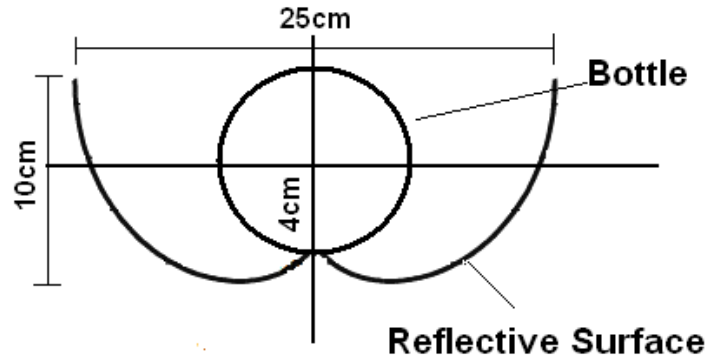


**Figure 4.8** Schematic of the compound parabolic curve (height 10 cm and width 25 cm) with 8 cm as the bottle diameter.

As solar collectors were fixed towards the same direction, their difference in sunlight concentrating efficiencies is considered to be mainly related to the difference in collector configuration and reflective area. CPC has been found to have the advantage of using both direct and diffuse irradiation. Thus, all light reaching CPC can be reflected to the sample located in the centre. That is:

$$Q_{\text{cpc}} = (I_{\text{dir}} + I_{\text{dif}}) A_{\text{cpc}} \quad (4.6)$$

where  $Q_{\text{cpc}}$  is the total solar energy received by HS solutions in CPC;  $I_{\text{dir}}$  and  $I_{\text{dif}}$  are the irradiation of direct and diffuse sunlight, respectively;  $A_{\text{cpc}}$  is the aperture area of CPC.

For the parabolic profile, assuming  $k_1$  as the concentrating factor ( $\leq 1$ ) for direct irradiation and  $k_2$  ( $\leq 1$ ) for diffuse irradiation, the total energy received by HS in two parabolic collectors is therefore expressed as:

$$Q_{\text{bpc}} = (k_1 I_{\text{dir}} + k_2 I_{\text{dif}}) A_{\text{bpc}} \quad (4.7)$$

$$Q_{\text{pc}} = (k_1 I_{\text{dir}} + k_2 I_{\text{dif}}) A_{\text{pc}} \quad (4.8)$$

The  $k_l$  value reaches its maximum (=1) at the moment when direct incident light is just perpendicular to the collector aperture during a day.

The sample in the flat tray can capture both direct and diffuse irradiation reaching the bottle area. That is:

$$Q_{\text{tray}} = (I_{\text{dir}} + I_{\text{dif}}) A_{\text{bottle}} \quad (4.9)$$

If the concentrating factors  $k_1$  and  $k_2$  both reach their maximum values, solar energy received by HS samples in different collectors under the same weather conditions is in a order as: Tray < PC = CPC < BPC. In this case, the concentrating efficiencies of solar collectors relative to the flat tray are estimated to be approximately 3 (CPC and PC) and 5 (BPC), according to the aperture size and bottle diameter. The order and concentrating efficiency can be influence by (1) the concentrating factors  $k_1$  and  $k_2$ , which are constantly changing with the position of sun and time of day, and (2) the relative amount of direct and diffuse irradiation in total solar irradiation. Therefore, the solar concentrating efficiency of solar collectors used in this research would be lower in practice.

In the photocatalytic applications, mirrors based on aluminium are considered to be the best option owing to its low cost and high reflectivity. The reflective aluminium mirror attached to a layer of high impact polystyrene sheet was purchased from Amari Plastics plc. (UK) and shaped according to the collector design to fit the supporting frame as previously described.

#### *4.5.4 Solar irradiation measurement*

A CS300 pyranometer was used to measure solar irradiation and connected with an EnviroMon data logger (Pico Technology Limited, UK). According to the

manual by the supplier (Campbell Scientific, UK), the CS300 pyranometer can accurately measure solar irradiation from 300 nm to 1100 nm. The conversion factor (5.00 W m<sup>-2</sup> per mV) was used to convert the voltage (mV) signal from the sensor head to solar intensity in the unit of W m<sup>-2</sup>, calculated as:

$$I = S \times \text{conversion factor} = S \times 5 \text{ W m}^{-2} \text{ per mV} \quad (4.10)$$

where  $I$ : solar intensity [W m<sup>-2</sup>];

$S$ : output of sensor head recorded by data logger [mV].

The total solar dose (J m<sup>-2</sup>) received by the earth surface of the experimental site was calculated from the accumulation of solar irradiation as:

$$E = \sum_{i=1}^n I_n \times t = \sum_{i=1}^n I_n \times 60s \quad (4.11)$$

where  $E$ : total solar dose [J m<sup>-2</sup>]

$I_n$ : average solar intensity recorded every minute [W m<sup>-2</sup>]

In addition, solar irradiation and UV data for the same period were obtained from the National Meteorological Library and Archive for comparison purposes.

## 4.6 Granular activated carbon adsorption experiment

### 4.6.1 Characterizing GAC

Adsorption studies of HS were performed with a commercial GAC (AquaSorb 101) purchased from Universal Mineral Supplies, UK. It is said to be a highly economical, medium activity GAC manufactured by steam activation from

selected grades of bituminous coal and typically used in municipal drinking water treatment and adsorption of taste and odour (information provided by the supplier). GAC was used as received without modifications and kept in a desiccator if not in use.

Characteristics of GAC determined in this work included surface area and pore size distribution. Surface area and porosity analysis was performed on a Coulter Omnisorp 100 (Beckman-Coulter, UK) at Imperial College, London, UK. In brief, the measurement was based on the adsorption isotherms of nitrogen onto a solid increasing with the pressure of gas at 77 K. Prior to analysis, GAC was degassed for 7-8 hours at 150 °C. Surface area was calculated from the Brunauer Emmett and Teller (BET) equation. Pore size distribution of GAC was determined using the t-plot method which indicates the amount of meso- and macropores in the carbon. Analytical results were provided by Imperial College and will be discussed in next chapter.

#### *4.6.2 Adsorption isotherm study (batch experiments)*

Batch adsorption experiments were conducted to determine the equilibrium isotherms which can be used to describe the adsorption behaviour of HS by GAC. Prior to adsorption, all flasks were soaked in a 10 % nitric acid bath overnight, washed with deionised water and dried in the oven at 105 °C for 24 hours. Isotherm experiments were performed in 100 ml flasks sealed with parafilm. The equilibrium adsorption was set to 6 days based on the preliminary kinetics studies. 0.005, 0.01, 0.02, 0.05, 0.1 and 0.2 g GAC were carefully weighed and added in a series of 50 ml HS solutions separately. The HS solutions were agitated in a temperature-control shaker (Stuart Orbital Incubator, Barloworld Scientific Ltd., UK) at 22±1 °C at 200 rpm. The shaker was equipped with dark

brown glass walls to avoid any light interference. Two types of blanks were served as controls - flasks containing HS solutions without GAC, and flasks containing GAC in contact with deionised water only. They were to ensure that HS did not attach to the wall of flasks to affect analytical results and no organic matter was released from GAC to interfere the measurement, respectively. After equilibration, an aliquot of solution was filtered through a pre-washed 0.45  $\mu\text{m}$  filter for further analysis as described in the “analytical methods” section.

The amount of HS adsorbed by GAC was calculated using the following equation:

$$q_{DOC} = \frac{DOC_0 - DOC_{eq}}{\frac{m}{0.05}} \quad (4.12)$$

where  $q_{DOC}$ : HS adsorbed by GAC in terms of DOC [ $\text{mg g}^{-1}$ ];

$DOC_0$ : initial DOC concentration of HS [ $\text{mg L}^{-1}$ ];

$DOC_{eq}$ : equilibrium DOC concentration of HS [ $\text{mg L}^{-1}$ ];

$m$ : mass of GAC in the flask [g].

The adsorption isotherms were plotted as the amount of HS remaining in solution ( $C_{eq}$ ) and against the amount of HS adsorbed per gram of adsorbent ( $q_e$ ).

#### 4.6.3 Small column experiments

Column experiments were carried out to obtain HS breakthrough curves under continuous flow conditions. The small column study was based on the rapid small scale column test (RSSCT) method.

#### 4.6.3.1 GAC preparation

The preparation of GAC followed the description in the standard RSSCT method (Crittenden *et al.*, 2005). GAC used for isotherm experiments was received as 12/40 mesh (particle size range of 420-1680  $\mu\text{m}$ ) and considered to be the GAC used in the full-scale column. The smaller GAC used in RSSCT studies was obtained by crushing the GAC for the full-scale column. The crushed carbon was sieved to obtain the 60/80 mesh size fraction (particle size range of 177-250  $\mu\text{m}$ ). Crushing and sieving were continued until all of the GAC passed through the upper sieve. The GAC retained on the bottom sieve was removed, washed with deionised water, dried overnight at 105 °C and kept in a desiccator until use.

#### 4.6.3.2 Column set-up

All RSSCT studies were carried out at room temperature. The schematic of the column experimental design is shown in Figure 4.9. A small glass column having an internal diameter of 1 cm and a total length of 20 cm was used. The influent water was supplied from a head tank to the small column and the flow rate was controlled by a flow meter connected with a Teflon tube to the column inlet. Wall effects were minimised because the ratio of column diameter to GAC particle size was  $\sim 50$  (Crittenden *et al.*, 1986 and 1991). The GAC bed was supported by a 100 micron mesh screen and both column ends were fitted with Teflon end adapters. All of these apparatus were cleaned thoroughly before use.

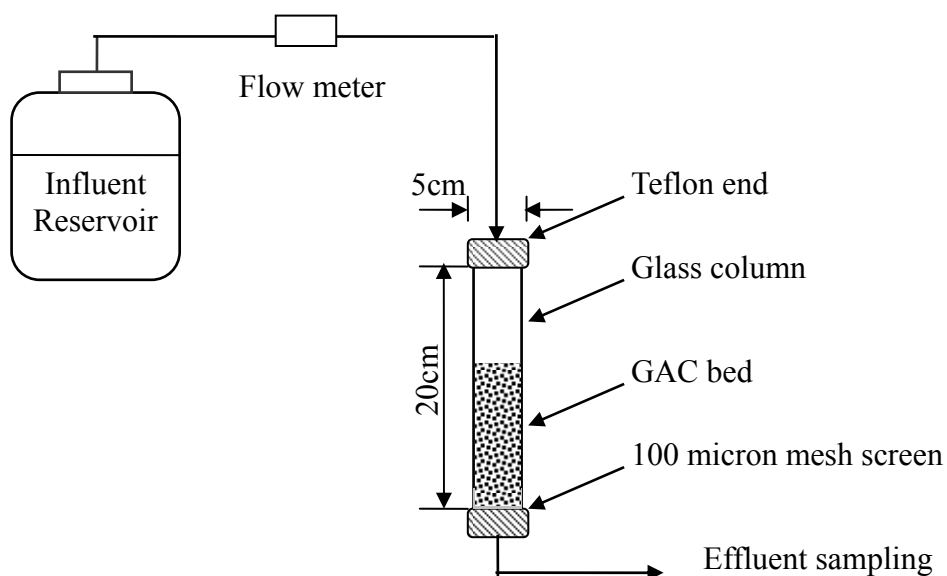


**Figure 4.9** Schematic of the rapid small scale column test (RSSCT) experiment.

**Table 4.3** A summary of the rapid small scale column test (RSSCT) parameters used in this study.

Particle diameter (mm)	0.21 (60/80)
Column diameter (cm)	1.0
Column length (cm)	20
Bed length (cm)	8.33
Mass of GAC (g)	3.4
EBCT (min)	1.05
Flow rate (ml/min)	6.23
Loading rate (m/h)	4.76

A summary of experimental parameters for RSSCT studies is tabulated (Table 4.3).

A designated amount of GAC was pre-wetted with deionised water and carefully

packed into the column using a spatula. The column was backwashed with deionised water during and after packing to eliminate air so as to reach the designated bed length at approximately 8.5 cm. HS samples were filled into the head tank and the flow rate was set at the desired value. A check on the small column system was undertaken every time when sampling to ensure no air was present in the influent tube and the flow rate was maintained within 5 % of the designated flow rate. Experiments were duplicated.

Column effluent samples were collected using 10ml pre-washed Pyrex glass vials from the tube connected to the outlet.  $UV_{254}$  absorbance was measured immediately. Samples for DOC and HPSEC analysis were stored in the fridge at 4 °C until use.

## CHAPTER 5

### RESULTS AND DISCUSSIONS

#### 5.1 Introduction

It has been concluded from the literature review that humic substances (HS) can be broken down into smaller organic molecules by solar irradiation. Furthermore, the adsorption capability of a given granular activated carbon (GAC) for HS is expected to increase with decreasing molecular size. In the search for effective HS removal treatment processes, it has been found that using artificial UV irradiation can enhance the removal of HS in the following biological activated carbon process. For example, Buchanan *et al.* (2008) reported that the removal of HS was improved by 26 % when UV irradiation was used as a pre-treatment method prior to GAC adsorption. This is due to UV irradiation fragmenting high molecular weight (MW) compounds into smaller molecules. However, using artificial UV light makes the treatment expensive. UV irradiation can also be found in natural sunlight spectrum. Despite this, solar effects on the properties and reactivity of HS with respect to the subsequent GAC adsorption have not been related nor studied in detail. No published report to date, known to the author, has encouraged a series of experiments to be carried out, aiming at evaluating the solar irradiation-GAC method and exploring the potential use of natural sunlight to enhance the removal of HS.

The discussion of the experimental results essentially consists of two main

sections - solar irradiation and GAC adsorption.

The first section discusses the effects of solar irradiation on HS properties with respect to UV absorbance at 254 nm ( $UV_{254}$ ), dissolved organic carbon (DOC) concentration and molecular weight (MW). Since natural sunlight was used as the source of energy, it is essential to know the characteristics of natural sunlight during the experimental period and therefore establish the correlation between solar irradiation and HS properties. The performance of different solar collectors which were applied to promote the photodegradation of HS is quantitatively evaluated by fitting kinetics models. Some parameters relevant to HS photodegradation, including pH and microbial activities, are discussed. Finally, solar irradiation effects on the properties of Suwannee River fulvic acid (SRFA) and a natural water sample are assessed, supporting the observations made on the Aldrich humic acid (AHA) which is a model material.

The second section discusses the removal of HS by GAC adsorption, subsequent to solar irradiation. For each set of experiments, isotherms are first examined to describe the adsorption behaviour of HS, followed by the application of adsorption models to fit experimental data to enable a quantitative description of the influence of the pre-treatment using solar irradiation on the GAC adsorption process. Results are further discussed on the basis of the high performance size exclusion chromatography (HPSEC) measurement. In addition, results from continuous flow studies using the rapid small scale column test (RSSCT) method are discussed, providing essential information to the effectiveness and feasibility of using solar irradiation to improve the GAC adsorption performance.

## 5.2 Effects of solar irradiation on the properties of HS

### 5.2.1 Evaluation of solar irradiation

Investigations on the photodegradation of HS were carried out under natural sunlight. It is clear that solar irradiation and the UV level are constantly changing from day to day and from season to season for a given location. The real-time solar irradiation values were recorded by a CS300 pyranometer (Campbell Scientific, UK) located on site. Details of the solar measurement can be found in Chapter 4. In the following content, the solar irradiance will be expressed as the ‘solar intensity’ in  $\text{W}/\text{m}^2$ , or the ‘solar dose’ in  $\text{kJ}/\text{m}^2$ , which is determined from the intensity and the irradiation time. A summary of the accumulative solar dose in each experiment is presented in Table 5.1. As shown, solar irradiation values greatly varied with season and duration of experiments. For example, the total solar irradiation in summer was four times more than that in winter for the same experimental duration.

**Table 5.1** Accumulative solar dose during irradiation experiments at Chadwick Building of UCL, London, UK.

Experiment	Accumulative solar dose ( $\times 10^5 \text{ kJ}/\text{m}^2$ )
Winter period	1.44
Spring period	2.61
Summer period	5.97
Initial pH effects	1.59
SRFA vs. AHA	1.96
Natural water vs. AHA	1.42

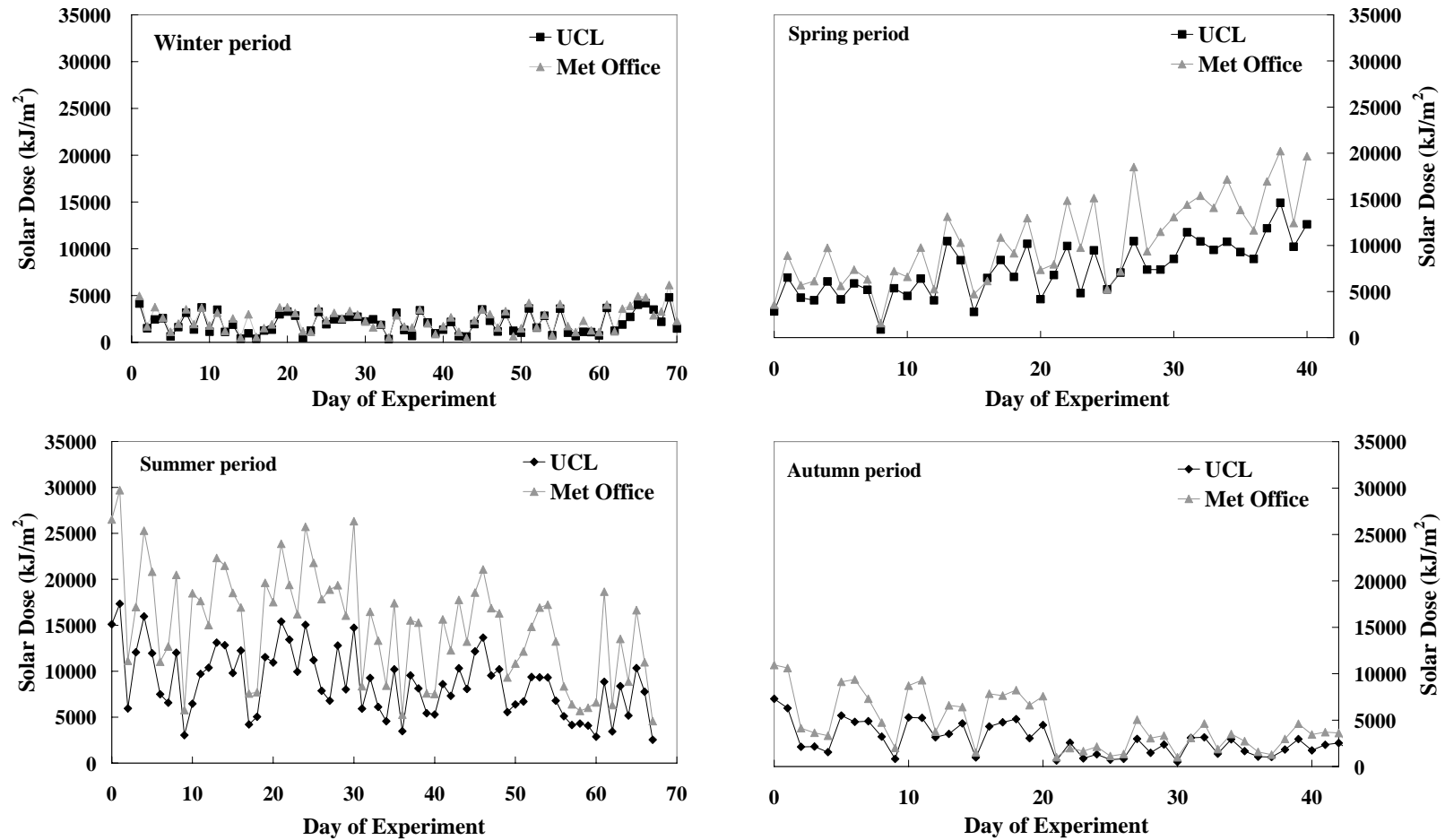


**Figure 5.1** Distribution of daily solar dose for four seasons: data recorded at UCL and by Met Office.

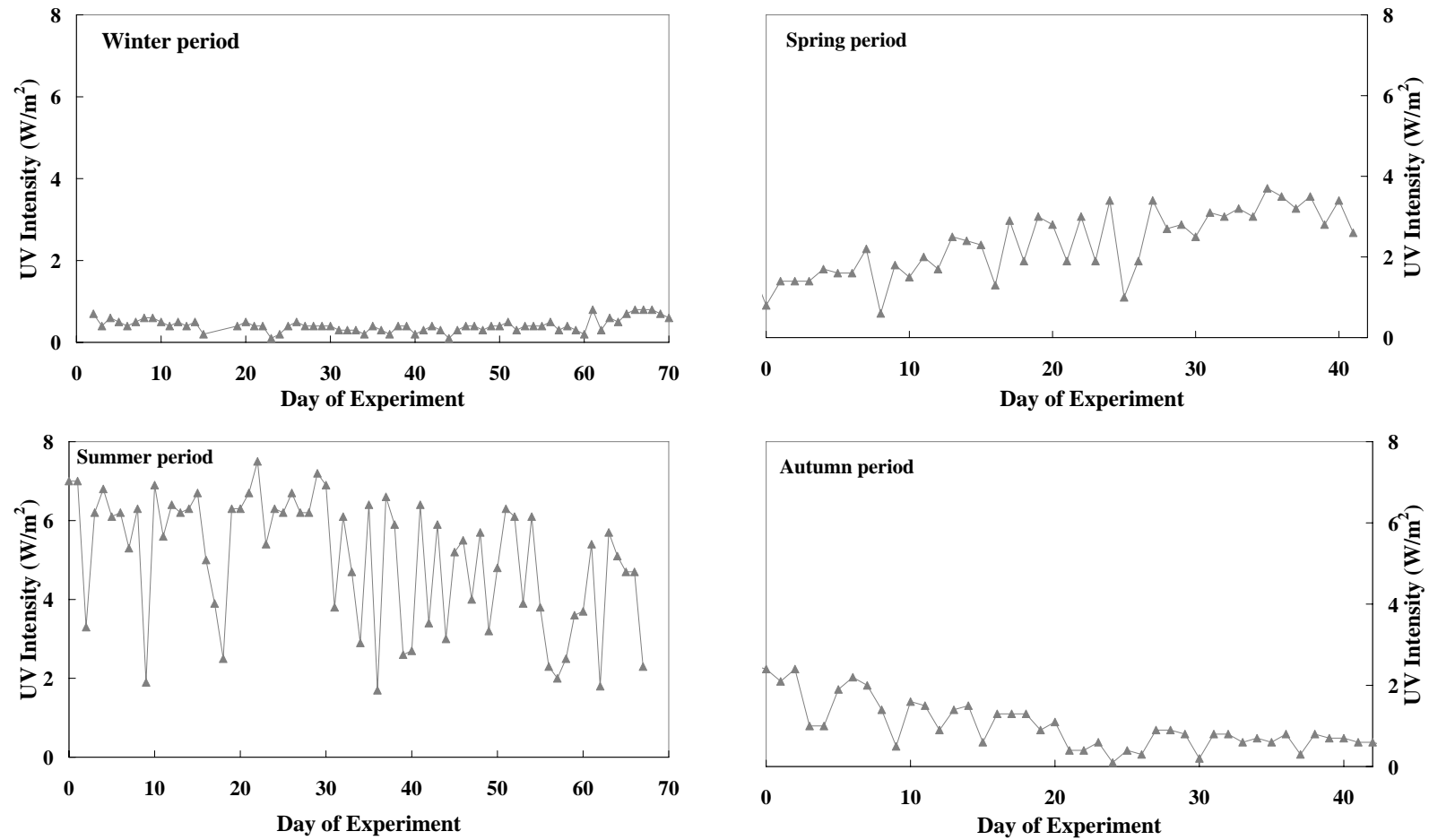


**Figure 5.2** Distribution of daily UV intensity for four seasons.

For comparison and validation purposes, solar irradiation data recorded by Meteorological Office (Met Office) during the same period were collected from the Met Office National Meteorological Library and Archive. The daily variations of solar data recorded at UCL and by the Heathrow meteorological station (which is the nearest meteorological station to UCL) for four seasonal experiments are illustrated in Figure 5.1. The followings were observed: (i) similar trend of UCL and Met Office data in each season; (ii) minor difference between UCL and Met Office data when solar intensity was low, such as in winter, early spring and late autumn; and (iii) significant difference when solar intensity was high, i.e. during the summertime.

The deviation of UCL experimental measurement from Met Office data can be attributed to the following potential reasons:

- The CS300 pyranometer measures both UV and visible irradiation ranging from 300 to 1100 nm (information from the supplier). The pyranometer used at the Heathrow meteorological station is the CM 11 type (Kipp & Zonen) which measures irradiation at spectral range 310-2800 nm. About 90 % of sunlight energy is between 300 and 1100 nm. Therefore, the observed data at UCL should be at least 10 % lower than the meteorological data.
- The accuracy of solar measurement may lead to the difference between experimental data and meteorological data. According to the supplier (Kipp & Zonen), the CS300 and CM 11 pyranometers have  $\pm 5$  % and  $\pm 3$  % accuracies, respectively, for the irradiation measurement.
- The location of the experimental site limited the incident light to the experimental installations. Some buildings nearby are taller than the

Chadwick Building where experiments were conducted. These taller buildings may directly affect the amount of solar irradiation reaching the experimental site, in particular the direct irradiation. In the summer, there is an increased proportion of direct irradiation in total solar irradiation compared to winter (McVeigh, 1983). This provides a plausible explanation for the big discrepancies in solar measurement taken during the summer.

It should be noted that the Heathrow meteorological station is about 25 kilometres (km) away from UCL. According to McVeigh (1983), in the UK it can be assumed that the average irradiation data from any meteorological station within 150 km are adequate for practical design purposes. Based on the observation in this research, it can be concluded that this assumption is probably applicable only to open sites without incident light being interfered by surroundings.

The above comparison validates the solar measurement at UCL. Results from this research can therefore well present the correlation between the photodegradation of HS and natural sunlight, and can be used as a reference for future research activities.

Considering the aim of this research, UV irradiation at the experimental site was not measured in detail. The daily maximum UV data obtained through Met Office are used here to provide general information for evaluating UV irradiation during the experimental period of this study. A summary of UV measurement results corresponding to Figure 5.1 is presented in Figure 5.2. As shown, the distribution of UV irradiation is generally similar to that of the total solar irradiation, with the highest intensity occurring in the summer period, and significantly lower in winter. According to the Met Office data, it is estimated that UV irradiation accounted for no more than 0.6 %, 1.5 %, 3.2 % and 1.3 % of

natural sunlight irradiation for winter, spring, summer and autumn periods, respectively. As expected, UV intensity in London is much lower compared to other regions. The maximum UV intensity during the experimental period was  $7.5 \text{ W/m}^2$ . As an example, the average UV intensity ranging between  $22 \text{ W/m}^2$  and  $44 \text{ W/m}^2$  was reported by McLoughlin *et al.* (2004) who conducted solar disinfection research in Spain.

### 5.2.2 Light transmission characteristics of experimental bottles

In HS photodegradation studies and solar applications, experiments are normally conducted using quartz or Pyrex borosilicate glass containers with small volumes of solutions (Schmitt-Kopplin *et al.*, 1998; Del Vecchio and Blough, 2002; Chow *et al.*, 2008). In this research, however, a large volume of water was required (at least 15 L in each set of experiment), which means a number of containers were needed. Therefore, when choosing experimental containers, availability should be firstly taken into account. In addition, compared to glasses, polyethylene terephthalate (PET) material has the advantage of being light and not easy to break. These advantages made it more appropriate to use PET bottles for convenient transportation and safety reasons as experimental site was on the roof of Chadwick building. Due to the good light transmission capability of PET material, PET bottles have been recommended for the SODIS method which makes use of the UV-A irradiation in sunlight to disinfect contaminated water. As discussed in the literature review, the UV-A irradiation also plays an important role in the photodegradation of HS. Based on the above considerations, PET bottles were chosen as containers in the solar irradiation experiments in this research.

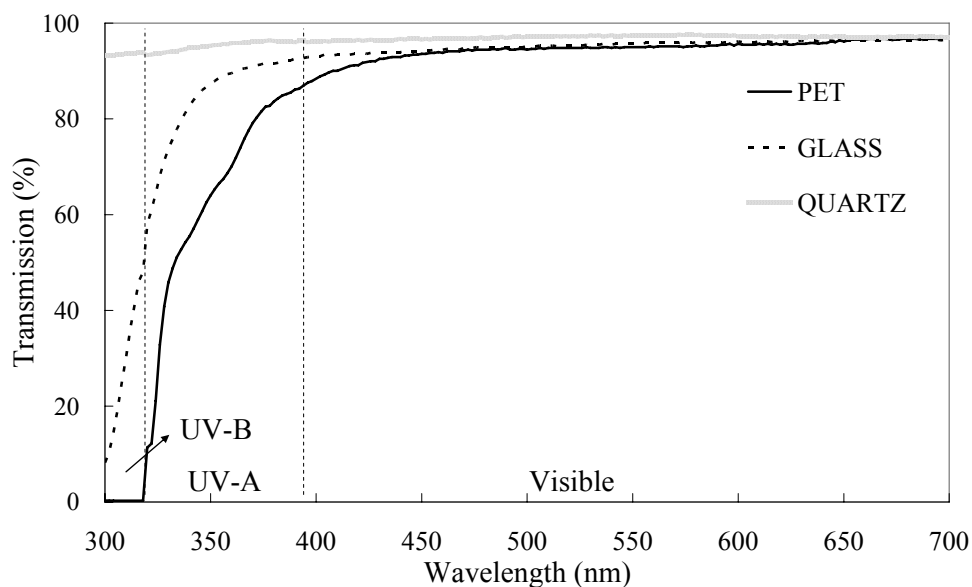


**Figure 5.3** Light transmission characteristics of quartz, borosilicate glass and PET materials as a function of wavelength, measured on a UV-visible spectrophotometer.

It was necessary to evaluate the difference in light transmission and photodegradation of HS when using PET, quartz and glass materials. The percentage of light transmission through quartz glass, borosilicate glass and PET bottles as a function of wavelength (300-700 nm) was measured on a UV-visible spectrophotometer, as illustrated in Figure 5.3. Quartz material showed the best light transmission capability, while borosilicate glass and PET materials selectively absorbed irradiation. As shown, quartz glass can transmit more than 95 % of irradiation over the entire wavelength range, with excellent transmission capacity at UV range. Borosilicate glass can transmit more than 95 % of visible light, 85 % on average of UV-A light, and 30 % of UV-B light. PET material has almost the same light transmission capability for visible light as does borosilicate glass, but reduced transmission at UV range, with about 66 % and only 2 % for UV-A and UV-B irradiation, respectively. The observed distribution of light

transmission characteristics of these materials is in good agreement with the observations made by Reche *et al.* (1999) and Mani *et al.* (2006). A comparison of light transmission characteristics of different materials reveals that the use of PET material does not affect the effect of visible light on the photodegradation of HS. However, by using PET material, the effect of UV irradiation on HS photodegradation is reduced compared to using quartz and borosilicate glass materials.

An investigation on the photodegradation of HS solutions in PET and borosilicate glass bottles was carried out during a sunny week in spring and a sunny week in summer, with total solar doses  $3.39 \times 10^4 \text{ kJ/m}^2$  and  $8.59 \times 10^4 \text{ kJ/m}^2$ , respectively. All samples were tested when they cooled down to the room temperature; however, temperature was not measured in the experiment. It is likely that the temperature in summer was higher, which may affect the photodegradation of HS. A decrease in  $UV_{254}$  and absorbance over the entire UV/visible spectrum was observed in all the irradiated HS solutions with initial  $UV_{254} 0.37 \text{ cm}^{-1}$  (Figure 5.4). Figure 5.4b shows a gradual decrease of absorbance with increasing wavelength, which is in agreement with previous observations (refer to section 2.2.1). This is due to the presence of numerous high energetic and aromatic structures that do not have distinguishable adsorption spectra. As there is no UV-C in natural sunlight, the absorbance decrease between 220 nm and 280 nm can be attributed to the indirect photodegradation by UV-A, UV-B and visible light. For the HS solutions in PET bottles, the absorbance decrease between 220 nm and 280 nm was caused by the indirect photodegradation by UV-A and visible light since UV-B irradiation was blocked by PET material (Figure 5.3). The absorbance decrease above 280 nm can be explained by both direct and indirect photodegradation (refer to section 2.3.2.1) as both UV-A and visible light were received by HS solutions (Figure 5.3). Figure 5.4 shows that: (1) under the same

irradiation condition, the absorbance decrease at 254 nm and the entire spectrum in borosilicate glass bottles was slightly more than that in PET bottles, probably due to the glass material being more transparent to the UV irradiation, as demonstrated in Figure 5.3; and (2) spectral changes of HS in PET and glass bottles followed a similar trend. These observations confirm that the use of PET bottles in HS photodegradation studies can provide comparable data to those using borosilicate glass bottles. If positive outcomes can be obtained through using PET bottles in the solar-GAC method, more pronounced results would be expected if the UV-transparent bottles, such as quartz and borosilicate glass bottles, are applied.

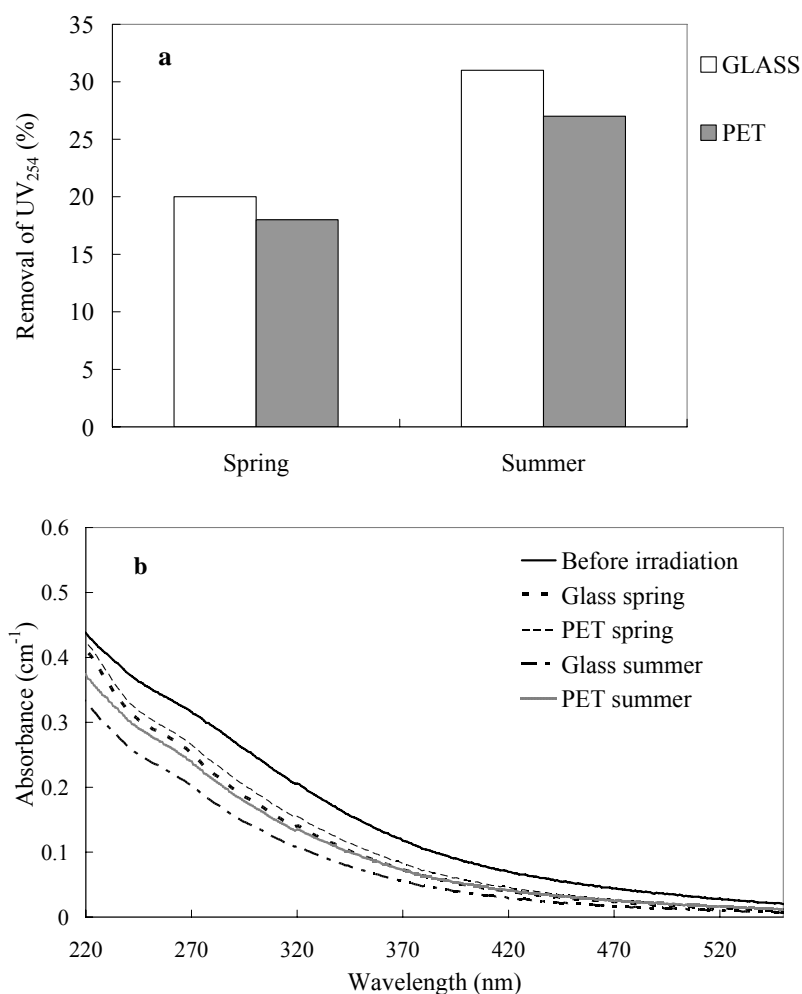


**Figure 5.4** Changes in (a) UV<sub>254</sub> absorbance and (b) UV/visible absorption spectrum of HS solutions in PET and glass bottles due to solar irradiation in

spring (solar dose  $3.39 \times 10^4$  kJ/m<sup>2</sup>) and summer (solar dose  $8.59 \times 10^4$  kJ/m<sup>2</sup>) with initial UV<sub>254</sub>=0.37 cm<sup>-1</sup>.

**Table 5.2** Characteristics of HS solutions prior to solar irradiation in winter experiments (solar dose  $1.44 \times 10^5$  kJ/m<sup>2</sup>).

pH	UV <sub>254</sub> (cm <sup>-1</sup> )	DOC (mg L <sup>-1</sup> )	SUVA (L mg <sup>-1</sup> m <sup>-1</sup> )	M <sub>n</sub> (Da)	M <sub>w</sub> (Da)	ρ
7.7	0.67	8.50	7.9	1561	4092	2.62

SUVA: specific UV absorbance

M<sub>n</sub>: number average molecular weight

M<sub>w</sub>: weight average molecular weight

ρ: polydispersity

### 5.2.3 Seasonal evaluation of solar irradiation on HS characteristics

#### 5.2.3.1 Winter experiment

Experiments were carried out during the winter period with a total solar dose of  $1.44 \times 10^5$  kJ/m<sup>2</sup>. Table 5.2 presents the characteristics of HS solutions prior to solar irradiation. The DOC concentration for HS solutions was selected to the range between 8 to 9 mg/L, as this range was considered to represent a typical level of HS in natural waters. As a consequence of solar irradiation, a reduction in DOC concentration was observed in all HS solutions, as shown in Figure 5.5. Each data point represents an average of results for duplicate samples in each collector. The DOC reduction due to irradiation can be explained by the production of CO, CO<sub>2</sub> and other forms of inorganic carbon matter (Moran and Zepp, 1997; Zuo and Jones, 1997; Xie *et al.*, 2004). CO and CO<sub>2</sub> may transfer to the atmosphere, with the latter possibly being dissolved in water and lowering the pH of water as a result (Patel-Sorrentino *et al.*, 2004). The DOC reduction increased with increasing solar irradiation, with a final removal of 11-15 %. The DOC reduction of HS solutions in solar collectors was slightly more than that in

the tray, but the difference was insignificant. A possible reason behind these minor variations is the lower solar intensity during the winter months being insufficient for a complete photodegradation of HS.

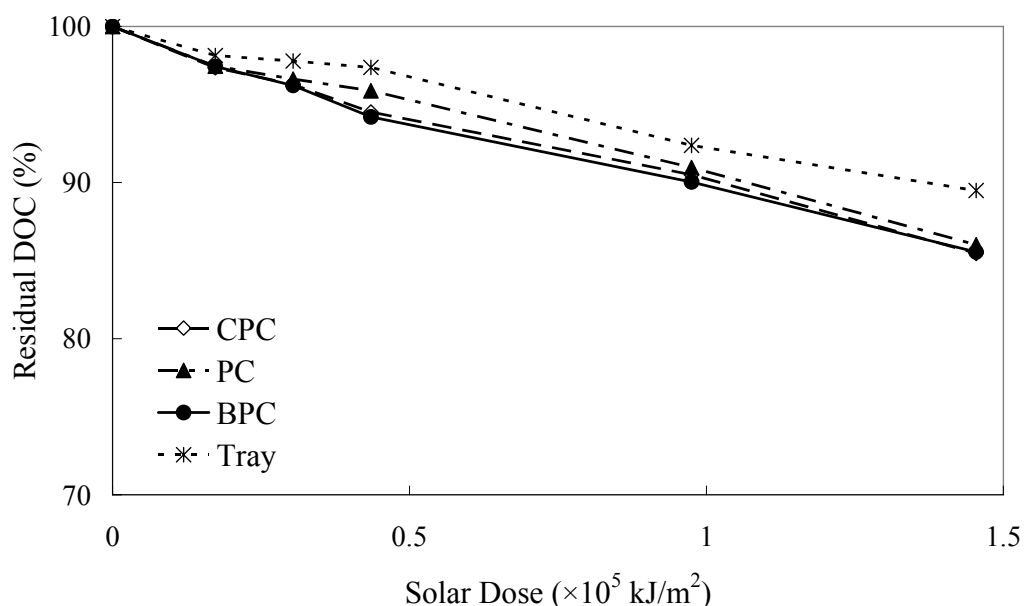


**Figure 5.5** Effect of solar irradiation on the DOC concentration of HS in different solar collectors in winter (initial DOC 8.50 mg/L, solar dose  $1.44 \times 10^5$  kJ/m<sup>2</sup>).

UV<sub>254</sub> absorbance was measured to evaluate solar irradiation effects on specific chromophoric groups of HS, rather than the total organic matter. It is a good indicator of the aromatic chromophores which have a high reactivity toward chlorination to form disinfection by-products (DBPs). A decrease in UV<sub>254</sub> therefore indicates the alteration and destruction of aromatic structures, as well as the reduced DBP formation potential. Under natural sunlight, the decrease of UV<sub>254</sub> can probably be explained by the indirect photodegradation pathway, as there is no UV-C irradiation reaching the earth. Figure 5.6 shows a gradual decrease of UV<sub>254</sub> with increasing solar irradiation, with approximately 14-20 % of UV absorbing chromophores finally being removed. In general, given a long

exposure time in winter, HS were ineffectively removed in terms of  $UV_{254}$  and DOC, due to the low solar intensity.

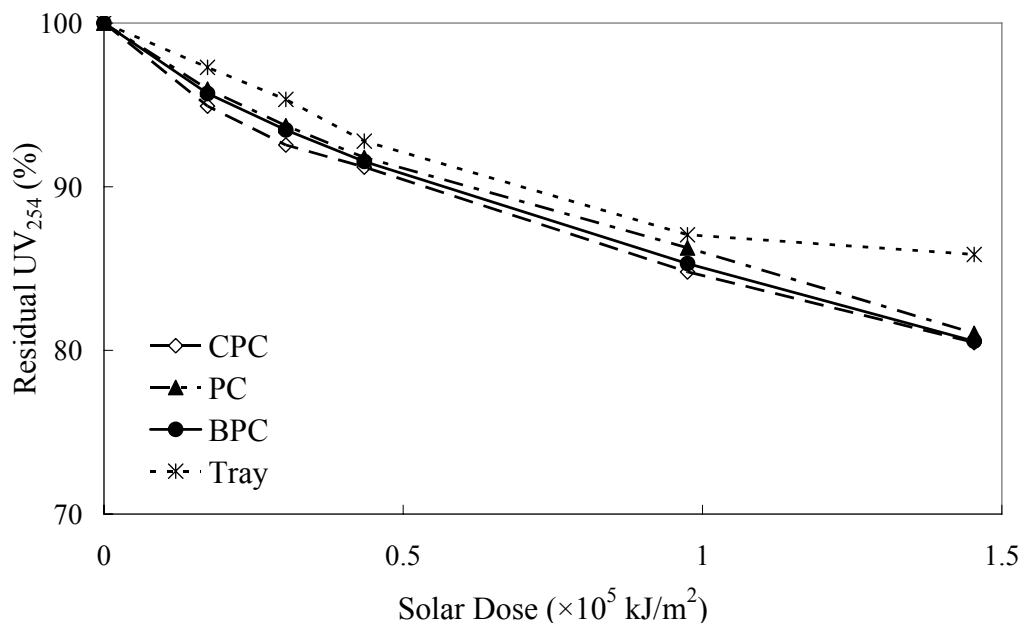


**Figure 5.6** Effect of solar irradiation on the  $UV_{254}$  absorbance of HS in different solar collectors in winter (initial  $UV_{254}$   $0.67 \text{ cm}^{-1}$ , solar dose  $1.44 \times 10^5 \text{ kJ/m}^2$ ).

It should be pointed that in Figures 5.5 and 5.6, the removal of HS is plotted against the accumulative solar dose which is the solar irradiation received by the earth surface of the experimental site. The actual solar irradiation received by HS solutions is a function of the incident sunlight and the solar collector configuration. It is also partially reduced by the PET material. The complexity of predicting the incident and reflected sunlight within collectors, however, does not allow for an accurate calculation or measurement of the solar irradiation actually received by HS solutions placed in solar collectors. Therefore, one can not directly plot the HS removal as a function of the actual solar irradiation received by HS solutions. If the removal of HS is only attributed to solar irradiation, then any observed difference in HS removal would reflect the

difference in solar irradiation received by samples. As a consequence, expressing experimental results as a function of solar irradiation received by the earth surface would allow for a direct comparison of the concentrating efficiencies between different collectors.

Photodegradation of HS has been previously reported to follow the first-order reaction, as presented in equation 5.1 (Kieber *et al.*, 1990; Zuo and Jones, 1997; Xie *et al.*, 2004; Chow *et al.*, 2008). Similarly, in this study, the HS removal fitted the first-order reaction with an  $R^2 > 0.96$  for most of HS solutions.

$$C = C_0 e^{-kt} \quad (5.1)$$

where  $C_0$  is the initial concentration of HS in mg/L,  $k$  is the first-order decay rate constant in  $s^{-1}$  and  $t$  is the reaction time in s. The reaction time can be substituted by the solar dose, which can be obtained from equation 4.11.

The kinetics of the photodegradation of HS, with respect to DOC concentration and  $UV_{254}$  absorbance, can therefore be calculated from the following equations:

$$\ln[\text{DOC}] = \ln[\text{DOC}]_0 - k_1 Q \quad (5.2)$$

$$\ln[\text{Abs}] = \ln[\text{Abs}]_0 - k_2 Q \quad (5.3)$$

where  $[\text{DOC}]_0$  is the initial DOC concentration in mg/L;  $[\text{DOC}]$  is the DOC value when sampling in mg/L;  $[\text{Abs}]_0$  is the initial  $UV_{254}$  absorbance in  $\text{cm}^{-1}$ ;  $[\text{Abs}]$  is the  $UV_{254}$  when sampling in  $\text{cm}^{-1}$ ;  $k_1$  is the first order decay rate constant for DOC and  $k_2$  is the first order decay rate constant for  $UV_{254}$ . A summary of the calculated first-order decay rate constants is presented in Table 5.3.

**Table 5.3** First-order decay rate constants of HS irradiated in different solar

collectors in winter experiment (DOC removal 11-15 %, UV<sub>254</sub> removal 14-20 %, solar dose  $1.44 \times 10^5$  kJ/m<sup>2</sup>).

Solar collectors	$k_1^*$	$k_2^*$
CPC	0.109	0.163
PC	0.102	0.152
BPC	0.110	0.159
Tray	0.077	0.121

\* unit:  $\times 10^{-5}$  m<sup>2</sup>/kJ

As shown, HS solutions in different solar collectors followed the same order of reactions, with varying  $k$  values. In a first-order reaction, the coefficient  $k$  stands for the slope of the ln-linear regression. The higher the value of  $k$ , the faster the photodegradation process is. The decay rate constant  $k$  depends on irradiation intensity, water characteristics and geometry of the solar collector (Ajona and Vidal, 2000; Vidal and Díaz, 2000). By comparing the  $k$  values of samples, a few observations were made as follows:

- Using solar collectors enhanced the removal of HS. When using compound parabolic collector (CPC), parabolic collector (PC) and big parabolic collector (BPC), the photobleaching (decrease in UV<sub>254</sub>) rate of HS was promoted by approximately 35 %, 26 % and 31 % relative to using the tray, respectively. The enhancement is attributed to more solar energy being collected and reflected to HS samples by solar collectors. Although solar irradiation in winter was fairly low, this result supports the view that solar collectors may be applied to improve the photodegradation of HS.
- Differences between solar collectors with regard to the enhancement of HS

removal were small. Although having a much smaller reflective surface area, CPC showed a similar photodegradation rate to that of BPC. According to Rodríguez *et al.* (2004), CPC has the advantage of concentrating diffuse solar irradiation. The diffuse irradiation accounts for more than 75 % of total solar irradiation in the winter in UK (McVeigh, 1983). The result in winter study therefore demonstrates that the compound parabolic profile can give a better diffuse sunlight capture than the parabolic profile.

- The decay rate constant of DOC was lower compared to that of  $UV_{254}$ . Assuming that the UV absorbing chromophores in HS were completely broken down to  $H_2O$ , CO and  $CO_2$  by solar irradiation, the rate of DOC reduction should be identical to, or higher than, the rate of  $UV_{254}$  reduction. The unequal rates indicate the destruction of aromatic structures resulting in the formation of some dissolved organic compounds that have less UV light absorptivity than their parent materials but still contribute to DOC value. Similar observations have been reported by Corin *et al.* (1996), Chow *et al.* (2008) and Rodríguez-Zúñiga *et al.* (2008). In addition, the greater reduction of  $UV_{254}$  relative to DOC has led to a slight decrease in the SUVA of the irradiated HS (from 7.9 to 7.4  $L\ mg^{-1}\ m^{-1}$ ), suggesting a decrease in the aromaticity following solar irradiation. The high SUVA value of HS also reflects the fact that the soil derived HS are of high aromatic character.

High performance size exclusion chromatography (HPSEC) was used to measure the change in the molecular size of HS following solar irradiation. Chromatograms of HS before and after solar irradiation are illustrated in Figure 5.7. Similar distributions were observed for all the irradiated HS solutions; therefore, only the results for HS solutions irradiated in BPC and tray are discussed here. No substantial changes were observed in the chromatograms of

the dark control during the experiment, reflecting the stability of HS.

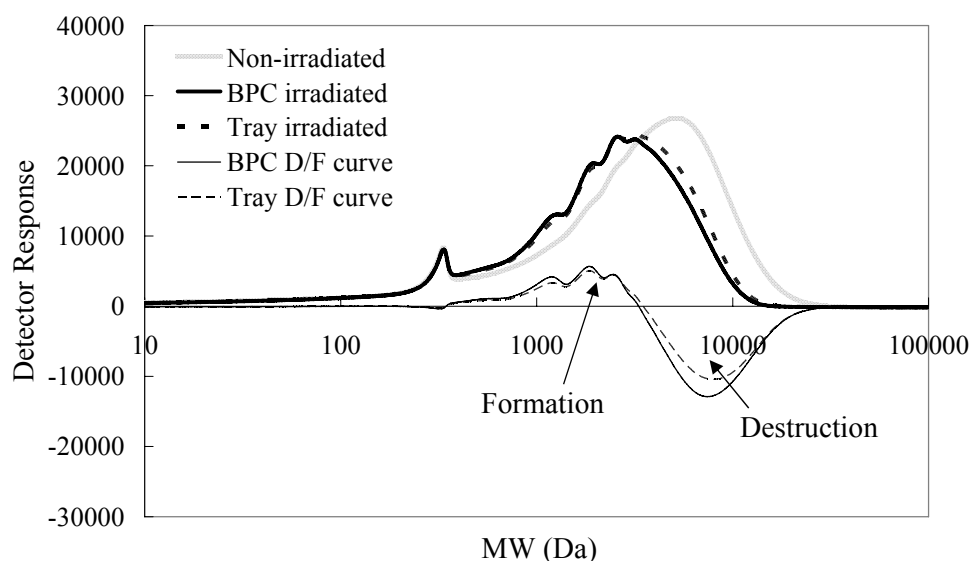


**Figure 5.7** Chromatograms of HS before and after solar irradiation in winter and destruction/formation (D/F) curves (initial DOC 8.50 mg/L and  $UV_{254}$   $0.67\text{ cm}^{-1}$ , DOC removal 11-15 % and  $UV_{254}$  removal 14-20 %, solar dose  $1.44 \times 10^5\text{ kJ/m}^2$ ).

The chromatogram of the non-irradiated HS showed a minor peak prior to the main peak, indicating a dominant proportion of high MW compounds and a small amount of low MW components in the un-treated solution. After exposure to sunlight, the main peak shifted to lower MW values, suggesting a decrease of the molecular size of HS. Solar irradiation also resulted in a decrease in the height and area of the chromatogram. The total area (or height) of a chromatogram is proportional to the sum of the concentrations of organic chromophores of various sizes (Lou and Xie, 2006). A decrease in the total area means the removal of some chromophores from the mixture due to solar irradiation. Corresponding to what was observed in Figures 5.5 and 5.6, using solar collectors resulted in more changes in the molecular weight distributions (MWD) of the irradiated HS solutions in BPC.

For a mixture of molecules such as HS, the MWD can be represented by several parameters, including  $M_n$ ,  $M_w$ , and polydispersity ( $\rho$ ). The  $M_w$  and  $M_n$  values of the untreated HS were 4092 Da and 1561 Da (Table 5.2), which are close to those values reported in the literature (Chin *et al.*, 1994; Karanfil *et al.*, 1996a). As a result of solar irradiation, the  $M_w$  was decreased by 23 %, 22 %, 25 % and 20 % for HS in CPC, PC, BPC and tray, respectively. It seems likely that solar irradiation had more pronounced influence on the HS properties with respect to the average molecular size rather than the DOC and  $UV_{254}$ . Solar irradiation not only reduced the MW, but also diminished the heterogeneities of HS ( $\rho$  decreased from 2.6 to 2.3), in accordance with previous observations by Lepane *et al.* (2003) as well as Lou and Xie (2006).

Additional information can be obtained from destruction/formation curves (Figure 5.7) by subtracting chromatograms of the irradiated HS from the non-irradiated HS, as suggested by Frimmel *et al.* (1998) and Lepane *et al.* (2003). Despite low solar intensity in winter, a significant removal of the high MW components was observed from the destruction curve, supporting the notion that the high MW compounds are readily photodegraded (Buchanan *et al.*, 2005; Carvalho *et al.*, 2008). The observed formation of smaller molecules can be attributed to the photoproducts from the breakdown of high MW components and these photoproducts still contributed to the DOC and  $UV_{254}$  values. Therefore, using solar irradiation in winter (or under low solar intensity) can effectively reduce the load of large molecules on the subsequent water treatment processes. A further treatment stage with good capability of removing smaller molecules will be necessary.

One should keep in mind that HPSEC can only measure the UV absorbing chromophores in HS. Some smaller molecules formed from the destruction of

high MW components may not be detected by the HPSEC measurement. Many components that do not absorb UV at 254 nm may also act as precursors for DBP formation (Matilainen *et al.*, 2002). However, study on the DBP formation potential is beyond the scope of this research.

**Table 5.4** Characteristics of HS solutions prior to solar irradiation in spring experiment (solar dose  $2.61 \times 10^5$  kJ/m<sup>2</sup>).

pH	UV <sub>254</sub> (cm <sup>-1</sup> )	DOC (mg L <sup>-1</sup> )	SUVA (L mg <sup>-1</sup> m <sup>-1</sup> )	M <sub>n</sub> (Da)	M <sub>w</sub> (Da)	ρ
7.3	0.67	8.29	8.1	1563	4241	2.71

SUVA: specific UV absorbance

M<sub>n</sub>: number average molecular weight

M<sub>w</sub>: weight average molecular weight

ρ: polydispersity

### 5.2.3.2 Spring experiment

A summary of the initial characteristics of HS is given in Table 5.4 and changes in DOC and UV<sub>254</sub> during solar irradiation in spring are shown in Figures 5.8 and 5.9, respectively. Following solar irradiation with an accumulative dose of  $2.61 \times 10^5$  kJ/m<sup>2</sup>, a removal of 28-45 % for UV<sub>254</sub> and 18-31 % for DOC were observed. It is clear that the increased removal of HS is linked to the increased solar irradiation.

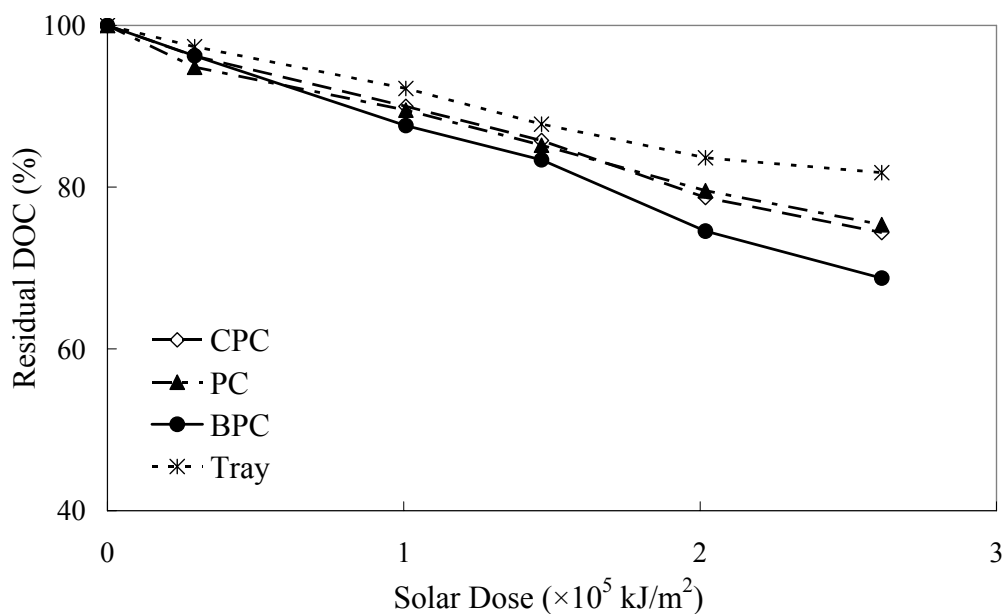


**Figure 5.8** Effect of solar irradiation on the DOC concentration of HS in different solar collectors in spring (initial DOC 8.29 mg/L, solar dose  $2.61 \times 10^5$  kJ/m<sup>2</sup>).

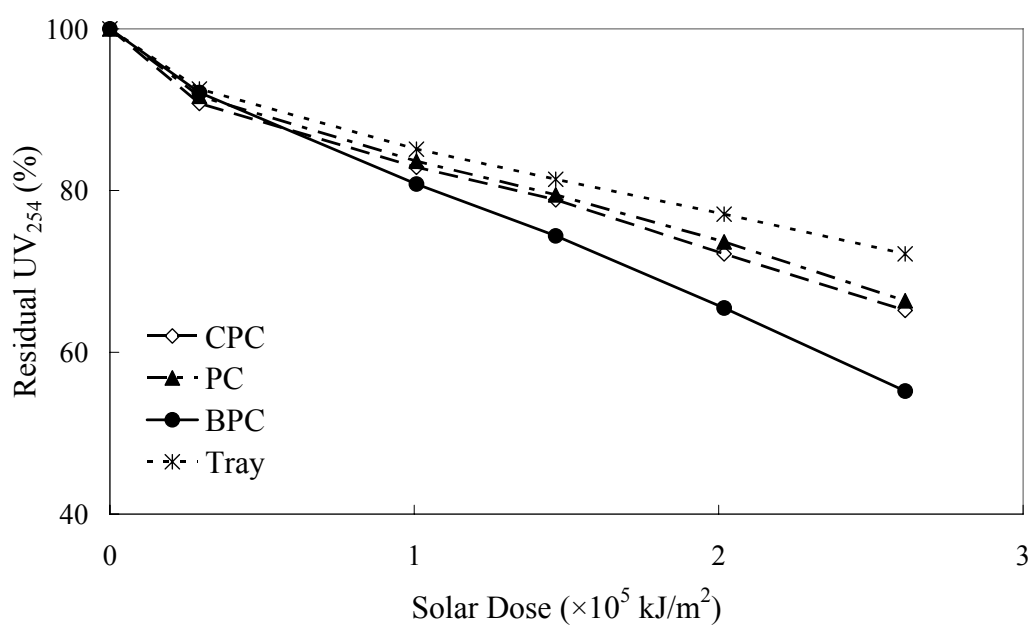


**Figure 5.9** Effect of solar irradiation on the UV<sub>254</sub> absorbance of HS in different solar collectors in spring (initial UV<sub>254</sub> 0.67 cm<sup>-1</sup>, solar dose  $2.61 \times 10^5$  kJ/m<sup>2</sup>).

**Table 5.5** First-order decay rate constants of HS irradiated in different solar collectors in spring experiment (DOC removal 18-31 %, UV<sub>254</sub> removal 28-45 %, solar dose  $2.61 \times 10^5$  kJ/m<sup>2</sup>).

Solar collectors	$k_1^*$	$k_2^*$
CPC	0.113	0.166
PC	0.110	0.158
BPC	0.140	0.218
Tray	0.082	0.132

\* unit:  $\times 10^{-5}$  m<sup>2</sup>/kJ

The photodegradation of HS in spring also followed the first-order reaction. With respect to DOC, a comparison between the decay rate constants demonstrates that the photodegradation rate of HS was promoted by 71 %, 38% and 34 % when using BPC, CPC and PC, respectively, relative to the HS irradiated without concentrating sunlight (Table 5.5). These results reveal a clear advantage of using BPC which has a larger reflective surface to capture more sunlight. The magnitude of enhancement for CPC samples was slightly higher compared to PC samples, indicating the advantage of CPC in collecting diffuse irradiation over PC of the similar scale.

HPSEC chromatograms of HS solutions before and after solar irradiation are illustrated in Figure 5.10. In addition to a shift of the peak to lower MW values and a decrease in the height and area of chromatograms, two distinct characteristics are observed in chromatograms of the irradiated HS.

Firstly, instead of a dominant peak, several new peaks and shoulders appears in

chromatograms of the irradiated HS in BPC. These peaks and shoulders were either caused by the lower MW fractions produced during irradiation so as to have their intensity increased at specific MW, or replaced by new peaks and shoulders from other low MW photoproducts (Lou and Xie, 2006). The pH value of HS solutions dropped following solar irradiation (from 7.3 to around 6.1), indicating that the important components of low MW photoproducts are small organic acids. A number of low MW organic acids have been identified as photochemical degradation products of HS, such as formic, acetic, malonic, oxalic and pyruvic acids (Moran and Zepp, 1997; Brinkmann *et al.*, 2003). In addition, CO<sub>2</sub> which was generated by the complete photodegradation of HS may dissolve in water and lower the pH.

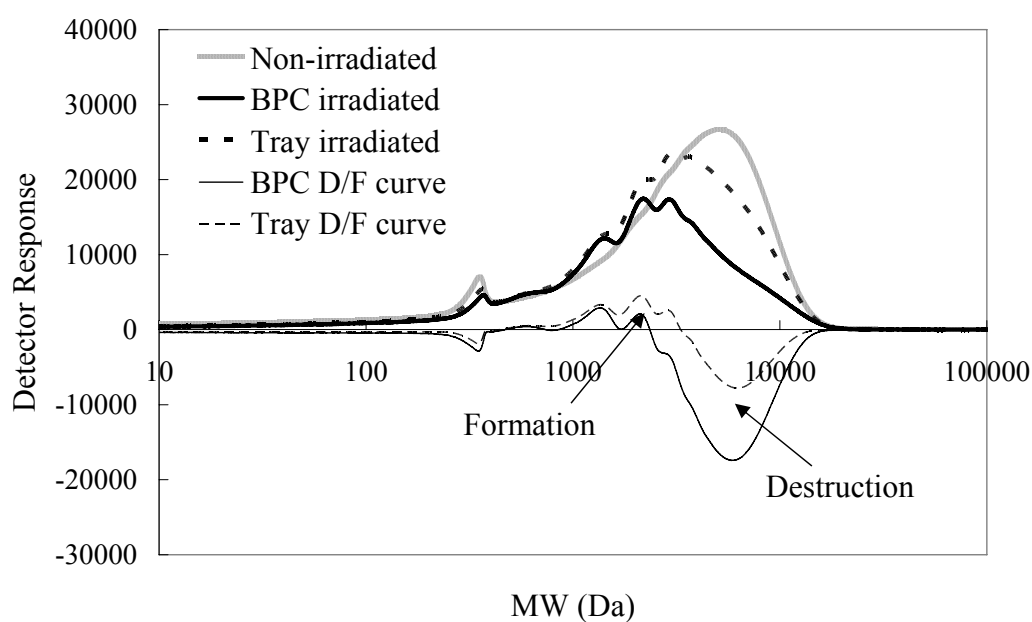


**Figure 5.10** Chromatograms of HS before and after solar irradiation in spring and destruction/formation (D/F) curves (initial DOC 8.29 mg/L and UV<sub>254</sub> 0.67 cm<sup>-1</sup>, DOC removal 18-31 % and UV<sub>254</sub> removal 28-45 %, solar dose 2.61×10<sup>5</sup> kJ/m<sup>2</sup>).

Secondly, as shown in the destruction and formation curves, after solar irradiation, there was a net removal of low MW fractions (< 1000 Da) and a reduced formation of intermediate MW fractions (approximately in the MW range of 1000-3000 Da), although more large molecular chromophores were removed. This is different from what was observed in Figure 5.7, where it shows less destruction of high MW components but more formation of intermediate and low MW fractions. It is likely that the increased solar intensity in spring was sufficient to remove some of the intermediate and low MW compounds in HS. These compounds could either be the intermediate and small size molecules present in the original HS or the photoproducts being generated and removed simultaneously. A simultaneous production and removal mechanism has been suggested by Buchanan *et al.* (2005) who studied the removal of humic fractions under UV-C irradiation. However, no information relevant to natural sunlight (in which the UV-C irradiation is absent) has been found in the consulted references. The increased UV intensity in the spring might be an important contributor to the enhanced removal of intermediate and smaller molecules.

The order of the decrease of  $M_w$  values was in agreement with the DOC and  $UV_{254}$  results, being the highest for HS in BPC (37 %), intermediate in CPC and PC (33 % and 31 %) and the lowest in the tray (24 %). A great photodegradation in spring resulted in a great decrease of polydispersity. For example, the value of polydispersity dropped from 2.7 to 2.2 for the HS solutions irradiated in BPC.

#### 5.2.3.3 Summer experiment

Characteristics of HS solutions prior to solar irradiation are given in Table 5.6. A significant removal of HS was obtained with a total solar dose of  $5.97 \times 10^5$  kJ/m<sup>2</sup>. The  $UV_{254}$  absorbance dropped by up to 84 % and the DOC concentration

dropped by up to 62 %, as illustrated in Figures 5.11 and 5.12. As a result, the SUVA value of the irradiated solutions was significantly reduced from 8.0 L mg<sup>-1</sup> m<sup>-1</sup> to 5.0, 5.3, 3.4 and 6.3 L mg<sup>-1</sup> m<sup>-1</sup> for HS in CPC, PC, BPC and tray, respectively, suggesting a significant reduction in the aromaticity of HS following solar irradiation. This significant removal is apparently attributed to the strong solar intensity in the summertime. UV<sub>254</sub> and DOC of HS decrease after exposure to light, as previously discussed in the literature review. The reported removal efficiencies vary, depending on the characteristics of HS, type and intensity of irradiation and exposure time (Tables 2.4 and 2.5). The result in summer experiments shows that the HS removal efficiencies that have been obtained using artificial UV irradiation can be achieved by using natural sunlight alone.

**Table 5.6** Characteristics of HS solutions prior to solar irradiation in summer experiment (solar dose  $5.97 \times 10^5$  kJ/m<sup>2</sup>).

pH	UV <sub>254</sub> (cm <sup>-1</sup> )	DOC (mg L <sup>-1</sup> )	SUVA (L mg <sup>-1</sup> m <sup>-1</sup> )	M <sub>n</sub> (Da)	M <sub>w</sub> (Da)	ρ
7.4	0.68	8.51	8.0	1680	4503	2.68

SUVA: specific UV absorbance

M<sub>n</sub>: number average molecular weight

M<sub>w</sub>: weight average molecular weight

ρ: polydispersity

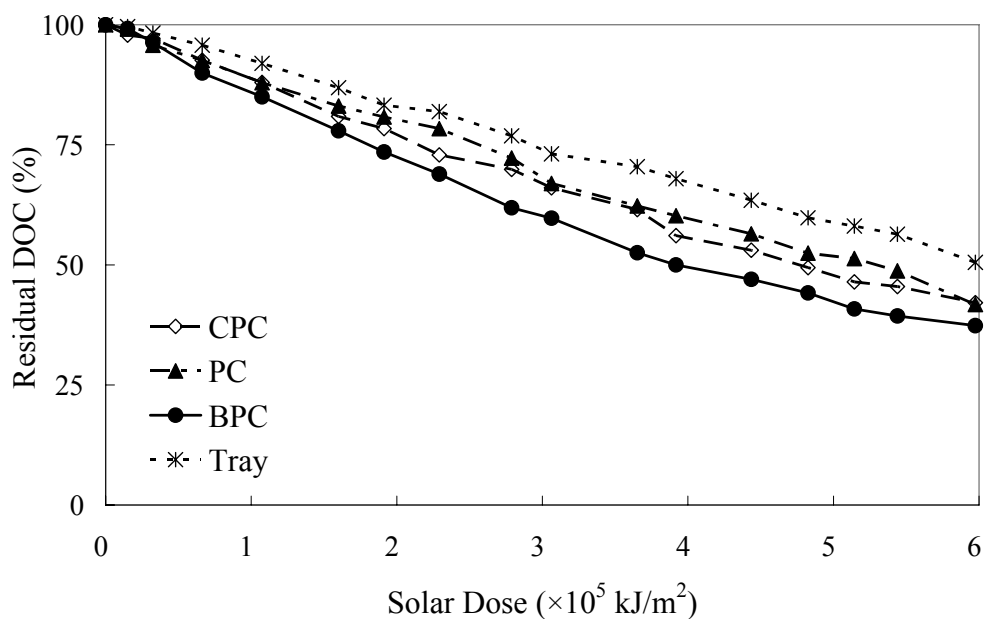


**Figure 5.11** Effect of solar irradiation on the DOC concentration of HS in different solar collectors in summer (initial DOC 8.51 mg/L, solar dose  $5.97 \times 10^5$  kJ/m<sup>2</sup>).

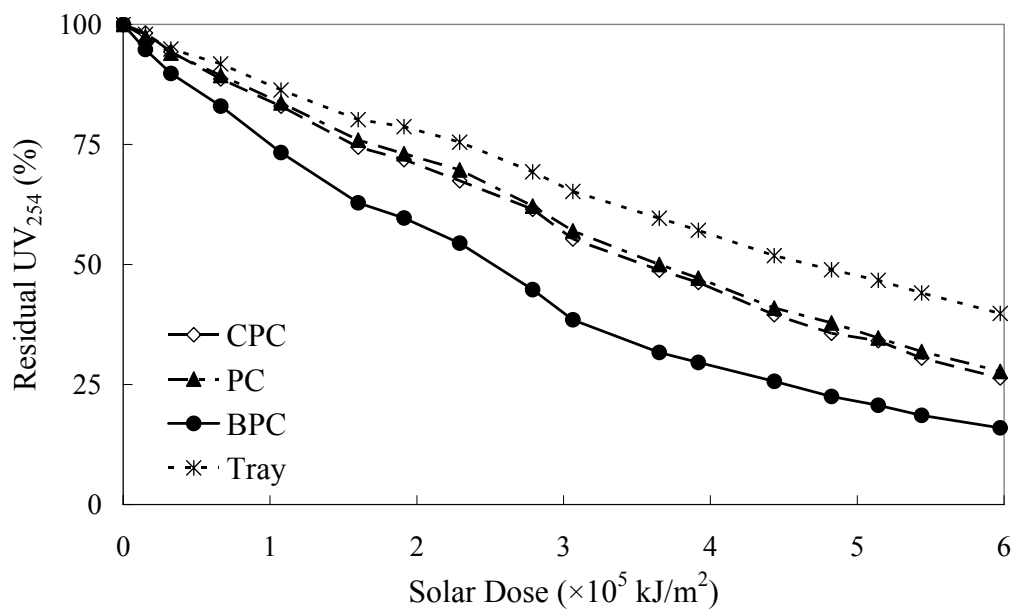


**Figure 5.12** Effect of solar irradiation on the UV<sub>254</sub> absorbance of HS in different solar collectors in summer (initial UV<sub>254</sub> 0.68 cm<sup>-1</sup>, solar dose  $5.97 \times 10^5$  kJ/m<sup>2</sup>).

**Table 5.7** First-order decay rate constants of HS irradiation in different solar collectors in summer (DOC removal 50-62 % and UV<sub>254</sub> removal 60-84 %, solar dose  $5.97 \times 10^5$  kJ/m<sup>2</sup>).

Solar collectors	$k_1^*$	$k_2^*$
CPC	0.143	0.207
PC	0.132	0.200
BPC	0.170	0.306
Tray	0.103	0.156

\* unit:  $\times 10^{-5}$  m<sup>2</sup>/kJ

Again, the photodegradation rate of HS was in a descending order as BPC > CPC > PC > tray. The DOC removal was enhanced by 65 %, 39 % and 28 % when using BPC, CPC and PC (Table 5.7). This observation, together with the other seasonal experimental results, demonstrates the large potential benefits of the use of parabolic solar collectors with large reflective surface. It also conforms to previous findings that the compound parabolic profile has better performance in concentrating sunlight relative to the parabolic profile of the similar scale (Vidal and Díaz, 2000; McLoughlin *et al.*, 2004).

It is worth noting that even after a long period of exposure duration the summer, a complete removal of HS by natural sunlight was not achieved in this study. As the photodegradation of HS followed the first-order reaction (equation 5.1), the relationship between the concentration of HS and solar dose can be described as an exponential function, implying that the 100 % photodegradation of HS would not be expected to achieve under prolonged sunlight exposure. This is in accordance with the hypothesis made by Lou and Xie (2006), who established the

relationship between MW and irradiation time with a single exponential function, and suggested that solar irradiation is incapable of completely oxidizing NOM even after a very long period of irradiation. Given the incomplete degradation of HS by sunlight, a further treatment stage is therefore required.

Significant differences in the MWD of HS following solar irradiation in summer are observed in Figure 5.13, suggesting remarkable structural changes of HS molecules. The high MW chromophores appear to be largely removed, leaving only a small amount of lower MW fractions in water. As can be seen from the destruction/formation curves, there was a destruction of chromophores across the entire range of MW, except that there was a slight accumulation of lower MW molecules in the HS solutions irradiated in the tray. This implies that strong solar irradiation during summer is sufficient to break down humic molecules with different sizes, even the smaller ones.

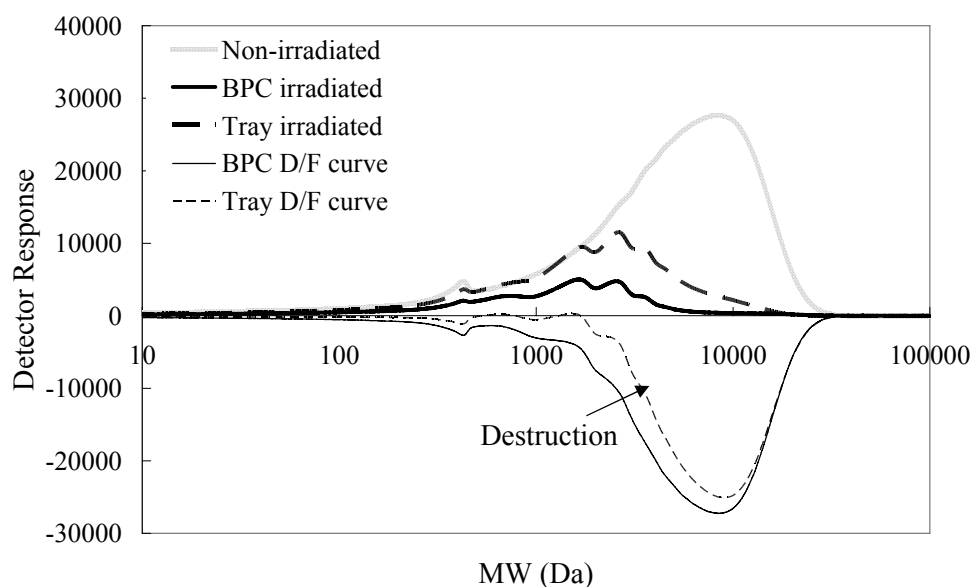


**Figure 5.13** Chromatograms of HS before and after solar irradiation in summer and destruction/formation (D/F) curves (initial DOC 8.51 mg/L and  $UV_{254}$  0.68  $cm^{-1}$ , DOC removal 50-62 % and  $UV_{254}$  removal 60-84 %, solar dose  $5.97 \times 10^5$

$\text{kJ/m}^2$ ).

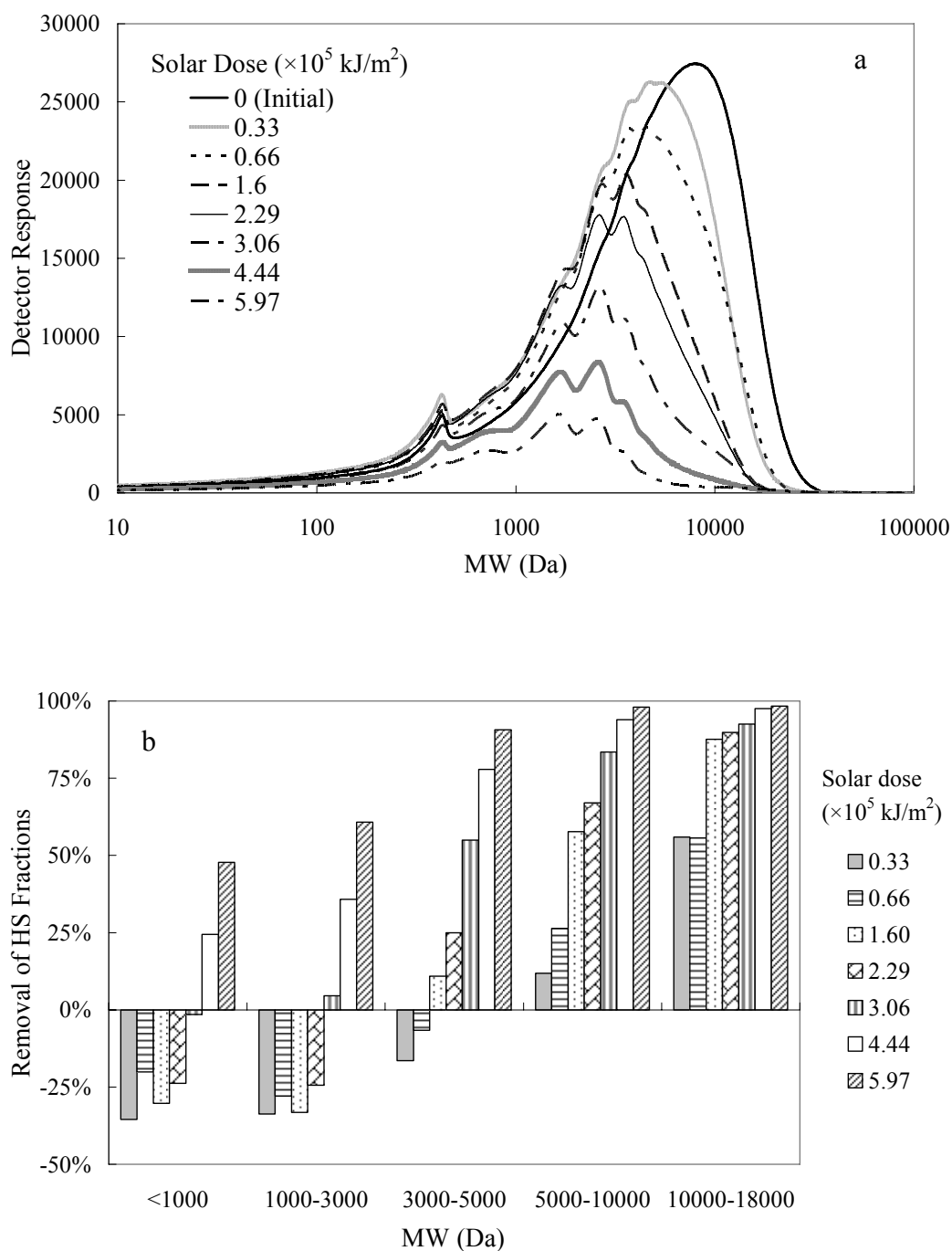


**Figure 5.14** (a) HPSEC chromatograms of HS irradiated in BPC during summer; (b) removal of different MW fractions of HS irradiated in BPC due to solar irradiation during summer.

A detailed investigation was carried out by measuring changes in the MWD of HS during solar irradiation. Chromatograms of HS in BPC and tray are shown as insets in Figures 5.14 and 5.15, respectively. To compare the performance of different MW fractions following solar irradiation, chromatograms of HS are roughly split into five MW fractions, as <1000 Da, 1000-3000 Da, 3000-5000 Da, 5000-10000 Da and 10000-18000 Da. The high MW fractions are here referred to those with the MW of more than 5000 Da, the intermediate MW fractions to those with the MW range of 5000-1000 Da, and the lowest MW fractions to those having the MW less than 1000 Da. The ratio of the decrease of the peak height (or area) to the initial peak height (or area) in chromatograms can be used as a measure for estimating the removal of HS fractions within the defined MW range. The efficiency of solar irradiation in removing different MW fractions can therefore be obtained.

The high MW fractions in HS irradiated in BPC were nearly completely removed after solar irradiation, and with just a small solar dose ( $0.33 \times 10^5$  kJ/m<sup>2</sup> for the first day) the highest MW fraction (10000-18000 Da) decreased by 56 %. The rapid initial breakdown confirms large molecules being preferentially photodegraded by solar irradiation. This is due to the large size and high conjugated character of these compounds which have a higher possibility of interaction with the incoming irradiation and oxidant radicals generated (Buchanan *et al.*, 2005). Following small solar doses of 0.33 and  $0.66 \times 10^5$  kJ/m<sup>2</sup>, a rapid increase in both intermediate and low MW fractions was observed, corresponding to the rapid breakdown of high MW fractions. Progressive changes in the MW fraction of 3000-5000 Da were observed with increasing solar irradiation, with more than 90 % of organic compounds within this MW range finally being removed. As to the smaller molecules, the removal process was

more complicated. It was expected that the smaller molecules would rapidly accumulate as a consequence of the breakdown of the high MW fractions after small solar doses and continuously accumulate due to the further breakdown of intermediate MW fractions. Instead, what was observed was that the amount of smaller molecules remained roughly constant for a period of time. A possible explanation could be that some low MW photoproducts were simultaneously formed and removed, and some small molecules originally in HS may also be photodegraded. Following solar irradiation, the total removal of smaller compounds was 48 % and 61 % for the MW <1000 Da and 1000-3000 Da fractions, respectively. These fractions are considered to be the ones mainly responsible for the final UV<sub>254</sub> of the irradiated HS, and partially contribute to the DOC concentration.

Likewise, as to the HS solutions in the tray, the highest MW fraction was rapidly removed, followed by the second highest MW fraction. The corresponding total removal efficiencies were approximately 94 % and 87 %, respectively. The removal of low and intermediate MW fractions was found to be significantly less relative to those in BPC. The removal of small fractions was only observed during the end of the solar exposure, with more than 83 % of smaller molecules still remaining in water. The removal of MW fractions of HS in CPC and PC showed a similar pattern to these in BPC and flat tray, and their values were between those illustrated in Figures 5.14 and 5.15.

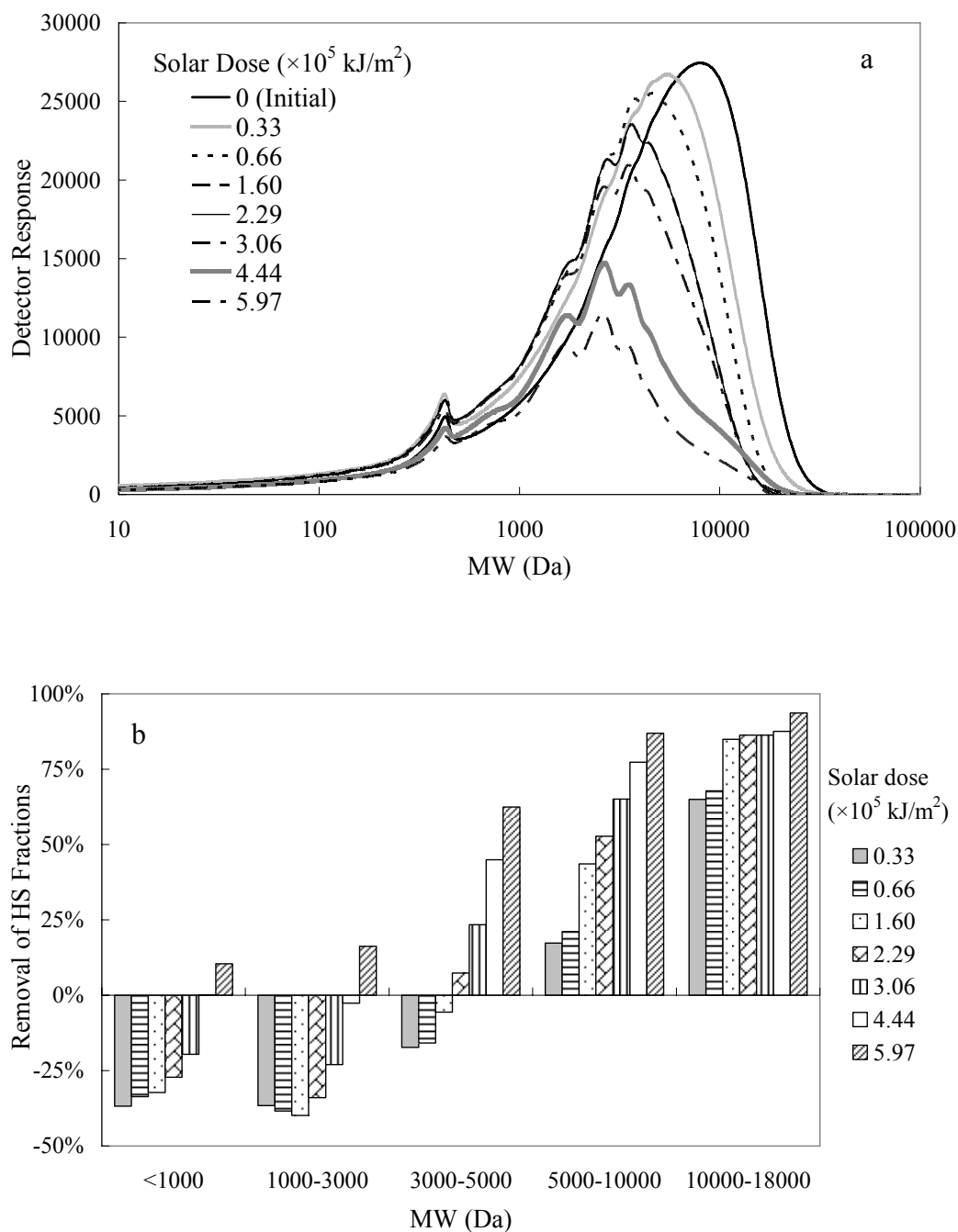


**Figure 5.15** (a) HPSEC chromatograms of HS irradiated in the tray during summer, (b) removal of different MW fractions of HS irradiated in the tray due to solar irradiation during summer.

The observations in Figures 5.14 and 5.15 imply that two possible processes may occur in the photodegradation of HS: (i) a primary cleavage or disaggregation of

high MW compounds and (ii) a secondary photodegradation of organic constituents. Schmitt-Kopplin *et al.* (1998) suggested that the fast disaggregation of HS may be initiated by oxidative cleavage of hydrogen binding functions and easily oxidizable phenolic linkages. The photodegradation of smaller organic compounds is shown to be related to the irradiation intensity. With the assistance of solar collectors, a significant removal of small molecules can be achieved. Since the solar collectors used in this research were simplified, non-solar tracking systems, it is assumed that the removal of HS will be greatly promoted by using sunlight-tracking collectors with higher concentrating ratios, i.e. 5 to 50 (Malato *et al.*, 2004). Also, significantly better HS removal may be expected if experiments are to be carried out for regions with stronger sunlight.

The effect of solar irradiation on the MW value was also significant. For example, the  $M_w$  value of HS irradiated in BPC was decreased by 76 %, together with a great decrease of polydispersity from 2.7 to 1.9, reflecting a decreased heterogeneity of the irradiated HS.

#### 5.2.4 Factors affecting the photodegradation of HS

Apart from solar intensity, the photodegradation of HS can be influenced by many factors, such as pH, concentration, microbial species, source of HS, carboxylic acidity, dissolved oxygen and ionic metals in the water (Collins *et al.*, 1986; Gao and Zepp, 1998; Schmitt-Kopplin *et al.*, 1998; Lepane *et al.*, 2003; Rodríguez-Zúñiga *et al.*, 2008). It is helpful to investigate those factors on the removal of HS for a better understanding of the solar-GAC method. Some of them were examined in this study.

#### 5.2.4.1 Microbial effects

Solar irradiation may have both direct and indirect effects on the microbial activity in water (Corin *et al.*, 1998). On one hand, solar irradiation, and in particular its UV fraction which is also known as germicidal irradiation, can inactivate microorganisms. On the other hand, exposure to sunlight stimulates the microbial growth in water, due to the formation of smaller organic molecules which are more biologically available than their parent molecules. The enhancement and inhibition of microbial activity in the irradiated water containing HS have been reported by several authors (Gjessing and Källqvist, 1991; Lund and Hongve, 1994; Corin *et al.*, 1998).

In theory, microbial degradation of HS is likely to occur in this study, since the solar exposure duration was long and the equipment was not sterilized. A key question therefore rises: was the removal of HS actually mainly attributed to the microbial degradation in this research? With this question, a regular check was made on the properties of the irradiated HS solutions after the completion of solar irradiation experiments. The check was conducted weekly within 6 to 10 weeks time. These irradiated solutions were kept in the dark after solar irradiation experiments. Therefore, microbial degradation, if any, is supposed to play a major role in changing the properties of HS. Figure 5.16 shows the evolution of the properties of the irradiated HS solutions in BPC after winter, spring and summer irradiation experiments. The y-axis represents the evolution of DOC and  $UV_{254}$ , normalized by dividing by the corresponding DOC and  $UV_{254}$  of HS at time zero (the final DOC and  $UV_{254}$  values of HS by the end of solar irradiation experiments). A random change in HS properties after solar irradiation experiments can be seen. The increase/decrease of  $UV_{254}$  and DOC values were less than 7 % and 5 %, respectively.

A direct comparison between the degradation of HS due to solar irradiation and the further degradation of the irradiated HS when kept in the dark is illustrated in Figure 5.17. It appears that the removal of HS due to the further degradation was insignificant compared to the solar-induced degradation of HS. In fact, if analytical uncertainties are taken into account, the variation resulting from the microbial activity, if any, can be considered negligible. This agrees well with Hongve (1994) who compared the photodegradation of sodium azide preserved and unpreserved HS and found that photodegradation of HS is primarily a photochemical process where microbial activity is suppressed.

It can therefore be concluded that the removal of HS in this research is mainly attributed to the photodegradation induced by solar irradiation. Microbial degradation may also occur, but the effects can be considered neglected.

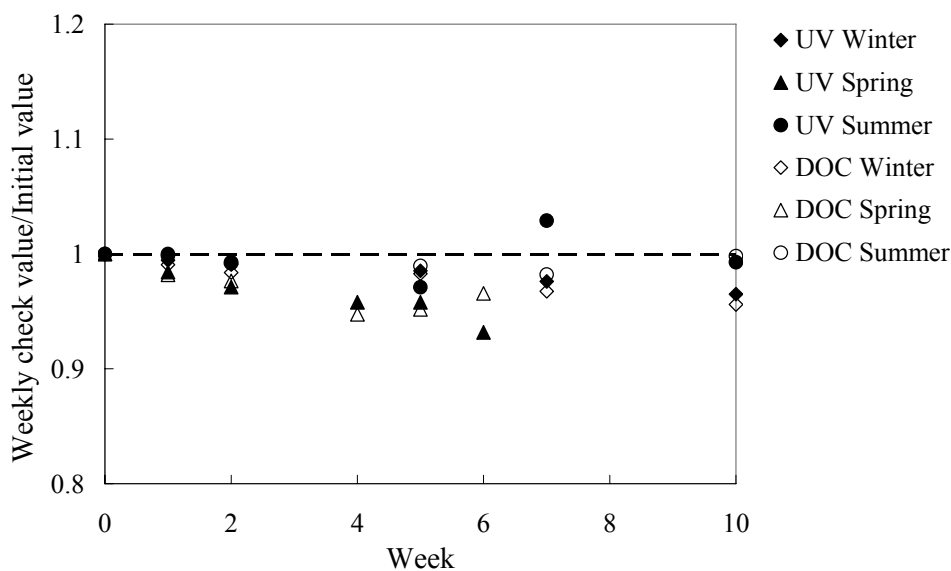


**Figure 5.16** Evolution of the properties of irradiated HS solutions in BPC after the completion solar irradiation experiments in winter (solar dose  $1.44 \times 10^5$  kJ/m<sup>2</sup>), spring (solar dose  $2.61 \times 10^5$  kJ/m<sup>2</sup>) and summer (solar dose  $5.97 \times 10^5$  kJ/m<sup>2</sup>).

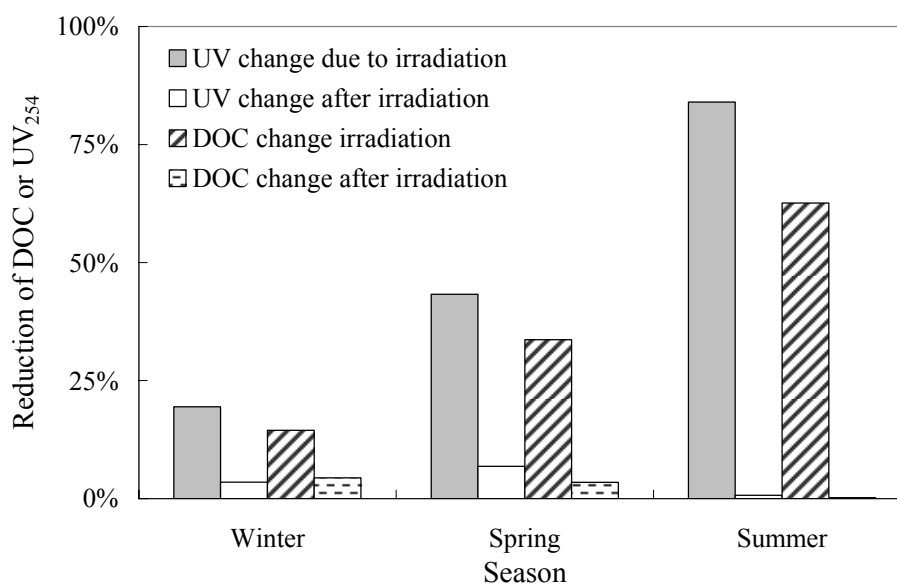


**Figure 5.17** Removal of HS in terms of  $UV_{254}$  and DOC due to solar irradiation and further degradation after irradiation.

#### 5.2.4.2 pH effects

pH is an important factor that affects the characteristics and reactivity of organics. Experiments were carried out under the same conditions with pH as a variable. Prior to solar irradiation, the water quality was:  $DOC = 8.30 \text{ mg L}^{-1}$ ,  $UV_{254}$  absorbance =  $0.67 \text{ cm}^{-1}$  and  $pH = 7.5$ . The pH of HS solutions was adjusted by adding sodium hydroxide (NaOH) and hydrochloric acid (HCl) to bring pH values to 4.2 (acidic) and 9.7 (basic), respectively. Solar collectors used for pH experiments were CPC and flat tray.

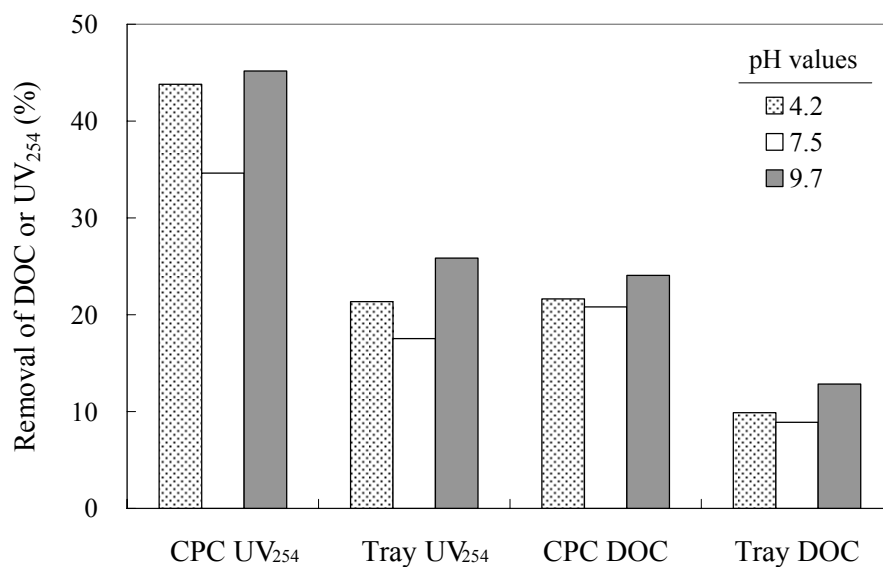


**Figure 5.18** Removal of HS with initial pH values of 4.2, 7.5 and 9.7 by solar irradiation (initial DOC 8.30 mg/L and  $UV_{254}$   $0.67 \text{ cm}^{-1}$ , solar dose  $1.59 \times 10^5 \text{ kJ/m}^2$ ).

Experiments were carried out in spring with a total solar dose of  $1.59 \times 10^5 \text{ kJ/m}^2$ . The total removal results are plotted in Figure 5.18. The DOC concentration was decreased by 9.9 %, 8.9 % and 12.8 % for the pH 4.2, 7.5 and 9.7 solutions irradiated in the tray, respectively. The corresponding  $UV_{254}$  absorbance reductions were 21.4 %, 17.5 % and 25.9 %. The photodegradation of HS irradiated using a solar collector was significantly promoted compared to that in the flat tray. It appears that the changes in  $UV_{254}$  were more pronounced for the pH adjusted HS solutions (acidic and basic) compared to the pH 7.5 solution, whereas the influence of pH on DOC reduction was relatively small. At high pH, the deprotonation of carboxylic and phenolic functional groups results in an increase of the electrostatic repulsive force among humic molecules; it may weaken some hydrogen bonds that hold molecules together, leaving humic molecules susceptible to disaggregation (Avena and Wilkinson, 2002; Brigante *et al.*, 2007). On the contrary, for lower pH values, HS are able to form large

aggregates due to the reduced electrostatic repulsion (Avena and Wilkinson, 2002). A hypothesis to explain the increased removal of HS under acidic conditions could be that the addition of acid might form associations with humic molecules that are more liable to photodegradation or/and weaken some interactions that hold molecules together. Some precipitation at low pH might also result in a larger decrease (Pullin *et al.*, 2004). The observed behaviour is in agreement with what has been previously reported by Gao and Zepp (1998), Brinkmann *et al.* (2003) and Pullin *et al.* (2004).

Irradiation led to a shift of the main peak to lower MW values and the removal of chromophores was more pronounced for the HS irradiated in the solar collector (Figure 5.19). The destruction/formation curves exhibit a pronounced removal of large molecules in the pH 9.7 solutions. This explains the observed higher removals of DOC and UV<sub>254</sub> of the pH 9.7 solutions. For the acidic HS solutions, it seems likely that the addition of acid increased the photodegradability of smaller molecules, which were either photoproducts from the breakdown of large molecules or those originally present in HS solutions.

It can therefore be concluded that pH adjustment can alter the interactions between HS constituting molecules, and hence affect their photodegradation performance by solar irradiation.

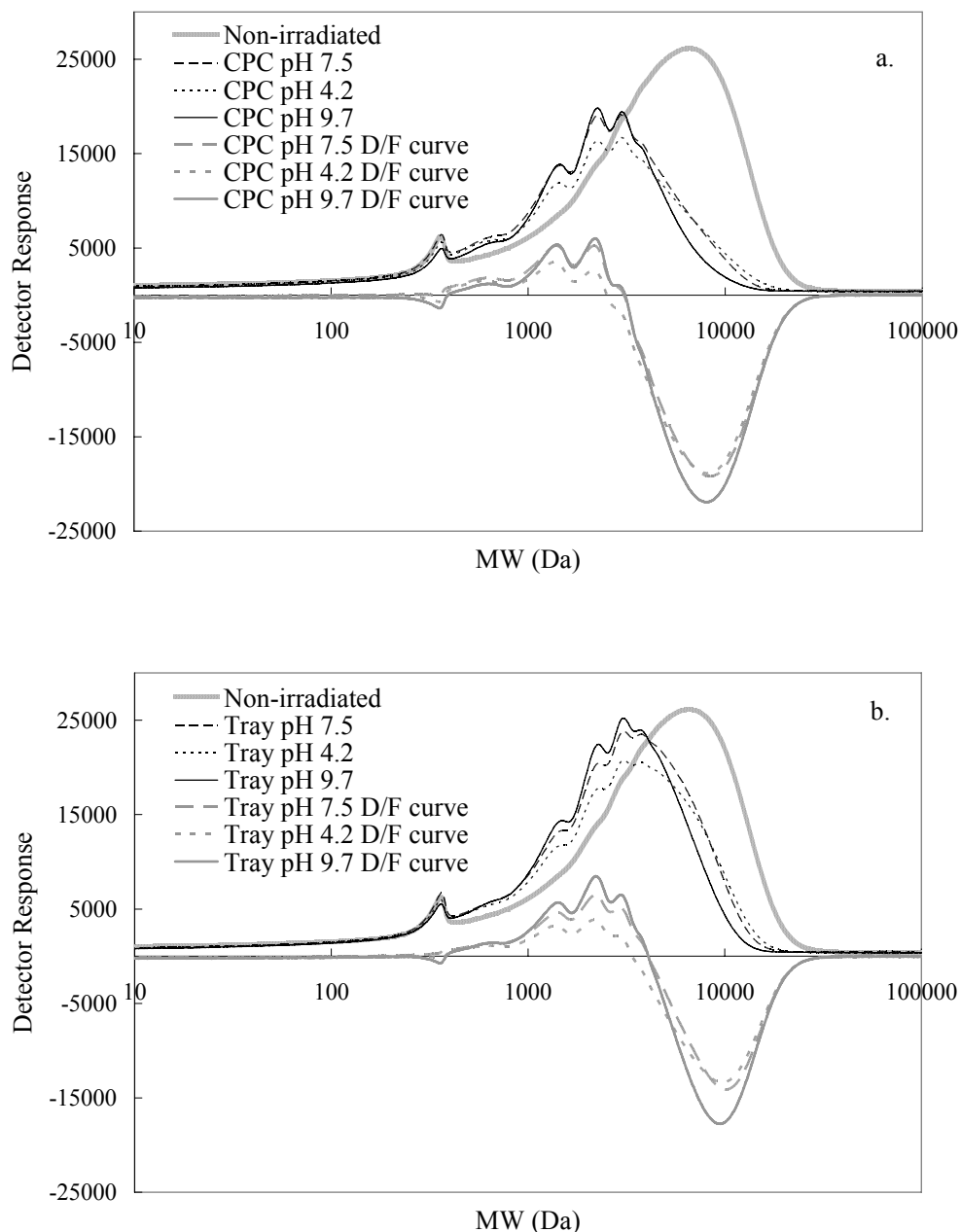


**Figure 5.19** HPSEC chromatograms and destruction/formation (D/F) curves of HS solutions at three different initial pH values (4.2, 7.5 and 9.7) before and after solar irradiation: (a) HS irradiated in CPC, and (b) HS irradiated in tray (initial DOC 8.30 mg/L and  $UV_{254}$   $0.67\text{ cm}^{-1}$ , solar dose  $1.59 \times 10^5\text{ kJ/m}^2$ ).

#### 5.2.4.3 Effects of solar irradiation on aquatic FA

A series of experiments carried out under natural sunlight give a practical and realistic demonstration that solar irradiation can effectively break down the large humic components and reduce the DOC concentration and  $UV_{254}$  absorbance of HS. However, HS in natural waters do not have the MW and degree of aromaticity as high as does the AHA. Fulvic acid (FA) is another important category of HS, accounting for 20-50 % of the organic matter pool in natural environments (Thurman, 1985). It is therefore essential to evaluate the treatability of FA using the solar irradiation–GAC adsorption method and the solar effect on FA properties will first be discussed here. Experimental solutions were prepared from approximately  $10 \text{ mg L}^{-1}$  SRFA and  $10 \text{ mg L}^{-1}$  AHA. Similar initial amount of SRFA and AHA resulted in different characteristics of solutions, as can be seen in Table 5.8, although the carbon assay values were similar (53.5 % for SRFA and 50.7 % for AHA). The big difference in DOC can be attributed to the filtration procedure when preparing samples. The large molecules were removed from the AHA mixture so as to reduce its DOC concentration. In contrast to the DOC concentration, the  $UV_{254}$  absorbance of HA was higher than that of SRFA, reflecting the fact that AHA contains a larger fraction of aromatic structures than does SRFA. According to Karanfil *et al.* (1996a), the aromaticity of AHA is 57.7 %, while it is only 24.8 % for SRFA.

Solar irradiation resulted in a continuous decrease in  $UV_{254}$  and DOC of AHA and SRFA solutions. The final removals are presented in Figure 5.20. In spite of the fact that the SRFA sample was more concentrated in terms of DOC, the observed photodegradation rate of SRFA was slightly faster compared to AHA. This difference is in accordance with some earlier studies. Allard *et al.* (1994) found that it took 58 h to remove 95 % of HA by exposure to UV-C light, while

only 12 h for FA to achieve 95 % removal. Kulovaara *et al.* (1996) measured total organic carbon (TOC) changes in the FA and HA isolates from a lake water by UV irradiation. The FA isolate was found to decrease faster at the beginning of irradiation and HA degradation proceeded at a relatively constant rate. The authors suggested that the photodegradation of FA structures proceeds faster relative to HA structures. Lepane *et al.* (2003) found that the loss in optical properties was in the order: natural seawater > FA > HA, under the UV-B irradiation.

**Table 5.8** Characteristics of AHA and SRFA solutions prior to solar irradiation (solar dose  $1.96 \times 10^5$  kJ/m<sup>2</sup>).

	DOC (mg L <sup>-1</sup> )	UV <sub>254</sub> (cm <sup>-1</sup> )	pH	M <sub>w</sub> (Da)	M <sub>n</sub> (Da)	ρ
AHA	3.80	0.25	7.1	4049	1719	2.36
SRFA	5.06	0.20	4.9	2234	1201	1.86

M<sub>n</sub>: number average molecular weight

M<sub>w</sub>: weight average molecular weight

ρ: polydispersity

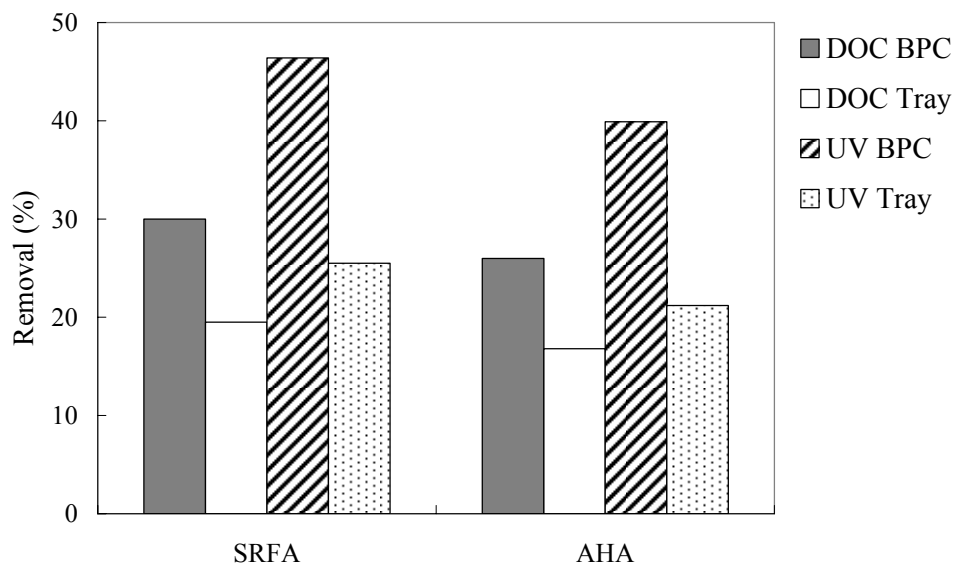


**Figure 5.20** Total removals of SRFA and AHA with respect to DOC and  $UV_{254}$  due to solar irradiation (initial DOC 5.06mg/L (SRFA) and 3.80 mg/L (AHA), initial  $0.20\text{ cm}^{-1}$  (SRFA) and  $0.25\text{ cm}^{-1}$  (AHA), solar dose  $1.96 \times 10^5\text{ kJ/m}^2$ ).

The  $M_w$  values of non-irradiated samples were 4049 Da (AHA) and 2234 Da (SRFA), as given in Table 5.8, confirming the notion that AHA possesses certain high MW components that are not present in SRFA. Following solar irradiation, there was a slightly higher reduction in MW values for SRFA. Similar observation has been reported by Lou and Xie (2006) who found that the aquatic humic samples (Suwannee River HA (SRHA), SRFA and a natural water) were more susceptible to the photoalternation of the MW by visible irradiation compared to a soil derived HA.

Thus, it can be concluded that FA is more prone to be photodegraded while HA is more resistant to photodegradation, possibly due to the high chemical stability of the aromatic structures. On the other hand, it can be deduced that results from studies employing the soil derived HS may lead to an underestimation of the photodegradation efficiency of natural humic rich waters (which consist of both

FA and HA) by solar irradiation. Consequently, it would be expected that when dealing with humic rich waters using natural sunlight, higher and faster photodegradation of humic waters might be obtained compared to the waters only containing HA.

### 5.2.5 Evaluation of natural water source

Results obtained from the above studies on humic model materials (AHA and SRFA) lead to the following initial conclusions: (i) if a water contains a high content of large humic molecules, it is likely that solar irradiation would effectively remove the high MW components, while the load of large molecules on the subsequent treatment processes would be successfully reduced; and (ii) if a water containing both FA and HA, as encountered in all natural waters, it is likely that solar irradiation would remove HS at a faster rate and to a greater extent than HA alone.

**Table 5.9** Characteristics of the natural CH water and AHA water prior to solar irradiation in autumn (solar dose  $1.42 \times 10^5$  kJ/m<sup>2</sup>).

	pH	DOC (mg L <sup>-1</sup> )	UV <sub>254</sub> (cm <sup>-1</sup> )	SUVA (L mg <sup>-1</sup> m <sup>-1</sup> )	M <sub>w</sub> (kDa)	M <sub>n</sub> (kDa)	ρ
CH water	6.4	12.90	0.72	5.58	4.67	2.43	1.92
AHA water	7.3	8.83	0.71	8.04	4.20	1.62	2.59

SUVA: specific UV absorbance

M<sub>n</sub>: number average molecular weight

M<sub>w</sub>: weight average molecular weight

ρ: polydispersity

To test these initial conclusions, the proposed solar irradiation-GAC adsorption method was then applied to a natural water sample collected from the Chellow Heights Water Treatment Plant of Yorkshire Water. This natural water sample is herein referred to as 'CH water'. Over the past ten years, Yorkshire Water has experienced a continual increase in the NOM content of raw water and difficulties in meeting trihalomethanes (THMs) regulations. The increase in colour of water is seasonal with peaks occurring in autumn (Goslan, 2003). Solar irradiation experiments were therefore carried out in autumn with an accumulative solar dose of  $1.42 \times 10^5$  kJ/m<sup>2</sup>. The quality of CH water prior to irradiation is summarized in Table 5.9 where some features of this natural water can be seen:

- Compared to AHA, there were possibly a higher content of acidic functional groups in CH raw water according to its lower pH value;
- With the similar UV<sub>254</sub> absorbance, CH water had a higher DOC content of 12.9 mg L<sup>-1</sup> than AHA water (DOC 8.8 mg L<sup>-1</sup>), indicating that a large portion of the organic components in this natural water sample did not have absorbance at 254 nm or did not possess aromatic or conjugated structures;
- Consequently, the SUVA value of CH water was lower than that of AHA water (Table 5.9), confirming a lesser hydrophobicity and aromaticity of the natural aquatic HS;
- CH water surprisingly had a higher MW (4.67 kDa) compared to AHA (4.20 kDa). As reflected in Figure 5.21, there were a larger number of organic components in CH water covering the entire MW range. The observed high MW can be linked to the characteristics of the source of the CH water – the upland water passing through peat. Due to the terrestrial origin, it is also possible that the ratio of HA to FA is higher in this upland water than in some other surface waters.

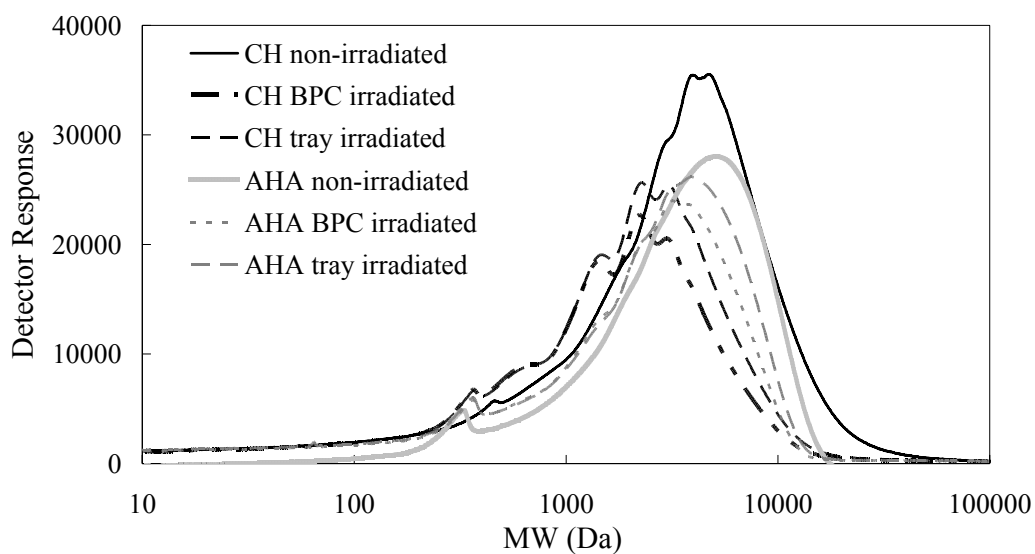


**Figure 5.21** HPSEC chromatograms of CH water and AHA water before and after solar irradiation in autumn (initial DOC 12.90 mg/L for CH water and 8.83 mg/L for AHA water, initial  $UV_{254}$  0.72  $cm^{-1}$  for CH water and 0.71  $cm^{-1}$  for AHA water, solar dose  $1.42 \times 10^5$   $kJ/m^2$ ).

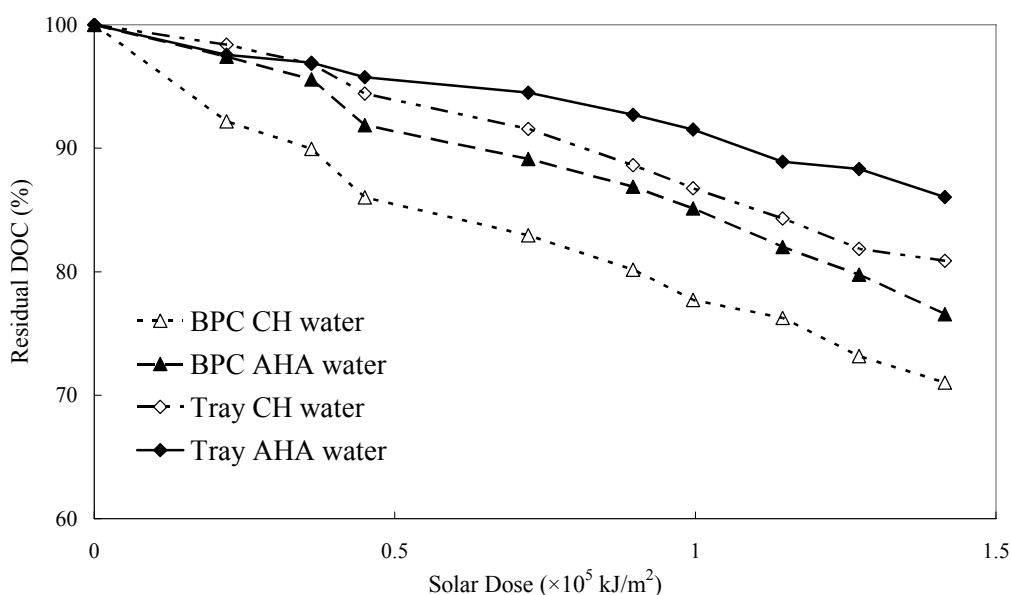


**Figure 5.22** Effect of solar irradiation on the DOC concentration of CH water and AHA water in BPC and flat tray in autumn (initial DOC 12.90 mg/L for CH water and 8.83 mg/L for AHA water, solar dose  $1.42 \times 10^5$   $kJ/m^2$ ).

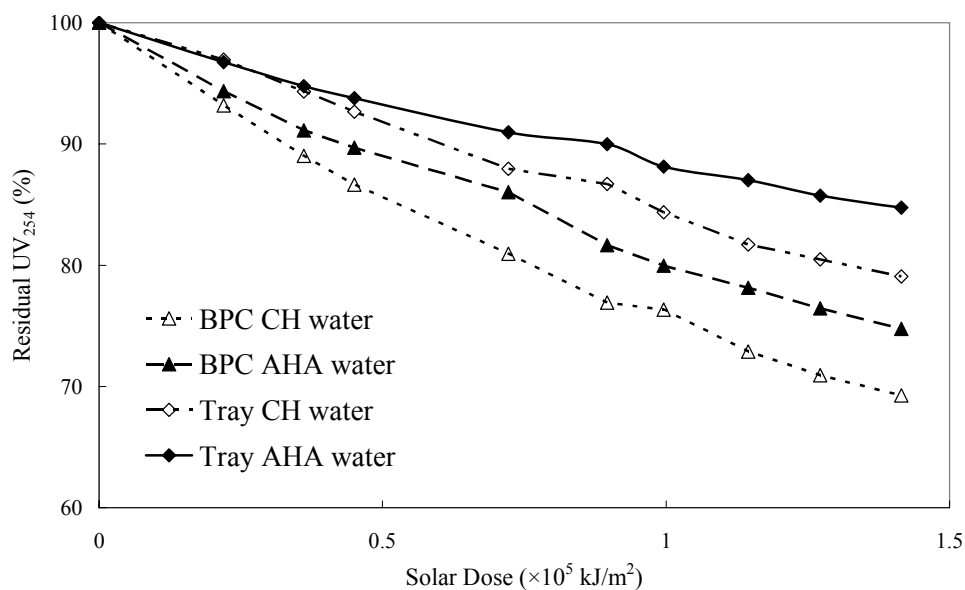


**Figure 5.23** Effect of solar irradiation on the  $UV_{254}$  absorbance of the CH water and AHA water in BPC and flat tray in autumn (initial  $UV_{254}$   $0.72\text{ cm}^{-1}$  for CH water and  $0.71\text{ cm}^{-1}$  for AHA water, solar dose  $1.42 \times 10^5\text{ kJ/m}^2$ ).

The DOC and  $UV_{254}$  of the dark control for both waters remained almost unchanged duration experiment, confirming the stability of HS. A gradual removal of HS was observed with increasing solar irradiation (Figures 5.22 and 5.23). The DOC of HS was removed by 21-29 % for CH water and 14-24 % for AHA water. Apparently, natural HS displayed a faster photodegradation rate. For example, for HS irradiated in tray, the photodegradation rate in terms of DOC was  $0.145 \times 10^{-5}\text{ m}^2/\text{kJ}$  for CH water and only  $0.097 \times 10^{-5}\text{ m}^2/\text{kJ}$  for AHA water. There are some possible explanations to this:

- Sharp *et al.* (2006) fractionated an upland water sample from Yorkshire Water by XAD resin adsorption technique and found that the FA fraction accounted for the greatest fraction of DOC, followed by HA fraction. Similar observations have also been reported by Ma *et al.* (2001) and Goslan (2003), who reported that the majority of DOC in upland water sources was presented as FA fraction, while HA

accounted for a lesser proportion. From previously published data and the measured low SUVA value of CH water, it can therefore be inferred that CH water contained more FA fraction than HA fraction. FA is more readily photodegraded than HA, as discussed in section 5.2.4.3. Thus, the natural water showed a faster degradation rate than AHA water.

- It is well-known that carboxyl containing compounds can form strong complexes with metals that undergo rapid photoreactions (Faust and Zepp, 1993; Brinkmann *et al.*, 2003; Xie *et al.*, 2004). A greater amount of carboxylic functional groups is expected in CH water, compared to AHA water. And the iron, for example, is one of the most commonly metals present in natural waters. The Fe(III)-carboxylate complexes may therefore promote the photodegradation process of the CH water;
- The indirect photodegradation of non-chromophoric organic materials can contribute to the DOC loss;
- As discussed in section 5.2.4.2, the pH value of water may also play a role in improving the photodegradation of HS.

The first-order decay rate constants presented in Table 5.10 show that the  $UV_{254}$  decreased faster than did the DOC concentration, suggesting a decrease in the SUVA value of HS following solar irradiation and hence a decrease in aromaticity. This is in agreement with the findings in other seasonal experiments. Using BPC significantly enhanced the photodegradation of CH water relative to the tray, with approximately 72 % and 63 % enhancement for the DOC and  $UV_{254}$  removal, respectively. The corresponding magnitude of enhancement for AHA water was 78 % (DOC) and 77 % ( $UV_{254}$ ).

**Table 5.10** First-order decay rate constants of CH water and AHA water irradiated in BPC and flat tray in autumn (DOC removal 21-29 % for CH water and 14-24 % for AHA water, solar dose  $1.42 \times 10^5$  kJ/m<sup>2</sup>).

Samples	$k_1^*$	$k_2^*$
CH water in BPC	0.249	0.275
CH water in tray	0.145	0.169
AHA water in BPC	0.173	0.216
AHA water in tray	0.097	0.122

\* unit:  $\times 10^{-5}$  m<sup>2</sup>/kJ

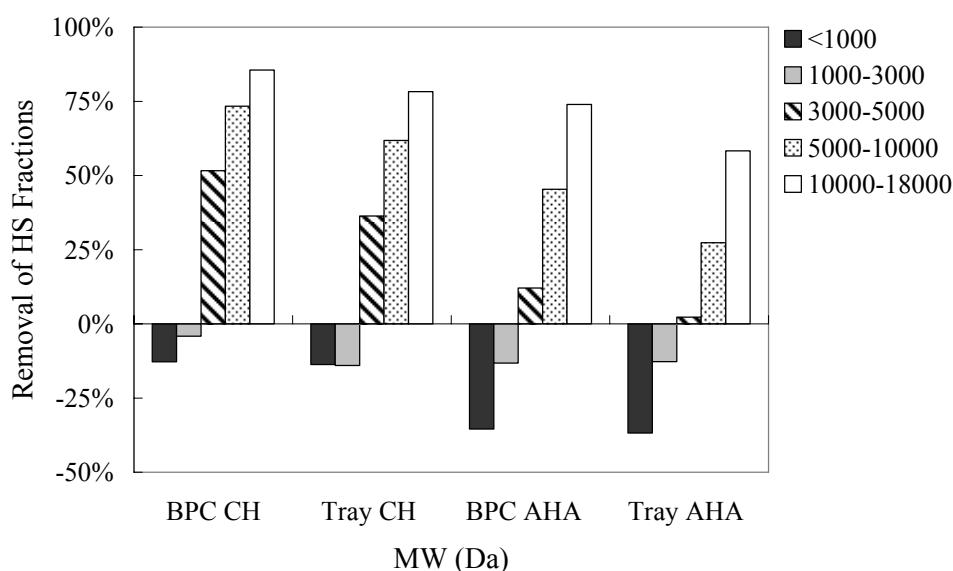


**Figure 5.24** Removal of different MW fractions of CH water and AHA water in BPC and tray due to solar irradiation in autumn (initial DOC 12.90 mg/L for CH water and 8.83 mg/L for AHA water, DOC removal 21-29 % for CH water and 14-24 % for AHA water, solar dose  $1.42 \times 10^5$  kJ/m<sup>2</sup>).

Although solar intensity during this experiment was not strong, a significant change in the MWD was observed (Figure 5.21). Apparently, solar irradiation

was more effective in altering the MWD of CH water, with more changes observed in the chromatograms. Figure 5.24 shows the photodegradation efficiencies of different MW fractions in HS. Compared to AHA, CH water had more large molecules removed and less smaller molecules remaining in water. It is possible that either many photoproducts were produced and degraded simultaneously, or/and more non-chromophoric photoproducts were formed in CH water. Observations in this experiment conclusively evidence the treatability of natural humic rich water subjected to solar irradiation. The influence on the subsequent GAC adsorption process will be discussed in the section 5.3.

#### 5.2.6 Summary of solar irradiation results

Solar irradiation undoubtedly alters the physicochemical characteristics of organic components that comprise HS, reflected by  $UV_{254}$ , DOC and MW changes. The total DOC removal of HS was up to 15 %, 31 % and 62 % after exposure to sunlight of  $1.44 \times 10^5$  kJ/m<sup>2</sup>,  $2.61 \times 10^5$  kJ/m<sup>2</sup> and  $5.97 \times 10^5$  kJ/m<sup>2</sup>, respectively. And the removal of DOC was up to 29 % for CH water with irradiation of  $1.42 \times 10^5$  kJ/m<sup>2</sup>. Winter *et al.* (2007) reported a 26 % DOC reduction of AHA solution (initial DOC 10.9 mg/L) exposed to natural sunlight for 13 days in summer in Waterloo, Canada, however, the solar dose was not measured in their work. Compared to the work by Winter *et al.* (2007), photodegradation of HS in this work was much slower (62 % DOC removal for 10 weeks in summer). This can be possibly attributed to the low solar intensity in London compared to Waterloo. Hongve (1998) also studied the photodegradation of HS under natural sunlight on a pond water sample with initial DOC 12 mg/L. After exposure to  $1.63 \times 10^5$  kJ/m<sup>2</sup> solar irradiation, a 32 % DOC removal was achieved. This value is higher than what was observed on AHA water and close to the DOC removal of CH water in autumn experiment (solar intensity  $1.44 \times 10^5$  kJ/m<sup>2</sup>),

confirming the treatability of natural humic waters by solar irradiation. Up to 84 %  $UV_{254}$  decrease and 62 % DOC decrease were achieved in this research. Comparisons between experimental data and published results (given in Tables 2.4 and 2.5) show that the removal of HS in terms of DOC and  $UV_{254}$  that has been obtained using artificial UV irradiation can be achieved by using natural sunlight alone. For example, Goslan *et al.* (2006) reported that by exposing an upland water under UV lamp at 254 nm ( $34 \text{ W/m}^2$ ), the  $UV_{254}$  of HS was reduced by 85 %.

A summary of the first-order decay rate constants for the photodegradation of HS in four seasonal experiments is presented in Figure 5.25. The main observations are:

- (1) the photodegradation rate varied with season due to varying solar intensities;
- (2) using solar collectors effectively improved the photodegradation of HS under any irradiation conditions (or any seasons). This is attributed to the increased solar irradiation within solar collectors. The magnitude of enhancement varied from 13 % to 65 % for DOC and from 26 % to 96 % for  $UV_{254}$ , depending on the solar collector configuration and solar intensity;
- (3) the  $UV_{254}$  absorbance was more remarkably reduced than the DOC concentration, leading to a decrease in the SUVA value. This demonstrates the aromaticity loss following solar irradiation, and the DBP formation potential may be reduced;
- (4) the natural humic rich water was more readily photodegraded compared to AHA water, suggesting the treatability of natural humic rich waters and confirming that the observed positive outcome from AHA is not only restricted to the model material.

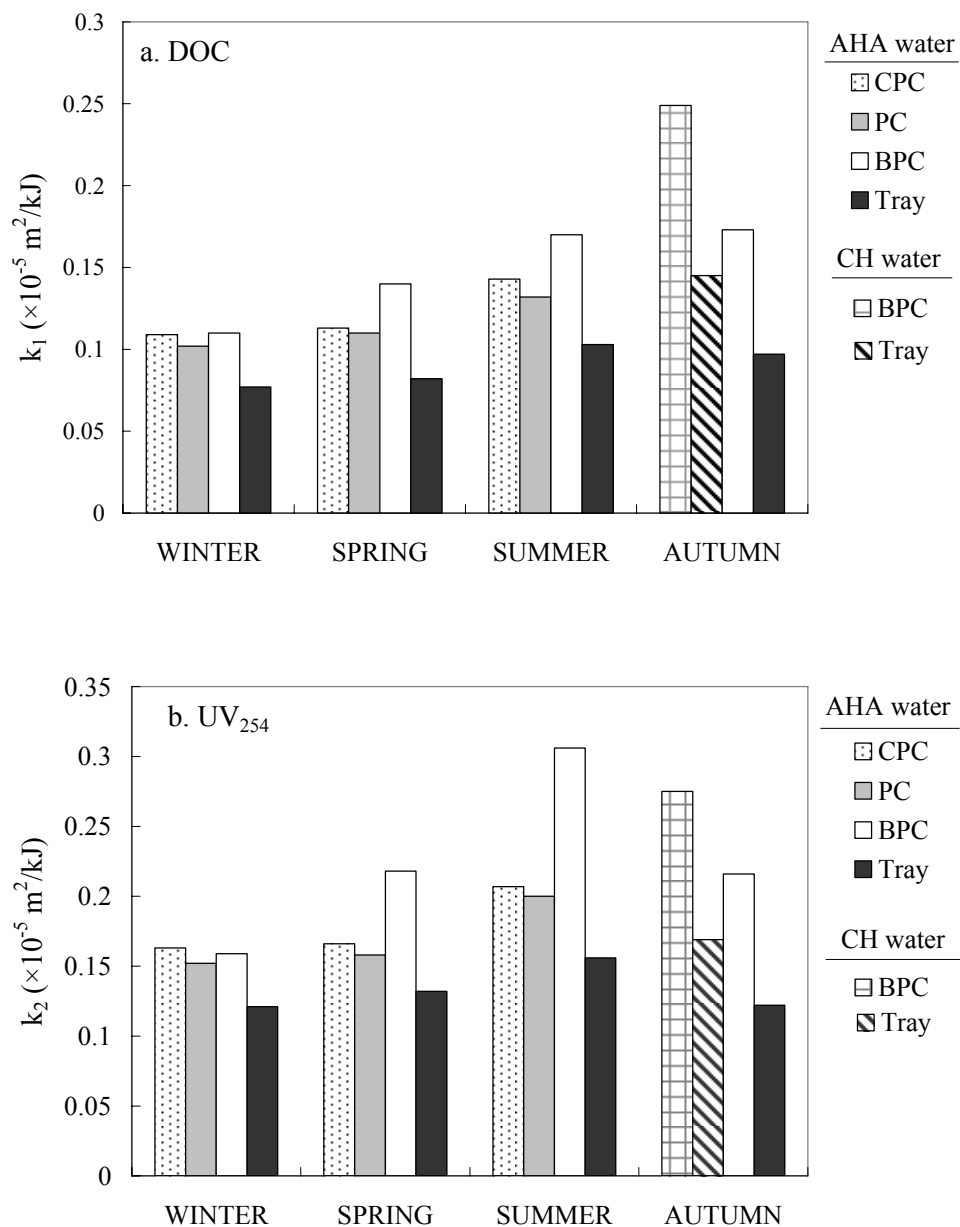


**Figure 5.25** Summary of the first-order decay rate constants for HS solutions irradiated in different seasons: (a)  $k_1$  for DOC, and (b)  $k_2$  for UV<sub>254</sub>.

The photodegradation rate is found to be strongly correlated with solar irradiation. In each seasonal experiment, the photodegradation of AHA was found to follow the first-order kinetics. The first-order decay rate constant  $k$  depends on irradiation intensity, water characteristics and geometry of the solar collector.

When the same AHA waters and the same solar collector were used,  $k$  is only related to the solar intensity. A direct correlation between the decay rate constants of AHA solutions in the tray (Tables 5.3, 5.5, 5.7 and 5.10) and solar dose in four seasonal experiments is illustrated in Figure 5.26. As can be seen,  $k$  values of AHA increase with increasing solar doses. There was a linear correlation between solar dose and decay rate constant  $k$  for UV<sub>254</sub>. However, a linear correlation for DOC was not found, which is caused by the apparent difference between  $k$  values obtained from winter ( $1.44 \times 10^5$  kJ/m<sup>2</sup>) and autumn experiments ( $1.42 \times 10^5$  kJ/m<sup>2</sup>) when the total solar dose was similar. This is possibly due to the DOC analytical error as the corresponding  $k$  values in relation to UV<sub>254</sub> were similar. The decay rate constant of CH water was noticeably higher than that of AHA water under the same irradiation condition, suggesting the good treatability of natural humic rich waters by solar irradiation.

It can therefore be concluded from Figure 5.26 that stronger solar intensity would lead to a faster photodegradation of HS. Even under natural sunlight, a significant HS removal is achievable. Solar irradiation as a sustainable energy source has the advantage of being freely and locally available. Solar irradiation in London is in fact much lower than many other regions, with the average daily intensity at the experimental site of approximately  $8.53 \times 10^3$  kJ/m<sup>2</sup> in summer. Solar data available from the published photodegradation or disinfection studies show that the daily intensities were  $14.03 \times 10^3$  kJ/m<sup>2</sup> for California,  $21.08 \times 10^3$  kJ/m<sup>2</sup> for Malaysia and  $15.12 \times 10^3$  kJ/m<sup>2</sup> for India (Kehoe *et al.*, 2000; Mani *et al.*, 2006; Chow *et al.*, 2008). As pronounced removals were achieved in this research, significantly better HS removal would be expected if experiments are conducted for regions with stronger sunlight.

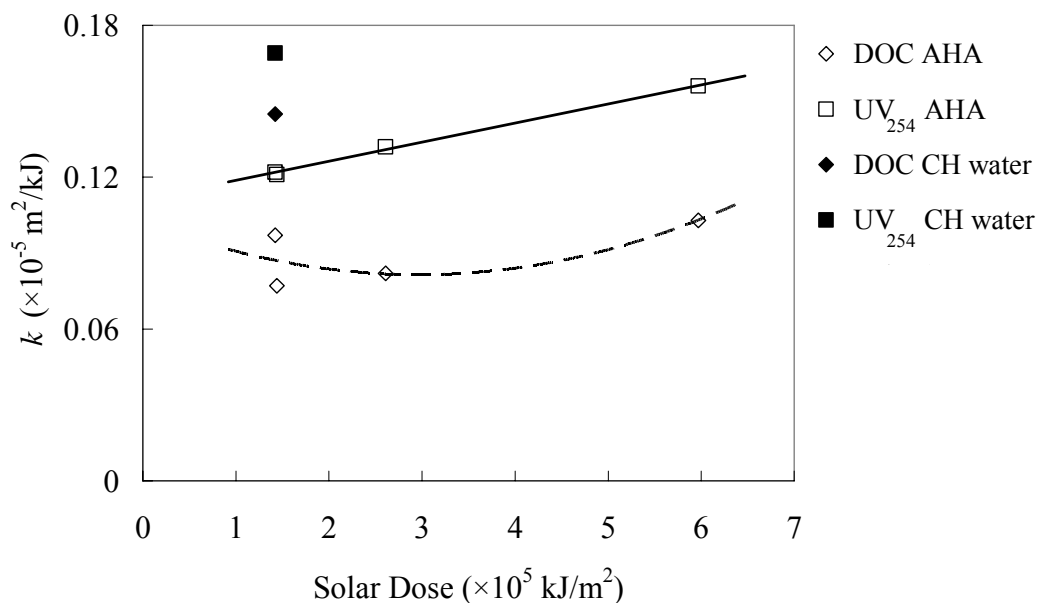


**Figure 5.26** Correlations between first-order decay rate constants of HS solutions irradiated in the flat tray and solar doses in four seasonal experiments.

### 5.3 Effects of solar irradiation on the adsorption of HS by GAC

#### 5.3.1 Characteristics of GAC

The Aquasorb 101 GAC was used as the adsorbent in this study. A summary of characteristics of this GAC relevant to the adsorption study is presented in Table 5.11. The value of the surface area measured was similar to the value stated by the supplier (950 m<sup>2</sup>/g). It is clear that the pore size distribution of the Aqua101 GAC was mainly in the microporous range (pore width < 2 nm), with a smaller portion (26 %) in the mesoporous (2 nm-50 nm) and macroporous (> 50 nm) range. Filtrasorb 400 (F400), a commonly used GAC in water treatment, has approximately 1000 m<sup>2</sup>/g specific surface area and about 86 % of the surface area falls into the pores smaller than 1 nm in width (Kilduff *et al.*, 1996). The Norit Row 0.8 Supra carbon used in water treatment applications was reported to have

only 15 % of the surface area of meso- and macropores (Świetlik *et al.*, 2002). It can be seen that the Aquasorb 101 carbon has the feature of many commercially available GAC in terms of the pore size distribution. It was selected as the representative carbon used in this research. Since the hypothesis of this research was based on the size exclusion effects, it is assumed that the observation made on the Aqua101 carbon would be also applicable to other commercial carbons with a higher portion of micropores and a smaller portion of meso- and macropores.

**Table 5.11** Basic characteristics of the Aquasorb 101 GAC (Universal Mineral Supplies, UK).

Surface area (m <sup>2</sup> /g)	919.4
Surface area <sub>micropore</sub> (m <sup>2</sup> /g)	682.9
Surface area <sub>meso+macropores</sub> (m <sup>2</sup> /g)	236.5
Pore volume (cm <sup>3</sup> /g)	0.88
pH <sub>PZC</sub>	9.5

pH<sub>PZC</sub>: Zero point of charge

### 5.3.2 Seasonal evaluation of solar irradiation effect on GAC adsorption of HS

The interactions between HS and GAC affect the adsorption of HS by GAC. Since the same type of GAC was used throughout this research, the properties of HS are considered to determine the extent of adsorption. Solar irradiation resulted in reductions in DOC, UV<sub>254</sub>, MW and pH of HS, which are expected to lead to the differences in the adsorption behaviour of the irradiated HS from the original.

### 5.3.2.1 Winter experiment

Adsorption isotherms of the irradiated and non-irradiated HS in winter experiments are presented in Figures 5.27. It is shown that the extent of adsorption increased with increasing equilibrium concentration or with decreasing GAC dose. Although no significant reduction in  $UV_{254}$ , DOC and MW was observed following solar irradiation in winter, the adsorption behaviour of HS was substantially influenced. Adsorption isotherms of the irradiated HS solutions differed slightly, corresponding to the minor differences in the  $UV_{254}$ , DOC and MW changes following solar irradiation (as can be seen in Figures 5.5, 5.6 and 5.7). From the isotherms, some information on the adsorption system can be obtained:

- higher loads of the irradiated HS on GAC when compared to the non-irradiated HS;
- steeper isotherm slopes of the irradiated HS, and in particular at high equilibrium concentrations;
- earlier adsorption starting points (or less delay) of the irradiated HS in those cases where the equilibrium concentration was low.

It is evident that solar irradiation improved the adsorption of HS over the entire concentration range of interest. For example, for an equilibrium concentration  $C_e$  value of 6 mg /L, the amount of HS adsorbed from the non-irradiated and irradiated HS solutions was approximately 3 and 6 mg/g, respectively. As previously discussed, there are two major factors, size exclusion effects and electrostatic interactions that can affect the adsorption of HS by GAC. According to the lab analysis, more than 74 % of the Aqua101 GAC surface was located within micropores (<2 nm). The average size of humic molecules has been reported to fall into the range of 0.4 and 4.2 nm (Cornel *et al.*, 1986; Aiken

and Malcolm, 1987; Karanfil *et al.*, 1999). According to the estimation by Cornel *et al.* (1986), the radius of AHA with MW larger than 5 kDa was more than 2 nm. Karanfil *et al.* (1999) reported that the radius of AHA (MW 4006 Da) had an average radius of 2.1 nm. According to Figure 5.7, most of the AHA used in this research was within the MW range of 100-10,000 Da. Clearly, some molecules with size larger than 2 nm were present in the non-irradiated HS solutions; therefore, they were not accessible to the fine carbon micropores. Solar irradiation decreased the molecular size of HS (Figure 5.7). The smaller molecules formed from the breakdown of high MW components were more accessible to the fine carbon pores than the larger ones due to the size exclusion effects. On the other hand, solar irradiation slightly increased the acidity of HS, according to a decrease in the pH value from 7.7 to 6.5 following solar irradiation. The GAC surface is more positively charged with increasing acidity, as indicated by the  $pH_{PZC}$  value, resulting in a stronger link between the irradiated HS and GAC surface. These physicochemical aspects justify the enhanced adsorption of the irradiated HS by GAC.

Further looking into each isotherm, a sharp rise was observed following a relatively slow increase of the load as the equilibrium concentration of the irradiated HS increased. The steep slope indicates a strong interaction between adsorbate and adsorbent (André, 2006). This strong interaction can be explained by the greater accessibility of the irradiated humic molecules to carbon pores, possibly due to the reduced size and increased surface attraction. As a result, for a small dose of carbon with limited adsorption sites, GAC became saturated and the load increased sharply. The slow change of the load with high carbon dose indicates that only a little surface was available for large molecules. This explains the slow change in the load of the non-irradiated HS by GAC, and also

corresponds to the fact that high MW compounds were still the dominant components in the irradiated HS solutions in winter experiment.

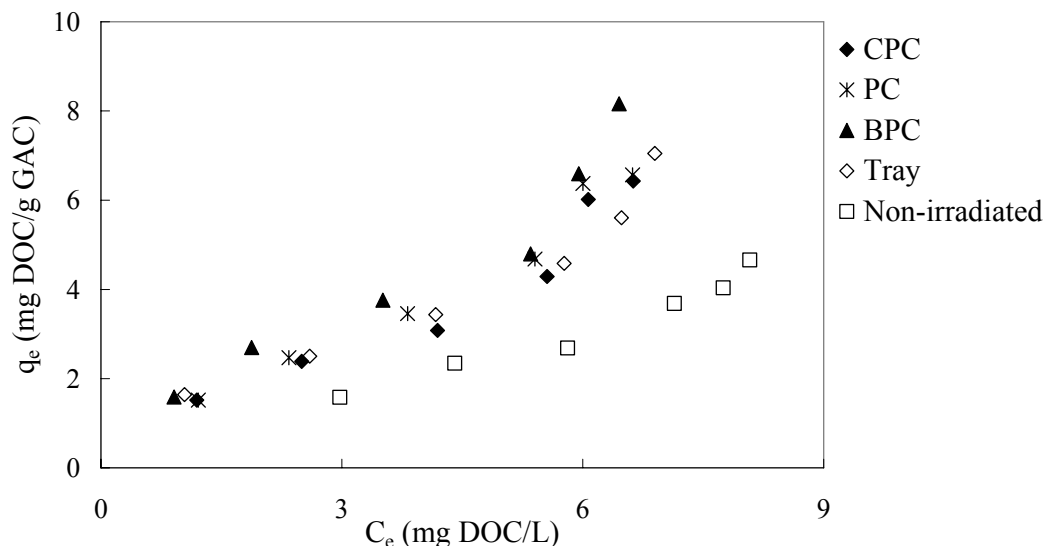


**Figure 5.27** Adsorption isotherms of the irradiated and non-irradiated HS solutions by GAC in winter experiment (initial DOC 8.50 mg/L, DOC removal 11-15 %, solar dose  $1.44 \times 10^5$  kJ/m<sup>2</sup>).

When examining the region of low equilibrium concentrations, a delay in adsorption was observed. The delay can be interpreted as the presence of non-adsorbable compounds in HS solutions for a carbon dose of 4000 mg/L (the maximum DOC dose in this study). For the irradiated HS, the starting point of adsorption was approximately 0.9 mg DOC/L, whereas a longer delay of 3 mg DOC/L was observed for the non-irradiated HS. The non-adsorbable compounds accounted for about 11 % (irradiated HS in BPC) and 35 % (non-irradiated HS) of the original HS. There are two possible reasons to this: either solar irradiation has completely photodegraded non-adsorbable compounds or the non-adsorbable compounds have been transformed into smaller adsorbable compounds by solar irradiation.

Several isotherm equations are available to model the adsorption behaviour (see Chapter 2). A good correlation of experimental data with models enables a better understanding of the adsorption process and a direct comparison between different systems. The conventional Langmuir (equation 2.2) and Freundlich (equation 2.4) models have been used more than 99 % of the time to describe the equilibrium adsorption of a variety of organic compounds onto activated carbon (Cooney, 1998). In addition to the conventional models, a modified Freundlich model (eq. 2.6) has been used by several researchers to describe the adsorption of commercial and natural HS by GAC (Summers and Roberts, 1988; Karanfil *et al.*, 1996a and 1996b; Kilduff *et al.*, 1996). It expresses the equilibrium condition in terms of the amount of unadsorbed components per unit of adsorbent, rather than the traditional equilibrium DOC concentration in solution (equation 2.6).

Initially the modified Freundlich model was compared with the conventional Langmuir and Freundlich models. The three equations were separately applied to model the GAC adsorption results of the non-irradiated HS and the irradiated HS in BPC (data have been shown in Figure 5.27). Parameters obtained through model fitting were then used to determine the new estimates of the DOC load on GAC,  $q_e$ , as the computed value. Results for the irradiated HS in BPC and the non-irradiated HS are illustrated in Figure 5.28. The X and Y axes, respectively, represent the experimental value  $q_e$  and its corresponding computed value from each model. If the model can perfectly represent experimental values, all computed values and their corresponding experimental values should meet and fall onto the same line (the solid line). A good model fitting should produce a minimum deviation between experimental values and computed values and certainly within the uncertainty of the overall measurement. Apparently, the modified Freundlich model represented adsorption data better, with all computed

values falling into the 10 % uncertainty region (between two dashed lines) relative to the experimental data over the investigated range. The conventional Langmuir and Freundlich models yielded much lower computed  $q_e$  values of the irradiated HS at the lowest GAC dose.

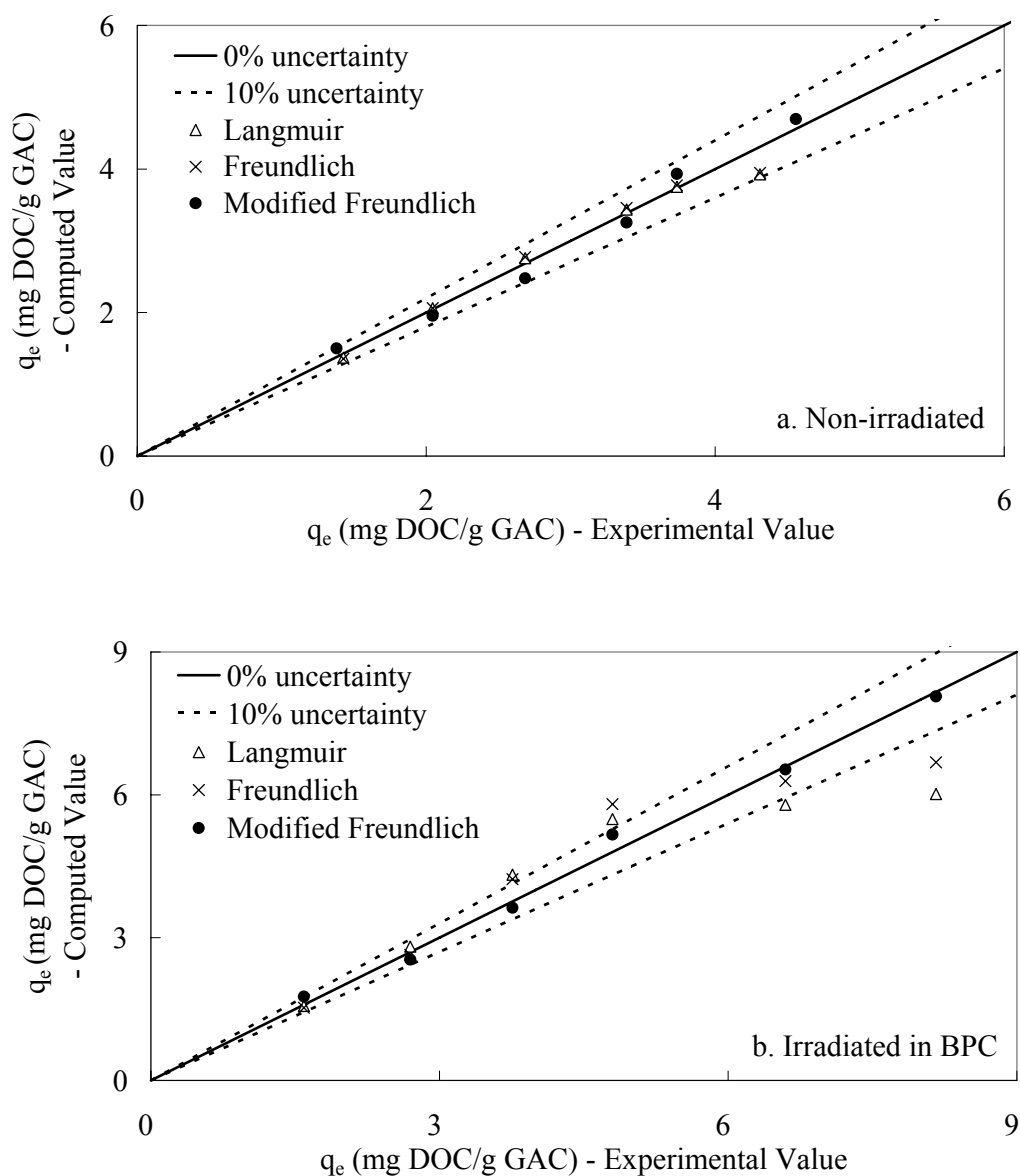


**Figure 5.28** Comparisons of experimental value and computed value of  $q_e$  based on the Langmuir, Freundlich and modified Freundlich models: (a) non-irradiated HS (DOC 8.50 mg/L) and (b) HS irradiated in BPC (DOC 7.23 mg/L). The

dashed lines represent 10 % uncertainty.

The Langmuir model considers the adsorption limited to one layer, corresponding to a unique type of adsorbent or adsorption energy. It is highly likely to be valid for a well-defined molecule or a homogenous adsorbent or at a low coverage for a heterogeneous adsorbent (André, 2006). The Freundlich model accounts for the heterogeneity of the adsorbent surface; however, it can not sufficiently model the polydisperse polymer adsorption (Summers and Roberts, 1988b). A maximum error in  $q_e$  at the lowest GAC dose when applying the Freundlich model was also observed by Summers and Roberts (1988a). Adsorption of polydisperse molecules (such as HS) by GAC is dose-dependent (Karanfil *et al.*, 1996a). When the GAC dose is low, the most adsorbable components are preferentially removed from the mixture. With increasing carbon dose, the less adsorbable components are also removed. Therefore, it is the composition of non-adsorbed HS at equilibrium that decides the extent of adsorption, rather than the residual liquid-phase concentration (Summers and Roberts, 1988a). A recommended parameter to represent the non-adsorbed HS composition is the amount of non-adsorbed solute per unit mass of adsorbent, resulting in a modified form of the Freundlich model (equation 2.6).

André (2006) used the same GAC as the one used in this research to adsorb Aldrich HS (with a DOC of 10 mg/L) from water and found that the Freundlich model and Henry model (which is identical to the Freundlich model when the exponent  $n^{-1}$  is equal to 1) fitted isotherms well, while the Langmuir model was suitable for only a few cases. The observation in Figure 5.28a justifies the validity of applying the conventional equations to model the adsorption of Aldrich HS by GAC, even though there is an approximately 10 % deviation at the lowest GAC dose. However, considering the original hypothesis of this research with

respect to the preferential adsorption of smaller photoproducts, and together with the excellent fits of the modified Freundlich model (Summers and Roberts, 1988; Karanfil *et al.*, 1996a and 1996b; Kilduff *et al.*, 1996) to experimental values (Figure 5.28b), it is more appropriate to employ the modified Freundlich equation for modeling the adsorption of irradiated HS, as it takes account of both the polydispersity of HS and the heterogeneity of GAC.

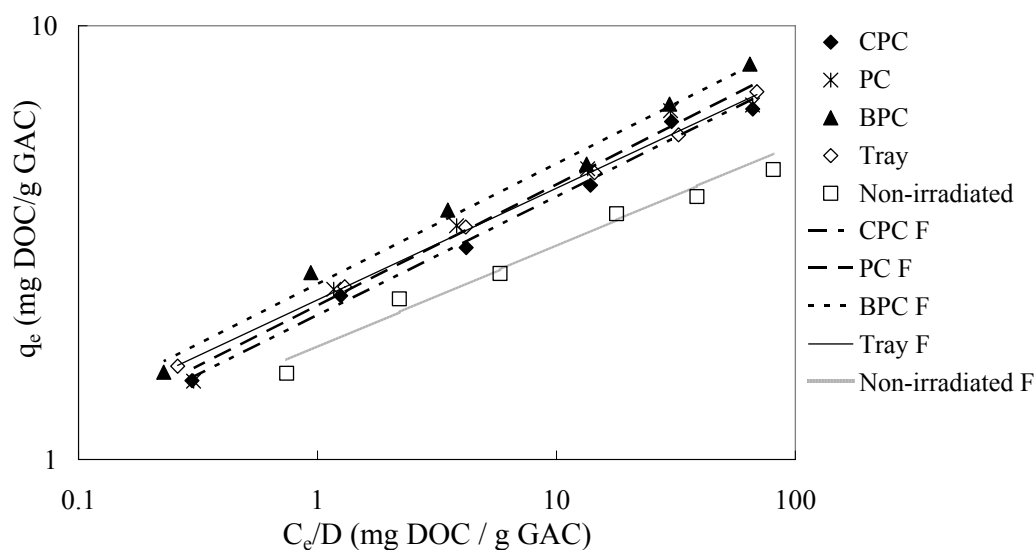


**Figure 5.29** Adsorption of the irradiated and non-irradiated HS solutions by GAC in winter experiments. Solid and dashed lines represent the fitting of the modified Freundlich model to experimental data (initial DOC 8.50 mg/L, DOC removal 11-15 %, solar dose  $1.44 \times 10^5$  kJ/m<sup>2</sup>).

The dose-normalized form of isotherms for winter HS solutions is illustrated in Figure 5.29. The lines represent the modified Freundlich model fits to experimental values. Parameters obtained from the modified Freundlich model are presented in Table 5.12. There were approximately parallel shifts of isotherms when plotting  $q_e$  vs.  $C_e/D$  on log-log axes. According to Karanfil *et al.* (1996a), the relatively parallel isotherms indicate different macromolecules

having a uniform chemical affinity for the GAC surface. It can therefore be deduced that with low solar intensity (or in winter), the chemical properties of HS did not greatly change. Size exclusion effects dominated the adsorption process and chemical aspect only played a minor role.

**Table 5.12** Modified Freundlich isotherm parameters for the irradiated and non-irradiated HS solutions in winter experiment (initial DOC 8.50 mg/L, DOC removal 11-15 %, solar dose  $1.44 \times 10^5$  kJ/m<sup>2</sup>).

Solar collectors	$K_F$	$n^{-1}$	$K_{F,irr}/K_{F,non}$	Maximum adsorption load (mg/g) <sup>b</sup>
CPC	2.15	0.273	1.16	7.05
PC	2.27	0.279	1.22	6.53
BPC	2.54	0.278	1.37	8.16
Tray	2.33	0.258	1.25	6.47
Non-irradiated	1.86	0.236	-	3.83

$K_F$ : (mg DOC/g GAC)<sup>1-1/n</sup>

Maximum adsorption load: DOC load on 100 mg GAC/L

The adsorbability of HS can be interpreted in terms of the Freundlich unit-capacity parameter ( $K_F$ ) which represents the adsorption capacity at  $C_e/D$  equal to unity. The ratio of the Freundlich parameters determined for the irradiated and non-irradiated HS,  $K_{F,irr}/K_{F,non}$ , can be used to compare the improvement of the HS adsorbability due to the pre-treatment with solar irradiation. It is clearly shown in Table 5.12 that as a result of exposing HS to solar irradiation, the magnitude of  $K_F$  was increased by 16-37 %. The lower enhancement of the HS adsorbability when using CPC and PC compared to using flat tray is possibly due to DOC analytical errors occurring to the lowest

equilibrium concentrations. The maximum adsorption load represents the amount of HS adsorbed on a GAC dose of 100 mg/L at equilibrium (which is the lowest carbon dose used in this study). Due to the preferential adsorption phenomenon, GAC of the lowest dose is presumed to adsorb the most adsorbable molecules from the mixture. The change in the maximum adsorption load therefore specifically refers to the change in the amount of the most adsorbable molecules following solar irradiation. As shown, solar irradiation increased the amount of the most adsorbable molecules in the irradiated HS solutions by 67-113% compared to the non-irradiated solutions. The results for  $K_F$  and maximum adsorption load evidence that HS components of different molecular sizes exhibit different adsorbability; more importantly, it shows that for humic rich waters, only a small dose of solar irradiation may greatly improve the performance of GAC adsorption.

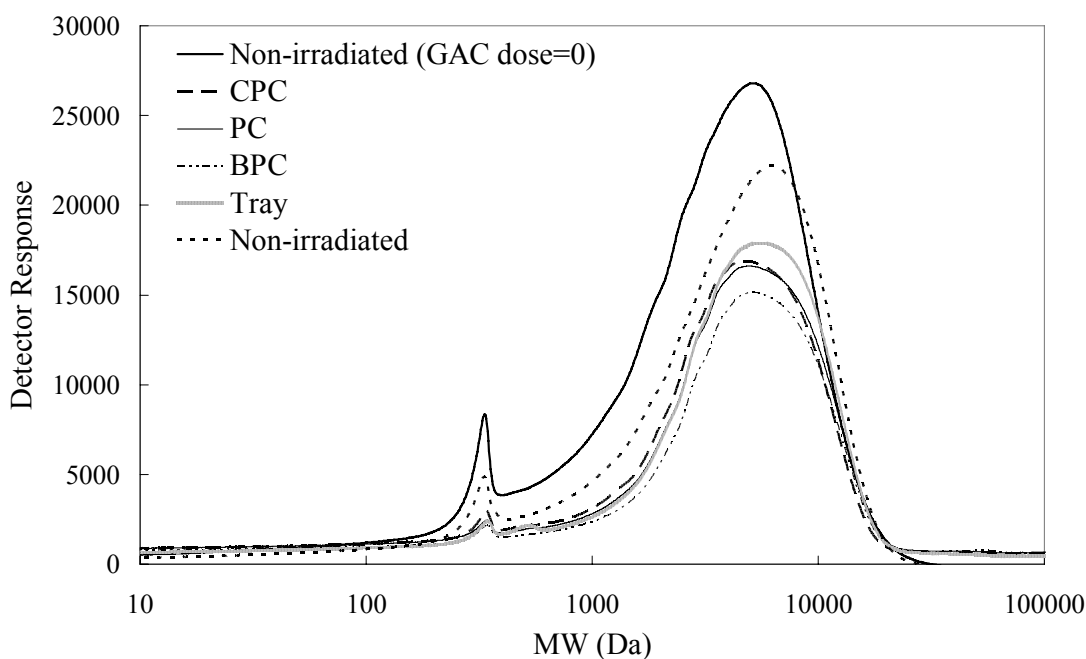


**Figure 5.30** Chromatograms of the non-irradiated and irradiated HS solutions after adsorption by GAC (1000 mg/L) in winter experiment (initial DOC

8.50mg/L, DOC removal 11-15 %, solar dose  $1.44 \times 10^5$  kJ/m<sup>2</sup>).

The HPSEC chromatograms of HS remaining in solutions after adsorption by 1000 mg GAC/L are plotted in Figure 5.30. After adsorption, the MWD of the non-irradiated HS shifted towards higher MW values, indicating the favourable adsorption of smaller molecules from the humic mixture by GAC. A considerable amount of high MW compounds still remained in the solutions after adsorption, due to the fact that large molecules were excluded from carbon pores. Solar irradiation improved the HS removal over the entire MW range, with a slightly more decrease in the chromatogram of the HS irradiated in BPC.

#### 5.3.2.2 Spring experiment

There is a noticeable difference between spring isotherms (Figure 5.31) and winter isotherms (Figure 5.27). The former exhibits higher loads on GAC and steeper slopes of isotherms, indicating stronger interactions between GAC and the irradiated HS molecules, and the irradiated HS solutions in spring more efficiently removed relative to the winter ones. This can be explained by the higher solar intensity in spring resulting in higher reductions in UV<sub>254</sub>, DOC and MW, as previously presented in section 5.2.3.2.

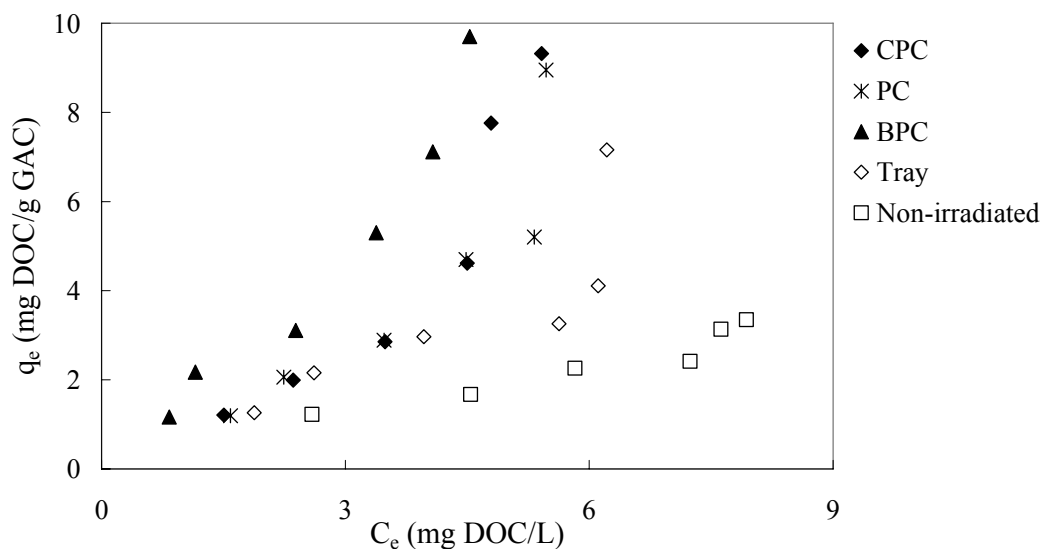


**Figure 5.31** Adsorption isotherms of irradiated and non-irradiated HS solutions by GAC in spring experiment (initial DOC 8.29 mg/L, DOC removal 18-31 %, solar dose  $2.61 \times 10^5$  kJ/m<sup>2</sup>).

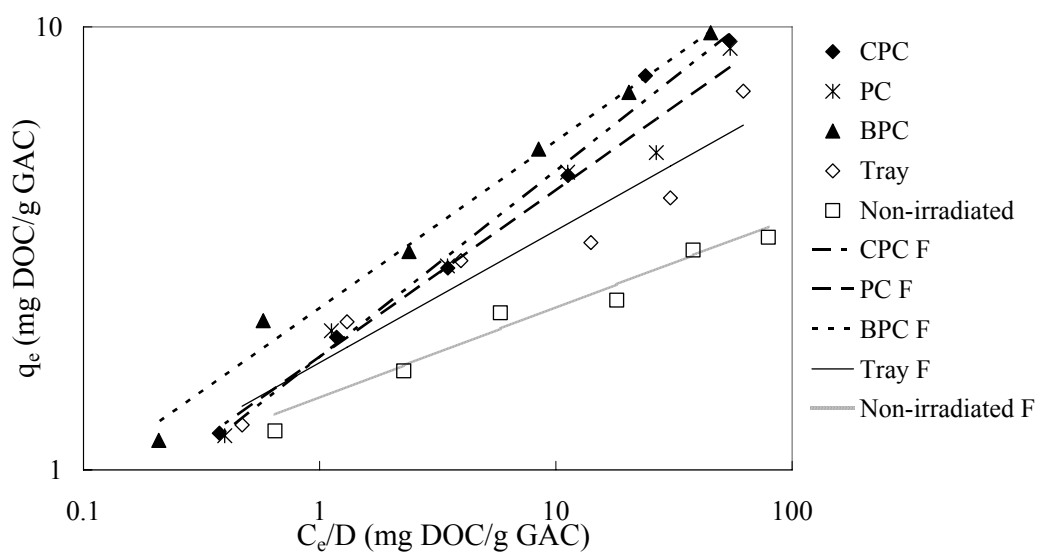


**Figure 5.32** Adsorption of irradiated and non-irradiated HS solutions by GAC in spring experiment. Solid and dashed lines represent the fitting of the modified Freundlich model to experimental data. (initial DOC 8.29 mg/L, DOC removal 18-31 %, solar dose  $2.61 \times 10^5$  kJ/m<sup>2</sup>).

Examining the low equilibrium concentration region, the amount of non-adsorbable compounds remaining in the solutions was in an ascending order: BPC < CPC  $\approx$  PC < tray < non-irradiated, indicating the different extent of the non-adsorbable compounds removal due to solar irradiation. A GAC dose of 100 mg/L adsorbed up to two times more humic molecules from the irradiated HS solutions than the non-irradiated solutions (Table 5.13). Given the same distribution of GAC adsorption sites for winter and spring HS solutions, the result reflects that there were more adsorbable molecules accessible to carbon pores in spring irradiated samples.

**Table 5.13** Modified Freundlich isotherm parameters for irradiated and non-irradiated HS solutions in spring experiment. (initial DOC 8.29 mg/L, DOC removal 18-31 %, solar dose  $2.61 \times 10^5$  kJ/m<sup>2</sup>).

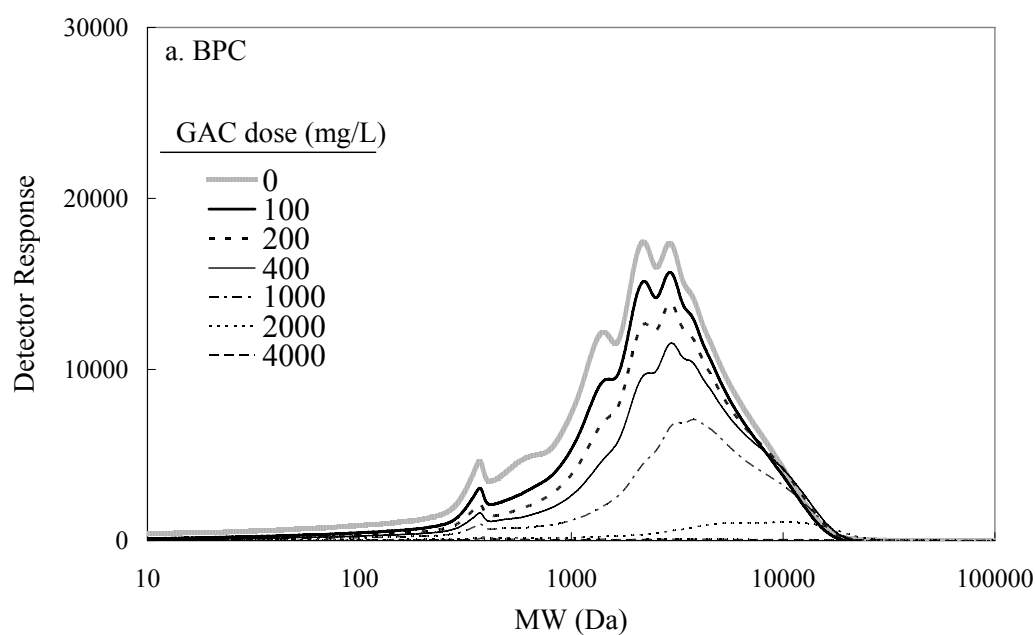
Solar collectors	$K_F$	$n^{-1}$	$K_{F,irr}/K_{F,non}$	Maximum adsorption load (mg/g)
CPC	1.80	0.420	1.28	9.32
PC	1.80	0.376	1.28	8.95
BPC	2.32	0.377	1.65	9.70
Tray	1.75	0.299	1.24	7.16
Non-irradiated	1.41	0.208	-	3.35

$K_F$ : (mg DOC/g GAC)<sup>1-1/n</sup>

Maximum adsorption load: DOC load on 100 mg GAC/L

Similarly, the conventional Langmuir and Freundlich models did not represent the experimental data well over the range of adsorption isotherms of interest. The modified Freundlich equation was applied as the adsorption model. Results are presented in Figure 5.32 and Table 5.13. Approximately 65 %, 28 %, 28 % and

24 % of the improvement in the HS adsorbability was observed due to pre-treatment with solar irradiation. The impact of solar irradiation on the Freundlich exponential coefficient ( $n^{-1}$ ) showed similar trends to that on  $K_F$ . The  $n^{-1}$  is related to the adsorption energy (adsorbent or adsorbate heterogeneity) or availability of adsorption sites (Weber *et al.*, 1991). An increase in  $n^{-1}$  value means that the energy of adsorption is more uniform (André, 2006). For a given adsorbent, HS components with various molecular sizes and structures are expected to adsorb with different energies. Solar irradiation reduced the heterogeneity of HS, and consequently reduced the heterogeneity of the adsorption system. This helps explain the increase of the exponential coefficient for the adsorption of the irradiated HS solutions.



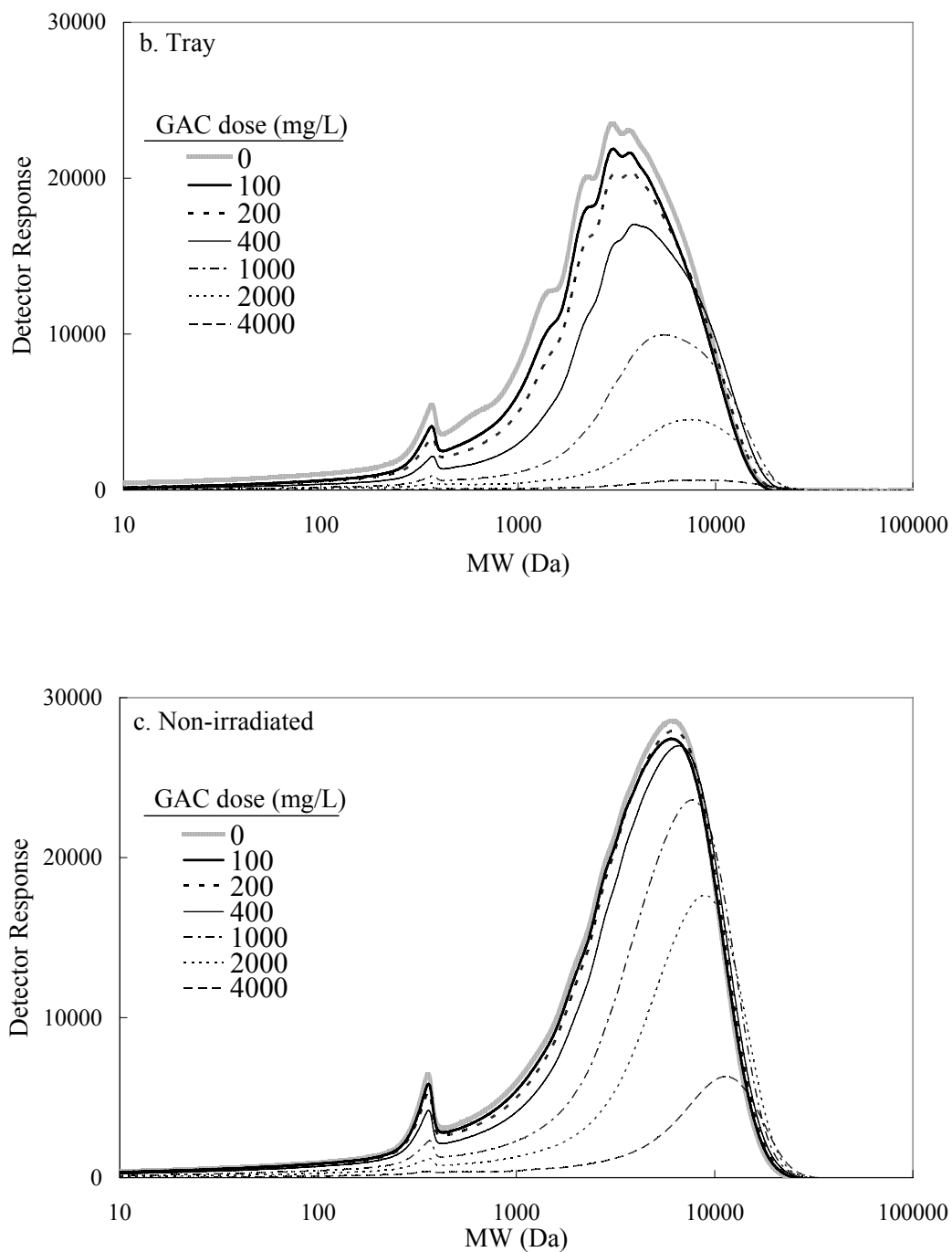
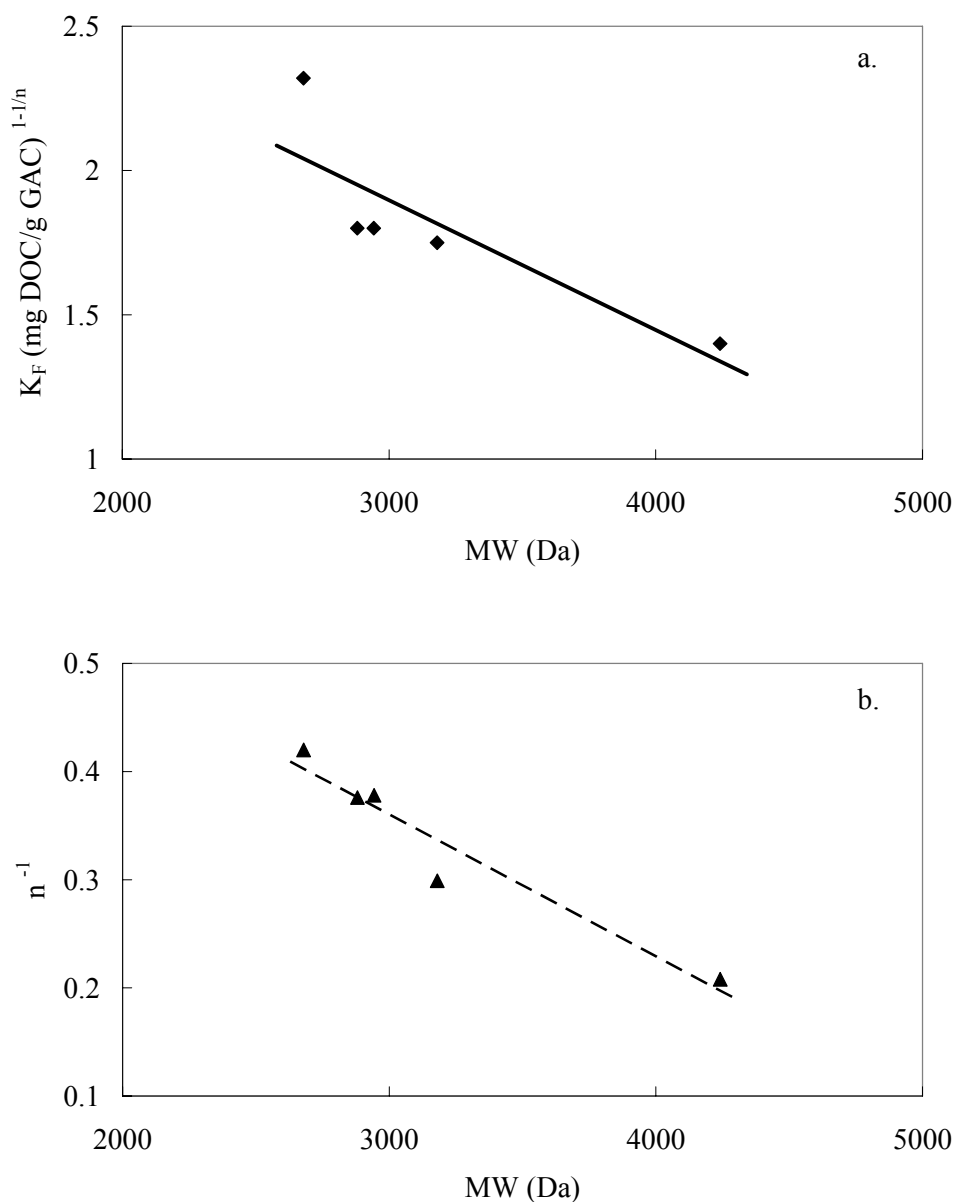


**Figure 5.33** HPSEC chromatograms of HS remaining in solution after GAC adsorption in spring experiment: (a) HS irradiated in BPC, (b) HS irradiated in tray, and (c) non-irradiated HS (DOC removal 18-31 %, solar dose  $2.61 \times 10^5$  kJ/m<sup>2</sup>).

Representative HPSEC chromatograms of HS remaining in solutions after adsorption by various doses of GAC are illustrated in Figure 5.33, showing that as the adsorbent dose increased, a greater amount of chromophoric HS was removed from the solution. It also demonstrates the fact that smaller molecules were readily removed from the mixture, mainly leaving larger organic compounds in the solutions after adsorption; this is reflected by the chromatograms shifting to larger MW values. At the highest GAC dose (4000 mg/L), almost no detectable chromophores remained in the irradiated HS solutions after adsorption, showing that all the irradiated chromophoric molecules were accessible to the GAC surface. It also implies that the non-adsorbable compounds, observed in the isotherms of irradiated HS in Figure 5.31, consisted of organic molecules that do not have the aromatic character. The non-adsorbable compounds observed in equilibrium isotherms accounted for 31 % (non-irradiated HS) and 10 % (irradiated HS in BPC) of the total DOC, respectively; whereas the non-adsorbable chromophores accounted for 15 % (non-irradiated HS) and 0 % (irradiated HS in BPC) of the total chromophoric HS. It can therefore be deduced that the non-adsorbable chromophores have been completely photodegraded or/and transformed into adsorbable compounds by solar irradiation; and the adsorbability of non-chromophoric compounds were partially changed, resulting from the indirect photodegradation.

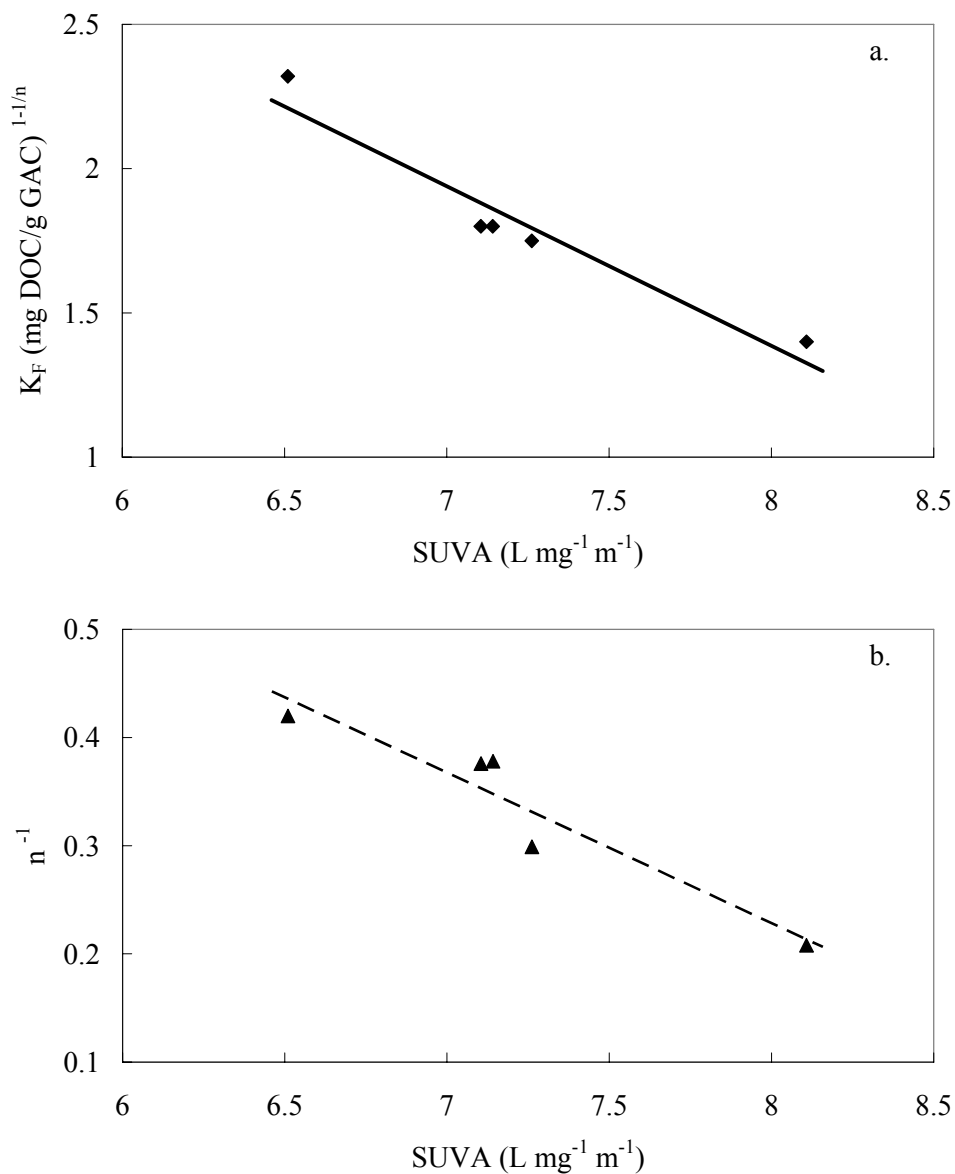
The Freundlich parameters  $K_F$  and  $n^{-1}$  (data shown in Table 5.13) as a function of the initial MW of the non-irradiated and irradiated HS prior to adsorption are plotted in Figure 5.34. The higher the initial MW, the lower the adsorption capacity was. This can be related to the observation in the chromatograms shown in Figure 5.10. Solar irradiation led to the destruction of high MW compounds and formation of smaller molecules which are more accessible to the

fine carbon pores. A lower MW value of the irradiated HS indicates that there were more high MW compounds photodegraded and more smaller molecules present in the irradiated HS. A good correlation between the Freundlich parameters and the MW of HS (Figure 5.34) indicates the important role of molecular size in determining the extent of adsorption of HS by GAC.



**Figure 5.34** Correlations between MW of the non-irradiated and irradiated HS and adsorption parameters: (a)  $K_F$  and (b)  $n^{-1}$ . (The solid and dashed lines suggest

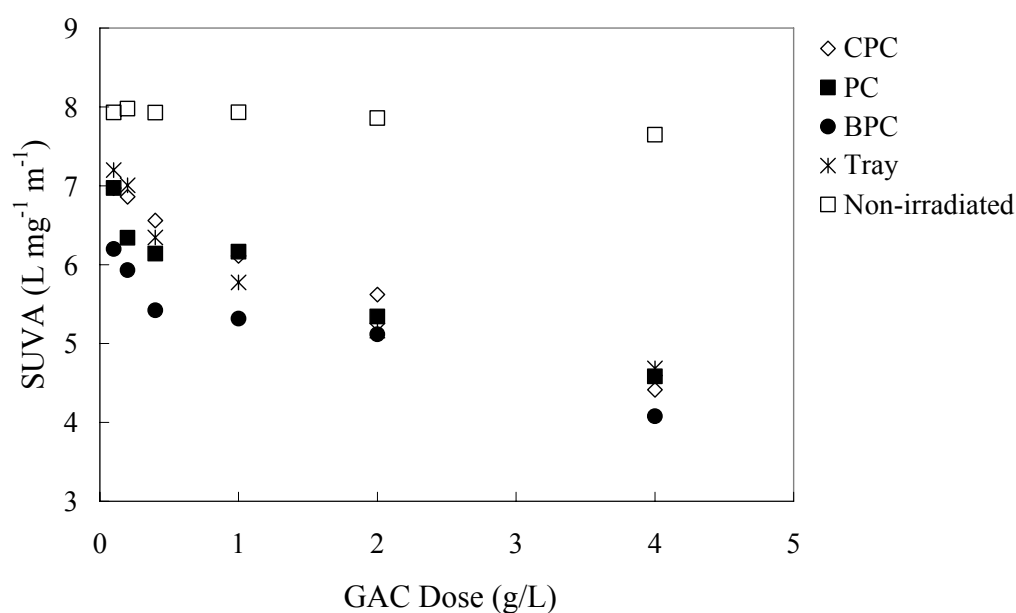
the trend)



**Figure 5.35** Correlations between the aromaticity of the non-irradiated and irradiated HS and adsorption parameters of HS: (a)  $K_F$ , and (b)  $n^{-1}$ . (The solid and dashed lines suggest the trend.)

The Freundlich parameters are also found to be well correlated with the SUVA of HS, as displayed in Figure 5.35. The SUVA is a good surrogate to indicate the aromaticity of organic compounds, allowing for an evaluation of the influence of

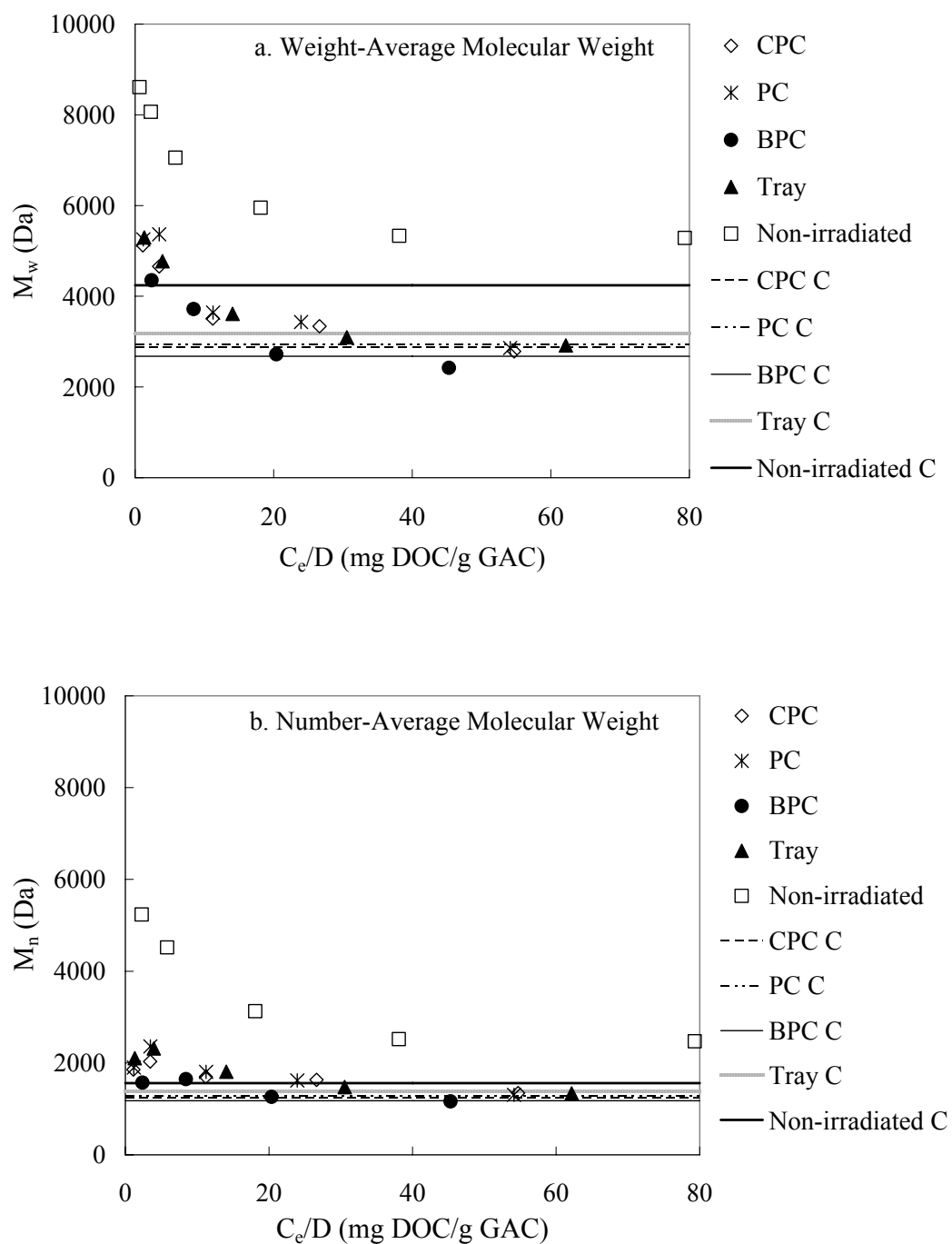
chemical structures in terms of aromaticity on the adsorption of HS. Photoproducts produced from the breakdown of high MW components are of lower MW and less aromaticity, thus more hydrophilic and more soluble in water compared to their parent compounds. Aromatic components of HS are hydrophobic in character, and therefore more readily adsorbed by GAC (Karanfil *et al.*, 2000). For example, McCreary and Snoeyink (1980) observed that a higher adsorption capacity for a soil derived HA than for the smaller fulvic molecules isolated from the same source. On the contrary, it is shown in Figure 5.35 that the adsorbability of HS increased with decreasing aromaticity. This observed trend is more likely to be a result of the impact of MW rather than the aromaticity, indicating that MW is the primary factor controlling the adsorption in this research.



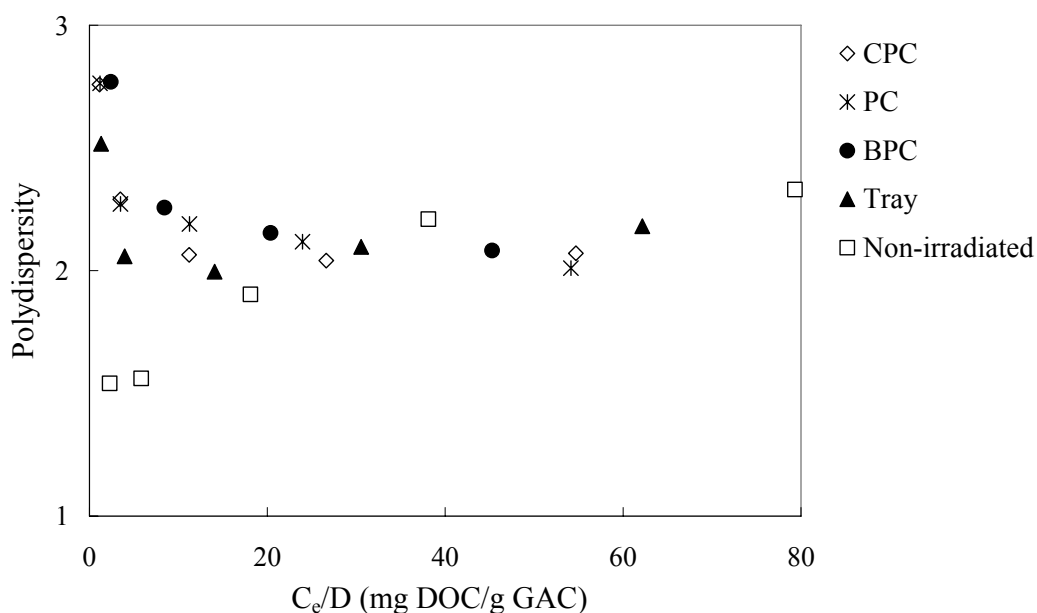
**Figure 5.36** SUVA values of the irradiated and non-irradiated HS remaining in solutions after adsorption by various doses of GAC in spring experiment (DOC removal 18-31 %, solar dose  $2.61 \times 10^5$  kJ/m<sup>2</sup>).

Figure 5.36 shows the SUVA value of HS remaining in solutions after adsorption by various GAC doses. As can be seen, the SUVA value of the irradiated HS remaining in solutions decreased with increasing GAC dose, indicating a decrease of the aromaticity. However, the SUVA of the non-irradiated HS only slightly changed after contacting various GAC doses. This means that using solar irradiation as a pre-treatment method can noticeably enhance the removal of aromatic compounds in the irradiated HS, which might be the aromatic photoproducts with lower MW. Since the aromatic compounds are known to be more reactive in the DBP formation, as a result, the DBP formation potential of the solar pre-treated humic water may be greatly reduced.

Due to the lack of analytical capabilities for characterizing functional groups, chemical structures of HS in terms of functional groups were not studied in this research. One should keep in mind that functional groups might influence the adsorption of HS. Carboxylic groups are predominate groups in HS. McCreary and Snoeyink (1980) found that the extent of HS adsorption decreased with increasing carboxylic acidity. Conversely, Karanfil *et al.* (1996a) reported an increasing extent of HS adsorption with increasing carboxylic groups. The two previous reports suggest that the impact of functional groups is specific to the system under study. However, a study by Xie *et al.* (2004) revealed that the concentration of carboxylic groups only slightly decreased or increased during irradiation. It is therefore considered that the influence of carboxylic groups was insignificant in this study.



**Figure 5.37** Changes in the MW of HS solutions remaining in the solutions after adsorption by various GAC doses in spring experiment: (a) weight-average MW, and (b) number-average MW.



**Figure 5.38** Changes in the polydispersity of the non-irradiated and irradiated HS solutions remaining in solution after adsorption by various GAC doses in spring experiment.

The average MWs ( $M_n$  and  $M_w$ ) of HS remaining in solutions as a function of  $C_e/D$  are plotted in Figure 5.37. As a result of the preferential removal of low MW compounds, the  $M_n$  and  $M_w$  of the residual HS were generally higher than the corresponding control value C ( $M_n$  and  $M_w$  of HS without contacting GAC). The greatest difference was observed when the carbon dose was high and mainly high MW compounds were left in the solutions. When the carbon dose was low, MW values of HS remaining in solution approached the control values.

It has become apparent that the smaller molecules are preferentially adsorbed by GAC due to the better accessibility to carbon pores. If complete preferential adsorption is exhibited for the low MW compounds, both the  $M_n$  and  $M_w$  will increase and the polydispersity will decrease (Kilduff *et al.*, 1996). This agrees well with the observed trend of all the irradiated HS solutions as displayed in

Figure 5.38. An opposite trend was noticed for the non-irradiated HS. The polydispersity of the non-irradiated HS increased with increasing equilibrium concentrations. If the  $M_n$ ,  $M_w$  and polydispersity increase simultaneously, the  $M_w$  must increase faster than the  $M_n$ . This means that some smaller molecules were non-adsorbable or adsorbed to a lesser extent than the larger ones (Kilduff *et al.*, 1996). The latter is more possible as there were only an insignificant amount of non-adsorbable small molecules observed in chromatograms at high GAC dose (Figure 5.33c). Therefore, some non-irradiated large HS molecules were also adsorbed by the GAC surface, more specifically, the external surface. As a result, the adsorption access was restricted for the smaller molecules and the preferential adsorption was incomplete. The greater adsorption of large molecules might be explained by the shorter diffusion distances to adsorption sites travelled by the larger molecules relative to the smaller ones (Newcombe *et al.*, 2002a). Based on this observation, the enhanced adsorption of the irradiated HS can also be attributed to the fact that solar irradiation broke down some high MW components that had greater adsorption on GAC, and consequently made more adsorption sites available for smaller molecules.

In addition, the improvement in the adsorption of the irradiated HS may also be caused by the dilution of HS solutions, as HS was removed by up to 43 % in terms of DOC concentration following solar irradiation in spring. When GAC dose is lower relative to the initial concentration of HS, there are limited sites available for adsorption. At high GAC dose relative to the initial concentration, there is a greater removal of HS as more adsorption sites are available. Consequently, at a constant GAC dose and a range of HS concentrations, the extent of adsorption decreases with increasing initial DOC value (Summers and Roberts, 1988a).

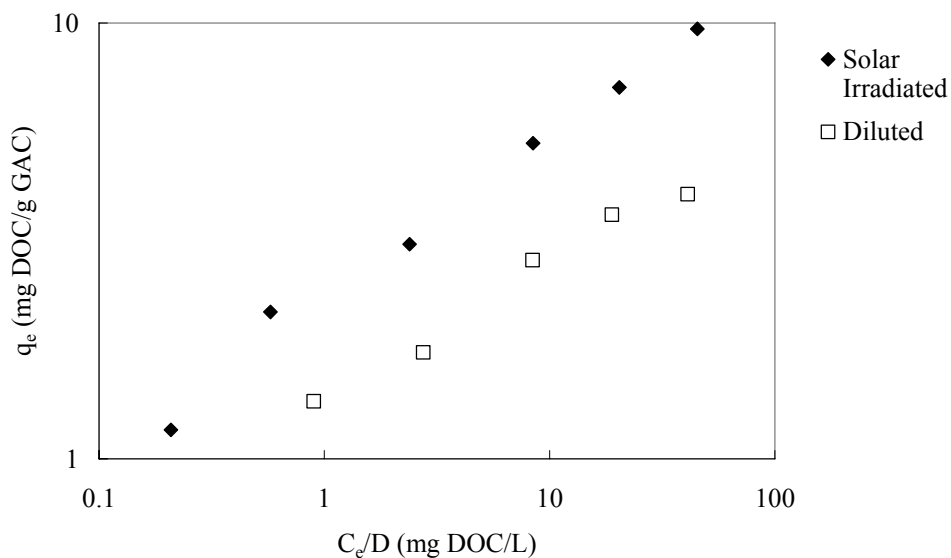


**Figure 5.39** Adsorption isotherms of the non-irradiated and irradiated HS with similar initial concentrations.

In order to eliminate the initial concentration effect and only to evaluate the effect of solar irradiation on adsorbability, isotherms of the irradiated and non-irradiated HS with similar initial concentrations were compared (Figure 5.39). It was achieved by diluting the non-irradiated solution to the similar concentration of the solar-irradiated solution in BPC. The Freundlich parameters for the diluted non-irradiated solution were found to be slightly higher than those of the original solution, confirming the notion that the adsorption capacity of HS increases upon dilution. However, more pronounced differences were observed between the irradiated and diluted HS solutions, as reflected in the isotherms shown in Figure 5.39 and the adsorption parameters shown in Figure 5.40. The adsorbability of the irradiated HS was almost two times that of the non-irradiated HS, the maximum adsorption load was increased by more than two times, and there were more non-adsorbable compounds in the diluted solutions. These results demonstrate that the dilution of HS solutions resulting from solar irradiation only

played a minor role in improving the removal of HS by GAC. It is the initial molecular composition of HS, rather than the solution concentration, determines the extent of adsorption. This notion fits well to the idea of using solar irradiation as a pre-treatment method. Although the extent of DOC removal varies among water sources as discussed in section 2.3.2.2, using solar irradiation can effectively change the molecular size distribution of HS, and consequently enhance their removal by the following adsorption process.

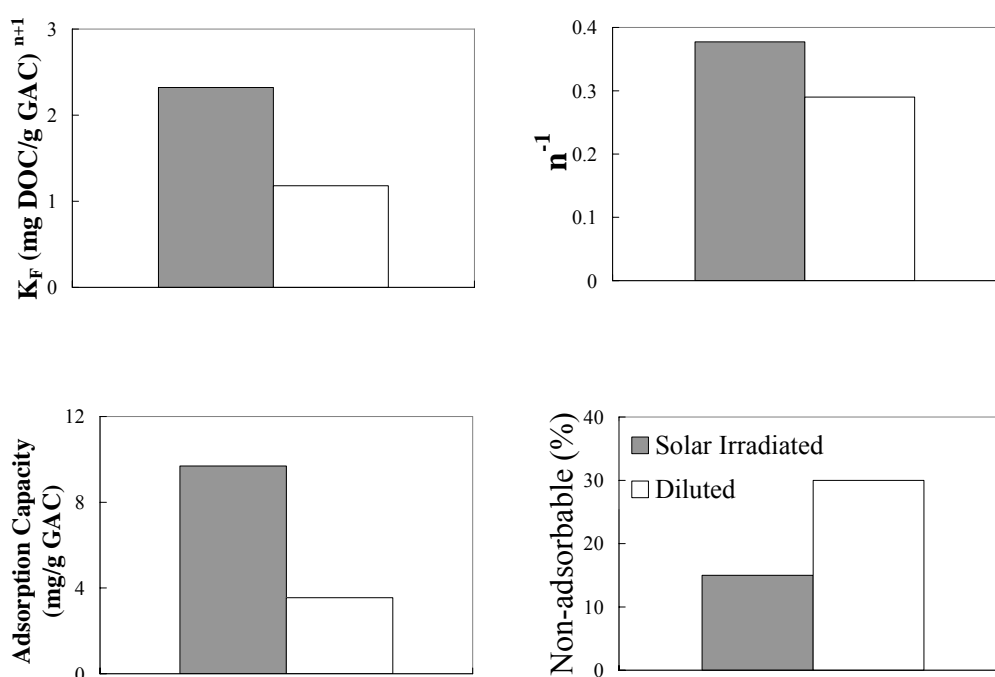


**Figure 5.40** Comparisons of the adsorption parameters of irradiated and diluted HS solutions with similar initial concentrations.

### 5.3.2.3 Summer experiment

As expected, significant differences were observed in the isotherms of the summer irradiated HS (Figure 5.41) from the winter and spring HS. The summer samples exhibited a rapid increase as the equilibrium concentration increased,

indicating all the irradiated molecules having strong interactions with the GAC surface. These molecules are considered to be smaller than 2 nm. There was also a noticeable advantage of using BPC. For example, at the equilibrium concentration of 2 mg/L, the DOC load of the BPC samples on GAC was approximately four times that of the CPC and PC samples. The advantage can be also seen from the maximum adsorption load on GAC, which was improved by up to 3.6 times due to pre-treatment using solar irradiation. The difference in isotherms between the irradiated HS in small solar collectors was insignificant, corresponding to the results from irradiation experiments. There were less than 5 % of the non-adsorbable compounds remaining in irradiated HS solutions after adsorption, indicating that the strong solar irradiation in summer effectively degraded non-adsorbable compounds which were also non-chromophoric, probably via the indirect photodegradation pathway.

A quantitative evaluation of the adsorption of HS in summer experiment is illustrated in Figure 5.42 and Table 5.14. The adsorbability of the irradiated HS was increased by 61 % (CPC), 71 % (PC), 99 % (BPC) and 42 % (Tray) as compared to the non-irradiated HS. As a result of the significant decrease in MW and heterogeneity of HS, the  $n^{-1}$  value and maximum adsorption load of the irradiated HS were significantly increased.

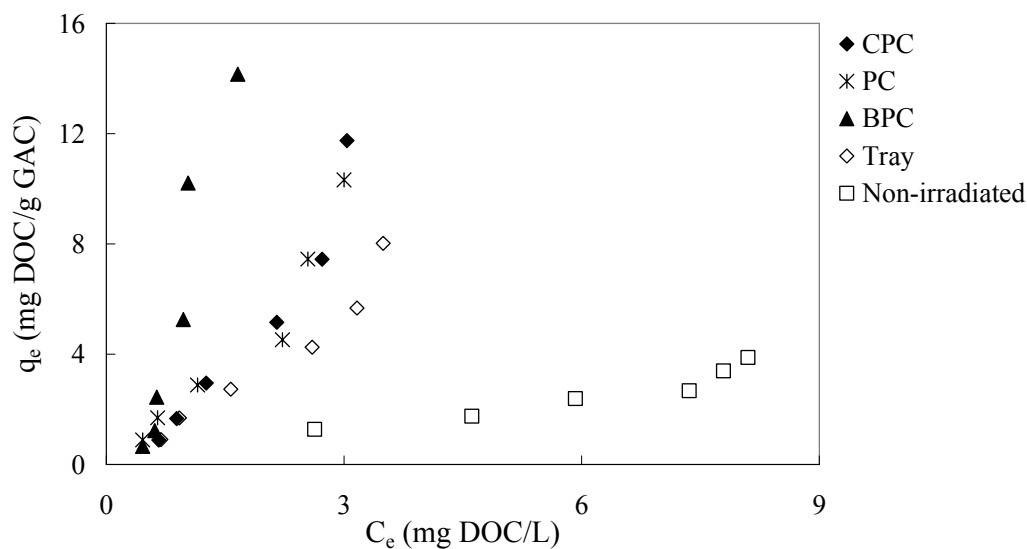


**Figure 5.41** Adsorption isotherms of the irradiated and non-irradiated HS solutions by GAC in summer experiment (initial DOC 8.51 mg/L, DOC removal 50-62 %, solar dose  $5.97 \times 10^5$  kJ/m<sup>2</sup>).

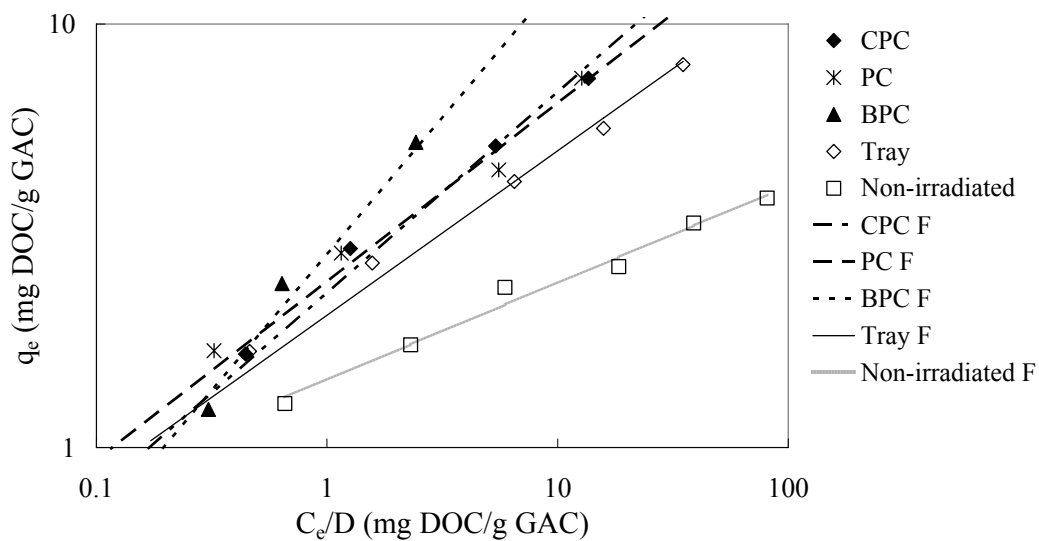


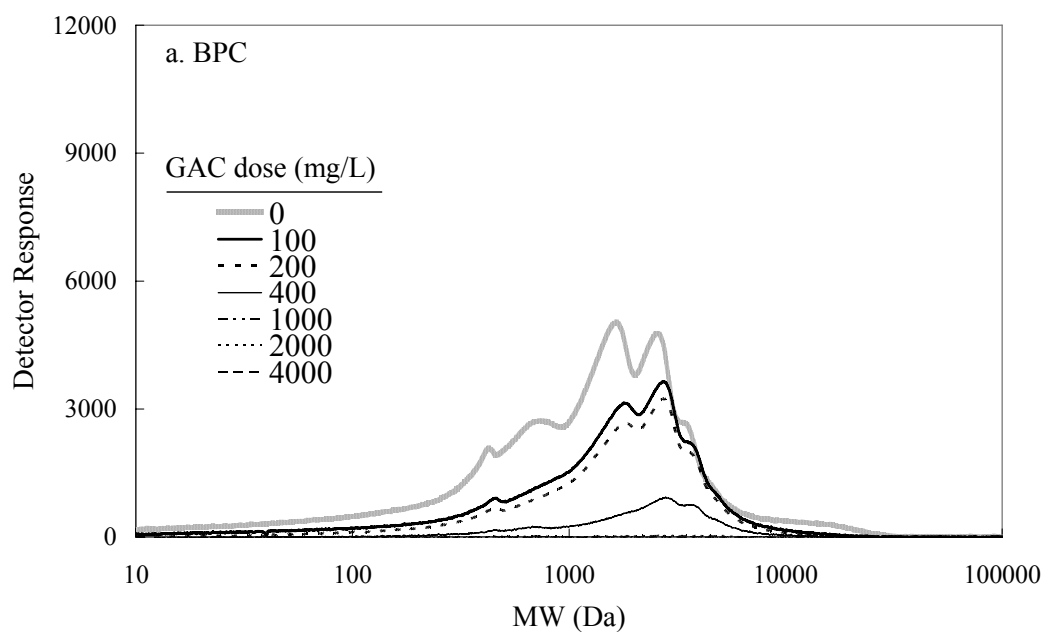
**Figure 5.42** Adsorption of the irradiated and non-irradiated HS by GAC in summer experiment. Solid and dashed lines show the fitting of the modified Freundlich model to the experimental data (initial DOC 8.51 mg/L, DOC removal 50-62 %, solar dose  $5.97 \times 10^5$  kJ/m<sup>2</sup>).

**Table 5.14** Modified Freundlich isotherm parameters for the irradiated and non-irradiated HS solutions in summer experiment (initial DOC 8.51 mg/L, DOC removal 50-62 %, solar dose  $5.97 \times 10^5$  kJ/m<sup>2</sup>).

Solar collectors	$K_F$	$n^{-1}$	$K_{F,irr}/K_{F,non}$	Maximum adsorption load (mg/g)
CPC	2.32	0.474	1.61	11.75
PC	2.46	0.421	1.71	10.32
BPC	2.86	0.644	1.99	14.16
Tray	2.05	0.388	1.42	8.02
Non-irradiated	1.44	0.229	-	3.88

$K_F$ : (mg DOC/g GAC)<sup>1-1/n</sup>

Maximum adsorption load: DOC load on 100 mg GAC/L



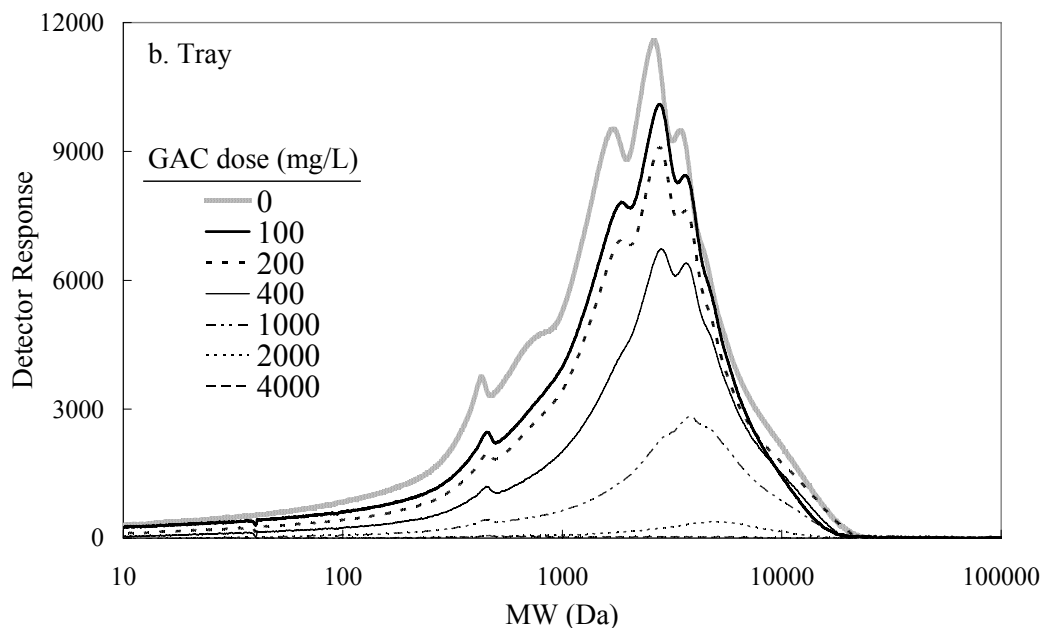


**Figure 5.43** Chromatograms of HS remaining in the solutions after adsorption by GAC in summer experiment: (a) HS irradiated in BPC, and (b) HS irradiated in the flat tray (DOC removal 50-62 %, solar dose  $5.97 \times 10^5$  kJ/m<sup>2</sup>).

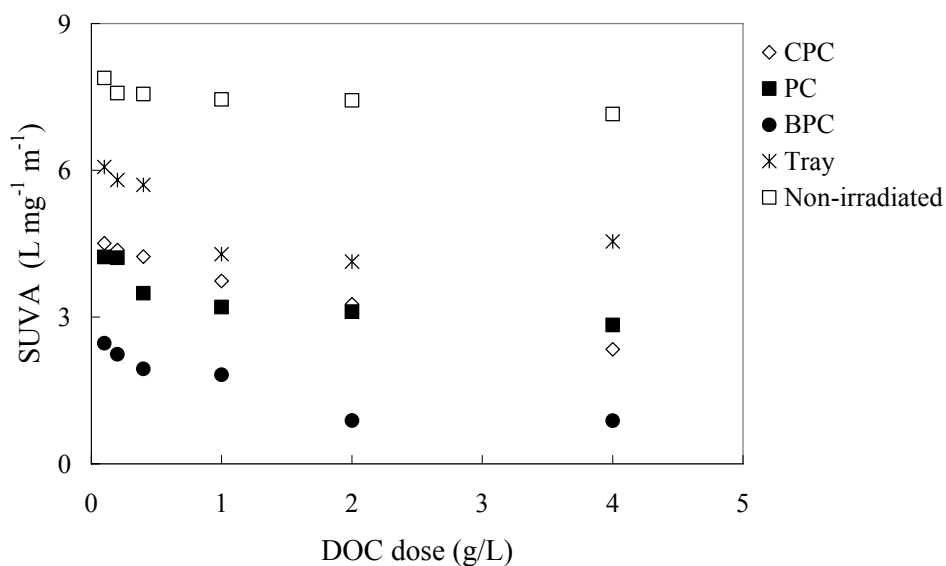


**Figure 5.44** SUVA values of HS remaining in the solutions after adsorption by various dose of GAC in summer experiment (DOC removal 50-62 %, solar dose  $5.97 \times 10^5$  kJ/m<sup>2</sup>).

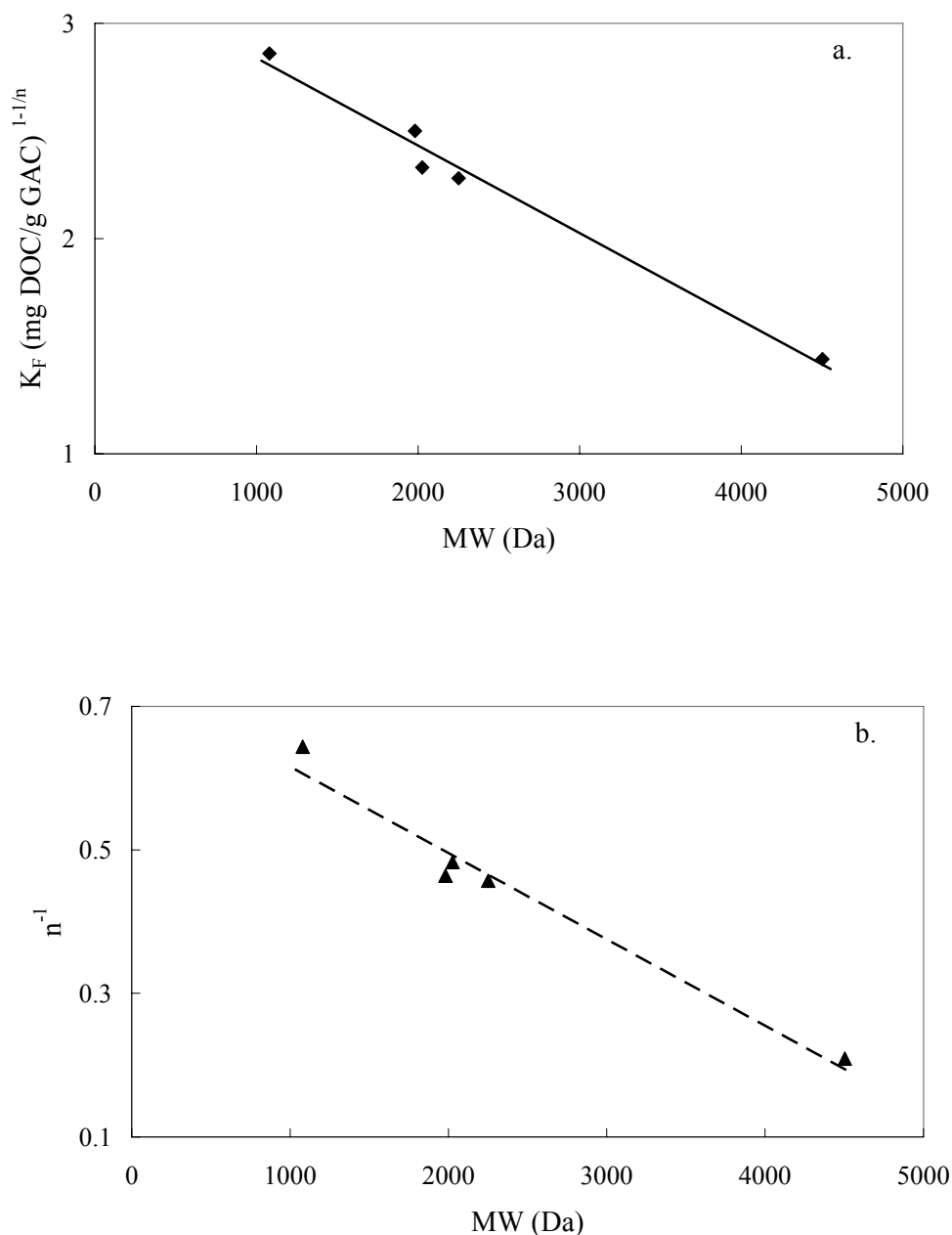


**Figure 5.45** Effect of MW on the adsorption behaviour of HS by GAC in summer experiment: (a)  $K_F$  and (b)  $n^{-1}$ . The solid and dashed lines suggest the trend.

The chromatograms of HS irradiated in BPC and tray after contacting different carbon doses are illustrated in Figure 5.43. Because the chromatograms of the non-irradiated HS solution exhibited a similar distribution to what was shown in Figure 5.33c, it is not presented here. Using BPC dramatically improved the

total removal of HS over the entire MW range. The chromophoric humic molecules remaining in BPC solutions were undetectable by HPSEC until carbon dose decreased to 400 mg/L (Figure 5.43a). This result demonstrates the accessibility of all irradiated molecules to GAC adsorption sites, and in particular the UV absorbing chromophores. As a result, the SUVA of HS remaining in the solutions after adsorption was significantly reduced, as can be seen in Figure 5.44. On the other hand, it suggests the greatly reduced DBP formation potential, as the aromaticity of HS was significantly reduced by the solar-GAC treatment.

Again, the Freundlich parameters  $K_F$  and  $n^{-1}$  exhibited a strong correlation with the MW, as illustrated in Figure 5.45, confirming the major role of size effects in the observed adsorption behaviour of HS.

### 5.3.3 Effect of pH

Irradiation experimental results have proven that the pH-adjusted HS solutions were more liable to be photodegraded. This may in turn influence their performance in the following GAC adsorption process. A comparison of the Freundlich parameter  $K_F$  in Figure 5.46 shows that:

- (1) for the non-irradiated HS solutions, the greatest adsorption was observed on the acidic solutions. Similar observations have been reported by Newcombe (1994) and Li *et al.* (2003). There are two possible reasons: (i) decrease in the negative charge of HS and increase in the positive charge of GAC surface (which had the  $pH_{pzc}$  of 9.5) created stronger attractive forces between HS and GAC surface, and (ii) decrease in the solubility of HS due to the protonation of the carboxylic groups increased the driving force for adsorption onto the hydrophobic carbon surface. Therefore, the removal of HS increased as pH

decreased.

(2) for the solar irradiated HS, it appears that the greatest removal was for the pH 9.7 solution, which has been proven to be more readily photodegraded. It should be noted that, the pH value of this solution decreased from 9.7 to 6.8 following solar irradiation, and no further pH adjustment was carried out prior to adsorption studies because the influence of the initial pH value on the removal of HS by the solar irradiation-GAC adsorption method was of research interest in this experiment. The enhanced removal is therefore largely attributed to the breakdown of high MW fractions and the increased proportion of smaller molecules due to solar irradiation, rather than pH effects. The higher removal of the acidic HS (which had pH value of 4.4-4.8 prior to adsorption) relative to the pH 7.5 HS might be mainly due to the surface attractive interactions, as no plausible explanation regarding molecular size can be found in the HPSEC results (Figure 5.18).

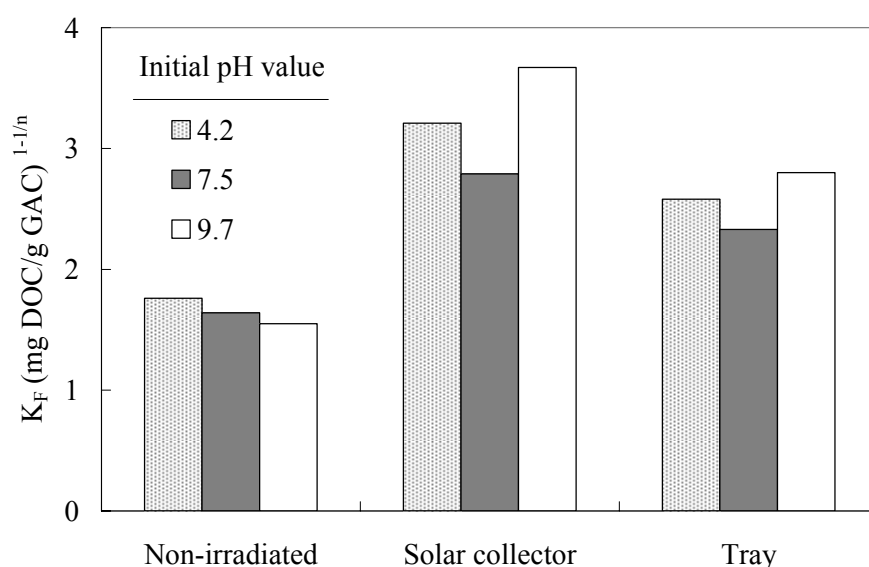


**Figure 5.46** Freundlich adsorption parameter  $K_F$  of the non-irradiated and irradiated HS solutions with different initial pH values (4.2, 7.5 and 9.7).

Similar trends were also obtained for other adsorption parameters. In addition to the fact that solar irradiation effectively improved the adsorption of HS by GAC, it demonstrates that the solar-GAC method is sensitive to pH adjustment. In water treatment applications, pH adjustment is sometimes applied to optimise the removal of target compounds. This will in turn affect the performance of the solar-GAC process in terms of HS removal, if solar irradiation is used as part of the water treatment.

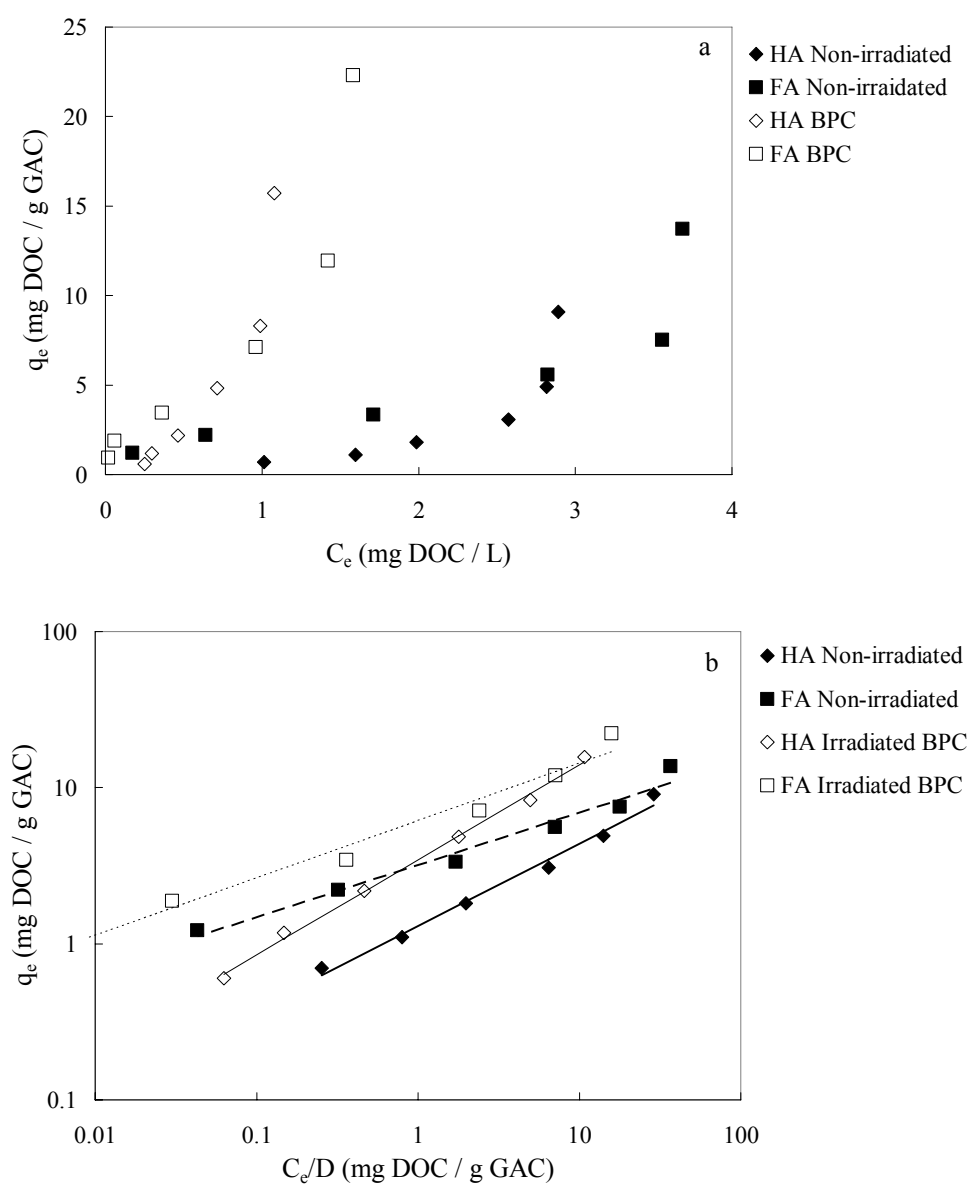


**Figure 5.47** Adsorption isotherms of AHA and SRFA solutions before and after

solar irradiation (solar dose  $1.96 \times 10^5$  kJ/m<sup>2</sup>): (a) conventional isotherms and (b) modified Freundlich isotherms.

### 5.3.4 Adsorption of FA

Here the adsorption isotherms of SRFA and AHA are compared (Figure 5.47). In general, SRFA exhibits higher carboxylic type of acidity, more hydrophilic and more soluble in water compared to AHA. This may consequently reduce its adsorption by GAC. However, it appears in isotherms and Freundlich parameters that the non-irradiated SRFA was adsorbed to a greater extent than the non-irradiated AHA. The observed behavior suggests that the size exclusion effects of SRFA are large enough to overcome the opposite effects of hydrophilicity and solubility in GAC adsorption.

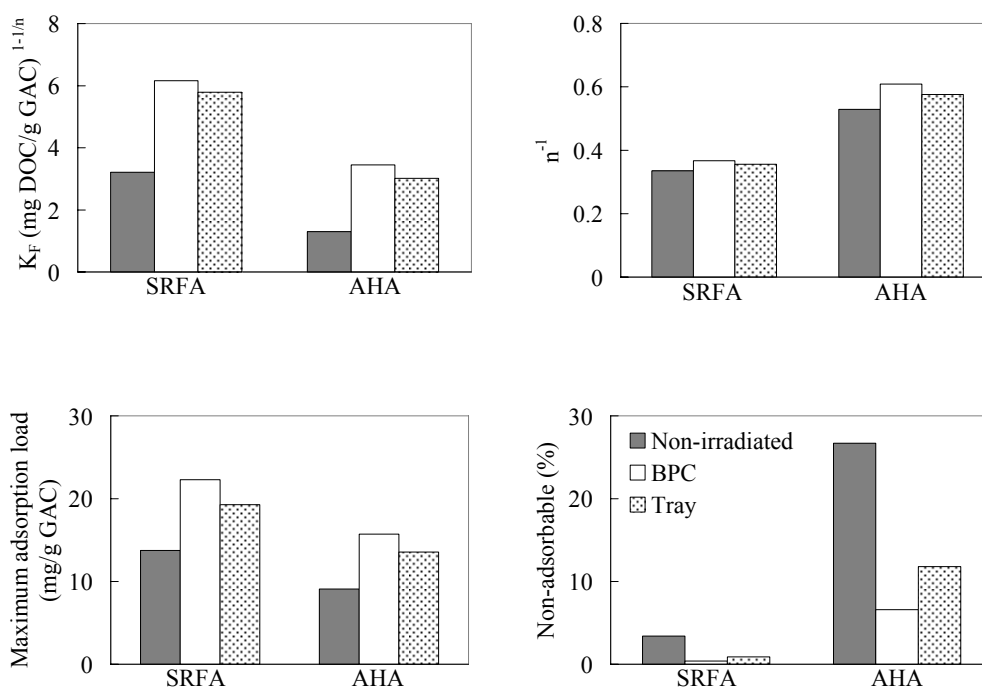


**Figure 5.48** Changes in adsorption parameters of the non-irradiated and irradiated SRFA and AHA solutions.

Solar irradiation improved the adsorbability of SRFA, as reflected by an increase in  $K_F$ ,  $n^{-1}$  and maximum adsorption load as well as a decrease in non-adsorbable components (Figure 5.48). Although SRFA was found to undergo the photodegradation to a greater extent (section 5.2.4.3), it appears solar irradiation had more pronounced influence on AHA than SRFA with respect to the subsequent GAC adsorption process. For example, following solar irradiation, the Freundlich parameter  $K_F$  was increased by about 92 % and 165 % for SRFA and AHA, respectively. A plausible explanation to this is that many of the FA molecules were small enough to be adsorbed, and therefore photodegradation of these small molecules did not greatly alter the overall removal of FA. The proportion of the non-adsorbable compounds in SRFA was reduced from 3.5 % to 0.4 % due to pre-treatment using solar irradiation (Figure 5.48). On one hand, this supports the notion that many of fulvic molecules are already accessible to carbon pores, as the non-adsorbable compounds in the non-irradiated AHA accounted for 26 % of the total DOC. On the other hand, it demonstrates the possibility of using solar irradiation to reduce molecular size of FA (which generally has much lower MW than HA) and increase the adsorbability. Given a water consists of both FA and HA, it is likely that sunlight would effectively work and reduce the molecular size of all humic components. This would in turn greatly benefit the subsequent treatment processes, in particular for those having high requirements of particle sizes of contaminants, such as GAC and membrane filtrations.

### 5.3.5 Evaluation of natural water source

The applicability of the findings with the model humic material (AHA) to a humic rich water (CH water) was investigated by carrying out batch equilibrium experiments using the same GAC. Results are presented in Figure 5.49 and

Table 5.15.

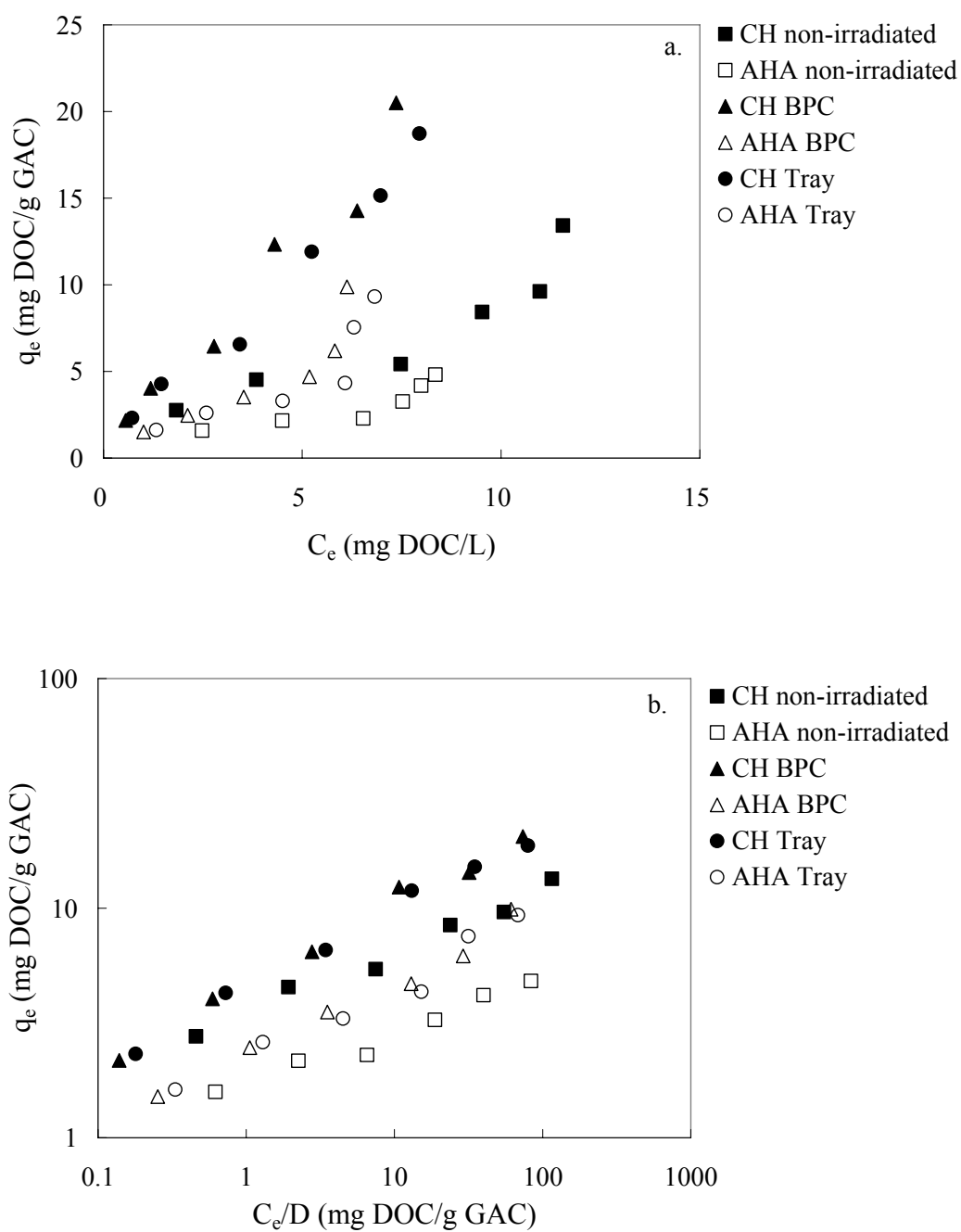


**Figure 5.49** Isotherms of the non-irradiated and irradiated CH water and AHA water by GAC: (a) conventional isotherms and (b) modified Freundlich isotherms (DOC removal 21-29 % for CH water and 14-24 % for AHA water, solar dose  $1.42 \times 10^5$  kJ/m<sup>2</sup>).

For the non-irradiated solutions, although CH water was of higher MW and more concentrated, the adsorbability of natural HS ( $K_F$  value of 3.47) was two times that of the AHA water ( $K_F$  value of 1.71). The maximum adsorption load of natural aquatic HS on GAC was three times higher than AHA. There are several possible reasons to this. First, this upland water is assumed to contain a greater amount of FA (see section 5.2.5) that has been proven more readily removed by GAC relative to the soil derived AHA. Second, surface attractive interactions are expected to be stronger between GAC surface and CH water according to the lower pH of natural water. Third, CH water is considered to have higher ionic strength which increased the adsorption capacity. Finally, CH water contains some adsorbable components that do not exist in AHA. These components have humic or non-humic characteristics and they are accessible to carbon pores, therefore contribute to the observed higher removal of natural HS.

The adsorbability of natural HS was increased by up to 33 % due to pre-treatment using solar irradiation. This result is similar to what was observed with AHA. The maximum removal in Table 5.15 refers to the DOC reduction of HS at the highest GAC dose (4 g/L). When solar irradiation was used prior to GAC adsorption, maximum removals of 94 % and 92 % were obtained for CH water irradiated in BPC and tray, respectively. It is evident that, even though solar intensity during experimental period was considerably low ( $1.42 \times 10^5$  kJ/m<sup>2</sup>), the adsorbability of natural aquatic HS was greatly improved. Since comparable results were obtained between CH water and AHA water, it can be deduced that a more pronounced removal of natural HS would be seen if there is strong solar irradiation provided.

**Table 5.15** Modified Freundlich isotherm parameters for CH water and AHA water on GAC (DOC removal 21-29 % for CH water and 14-24 % for AHA water, solar dose  $1.42 \times 10^5$  kJ/m<sup>2</sup>).

Samples	$K_F$	1/n	$K_{F,irr}/K_{F,non}$	Maximum adsorption load <sup>b</sup> (mg/g)	Maximum removal (%)
CH water in BPC	4.60	0.353	1.33	20.50	94
CH water in tray	4.46	0.344	1.29	18.73	92
CH water non-irradiated	3.47	0.271	-	13.43	86
AHA water in BPC	2.33	0.327	1.36	9.89	89
AHA water in tray	2.22	0.311	1.30	9.32	85
AHA water non-irradiated	1.71	0.228	-	4.18	72

$K_F$ : (mg DOC/g GAC)<sup>1-1/n</sup>

Maximum adsorption load: DOC load on 100 mg GAC/L

Maximum removal: DOC removal by 4000 mg GAC/L

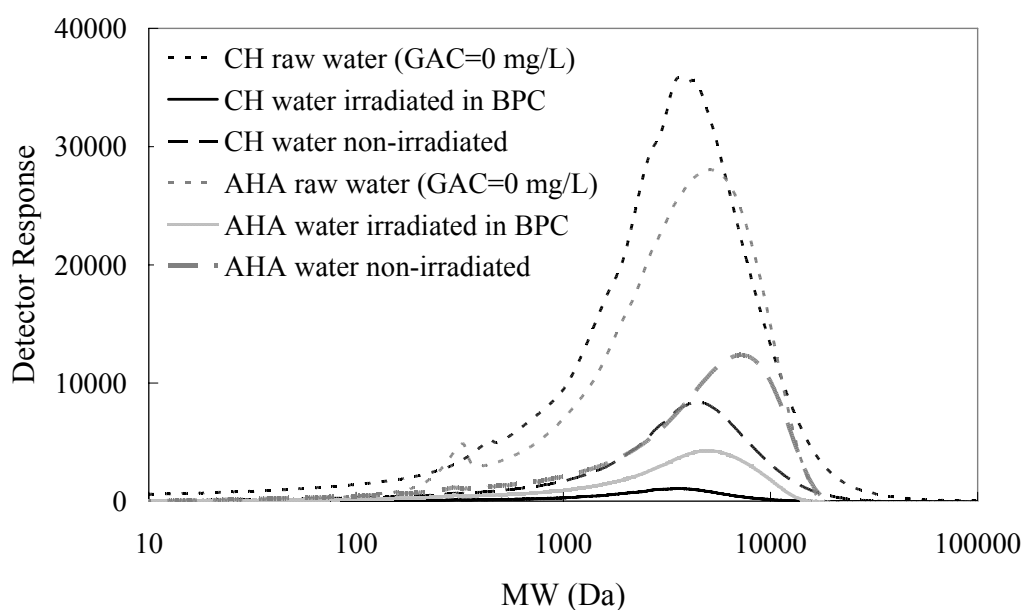


**Figure 5.50** Chromatograms of the non-irradiated and irradiated CH water and

AHA water before and after adsorption by 2000 mg GAC/L (DOC removal 21-29 % for CH water and 14-24 % for AHA water, solar dose  $1.42 \times 10^5$  kJ/m<sup>2</sup>).

Representative HPSEC results for the MWD of CH water and AHA water after adsorption by GAC of 2000 mg/L are plotted in Figure 5.50. When solar irradiation was applied, HS molecules in the CH water of all molecular sizes were effectively removed by GAC, leaving an almost undetectable portion of organic matter in water, confirming the effectiveness of the solar-GAC method and treatability of this natural humic rich water.

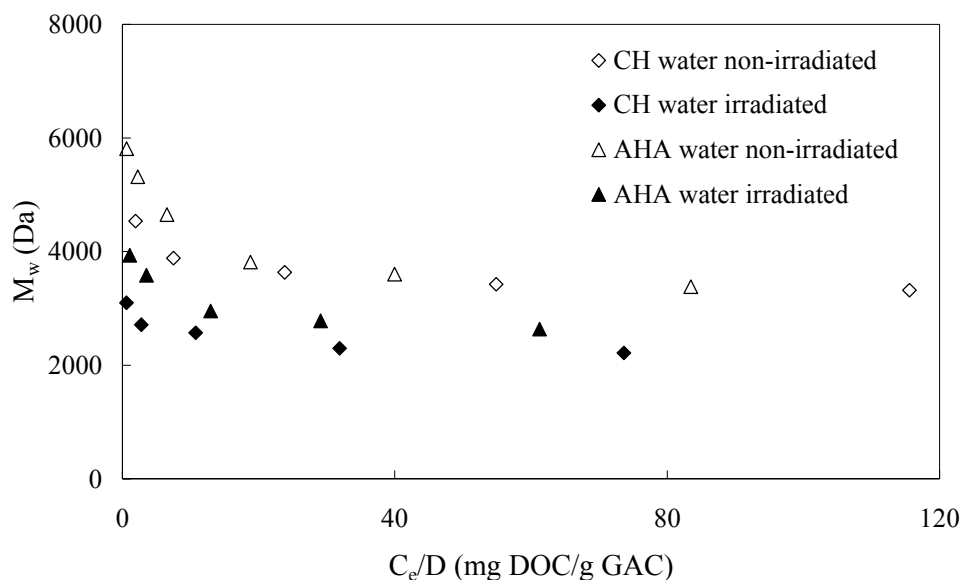


**Figure 5.51** Changes in the MW of CH water and AHA water remaining in solutions after adsorption by various doses of GAC.

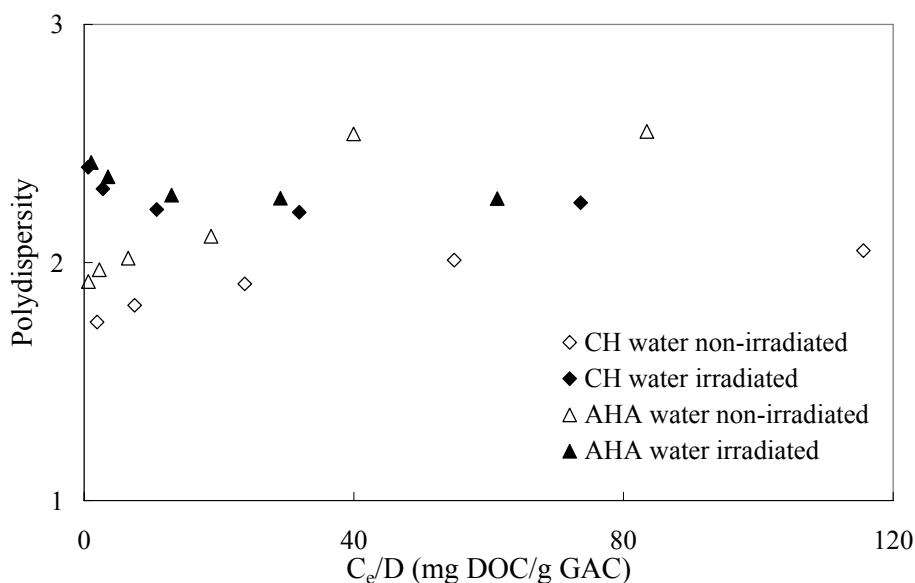


**Figure 5.52** Changes in the polydispersity of CH water and AHA water remaining in solutions after adsorption by various doses of GAC.

As illustrated in Figures 5.51 and 5.52, the measured  $M_w$  and polydispersity of CH water and AHA water as a function of  $C_e/D$  followed a similar trend, suggesting what has been learned from AHA with respect to size effects on adsorption is also applicable to this natural water. Solar irradiation can break down large molecules, leaving more GAC adsorption sites available to the smaller photoproducts or already existing smaller molecules; and the smaller photoproducts can be preferentially removed by GAC.

### 5.3.6 GAC column adsorption

The batch equilibrium adsorption studies provide useful information regarding the adsorption of HS by GAC. However, batch studies are usually limited to the treatment of small volumes of solutions. In drinking water treatment applications, GAC adsorption is normally operated on a continuous flow basis and the fixed-bed adsorber is considered more efficient (Al-Ghouti *et al.*, 2007). The

complex characteristics of HS are found to adversely affect the performance of GAC adsorbers. As a result, the operational life of fixed-bed GAC adsorbers is significantly reduced and the operating cost is increased due to frequent replacement and regeneration. Compared to batch studies, very few results have been reported in the literature regarding the removal of HS under a continuous adsorption condition. The effect of solar irradiation as a pre-treatment method on the breakthrough behaviours of HS has not been published to date. Therefore, further investigations under continuous flow conditions are necessary to provide more information regarding the effective use of solar irradiation to improve the performance of GAC adsorption for HS removal.

**Table 5.16** Characteristics of HS solutions used in small column studies.

	UV <sub>254</sub> (cm <sup>-1</sup> )	DOC (mg/L)	M <sub>w</sub> (Da)	M <sub>n</sub> (Da)
Non-irradiated	0.585	7.21	3963	1484
Irradiated A	0.498	6.75	2355	982
Irradiated B	0.181	3.12	1115	620

M<sub>n</sub>: number average molecular weight

M<sub>w</sub>: weight average molecular weight

In this study, small-scale columns were used and the operational parameters were determined using the rapid small scale column test (RSSCT) method. It has been suggested that the parameters obtained through RSSCT studies could satisfactorily predict the fixed-bed performance for large column runs (Crittenden *et al.*, 2005).

A summary of the characteristics of influent HS solutions to small GAC columns is shown in Table 5.16 and the corresponding chromatograms are illustrated in

Figure 5.53. All samples were diluted from the same stock solution to the same initial concentration. The non-irradiated HS were those kept in the dark, while the irradiated A and B samples were exposed to sunlight for a shorter and longer period, respectively. Due to unexpected technical problems, the reading of solar intensity was not recorded for this period. As can be seen in Table 5.16, solar irradiation removed 6.4 % of HS from sample A and 56.7 % from sample B with respect to the DOC concentration. High MW components were preferentially removed, resulting in a shift of the MWD to smaller MW values (Figure 5.53). A significant removal of HS over the entire MW range was observed for sample B.

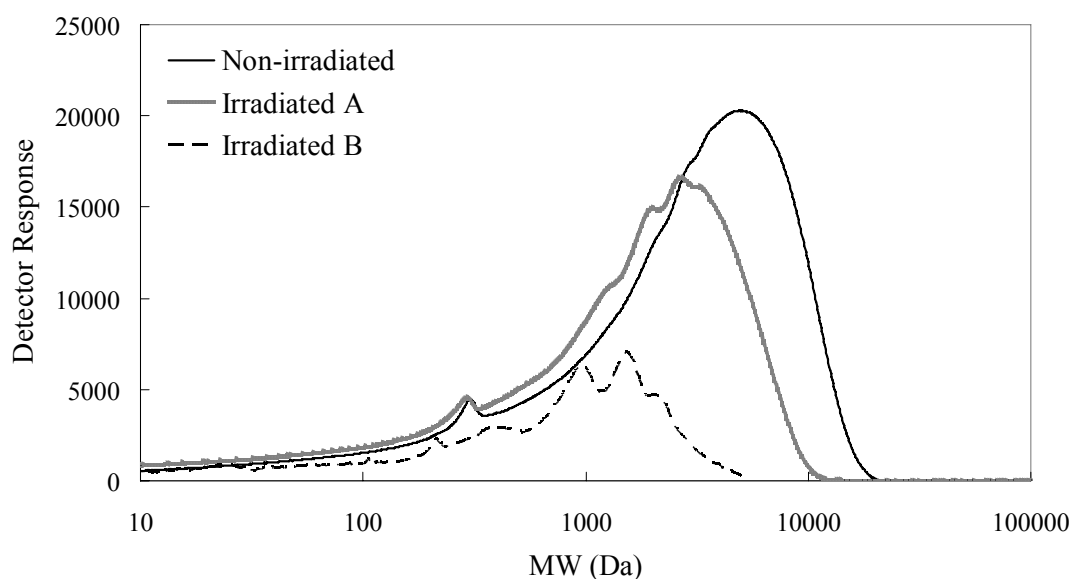


**Figure 5.53** MWD of the non-irradiation and irradiated HS solutions measured by HPSEC before column feeding (initial DOC 7.2, 6.8 and 3.1 mg/L for the non-irradiated, irradiated A and irradiated B samples, respectively).

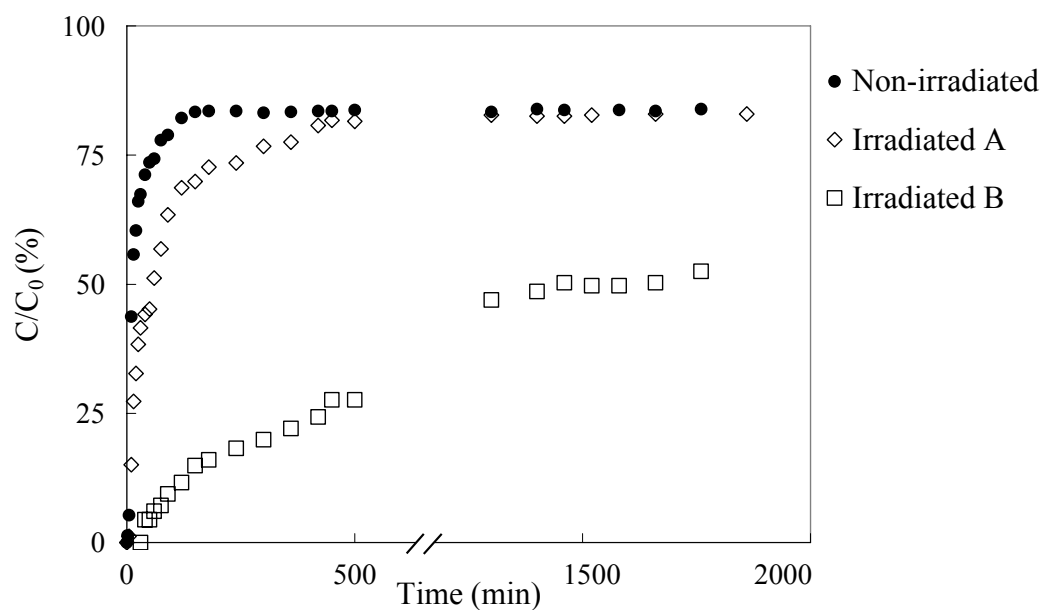


**Figure 5.54** Breakthrough curves of the non-irradiated and irradiated HS solutions by small GAC columns using the RSSCT method (initial DOC 7.2, 6.8 and 3.1mg/L for the non-irradiated, irradiated A and irradiated B samples, respectively).

The observed breakthrough curves of all samples are illustrated in Figure 5.54, plotted as the relative residual concentration  $C/C_0$  (effluent DOC concentration at sampling time to influent DOC concentration at time zero) versus the volume of water treated. All experiments were duplicated and each data point in Figure 5.54 represents an average of results for duplicate samples. The breakthrough curves generally exhibit a characteristic convex shape, which is in agreement with previous findings by Li *et al.* (2003) and André (2006).

Influent DOC of the non-irradiated HS was 7.2 mg/L. The breakthrough of the non-irradiated HS occurred very quickly (Figure 5.54). Actually an initial DOC was immediately measured in the effluent. This agrees well with what was found from the previous equilibrium studies, for example, approximately 35 % of

HS still remained in water after contacting GAC of the highest dose (4000 mg/L). The non-adsorbable HS are high MW compounds which do not adsorb well on GAC due to the size exclusion effects. Similar observations have been obtained by Schreiber *et al.* (2005) and André (2006) for the adsorption of a pond water and AHA water on GAC, respectively. The authors reported an earlier breakthrough of high MW compounds from small GAC columns. The earlier breakthrough of large molecules is validated by Figure 5.55a, which shows the chromatograms of the non-irradiated HS remaining in the effluent after passing through the small GAC column. The high MW compounds immediately appeared in the effluent, and the peak of the chromatogram at high MW values rapidly became nearly identical to that of the influent. This indicates that the high MW compounds are only adsorbed on GAC to some extent. An immediate presence of a small number of low and intermediate MW compounds in the effluent of the non-irradiated HS solutions was also observed, suggesting that inside the column, some high MW compounds are adsorbed which block access for smaller molecules to the carbon surface. As the non-irradiated humic solution continued to flow, the effluent concentration increased. The final effluent concentration rose to 82 % of the influent concentration ( $C_0=7.21$  mg/L) and remained stable till the end of the column experiments at about 2000 min. The chromatograms of the effluent also remained relatively unchanged after the effluent concentration became constant (i.e. the MWD of the effluent at 6h in Figure 5.55a), showing that some molecules can still be adsorbed by GAC.

Adsorption of HS was enhanced by applying solar irradiation as a pre-treatment method, as reflected by a later breakthrough of the irradiated A sample in Figure 5.54. The influent concentration was 6.8 mg/L. The irradiated A sample showed a similar shape of the breakthrough curve to the that of the non-irradiated

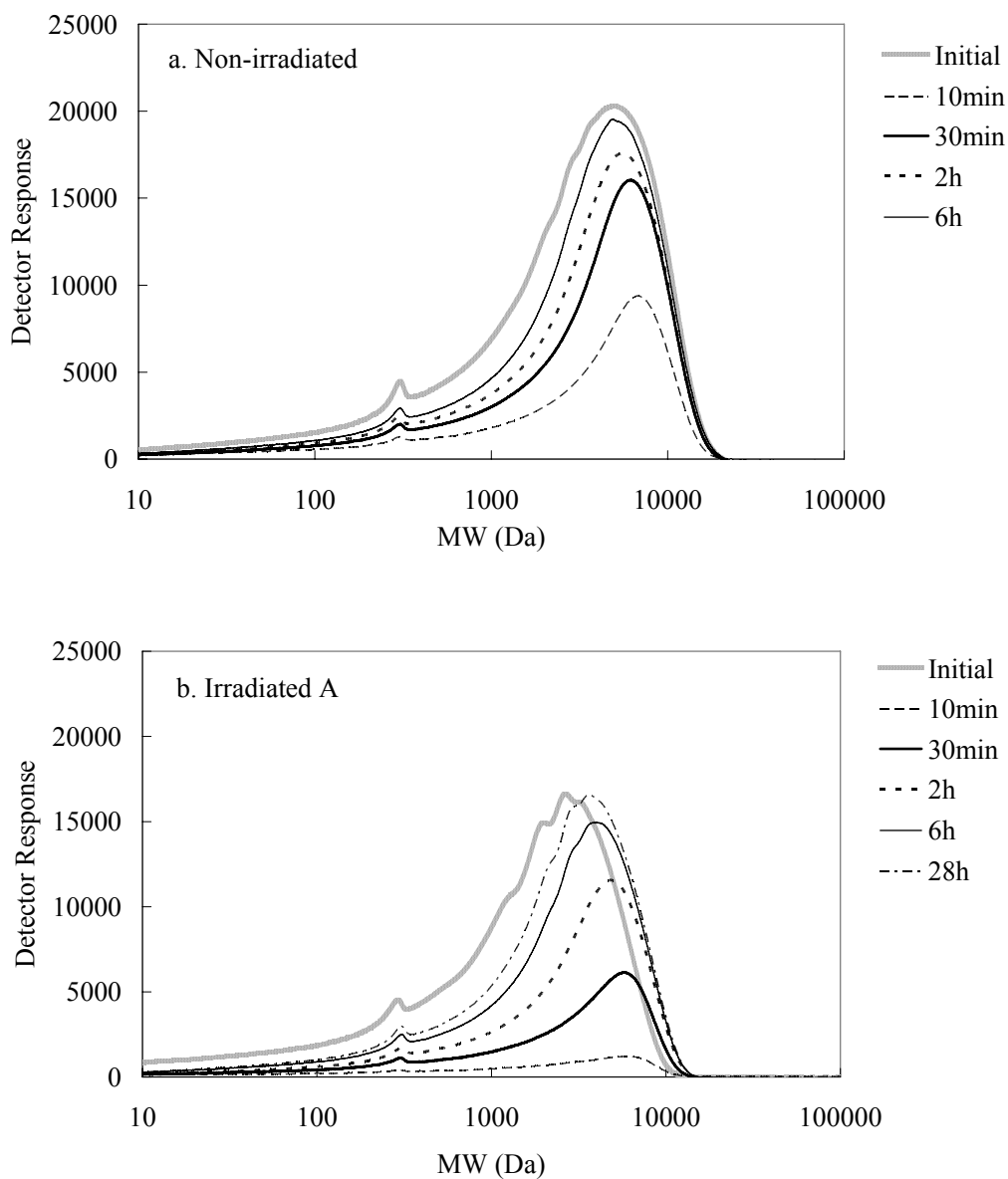
HS. The initial breakthrough took place after 8 min. The effluent concentration rapidly increased after breakthrough and rose to 80 % of the influent concentration (6.8 mg/L). From Figure 5.55b, chromatograms show that there were almost no detectable chromophoric molecules in the effluent during the first ten minutes of running. This means that the adsorbability of the non-adsorbable compounds that were immediately found in the effluent of the non-irradiated HS have been improved by solar irradiation. Similar to the non-irradiated HS, as the adsorption of the irradiated A sample proceeded, the peak of the chromatogram at high MW values gradually approached that of the influent. This means that the high MW compounds were eluted from the column. However, the process was much slower compared to the non-irradiated HS.

The influent concentration of sample B was 3.1 mg/L. The removal trend of this sample was different from the others. The initial breakthrough of sample B occurred at 60 min, showing a significant improvement in the adsorbability of HS due to the pre-treatment using solar irradiation. The improvement is apparently attributed to the decreased molecular size, and also to the reduced initial concentration. The effect of the molecular size on the breakthrough of AHA by GAC columns has been previously studied by André (2006) who fractionated AHA into different MW fractions. The author found that GAC adsorb HS with MW less than 5 kDa well. The breakthrough for the low MW fractions was observed after 90 hours, while for the 5-10 kDa fractions the breakthrough took place after 5 hours. After the breakthrough, the effluent concentration of the irradiated B sample gradually increased till the end of column experiments, as illustrated in Figure 5.54. This indicates that all the irradiated molecules in sample B were accessible to the carbon surface. Although the DOC concentration was measured from the effluent since after 60 min, there were no

observable HS components in the HPSEC chromatograms until after approximately 30 h of column running (Figure 5.55c). Since DOC is not only a surrogate for the aromatic molecules but also for the weak UV absorbing molecules, for example aliphatic and alicyclic compounds, such behaviour means that the aromatic humic molecules can be preferentially removed from the influent and can also replace the other weakly adsorbed non-chromophoric organic compounds that have been initially adsorbed. This is explained by the better accessibility of smaller aromatic molecules to GAC pores and strong hydrophobic interactions with the GAC surface. The aromaticity of the effluent water is therefore largely reduced, implying the reduced DBP formation potential. In addition, the observation in Figures 5.54 and 5.55c confirms the different trends in breakthrough curves when DOC and UV<sub>254</sub> are used as analytical surrogates, in agreement with previous findings by Schreiber *et al.* (2005). A faster breakthrough curve is obtained if the DOC concentration is used as a measure for HS.

The combined solar-GAC treatment significantly improved the DOC removal by 60 % relative to the non-irradiated HS. Using pre-treatment methods to enhance the HS removal by carbon columns has been previously reported (Urfer and Huck, 1997; Gauden *et al.*, 2006; Toor and Mohseni, 2007; Buchanan *et al.*, 2008). For example, UV pre-treatment increased the overall HS removal from 29 % (without pre-treatment) to 54 % by GAC adsorption (Buchanan *et al.*, 2008). UV-H<sub>2</sub>O<sub>2</sub> pre-treatment improved the HS removal by the following biological carbon adsorption by 52 % (Toor and Mohseni, 2007). As can be seen, the observation in this research is comparable to the published data. The characteristics of HS, activated carbon employed, and extent of pre-treatment determine the effectiveness of column performance on HS removal. A sufficient pre-treatment,

i.e. high UV dose, would greatly benefit the subsequent adsorption performance. However, using artificial light and chemicals makes the treatment expensive. More research is necessary to explore the potential use of natural sunlight instead of artificial light prior to adsorption.



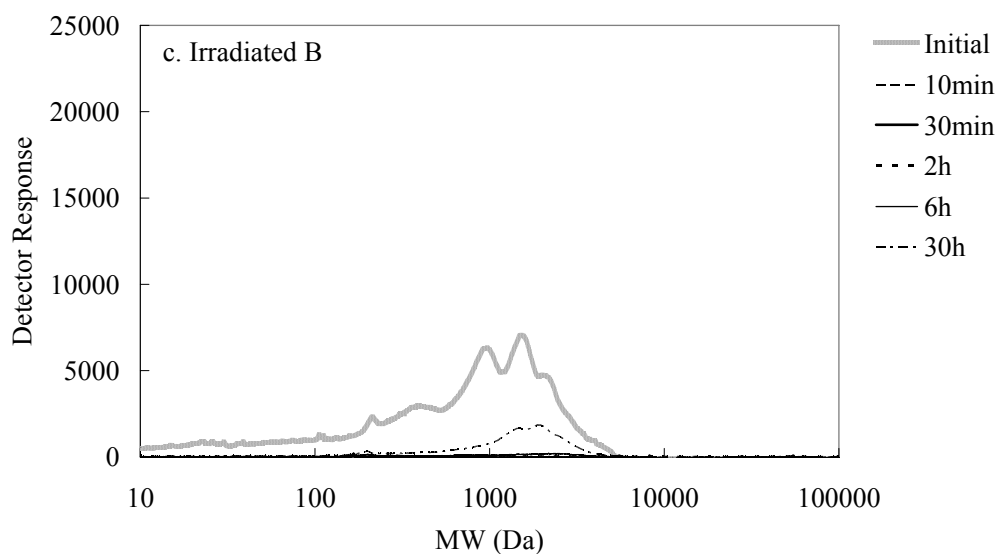


**Figure 5.55** Chromatograms of HS remaining in the effluent after passing through the small GAC column: (a) non-irradiated HS, (b) irradiated A HS, and (c) irradiated B HS (initial DOC 7.2, 6.8 and 3.1 mg/L for non-irradiated, irradiated A and irradiated B, respectively).

As the RSSCT can well represent the large scale operations, from the above findings, it can be concluded that using solar irradiation as a pre-treatment method can successfully improve the performance of GAC adsorbers with respect to HS removal, increase the column operational life and improve the water quality.

### 5.3.7 Summary of GAC adsorption results

The maximum DOC removal efficiencies of HS following solar irradiation and adsorption treatment are summarized and compared in Figure 5.56. Using GAC alone can provide reasonable removals of 60-70 % of AHA and 84 % of CH water. However, GAC does not effectively remove HS of all molecular sizes and rapidly gets saturated. The enhanced HS removal by employing solar irradiation prior to GAC adsorption process is clearly illustrated, with the total removal efficiency

rising up to 96 %.

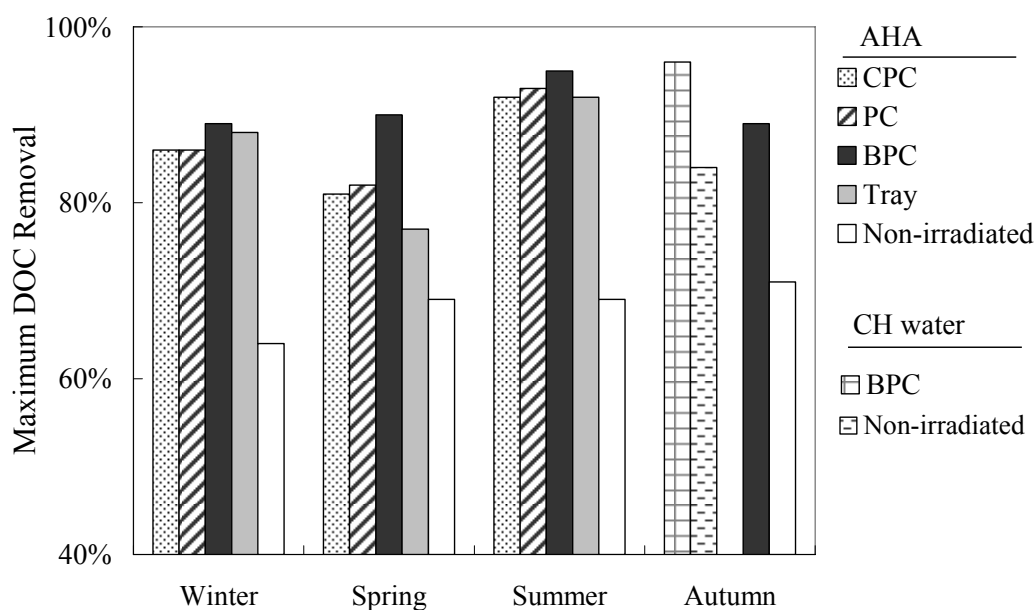


**Figure 5.56** Maximum removals of HS following solar irradiation and GAC adsorption.

The change in the Freundlich parameter  $K_F$  of the irradiated HS relative to the non-irradiated HS can be used as a measure to assess the magnitude of the adsorbability enhancement, as illustrated in Figure 5.57. It proves that even solar irradiation of low intensity can effectively enhance the adsorbability of HS molecules; for example, 16-37 % enhancement was found in winter. As a result of the enhanced adsorbability, the GAC adsorption capacity was more efficiently utilized (Figure 5.58). All those parameters are closely related to the extent of photodegradation in the pre-treatment process.

The effective use of the solar-GAC method was further proven with a natural water sample (CH water), which showed a more pronounced removal. This confirms the applicability of the observation based on AHA. Furthermore, using

solar collectors noticeably improved the overall removal of HS with respect to all parameters investigated and in particular for the one with larger reflective surface.

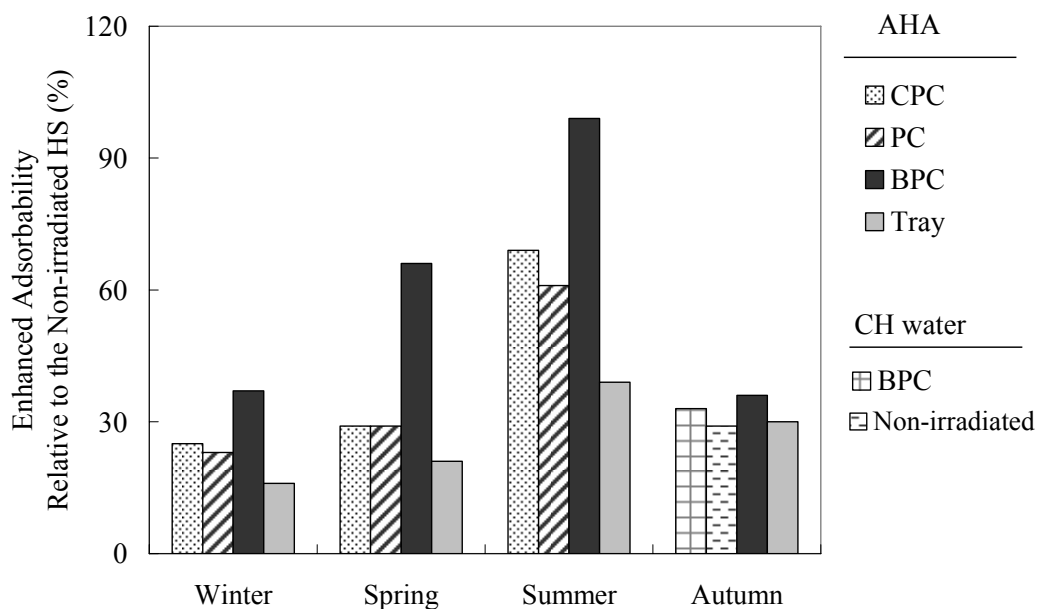


**Figure 5.57** Enhancement in the adsorbability of HS by GAC due to solar irradiation.

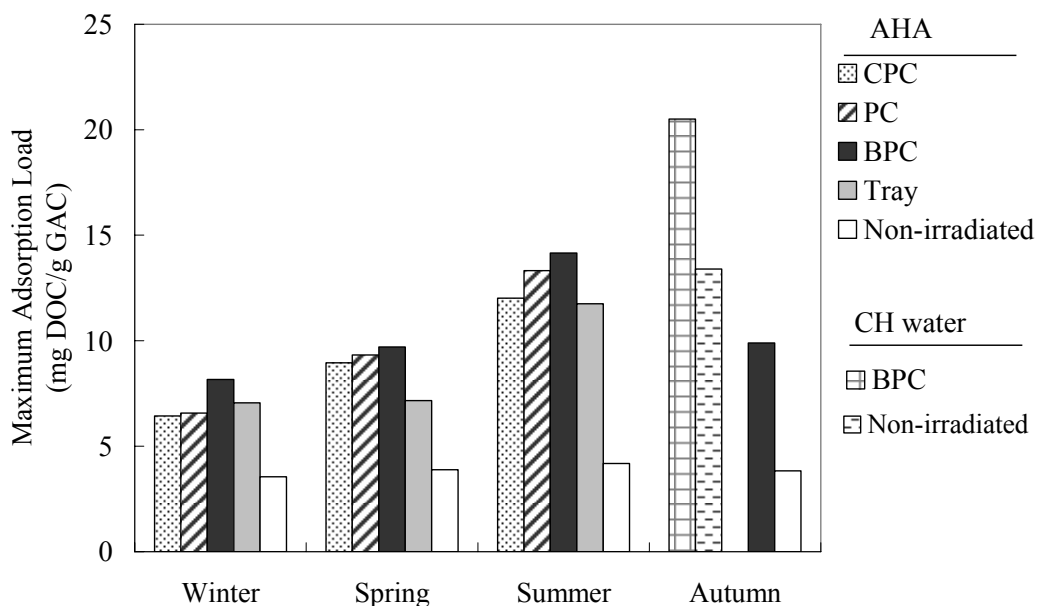


**Figure 5.58** Maximum adsorption load of HS on GAC following solar irradiation and GAC adsorption.

## CHAPTER 6

### OVERALL COMPARISONS AND DISCUSSIONS

#### 6.1 Introduction

The drivers for the introduction of solar irradiation to humic substances (HS) removal are to (1) explore a new and sustainable approach for HS removal; (2) improve the removal of HS in granular activated carbon (GAC) adsorbers; and (3) reduce the energy consumption. Sunlight presents a good opportunity, being low cost and available globally. Experimental work has shown that solar irradiation could effectively enhance the adsorption of HS by GAC.

A comparison of the findings in this research with the results from other studies on the HS removal is necessary. From the literature consulted, no researchers have linked solar irradiation and GAC adsorption to the treatment of HS. The heterogeneous nature of HS further complicates the comparison. Here, the Aldrich humic acid (AHA) is selected as the target compound to allow comparisons of different processes based on the literature data. This is because AHA is a model material that has been widely studied and it is also the main material used in this research. The following section brings together the best

available information regarding the performance of different processes on the removal of the commercial AHA.

## 6.2 Overall comparisons of different processes on HS removal

Published data are collected from the work by Allard *et al.* (1994), Rebhun *et al.* (1998), Wiszniowski *et al.* (2002 and 2004) Chen and Wu (2004), Murray and Parsons (2004) and Listiarini *et al.* (2009) whose research involved the treatment of AHA. The treatment processes include nanofiltration (NF), NF/alum pre-treatment, GAC adsorption, TiO<sub>2</sub>/natural or simulating solar irradiation, UVC irradiation, UV/H<sub>2</sub>O<sub>2</sub>, Fenton (Fe<sup>2+</sup>/H<sub>2</sub>O<sub>2</sub>) process and coagulation, together with the solar-GAC method in this research. Results are presented comparatively on the basis of the removal of UV absorbance at 254nm (UV<sub>254</sub>) and dissolved organic carbon (DOC), which are illustrated in Figures 6.1 and 6.2, respectively.

-UV<sub>254</sub>

UV<sub>254</sub> has been widely used as a surrogate parameter to indicate the aromaticity of HS. As discussed in the literature review, the high UV<sub>254</sub> value also reflects the HS fractions with hydrophobic properties and high MW for the water with a high humic content. Figure 6.1 shows that most of the consulted processes well performed with respect to UV<sub>254</sub>, with more than 80 % of AHA being removed. This is not surprising as humic compounds with aromatic structures,

hydrophobic properties and high MW are more readily removed by physicochemical treatments (Buchanan *et al.*, 2008).

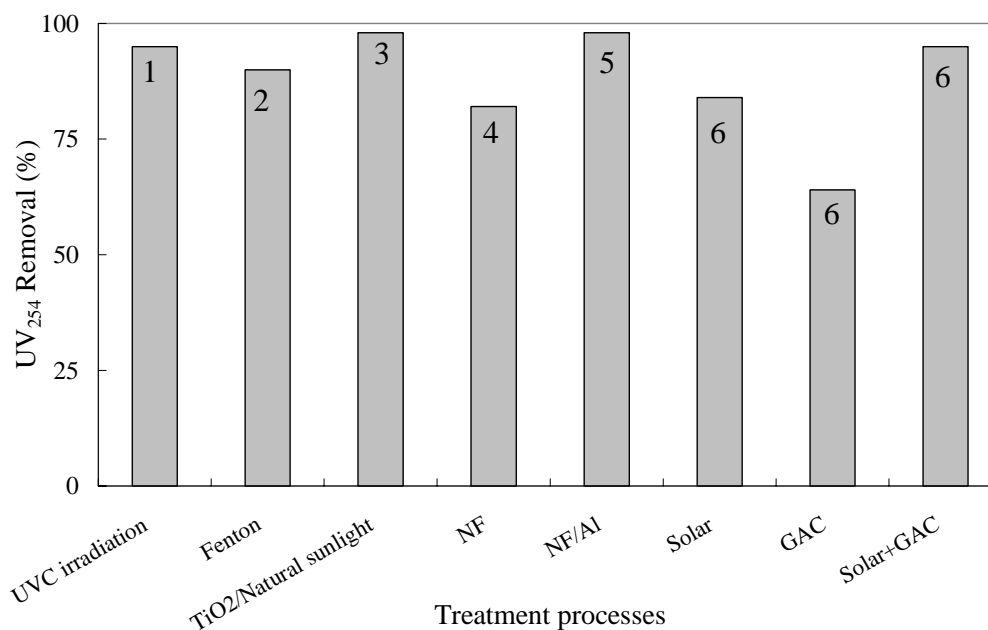


**Figure 6.1** Comparison of different treatment processes for the removal of UV<sub>254</sub> absorbance of AHA. (1) Allard *et al.* (1994); (2) Murray and Parsons (2004); (3) Wiszniowski *et al.* (2004); (4) and (5) Listiarini *et al.* (2009); (6) results in this research.

The efficiency of AHA removal varies, depending on the treatment process employed, operational conditions and physicochemical properties of AHA solutions. A summary of the experimental conditions corresponding to the treatment processes in Figure 6.1 are listed in Table 6.1. A comparison and discussion of each process in comparison with the solar-GAC method is given below.

**Table 6.1** Experimental conditions corresponding to the treatment process listed in Figure 6.1 regarding the removal of UV<sub>254</sub> of AHA (Allard *et al.*, 1994; Murray and Parsons, 2004; Wiszniowski *et al.*, 2004; Listiarini *et al.*, 2009).

Treatment process	Experimental conditions	Reference
UVC irradiation	UV intensity of 16 W/m <sup>2</sup> for 58 h, DOC 10 mg/L	Allard <i>et al.</i> , 1994
Fenton	0.25 mM Fe <sup>2+</sup> , Fe <sup>2+</sup> :H <sub>2</sub> O <sub>2</sub> 1:10, DOC 10.5 mg/L	Murray and Parsons, 2004;
TiO <sub>2</sub> /natural sunlight	Q <sub>UV</sub> 60 kJ/L, 0.7g/L TiO <sub>2</sub> , DOC 100 mg/L	Wiszniowski <i>et al.</i> , 2004
NF	NF270, size 9.0 ± 4.2 nm, DOC 10 mg/L	Listiarini <i>et al.</i> , 2009
NF/alum	NF270, size 9.0 ± 4.2 nm, 30 mg/L alum, DOC 10 mg/L	
Solar*	Solar dose 5.97 × 10 <sup>5</sup> kJ/m <sup>2</sup> , DOC 8.5 mg/L	
GAC adsorption*	Aquasorb 101 GAC 2g/L, DOC 8.5 mg/L	this research
Solar/GAC*	Solar dose 5.97 × 10 <sup>5</sup> kJ/m <sup>2</sup> , Aquasorb 101 GAC 2g/L, DOC 8.5 mg/L	

As a result of UV-C irradiation for 58 h, 95 % UV<sub>254</sub> removal of AHA (initial DOC 10 mg/L) was observed by Allard *et al.* (1994). Compared to the 84 % removal of AHA (initial DOC 8.5 mg/L) under natural sunlight for 10 weeks in London, the degradation rate under UV lamp was much faster. This is because UV irradiation is strongly absorbed by humic molecules (Frimmel, 1994) and

UV-C irradiation has the highest photo energy that can directly photodegrade organic compounds. In natural sunlight, UV-C irradiation is absent (see section 2.3.1.1), while UV-A and UV-B irradiation only account for a small portion (no more than 4 %). In addition, using PET bottles in this research only partly let through the UV-A and UV-B irradiation and thus reduced the extent of photodegradation of HS (see section 5.2.2). Therefore, the photodegradation of HS under natural sunlight is a slow process. However, using artificial light source makes the water treatment expensive.

Advanced oxidation processes (AOPs) are of growing interest in current drinking water treatment (see section 2.5.3). A number of AOPs, such as UV/H<sub>2</sub>O<sub>2</sub>, UV/O<sub>3</sub>, Fenton process, and UV/TiO<sub>2</sub>, have been investigated for treating refractory organics. Murray and Parsons (2004) studied the use of Fenton (Fe<sup>2+</sup>/H<sub>2</sub>O<sub>2</sub>) to treat AHA water with initial DOC 10.5 mg/L. The optimum condition to obtain 90 % UV<sub>254</sub> removal was Fe<sup>2+</sup> of 0.25 mM and Fe<sup>2+</sup>:H<sub>2</sub>O<sub>2</sub> ratio of 1:10 at pH 4. The process only took up to 30 min. The Fe<sup>2+</sup> concentration and Fe<sup>2+</sup>:H<sub>2</sub>O<sub>2</sub> ratio influence the overall performance. For example, only 40 % UV<sub>254</sub> was removed when Fe<sup>2+</sup>:H<sub>2</sub>O<sub>2</sub> ratio was 1:10 and Fe<sup>2+</sup> concentration was 0.5 mM. Therefore, one should carefully tailor the treatment conditions according to the humic water characteristics. An improper Fe<sup>2+</sup> dose or Fe<sup>2+</sup>:H<sub>2</sub>O<sub>2</sub> ratio may not only reduce the HS removal efficiency but also increase the chemical residuals and operating cost. Instead of UV irradiation, Wiszniowski *et al.* (2004) investigated natural sunlight combined with TiO<sub>2</sub> to treat AHA water. Up to 98 % UV<sub>254</sub> reduction was

achieved with 0.7 g/L TiO<sub>2</sub> and Q<sub>UV</sub> 60 kJ/L. It should be noted that the initial DOC concentration of AHA in the work by Wiszniowski *et al.* (2004) was 100 mg/L, which is much higher than other listed studies. Such a high AHA concentration is also not common in natural waters. The high AHA concentration and removal efficiency prove the effectiveness of using TiO<sub>2</sub>/natural sunlight method to treat water with a high humic content. It also presents a good example of replacing artificial light by natural sunlight in treating humic waters. Apparently, AOPs are significantly faster than the solar-GAC process. The advantage of AOPs is the high efficiency achieved within a short time. Due to the addition of chemical agents, problems with operating cost and chemical residuals handling are inevitable. Using solar irradiation prior to GAC can successfully reduce the energy consumption and chemical residual problems.

NF process features many advantages over conventional treatment methods, such as smaller size, easier operation and maintenance as well as good water quality. Using NF alone, the removal of AHA with an initial concentration of 10 mg/L was 82 % (Listiarini *et al.*, 2009). A fouling problem was noticed due to the large molecular size of AHA. By introducing alum prior to NF, the removal of AHA was increased from 82 % to 98 %. This is attributed to alum coagulant aggregating fine particles to form a highly porous and less dense cake on the NF surface that can be easily removed by backwashing (Fabris *et al.*, 2007). However, problems with the sludge production by addition alum coagulant prior to NF should be taken into account when employing the

NF/alum method.

In the work presented in this thesis, 84 % and 64 %  $UV_{254}$  removal of AHA was achieved using natural solar irradiation alone and GAC adsorption alone (2 g/L), respectively. The low removal of AHA by GAC is attributed to the fact that the high MW compounds did not adsorb well on the GAC surface. When solar irradiation employed prior to GAC adsorption, up to 95 % of AHA was removed. The high removal efficiency verifies the hypothesis that solar irradiation breaks down high MW compounds to smaller molecules therefore improves the adsorption behaviour of the irradiated HS by GAC.

*-DOC*

A comparison of the removal efficiency of AHA in terms of DOC concentration by different treatment processes is presented in Figure 6.2 and a summary of the corresponding experimental conditions is given in Table 6.2. The removal of DOC is linked to the degradation of both aromatic and non-aromatic organic components, while the  $UV_{254}$  reduction mainly reflects the changes in aromatic compounds. Some of the non-aromatic components have been found to contribute to the DBP formation (Bond *et al.*, 2010). It is therefore necessary to investigate the removal efficiencies of AHA in terms of DOC by different processes.

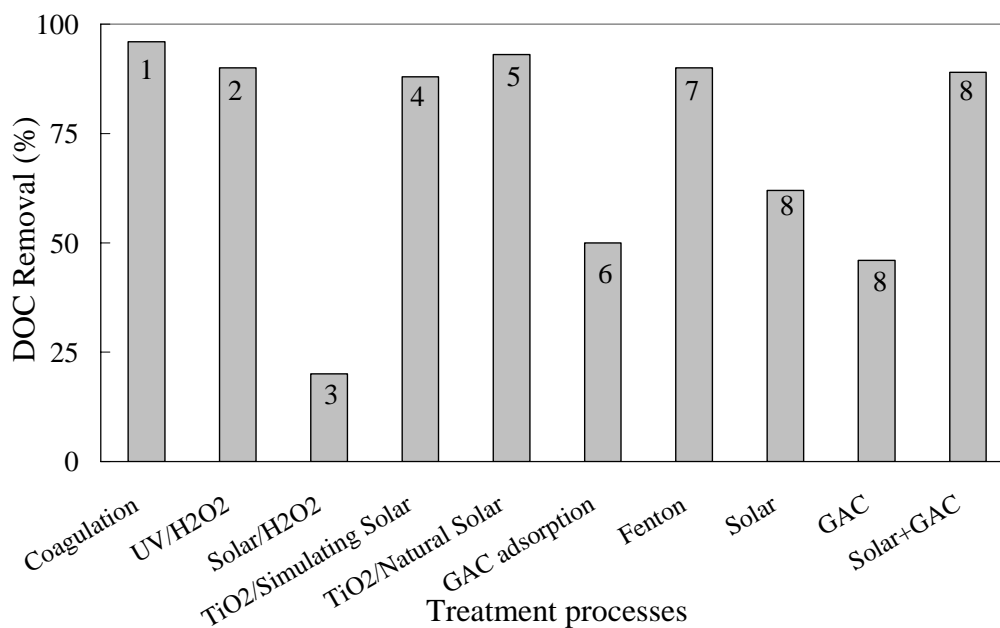


**Figure 6.2** Comparison of different treatment processes for the removal of DOC content of AHA. (1) Rebhun *et al.* (1998); (2) and (3) Wang *et al.* (2000); (4) Wiszniowski *et al.* (2002); (5) Wiszniowski *et al.* (2004); (6) Chen and Wu (2004); (7) Murray and Parsons (2004); (8) results in this research.

Coagulation has been recommended as one of the best available technologies for the removal of HS from water (Jacangelo *et al.*, 1995). It was found that both Al<sub>2</sub>O<sub>3</sub> and FeCl<sub>3</sub> can successfully remove AHA of a wide range of concentrations (16.5 to 50 mg/L), depending on the coagulant dose (Rebhun *et al.*, 1998). When the coagulant dose exceeded 40 mg/L, nearly 98 % of AHA was removed. Increasing coagulant dose inevitably results in an increasing sludge production and handling cost. The sludge generated by coagulation process is difficult to dewater due to the increased metal ion and organic content (Murray and Parsons, 2004).

**Table 6.2** Experimental conditions corresponding to the treatment process listed in Figure 6.2 regarding the removal of DOC of AHA (Rebhun *et al.*, 1998; Wang *et al.*, 2000; Wiszniowski *et al.*, 2002 and 2004; Chen and Wu, 2004; Murray and Parsons, 2004).

Treatment process	Experimental conditions	Reference
Coagulation	Al <sub>2</sub> O <sub>3</sub> or FeCl <sub>3</sub> 40 mg/L, DOC 16.5, 30 or 50 mg/L	Rebhun <i>et al.</i> , 1998
UV/H <sub>2</sub> O <sub>2</sub>	1h, UV intensity 275.8 W/m <sup>2</sup> , 0.1 % H <sub>2</sub> O <sub>2</sub>	Wang <i>et al.</i> , 2000
Solar/H <sub>2</sub> O <sub>2</sub>	2h, UV intensity 23.2 W/m <sup>2</sup> , 0.1 % H <sub>2</sub> O <sub>2</sub>	
TiO <sub>2</sub> /simulating sunlight	6h, 1 g/L TiO <sub>2</sub> , DOC 100 mg/L	Wiszniowski <i>et al.</i> , 2002
TiO <sub>2</sub> /natural sunlight	Q <sub>UV</sub> 33 kJ/L, 1 g/L TiO <sub>2</sub> , DOC 100 mg/L	Wiszniowski <i>et al.</i> , 2004
GAC adsorption	F200 GAC 2.5 g/L, DOC 10 mg/L	Chen and Wu, 2004
Fenton	0.1 mM Fe <sup>2+</sup> , Fe <sup>2+</sup> :H <sub>2</sub> O <sub>2</sub> 1:10, DOC 10.5 mg/L	Murray and Parsons, 2004
Solar*	Solar dose 5.97× 10 <sup>5</sup> kJ/m <sup>2</sup> , DOC 8.5 mg/L	this research
GAC adsorption*	Aquasorb 101 GAC 2g/L, DOC 8.5 mg/L	
Solar/GAC*	Solar dose 5.97× 10 <sup>5</sup> kJ/m <sup>2</sup> , Aquasorb 101 GAC 2g/L, DOC 8.5 mg/L	

Wang *et al.* (2000), Wiszniowski *et al.* (2002 and 2004) and Murray and Parsons (2004) used a variety of AOPs to treat AHA water. Different from the optimum

condition for the  $UV_{254}$  removal as discussed before, Murray and Parsons (2004) found that the maximum DOC removal was achieved when the  $Fe^{2+}$  concentration was 0.1 mM and there was only a slight difference for the DOC removal when different  $Fe^{2+}:H_2O_2$  ratio was applied. This creates the difficulty in determining the operational conditions to achieve the high removal of both  $UV_{254}$  and DOC of humic waters. There was a dramatic difference between UV/ $H_2O_2$  and solar/ $H_2O_2$  on the removal of AHA water (Wang *et al.*, 2000). 90 % DOC removal was achieved for the former after 1 h treatment, while only 20 % removal for the latter after 2 h. This observation is attributed to the difference in the UV intensity between artificial light and natural sunlight. The UV irradiation is more effective in the activation of  $H_2O_2$ . Wiszniowski *et al.* (2002 and 2004) investigated solar photocatalytic degradation of AHA by  $TiO_2$  under simulating sunlight and natural sunlight. 88 % DOC removal of AHA was obtained within 6 h using  $TiO_2$ /simulating sunlight. The DOC removal of AHA using  $TiO_2$ /natural sunlight was slightly higher (93 %). This is due to the longer exposure time under natural sunlight (3 days) resulting in more irradiation received and used for the photodegradation process. The above examples demonstrate the effectiveness of using AOPs in HS removal in terms of efficiency and reaction time. It also shows that when solar irradiation is involved in the treatment, the process is relatively slower. Either chemical addition or additional treatment step is therefore necessary to improve the water quality.

A relatively lower removal of AHA (50 %) with initial DOC 10 mg/L was

obtained using 2.5 g/L F200 carbon (Chen and Wu, 2004). The DOC removal value validates the observation in this research (46 % removal of AHA by 2g/L Aquasorb 101 GAC). This can be explained by the similarity of the pore size distribution of the two carbons. The F200 carbon has 65 % surface area of micropores (610 m<sup>2</sup>/g out of 934 m<sup>2</sup>/g) and 35 % of meso- and macropores (324 m<sup>2</sup>/g out of 934 m<sup>2</sup>/g). And the Aquasorb 101 carbon has 26 % surface area (236 m<sup>2</sup>/g out of 919 m<sup>2</sup>/g) in the meso- and macroporous range and 74 % (683 m<sup>2</sup>/g out of 919 m<sup>2</sup>/g) in the microporous range. The low degree of AHA removal by commercial carbons suggests that a majority of the micropores are not accessible by large AHA molecules. On the other hand, it indicates that the findings in this research on the Aquasorb 101 carbon may be applicable to other commercial carbons.

Solar irradiation showed a major improvement in removing HS by GAC adsorption, increasing the DOC removal from 46 % (using GAC alone) to 90 % (solar + GAC), due to the decrease of large molecules and increase of smaller adsorbable components. Even in winter with low solar intensity, the removal of AHA by GAC was increased by 30 % due to solar irradiation (see section 5.3.2.1), indicating the effectiveness of using solar irradiation as a pre-treatment method to GAC adsorption.

This chapter compared the removal of AHA water using different treatment processes. As can be seen, most of the consulted processes seem to perform well and can be considered as options for HS control. Using solar irradiation

prior to GAC adsorption was proven to significantly improve the adsorption of AHA and be able to achieve the AHA removal that can be achieved by AOPs, NF and coagulation processes. Compared to these processes, the solar-GAC method does not require the consumption of artificial energy and chemicals, and therefore does not have the chemical residual handling problems. It favours the environment. However, when the removal and treatment time are considered together, it appears that the solar-GAC process is not as effective as other processes. For example, the consulted processes only took 30 min to 3 days to complete the reaction, while the solar-GAC process took up to 10 weeks in this research. Despite this, experimental observations are evidence for the potential use of solar irradiation as a pre-treatment method to assist the water treatment process for improving HS removal. Sunlight presents a good opportunity in many fields, being low cost, available in significant quantities as well as preventing the pollution from the waste generated from chemical addition. Conducting solar irradiation tests in the sunlight-rich regions, using high performance solar collectors and employing GAC with a higher portion of meso- and macropores may help shorten the treatment time. Further investigations are suggested to better understand the proposed method in this research.

## CHAPTER 7

### CONCLUSIONS AND RECOMMENDATIONS

#### 7.1 Conclusions

A novel method for removing humic substances (HS) was proposed in this research, comprising a combination of solar irradiation and granular activated carbon (GAC) adsorption. This method is based on the fact that solar irradiation can break down large HS components into smaller molecules which are preferentially adsorbed by GAC. This is the first study to evaluate the use of solar irradiation as a pre-treatment method for improving the subsequent GAC adsorption performance with respect to HS removal; it therefore makes an important contribution to the knowledge of this method. The main findings coming out of this study are as follows:

- Solar irradiation reduced the dissolved organic carbon (DOC) concentration, UV absorbance at 254 nm ( $UV_{254}$ ), aromaticity and molecular weight (MW) of HS. An up to 84 % decrease of  $UV_{254}$  and up to 62 % decrease of DOC following solar irradiation were achieved in this research, showing that the HS removal efficiencies that have been reported by using artificial UV irradiation can be achieved by using natural sunlight alone (solar dose  $5.97 \times 10^5$  kJ/m<sup>2</sup>).
- The photodegradation of DOC and  $UV_{254}$  followed the first-order kinetics.

For waters of similar characteristics, the first-order decay rate constants were well correlated with solar doses. Not only UV irradiation but also visible irradiation in sunlight contributed to the photodegradation of HS.

- The high MW components in HS were more readily photodegraded, leading to the formation of smaller molecules. With the lower solar intensity in winter, there was an accumulation of intermediate and low MW fractions due to the breakdown of large molecules. While with increased solar intensity in spring and summer, solar irradiation alone removed HS fractions of all molecular sizes. A significant removal of the low MW compounds was shown to be achievable under strong sunlight.
- The application of solar collectors provided an efficient and viable way to promote the photodegradation of HS, and therefore benefited their removal by the subsequent GAC adsorption process. For example, the photodegradation rate of HS in BPC was two times that of HS in tray in summer experiment. And the maximum adsorption load of HS in BPC on GAC was enhanced by three times compared to that of HS in tray. For small scale applications, static solar collectors with large reflective surface would effectively work.
- Pre-treatment using solar irradiation substantially improved the GAC adsorption performance with regard to HS removal. Even though the solar intensity (or dose) in winter was fairly low, the adsorbability of HS was improved by up to 37 % and the maximum adsorption load was increased by 113 %. The improved adsorption behaviour was attributed to: (1) the increased amount of smaller molecules which were preferentially adsorbed by GAC from the mixture; (2) the decreased amount of large molecules that had great adsorption affinities to GAC surface and restricted access of smaller

molecules to carbon pores; (3) the dilution of solution concentration; and (4) the increased surface attractive interactions as a result of the decreased pH of HS solutions. Among them, the size effects were proven to play a major role.

- High performance size exclusion chromatography (HPSEC) data showed that the irradiated humic molecules could be completely removed by GAC. As the UV absorbing chromophores are known to be more reactive in disinfection by-product (DBP) formation for a water with a high humic content, this observation hence gives a good indication for the reduced DBP formation potential of the solar-treated water.
- Fulvic acid (FA) was found to be more prone to photodegradation than humic acid (HA). An improvement was also found for the adsorption of irradiated FA. Thus the effectiveness of the proposed solar-GAC method is likely to be seen when treating natural waters which contain both FA and HA.
- Comparable results were obtained between a natural water and Aldrich HA (AHA), showing the potential of using solar irradiation for improving the GAC adsorption of humic rich waters.
- Solar irradiation significantly improved the GAC adsorber performance based on smaller column studies, resulting in a longer operational life of the GAC adsorber and better effluent water quality. Since the rapid small scale column test (RSSCT) can well represent the full-scale filtration process, the use of solar irradiation as a pre-treatment method would be expected to reduce the regeneration or replacement frequency of GAC adsorbers, and therefore reduce the cost.

- The combination of solar irradiation with GAC adsorption exhibits the possibility of removing HS from water in a sustainable way. It improves the performance of the already existing GAC adsorption process, and does not require chemical addition, hence reducing the formation of chemical residues and associated waste handling cost simultaneously.

## 7.2 Recommendations

This work has proven the idea of using natural sunlight prior to GAC adsorption process to enhance the removal of HS from water. Future work is necessary to assist in understanding and evaluating this new approach. The following points are recommended for future work:

- Different water sources – HS from different water sources have varying characteristics and treatability. Investigations on different waters would give a more realistic idea of the effectiveness and applicability of the solar irradiation-GAC adsorption method. HS collected from the same water source during different times of the year should also be examined.
- Sunlight-rich regions – solar irradiation in London is in fact much lower than many other regions. The research conducted in London, however, has successfully proven the effective use of natural sunlight to improve HS removal by GAC. Further research in the sunlight-rich regions is strongly recommended to verify the observation in this research.
- Chemical mechanisms – if different waters with varying characteristics are examined as suggested above, it is also of interest to examine whether the chemical aspects play an important role in determining the removal of HS and

to what extent, in order to gain an insight into the mechanisms.

- Different GAC – The Aquasorb 101 GAC is mainly microporous and GAC containing more meso- and macropores has been found to better adsorb HS. The effects of solar irradiation on the adsorption of HS by GAC with different pore size distributions could be different.
- DBP formation – the effectiveness of HS removal by the solar-GAC method in this research was based on the changes in  $UV_{254}$ , DOC and HPSEC data. Although  $UV_{254}$  and aromaticity are well correlated with the DBP formation, further analysis on the DBP formation potential could give a better understanding of the effectiveness of the solar-GAC method in terms of drinking water safety.
- High performance solar collectors – with simplified and static solar collectors, the removal of HS was significantly improved. The estimated maximum solar concentrating efficiencies of static solar collectors employed in this research were 3-5 (see section 4.5.3). If high performance solar collectors (i.e. with solar concentrating efficiency more than 50) are applied, the experimental duration can be greatly shortened and higher removal efficiency would be expected.
- Effects on other processes – using natural sunlight as a pre-treatment method offers a sustainable and viable option to reduce the HS load, in particular the large molecules, on the subsequent treatment processes. Further research on a combination of solar irradiation with other water treatment processes is also recommended.

## CHAPTER 8

### REFERENCES

- Acra A., Raffoul Z. and Karahagopian Y. (1984). *Solar Disinfection of Drinking Water and Oral Rehydration Solutions*. Illustrate Publications S.A.L., Beirut, Lebanon.
- Aiken G. R. and Malcolm R. L. (1987). Molecular weight of aquatic fulvic acids by vapour pressure osmometry. *Geochimica et Cosmochimica Acta*, **51**(8), 2177-2184.
- Ajona J. I. and Vidal A. (2000). The use of CPC collectors for detoxification of contaminated water: Design, construction and preliminary results. *Solar Energy*, **68**(1), 109-120.
- Al-Ghouti M. A., Khraisheh M. A. M., Ahmad M. N. and Allen S. J. (2007). Microcolumn studies of dye adsorption onto manganese oxides modified diatomite. *Journal of Hazardous Materials*, **146**(1-2), 316-327.
- Allard B., Borén H., Pettersson C. and Zhang G. (1994). Degradation of humic substances by UV irradiation. *Environment International*, **20**(1), 97-101.
- Amy G. and Cho J. (1999). Interactions between natural organic matter and membranes: Rejection and fouling. *Water Science and Technology*, **40**(9), 131-139.
- André C. M. (2006). *Adsorption Treatment for the Removal of Humic Substances from Water Supply, Using Granular Activated Carbon and Iron-containing Adsorbents*. PhD thesis, University of London, London, UK.
- Archibald F. and Roy-Arcand L. (1995). Photodegradation of high molecular weight kraft bleachery effluent organochlorine and color. *Water Research*, **29**(2), 661-669.
- ASTM G173-03. (1992). *Standard Tables for Reference Solar Spectral Irradiances: Direct Normal and Hemispherical on 37° Tilted Surface*. American Society for Testing and Material, West Conshohocken.
- Ates N., Kitis M. and Yetis U. (2007). Formation of chlorination by-products in waters with low SUVA-correlations with SUVA and differential UV spectroscopy. *Water Research*, **41**(18), 4139-4148.

- Avena M. J. and Wilkinson K. J. (2002). Disaggregation kinetics of a peat humic acid: Mechanism and pH effects. *Environmental Science and Technology*, **36**(23), 5100-5105.
- Barrett S. E., Krasner S. W. and Amy G. L. (2000). *Natural Organic Matter and Disinfection By-Products: Characterization and Control in Drinking Water*. American Chemical Society, Washington D. C.
- Bennett L. E. and Drikas M. (1993). The evaluation of colour in natural waters. *Water Research*, **27**(7), 1209-1218.
- Bergamaschi B. A., Fram M. S., Fujii R., Aiken G. R., Kendall C. and Silva S. R. (2000). Trihalomethanes formed from natural organic matter isolates: Using isotopic and compositional data to help understand sources. In: *Natural Organic Matter and Disinfection By-Products: Characterization and Control in Drinking Water*. S. E. Barrett (ed.), S. W. Krasner (ed.) and G. L. Amy (ed.), American Chemical Society, Washington D. C., pp. 206-222.
- Bertilsson S. and Wildenfalk A. (2002). Photochemical degradation of PAHs in freshwaters and their impact on bacterial growth – influence of water chemistry. *Hydrobiologia*, **469**(1-3), 23-32.
- Blanco J., Malato S., Fernández P., Vidal A., Morales A., Trincado P., Oliveira J. C., Minero C., Musci M., Casalle C., Brunotte M., Tratzky S., Dischinger N., Funken K.-H., Sattler C., Vincent M., Collares-Pereira M., Mendes J. F. and Rangel C. M. (1999). Compound parabolic concentrator technology development to commercial solar detoxification applications. *Solar Energy*, **67**(4-6), 317-330.
- Bond T., Goslan E. H., Parsons S. A., Jefferson B. (2010). Disinfection by-product formation of natural organic matter surrogates and treatment by coagulation, MIEEX and nanofiltration. *Water Research*, **44**(5), 1645-1653.
- Brigante M., Zanini G. and Avena M. (2007). On the dissolution kinetics of humic acid particles: Effects of pH, temperature and  $\text{Ca}^{2+}$  concentration. *Colloid and Surfaces A: Physicochemical and Engineering Aspects*, **294**(1-3), 64-70.
- Brinkmann T., Hörsch P., Sartorius D. and Frimmel F. H. (2003). Photoformation of low-molecular-weight organic acids from brown water dissolved organic matter. *Environmental Science and Technology*, **37**(18), 4190-4198.
- Buchanan W., Roddick F., Porter N. and Drikas M. (2005). Fractionation of UV and VUV pretreatment natural organic matter from drinking water. *Environmental Science and Technology*, **39**(12), 4647-4654.
- Buchanan W., Roddick F. and Porter N. (2008). Removal of VUV pre-treated natural organic matter by biologically activated carbon columns. *Water Research*, **42**(13), 3335-3342.
- Cabaniss S. E., Zhou Q., Maurice P. A., Chin Y-P. and Aiken G. R. (2000). A Log-normal distribution model for the molecular weight of aquatic fulvic acids.

*Environmental Science and Technology*, **34**(6), 1103-1109.

Carter M. C. and Weber Jr. W. J. (1994). Modelling adsorption of TCE by activated carbon preloaded by background organic matter. *Environmental Science and Technology*, **28**(4), 614-623.

Carvalho S. I. M., Otero M., Duarte A. C. and Santos E. B. H. (2008). Effects of solar irradiation on the fluorescence properties and molecular weight of fulvic acids from pulp mill effluents. *Chemosphere*, **71**(8), 1539-1546.

Caslake L. F., Connolly D. J., Menon V., Duncanson C. M., Rojas R. and Tavakoli J. (2004). Disinfection of contaminated water by using solar irradiation. *Applied and Environmental Microbiology*, **70**(2), 1145-1150.

Chen J., Gu B., LeBoeuf E. J., Pan H. and Dai S. (2002). Spectroscopic characterization of the structural and functional properties of natural organic matter fractions. *Chemosphere*, **48**(1), 59-68.

Chen J. P. and Wu S. (2004). Simultaneous adsorption of copper ions and humic acid onto an activated carbon. *Journal of colloid and interface science*, **280**(2), 334-342.

Cheng W., Dastgheib S. A. and Karanfil T. (2005). Adsorption of dissolved natural organic matter by modified activated carbons. *Water Research*, **39**(11), 2281-2290.

Chin Y. P., Alken G. and O'Loughlin E. (1994). Molecular weight, polydispersity, and spectroscopic properties of aquatic humic substances. *Environmental Science and Technology*, **28**(11), 1853-1858.

Chin A. and Bérubé P. R. (2005). Removal of disinfection by-product precursors with ozone-UV advanced oxidation process. *Water Research*, **39**(10), 2136-2144.

Cho M., Chung H., Choi W. and Yoon J. (2005). Different inactivation behaviours of MS-2 phage and *Escherichia coli* in TiO<sub>2</sub> photocatalytic disinfection. *Applied and Environmental Microbiology*, **71**(1), 270-275.

Chow A. T., Leech D. M., Boyer T. H. and Singer P. C. (2008). Impact of simulated solar irradiation on disinfection byproduct precursors. *Environmental Science and Technology*, **42**(15), 5586-5593.

Chow C. W. K., Van Leeuwen J. A., Drikas M., Fabris R., Spark K. M. and Page D. W. (1999). The impact of the character of natural organic matter in conventional treatment with alum. *Water Science and Technology*, **40**(9), 97-104.

Chow C. W. K., Van Leeuwen J. A., Fabris R. and Drikas M. (2009). Optimised coagulation using aluminium sulphate for the removal of dissolved organic carbon. *Desalination*, **245**(1-3), 120-134.

Collins M. R., Amy G. L. and Steelink C. (1986). Molecular weight distribution, carboxylic acidity, and humic substances content of aquatic organic matter:

- Implications for removal during water treatment. *Environmental Science and Technology*, **20**(10), 1028-1032.
- Conte P. and Piccolo A. (1999). High pressure size exclusion chromatography (HPSEC) of humic substances: Molecular sizes, analytical parameters, and column performance. *Chemosphere*, **38**(3), 517-528.
- Cook R. L. and Langford C. H. (1998). Structural characterization of a fulvic acid and a humic acid using solid state ramp-CP-MAS C-13 nuclear magnetic resonance. *Environmental Science and Technology*, **32**(5), 719-725.
- Cooney D. O. (1999). *Adsorption Design for Wastewater treatment*. CRC Press LLC, Florida.
- Corin N., Backlund P. and Kulovaara M. (1996). Degradation products formed during UV-irradiation of humic waters. *Chemosphere*, **33**(2), 245-255.
- Corin N., Backlund P. and Wiklund T. (1998). Bacterial growth in humic water exposed to UV-radiation and simulated sunlight. *Chemosphere*, **36**(9), 1947-1958.
- Cornel P. K., Summers R. S. and Roberts P. V. (1986). Diffusion of humic-acid in dilute aqueous solution. *Journal of Colloid and Interface Science*, **110**(1), 149-164.
- Crittenden J. C., Berrigan J. K. and Hand D. W. (1986). Design of rapid small-scale adsorption tests for a constant diffusivity. *Journal of Water Pollution Control Federation*, **58**(4), 312-319.
- Crittenden J. C., Berrigan J. K., Hand D. W. and Lykins B. (1987). Design of rapid fixed-bed adsorption tests for nonconstant diffusivity. *Journal of Environmental Engineering*, **113**(2), 243-259.
- Crittenden J. C., Reddy P. S., Arora H., Trynoski J., Hand D. W., Perram D. L. and Summers R. S. (1991). Predicting GAC performance with rapid small-scale column tests. *Journal of American Water Works Association*, **95**(3), 77-87.
- Crittenden J. C., Trussell R. R., Hand D. W., Howe K. J., and Tchobanoglous G. (2005). *Water Treatment Principle and Design*. 2<sup>nd</sup> edn. John Wiley & Sons.
- Dastgheib S. A., Karanfil T. and Cheng W. (2004). Tailoring activated carbons for enhanced removal of natural organic matter from natural waters. *Carbon*, **42**(3), 547-557.
- Deflandre B. and Gagne J.-P. (2001). Estimation of dissolved organic carbon (DOC) concentrations in nanoliter samples using UV spectroscopy. *Water Research*, **35**(13), 3057-3062.
- Del Vecchio R. and Blough N. V. (2002). Photobleaching of chromophoric dissolved organic matter in natural waters: kinetics and modelling. *Marine Chemistry*, **78**(4), 231-253.

- Ding J. Y. and Wu S. C. (1997). Transport of organochlorine pesticides in soil columns enhanced by dissolved organic carbon. *Water Science and Technology*, **35**(7), 139-145.
- Dobbs R. A., Wise R. H. and Dean R. B. (1972). The use of ultra-violet absorbance for monitoring the total organic carbon content of water and wastewater. *Water Research*, **6**(10), 1173-1180.
- Doll T. E. and Frimmel F. H. (2003). Fate of pharmaceuticals-photodegradation by simulated solar UV-light. *Chemosphere*, **52**(10), 1757-1769.
- Edzwald J. K. and Tobiason J. E. (1999). Enhanced coagulation: US requirements and a broader view. *Water Science and Technology*, **40**(9), 63-70.
- Fabris R., Lee E. K., Chow C. W. K., Chen V. and Drikas M. (2007). Pre-treatment to reduce fouling of low pressure micro-filtration (MF) membranes. *Journal of Membrane Science*, **289**(1-2), 231-240.
- Fan L., Harris J. L., Roddick F. A. and Booker N. A. (2001). Influence of the characteristics of natural organic matter on the fouling of microfiltration membranes. *Water Research*, **35**(18), 4455-4463.
- Faust B. C. and Zepp R. G. (1993). Photochemistry of Aqueous Iron(III)-polycarboxylate complexes: Roles in the chemistry of atmospheric and surface waters. *Environmental Science and Technology*, **27**(12), 2517-2522.
- Fearing D. A., Banks J., Guyetand S., Eroles C. M., Jefferson B., Wilson D., Hillis P., Campbell A. and Parsons S. A. (2004). Combination of ferric and MIEX® for the treatment of a humic rich water. *Water Research*, **38**(10), 2551-2558.
- Fernández-Ibáñez P., Blanco J., Malato S. and de las Nieves F. J. (2003). Application of the colloidal stability of TiO<sub>2</sub> particles for recovery and reuse in solar photocatalysis. *Water Research*, **37**(13), 3180-3188.
- Fettig J. (1999). Removal of humic substances by adsorption/ion exchange. *Water Science and Technology*, **40**(9), 173-182.
- Freeman C., Evans C. D., Monteith D. T., Reynolds B. and Fenner N. (2001). Export of organic carbon from peat soils. *Nature*, **412**(6849), 785-785.
- Frimmel F. H. (1994). Photochemical aspects related to humic substances. *Environmental International*, **20**(3), 373-385.
- Frimmel F. H. (1998). Impact of light on the properties of aquatic natural organic matter. *Environment International*, **24**(5/6), 559-571.
- Fu P., Ruiz H., Thompson K. and Spangenberg C. (1994). Selecting membranes for removing NOM and DBP precursors. *Journal of American Water Works Association*, **86**(12), 55-72.
- Gao H. and Zepp R. G. (1998). Factors influencing photoreactions of dissolved

- organic matter in a coastal river of the southeastern United States. *Environmental Science and Technology*, **32**(19), 2940-2946.
- Gauden P. A., Szmechtig-Gauden E., Rychlicki G., Duber S., Garbacz J. K. and Buczkowski R. (2006). Changes of the porous structure of activated carbons applied in a filter bed pilot operation. *Journal of colloid and interface science*, **295**(2), 327-347.
- Gjessing E. T. and Källqvist T. (1991). Algicidal and Chemical effect of UV-radiation of water containing humic substances. *Water Research*, **25**(4), 491-494.
- Goel S., Hozalski R. M. and Bouwer E. J. (1995). Biodegradation of NOM - Effect of NOM source and ozone dose. *Journal of American Water Works Association*, **87**(1), 90-105.
- Goldstone J. V., Pullin M. J., Bertilsson S. and Voelker B. M. (2002). Reactions of hydroxyl radiation with humic substances: Bleaching, mineralization, and production of bioavailable carbon substrates. *Environmental Science and Technology*, **36**(3), 364-372.
- Goslan E. H. (2003). *Natural Organic Matter Character and Reactivity: Assessing Seasonal Variation in a Moorland Water*. EngD thesis, Cranfield University, UK.
- Goslan E. H., Gurses F., Banks J. and Parsons S. A. (2006). An investigation into reservoir NOM reduction by UV photolysis and advanced oxidation processes. *Chemosphere*, **65**(7), 1113-1119.
- Graham N. J. D. (1999). Removal of humic substances by oxidation/biofiltration processes – a review. *Water Science and Technology*, **40**(9), 141-148.
- Gray A., Abbena E. and Salamon S. (1997). *Modern Differential Geometry of Curves and Surfaces with Mathematica(Studies in Advanced Mathematics)*. Chapman and Hall/CRC.
- Hautala K., Peuravuori J. and Pihlaja K. (2000). Measurement of aquatic humus content by spectroscopic analyses. *Water Research*, **34**(1), 246-258.
- Hayes M. H. B. and Clapp C. E. (2001). Humic substances: considerations of compositions, aspects of structure, and environmental influences. *Soil Science*, **166**(11), 723-737.
- Hongve D. (1994). Sunlight degradation of aquatic humic substances. *Acta Hydrochimica et Hydrobiologica*, **22**(3), 117-120.
- Hooper S. M., Summers R. S., Solarik G. and Owen D. M. (1996). Improving GAC performance by optimized coagulation. *Journal of American Water Works Association*, **88**(8), 107-120.
- Jacangelo J. G., Demarco J., Owen D. M. and Randtke S. J. (1995). Selected

- processes for removing NOM-an overview. *Journal of American Water Works Association*, **87**(1), 64-77.
- Jacangelo J. G., Trussell R. R. and Watson M. (1997). Role of membrane technology in drinking water treatment in the United States. *Desalination*, **113**(2-3), 119-127.
- Jiang J. Q. and Graham N. J. D. (1996). Enhanced coagulation using Al/Fe(III) coagulants: Effect of coagulant chemistry on the removal of colour-causing NOM. *Environmental Technology*, **17**(9), 937-950.
- Kam S.-K. and Gregory J. (1999). Charge determination of synthetic cationic polyelectrolytes by colloid titration. *Colloid and Surfaces A: Physicochemical and Engineering Aspects*, **159**(1), 165-179.
- Karanfil T., Kilduff J. E., Schlautman M. A. and Weber Jr. W. J. (1996a). Adsorption of macromolecules by granular activated carbon. 1. Influence of molecular properties under anoxic solution conditions. *Environmental Science and Technology*, **30**(7), 2187-2194.
- Karanfil T., Schlautman M. A., Kilduff J. E. and Weber Jr. W. J. (1996b). Adsorption of macromolecules by granular activated carbon. 2. Influence of dissolved oxygen. *Environmental Science and Technology*, **30**(7), 2195-2201.
- Karanfil T., Kitis M., Kilduff J. E. and Wigton A. (1999). Role of granular activated carbon surface on the adsorption of organic compounds. 2. natural organic matter. *Environmental Science and Technology*, **33**(18), 3225-3233.
- Karanfil T., Kitis M., Kilduff J. E. and Wigton A. (2000). The use of granular activated carbon adsorption for natural organic matter control and its reactivity to disinfection by-products formation. In: *Natural Organic Matter and Disinfection By-Products: Characterization and Control in Drinking Water*. S. E. Barrett (ed.), S. W. Krasner (ed.) and G. L. Amy (ed.), American Chemical Society, Washington D. C., pp. 190-205.
- Karanfil T., Erdogan I. and Schlautman M. A. (2003). Selecting filter membranes for measuring DOC and UV<sub>254</sub>. *Journal of American Water Works Association*, **95**(3), 86-100.
- Kehoe S. C., Joyce T. M., Ibrahim P., Gillespie J. B., Shahar R. A. and McGuigan K. G. (2001). Effect of agitation, turbidity, aluminium foil reflectors and container volume on the inactivation efficiency of batch-process solar disinfectors. *Water Research*, **35**(4), 1061-1065.
- Khan E. and Subramania-Pillai S. (2007). Interferences contributed by leaching from filters on measurement of collective organic constituents. *Water Research*, **41**(9), 1841-1850.
- Kieber R. J., Zhou X. and Mopper K. (1990). Formation of carbonyl compounds from UV-induced photodegradation of humic substances in natural waters: Fate of

- riverine carbon in the sea. *Limnology and Oceanography*, **35**(7), 1503-1515.
- Kilduff J. E., Karanfil T., Chin Y.-P. and Weber Jr. W. J. (1996). Adsorption of natural organic polyelectrolyte by activated carbon: a size-exclusion chromatography study. *Environmental Science and Technology*, **30**(4), 1336-1343.
- Kitis M., Karanfil T., Kilduff J. E. and Wigton A. (2001). The reactivity of natural organic matter to disinfection byproducts formation and its relation to specific ultraviolet absorbance. *Water Science and Technology*, **43**(2), 9-16.
- Korshin G. V., Li C.-W. and Benjamin M. M. (1996). Monitoring the properties of natural organic matter through UV spectroscopy: a consistent theory. *Water Research*, **31**(7), 1787-1795.
- Korshin G. V., Wu W. W., Benjamin M. M. and Hemingway O. (2002). Correlations between differential absorbance and formation of individual DBPs. *Water Research*, **36**(13), 3273-3282.
- Lambert S. D. and Graham N. J. D. (1995). Removal of non-specific dissolved organic matter from upland potable water supplies – I. Adsorption. *Water Research*, **29**(10), 2421-2426.
- Leenheer J. A., Brown G. K., MacCarthy P. and Cabaniss S. E. (1998). Models of metal binding structures in fulvic acid from the Suwannee River, Georgia. *Environmental Science and Technology*, **32**(16), 2410-2416.
- Legrini O., Oliveros E. and Braun A. M. (1993). Photochemical processes for water treatment. *Chemical Reviews*, **93**(2), 671-698.
- Lehtola M. J., Miettinen I. T., Vartiainen T., Rantakokko P., Hirvonen A. and Martikainen P. J. (2003). Impact of UV disinfection on microbially available phosphorus, organic carbon, and microbial growth in drinking water. *Water Research*, **37**(5), 1064-1070.
- Lepane V., Persson T. and Wedborg M. (2003). Effects of UV-B radiation on molecular weight distribution and fluorescence from humic substances in riverine and low salinity water. *Estuarine Coastal and Shelf Science*, **56**(1), 161-173.
- Li C. W., Korshin G. V. and Benjamin M. M. (1998). Monitoring DBP formation with differential UV spectroscopy. *Journal of American Water Works Association*, **90**(8), 88-100.
- Li F., Yuasa A., Ebie K. and Azuma Y. (2003). Microcolumn test and model analysis of activated carbon adsorption of dissolved organic matter after pre-coagulation: effects of pH and pore size distribution. *Journal of Colloid and Interface Science*, **262**(2), 331-341.
- Listiarini K., Sun D. D. and Leckie J. O. (2009). Organic fouling of nanofiltration membranes: Evaluating the effects of humic acid, calcium, alum coagulant and their combinations on the specific cake resistance. *Journal of membrane science*, **262**(2), 331-341.

- Lou T. and Xie H. (2006). Photochemical alteration of the molecular weight of dissolved organic matter. *Chemosphere*, **65**(11), 2333-2342.
- Lund V. and Hongve D. (1994). Ultraviolet-irradiated water containing humic substances inhibits bacterial metabolism. *Water Research*, **28**(5), 1111-1116.
- Ma H. Z., Allen H. E. and Yin Y. J. (2001). Characterization of isolated fractions of dissolved organic matter from natural waters and a wastewater effluent. *Water Research*, **35**(4), 985-996.
- MacCarthy P. (2001). The principles of humic substances. *Soil Science*, **166**(11), 738-751.
- Malato S., Blanco J., Richter C., Curc3 D. and Gim3nez J. (1997). Low-concentrating CPC collectors for photocatalytic water detoxification: comparison with a medium concentrating solar collector. *Water Science and Technology*, **35**(4), 157-164.
- Malato S., Blanco J., Vidal A. and Richter C. (2002). Photocatalysis with solar energy at a pilot-plant scale: an overview. *Applied Catalysis B: Environmental*, **37**(1), 1-15.
- Mani S. K., Kanjur R., Singh I. S. B. and Reed R. H. (2006). Comparative effectiveness of solar disinfection using small-scale batch reactors with reflective, absorptive and transmissive rear surfaces. *Water Research*, **40**(4), 721-727.
- Matamoros V., Duhec A., Albaiges J. and Bayona J. M. (2009). Photodegradation of Carbamazepine, Ibuprofen, Ketoprofen and 17 alpha-Ethinylestradiol in Fresh and Seawater. *Water, air, and soil pollution*, **196**(1-4), 161-168.
- Matilainen A., Lindqvist N., Korhonen S. and Tuhkanen T. (2002). Removal of NOM in the different stages of the water treatment process. *Environment International*, **28**(6), 457-465.
- Matilainen A., Iivari P., Sallanko J., Heiska E. and Tuhkanen T. (2006). The role of ozonation and activated carbon filtration in the natural organic matter removal from drinking water. *Environmental Technology*, **27**(10), 1171-1180.
- Mavronikola C., Demetriou M., Hapeshi E., Partassides D., Michael C., Mantzavinos D., Kassinos D. (2009). Mineralisation of the antibiotic amoxicillin in pure and surface waters by artificial UVA- and sunlight-induced Fenton oxidation. *Journal of chemical technology and biotechnology*, **84**(8), 1211-1217.
- McCreary J. J. and Snoeyink V. L. (1980). Characterization and activated carbon adsorption of several humic substances. *Water Research*, **14**(9), 151-160.
- McLoughlin O. A., Kehoe S. C., McGuigan K. G., Duffy E. F., Al Touati F., Gernjak W., Alberola O. I., Rodr3guez S. M. and Gill L. W. (2004). Solar disinfection of contaminated water: a comparison of three small scale reactors. *Solar Energy*, **77**(5), 657-664.

- McVeigh J. C. (1983). *Sun Power: An Introduction to the Applications of Solar Energy*. Pergamon Press Ltd., England.
- Methods for the Examination of Water and Wastewater (1998). 20th edn, American Public Health Association/American Water Works Association/Water Environment Federation, Washington DC, USA.
- Moncayo-Lasso A., Pulgarin C. and Benitez N. (2008). Degradation of DBPs' precursors in river water before and after slow sand filtration by photo-Fenton process at pH 5 in a solar CPC reactor. *Water Research*, **42**(15), 4125-4132.
- Moran M. A. and Zepp R. G. (1997). Role of photoreactions in the formation of biologically labile compounds from dissolved organic matter. *Limnology and Oceanography*, **42**(6), 1307-1316.
- Murray C. A. and Parsons S. A. (2004). Removal of NOM from drinking water: Fenton's and photo-Fenton's processes. *Chemosphere*, **54**(7), 1017-1023.
- Murray C. A. and Parsons S. A. (2006). Preliminary laboratory investigation of disinfection by-product precursor removal using an advanced oxidation process. *Water and environment journal*, **20**(3), 123-129.
- Navntoft C., Ubomba-Jaswa E., McGuigan K. G. and Fernández-Ibáñez P. (2008). Effectiveness of solar disinfection using batch reactors with non-imaging aluminium reflectors under real conditions: Natural well-water and solar light. *Journal of Photochemistry and Photobiology B: Biology*, **93**(3), 155-161.
- Newcombe G. (1994). Activated carbon and soluble humic substances: Adsorption, desorption, and surface charge effects. *Journal of Colloid and Interface Science*, **164**, 452-462.
- Newcombe G. (1999). Charge vs. porosity - some influences on the adsorption of natural organic matter (NOM) by activated carbon. *Water Science and Technology*, **40**(9), 191-198.
- Newcombe G., Morrison J. and Hepplewhite C. (2002a). Simultaneous adsorption of MIB and NOM onto activated carbon. I. Characterisation of the system and NOM adsorption. *Carbon*, **40**(12), 2135-2146.
- Newcombe G., Morrison J. and Hepplewhite C. (2002b). Simultaneous adsorption of MIB and NOM onto activated carbon. II. Competitive effects. *Carbon*, **40**(12), 2147-2156.
- Newcombe G. (2006). Removal of natural organic material and algal metabolites using activated carbon. In: *Interface Science in Drinking Water Treatment: Theory and Applications*. G. Newcombe (ed.) and D. Dixon (ed.), Elsevier, UK, pp. 133-153.
- Nikolaou A. D. and Lekkas T. D. (2001). The role of natural organic matter during formation of chlorination by-products: a review. *Acta Hydrochimica et Hydrobiologica*, **29**(2-3), 63-77.

- Nokes C. J., Fenton E. and Randall C. J. (1999). Modelling the formation of brominated trihalomethanes in chlorinated drinking waters. *Water Research*, **33**(17), 3557-3568.
- Paleologou A., Marakas H., Xekoukoulotakis P., Moya A., Vergara Y., Kalogerakis N., Gikas P. and Mantzavinos D. (2007). Disinfection of water and wastewater by TiO<sub>2</sub> photocatalysis, sonolysis and UV-C irradiation. *Catalysis Today*, **129**(1-2), 136-142.
- Parkinson A., Roddick F. A. and Hobday M. D. (2003). UV photooxidation of NOM: Issues related to drinking water treatment. *Journal of Water Supply: Research and Technology-Aqua*, **52**(8), 577-586.
- Patel-Sorrentino N., Mounier S., Lucas Y. and Benaim J. Y. (2004). Effects of UV-visible irradiation on natural organic matter from the Amazon basin. *Science of the Total Environment*, **321**(1-3), 231-239.
- Paul A., Stösser R., Zehl A., Zwirnmann E., Vogt R. D. and Steinberg C. E. W. (2006). Nature and abundance of organic radicals in natural organic matter: Effect of pH and irradiation. *Environmental Science and Technology*, **40**(19), 5897-5903.
- Pelekani C., Newcombe G., Snoeyink V. L., Hepplewhite C., Assemi S. and Beckett R. (1999). Characterization of natural organic matter using high performance size exclusion chromatography. *Environmental Science and Technology*, **33**(16), 2807-2873.
- Peuravuori J. and Pihlaja K. (1997). Molecular size distribution and spectroscopic properties of aquatic humic substances. *Langford C. H.*, **337**(2), 133-149.
- Piccolo A. (2001). The supramolecular structure of humic substances. *Soil Science*, **166**(11), 810-832.
- Pullin M. J., Progg C. A. and Maurice P. A. (2004). Effects of photoirradiation on the adsorption of dissolved organic matter to goethite. *Geochimica et Cosmochimica Acta*, **68**(18), 3643-3656.
- Ratnaweera H., Gjessing E. and Oug E. (1999). Influence of physical-chemical characteristics of natural organic matter (NOM) on coagulation properties: an analysis of eight Norwegian water sources. *Water Science and Technology*, **40**(4-5), 89-95.
- Rebhun M., Meir S. and Laor Y. (1998). Using dissolved humic acid to remove hydrophobic contaminants from water by complexation-flocculation process. *Environmental Science and Technology*, **32**(7), 981-986.
- Reche I., Pace M. L. and Cole J. J. (1999). Relationship of trophic and chemical conditions to photobleaching of dissolved organic matter in lake ecosystems. *Biogeochemistry*, **44**(3), 259-280.
- Reckhow D. A., Singer P. C. and Malcolm R. L. (1990). Chlorination of humic materials: Byproduct formation and chemical interpretations. *Environmental*

*Science and Technology*, **24**(11), 1655-1664.

Remoundaki E., Vidali R., Kousi P., Hatzikioseyan A. and Tsezos M. (2009) Photolytic and photocatalytic alterations of humic substances in UV (254 nm) and Solar Cocentric Parabolic Concentrator (CPC) reactors. *Desalination*, **248**(1-3), 843-851.

Rice J. A. and MarCarthy P. (1991). Statistical evaluation of the chemical composition of humic substances. *Organic Geochemistry*, **17**(5), 635-648.

Rodríguez M. (2003). *Fenton and UV-vis Based Advanced Oxidation Processes in Wastewater Treatment: Degradation, Mineralization and Biodegradability Enhancement*. PhD thesis, University of Barcelona, Barcelona, Spain.

Rodríguez S. M., Gálvez J. B., Rubio M. I. M., Ibáñez P. F., Padilla D. A., Pereira M. C., Mendes J. F. and Oliveira J. C. (2004). Engineering of solar photocatalytic collectors. *Solar Energy*, **77**(5), 513-524.

Rodríguez-Zúñiga U. F., Milori D. M. B. P., Da Silva W. T. L., Martin-Netro L., Oliveira L. C. and Rocha J. C. (2008). Changes in optical properties caused by UV-irradiation of aquatic humic substances from the Amazon river basin: Seasonal variability evaluation. *Environmental Science and Technology*, **42**(6), 1948-1953.

Rook J. J. (1974). Formation of halogens during chlorination of natural waters. *Water Treatment Examination*, **23**, 234-243.

Schmitt-Kopplin P., Hertkorn N., Schulten H. R. and Kettrup A. (1998). Structural changes in a dissolved soil humic acid during photochemical degradation processes under O<sub>2</sub> and N<sub>2</sub> atmosphere. *Environmental Science and Technology*, **32**(17), 2531-2541.

Schreiber B., Brinkmann T., Schmalz V. and Worch E. (2005). Adsorption of dissolved organic matter onto activated carbon-the influence of temperature, adsorption wavelength, and molecular size. *Water Research*, **39**(15), 3449-3456.

Selcuk H., Sene J. J. and Anderson M. A. (2003). Photoelectrocatalytic humic acid degradation kinetics and effect of pH, applied potential and inorganic ions. *Journal of Chemical Technology and Biotechnology*, **78**(9), 979-984.

Sharp E. L., Jarvis P., Parsons S. A. and Jefferson B. (2006). Impact of fractional character on the coagulation of NOM. *Colloids and surfaces. A, Physicochemical and engineering aspects*, **286**(1-3), 104-111.

Singer P. C. (1999). Humic substances as precursors for potentially harmful disinfection by-products. *Environmental Science and Technology*, **40**(9), 25-30.

Singer P. C. and Bilyk K. (2002). Enhanced coagulation using a magnetic ion exchange resin. *Water Research*, **36**(16), 4009-4022.

Skjelkvåle B. L., Stoddard J. L., Jeffries D. S., Tørseth K., Høgåsen T., Bowman

- J., Mannio J., Monteith D. T., Mosello R., Rogora M., Rzychon D., Vesely J., Wieting J., Wilander A. and Worsztynowicz A. (2005). Regional scale evidence for improvements in surface water chemistry 1990-2001. *Environmental Pollution*, **137**(1), 165-176.
- Stevenson F. J. (1982). *Humus chemistry. Genesis, composition, reactions*. John Wiley and Sons Limited, New York.
- Summers R. S. and Roberts P. V. (1988a). Activated carbon adsorption of humic substances: I. Heterodisperse mixtures and desorption. *Environmental Science and Technology*, **122**(2), 367-381.
- Summers R. S. and Roberts P. V. (1988b). Activated carbon adsorption of humic substances: I. Size exclusion and electrostatic interactions. *Environmental Science and Technology*, **122**(2), 382-397.
- Summers R. S., Hooper S. M., Solarik G., Owen D. M. and Hong S. (1995). Batch-scale evaluation of GAC for NOM control. *Journal of American Water Works Association*, **87**(8), 69-80.
- Świetlik J., Raczyk-Stanisławiak U., Biłozor S., Ilecki W. and Nawrocki J. (2002). Adsorption of natural organic matter oxidized with ClO<sub>2</sub> on granular activated carbon. *Water Research*, **36**(9), 2328-2336.
- Thomas-Smith T. E. and Blough N. V. (2001). Photoproduction of hydrated electron from constituents of natural waters. *Environmental Science and Technology*, **35**(13), 2721-2726.
- Thomson J., Roddick F. and Drikas M. (2002). Natural organic matter removal by enhancement photooxidation using low pressure mercury vapour lamps. *Water Science and Technology*, **2**(5-6), 435-443.
- Thurman E. M. (1985). *Organic Geochemistry of Natural Waters*. Martinus Nijhoff / Dr. W. Junk, Dordrecht.
- Toor R. and Mohseni M. (2007). UV-H<sub>2</sub>O<sub>2</sub> based AOP and its integration with biological activated carbon treatment for DBP reduction in drinking water. *Chemosphere*, **66**(11), 2087-2095.
- Ubomba-Jaswa E., Navntoft C., Polo-Lopez M. I., Fernandez-Ibanez P. and McGuigan K. G. (2009). Solar disinfection of drinking water (SODIS): an investigation of the effect of UV-A dose on inactivation efficiency. *Photochemical & Photobiological Sciences*, **8**(5), 587-595.
- Urfer D. and Huck P. M. (1997). Effects of hydrogen peroxide residuals on biologically active filters. *Ozone: science and engineering*, **19**(4), 371-386.
- Vidal A. and Díaz A. I. (2000). High-performance, low-cost solar collectors for disinfection of contaminated water. *Water Environment Research*, **72**(3), 271-275.
- Volk C., Bell K., Ibrahim E., Verges D., Amy G. and Lechevallier M. (2000).

- Impact of enhanced and optimized coagulation on removal of organic matter and its biodegradable fraction in drinking water. *Water Research*, **34**(12), 3247-3257.
- Vuorenmaa J., Forisius M. and Mannio J. (2006). Increasing trends of total organic carbon concentrations in small forest lakes in Finland from 1987 to 2003. *Science of the Total Environment*, **365**(1-3), 47-65.
- Walker D. C., Len S-V. and Sheehan B. (2004). Development and Evaluation of a reflective solar disinfection pouch for treatment of drinking water. *Applied and Environmental Microbiology*, **70**(4), 2545-2550.
- Wang Z., Pant B. C. and Langford C. H. (1990). Spectroscopic and structural characterization of a Laurentian fulvic-acid – Notes on the origin of the color. *Analytica Chimica Acta*, **232**(1), 43-49.
- Wang G-S., Hsieh S.-T. and Hong C.-S. (2000). Destruction of humic acid in water by UV light – Catalyzed oxidation with hydrogen peroxide. *Water Research*, **34**(15), 3882-3887.
- Watts C. D., Naden P. S., Machell J. and Banks J. (2001). Long term variation in water colour from Yorkshire catchments. *Science of the Total Environmen*, **278**(1-3), 57-72.
- Weber Jr. W. J., McGinley P. M. and Katz L. E. (1991). Sorption phenomena in subsurface systems: Concept, models and effects on contaminant fate and transport. *Water Research*, **25**(5), 499-528.
- Weishaar J. L., Aiken G. R., Bergamaschi B. A., Fram M. S., Fujii R. and Mopper K. (2003). Evaluation of specific ultraviolet absorbance as an indicator of the chemical composition and reactivity of dissolved organic carbon. *Environmental Science and Technology*, **37**(20), 4702-4708.
- White D. M., Garland D. S., Narr J. and Woolard C. R. (2003). Natural organic matter and DBP formation potential in Alaskan water supplies. *Water Research*, **37**(4), 939-947.
- Winter A. R., Fish T. A. E., Playle R. C., Smith D. S. and Curtis P. J. (2007). Photodegradation of natural organic matter from diverse freshwater sources. *Aquatic Toxicology*, **84**(2), 215-222.
- Wiszniewski J., Robert D., Surmacz-Gorska J., Miksch K. and Weber J. V. (2002). Photocatalytic decomposition of humic acids on TiO<sub>2</sub> Part I: Discussion of adsorption and mechanism. *Journal of photochemistry and photobiology. A, Chemistry*, **152**(1-3), 267-273.
- Wiszniewski J., Robert D., Surmacz-Gorska J., Miksch K., Malato S. and Weber J.-V. (2004). Solar photocatalytic degradation of humic acids as a model of organic compounds of landfill leachate in pilot-plant experiments: influence of inorganic salts. *Applied Catalysis B: Environmental*, **53**(2), 127-137.
- Worrall F., Harriman R., Evans C. D., Watts C. D., Adamson J., Neal C., Tipping

- E., Burt T., Grieve I., Monteith D., Naden P. S., Nisbet T., Reynolds B. and Stevens P. (2004). Trends in dissolved organic carbon in UK rivers and lakes. *Biogeochemistry*, **70**(3), 369-402.
- Xie H., Zafiriou O. C., Cai W.-J., Zepp R. G. and Wang Y. (2004). Photooxidation and its effects on the carboxyl content of dissolved organic matter in two coastal rivers in the Southeastern United States. *Environmental Science and Technology*, **38**(15), 4113-4119.
- Yuasa A., Li F., Matsui Y. And Ebie K. (1997). Characteristics of competitive adsorption of aquatic humic substances onto activated carbon. *Water Science and Technology*, **36**(12), 231-238.
- Zhou Q., Cabaniss S. E. and Maurice P. A. (2000). Considerations in the use of high-pressure size exclusion chromatography (HPSEC) for determining molecular weights of aquatic humic substances. *Water Research*, **34**(14), 3505-3514.
- Zhou Q., Maurice P. A. and Cabaniss S. E. (2001). Size fractionation upon adsorption of fulvic acid on goethite: Equilibrium and kinetics studies. *Geochimica et Cosmochimica Acta*, **65**(5), 803-812.
- Zularisam A. W., Ismail A. F. and Salim R. (2006). Behaviours of natural organic matter in membrane filtration for surface water treatment – a review. *Desalination*, **194**(1-3), 211-231.
- Zuo Y. and Jones R. D. (1997). Photochemistry of natural dissolved organic matter in lake and wetland waters-production of carbon monoxide. *Water Research*, **31**(4), 850-858.

## PAPERS AND COMMUNICATIONS

This work has been presented to:

- The 1<sup>st</sup> HYDRA Postgraduate Research Poster Meeting, UCL, UK, 12/2007.
- The 5<sup>th</sup> IWA Leading-Edge Conference and Exhibition on Water and Wastewater Technologies, Zurich, Switzerland, 06/2008.
- The 4<sup>th</sup> IWA Specialist Conference - Natural Organic Matter: from Source to Tap, Bath, UK, 09/2008.
- The 10<sup>th</sup> IWA UK Young Water Professional Conference, London, UK, 04/2009.

The results of this research are presented in three journal papers:

- Removal of Humic Substances Using Solar Irradiation Followed by Granular Activated Carbon Adsorption. *Water Science and Technology: Water Supply*. (accepted 1 December, 2009).